ZIRCONIUM COMPLEXES AS CATALYSTS IN THE OLIGOMERISATION OF ETHYLENE

by

David John Jones B.Sc. (Hons.)

A thesis submitted in fulfilment of the requirements for the degree of

Doctor of Philosophy

Chemistry Department,
University of Tasmania,
Hobart, Tasmania,
Australia, 1994.

This thesis contains no material which has been accepted for the award of any other degree or diploma in any University, and to the best of my knowledge, contains no copy or paraphrase of material previously presented by another person, except where due reference is made in the text.

ACKNOWLEDGEMENTS

It is with pleasure that I acknowledge my supervisor, Assoc. Prof. K.J. Cavell, for his support, interest and encouragement during the difficult early months of this research continuing through to its completion. Sincere thanks are also extended to my co-supervisor, Prof. Dr. W.I. Keim, who made possible an enjoyable and rewarding period in his laboratory in Aachen, Germany. I extend my thanks to Prof. A.J. Canty for his support and interest during my time studying the chemistry of palladium.

I would like to extend my thanks to the technical and academic staff, both at the University of Tasmania and Institut für Technische Chemie und Petrolchemie der RWTH, Aachen for their support and assistance. Special thanks go to Mike Brandon for the extensive supply of new glassware, Evan Peacock for his valued assistance during many NMR studies and Dr. P. Trail for helping me understand the art of air sensitive and palladium chemistry.

For their valued friendship and support I thank fellow students, who helped make the process of learning fun, especially Dr. A. Seen, Mr. I. Setiawan, Ms. S. Desjardins, Mr A. Roberts, Mr. R. Hecker, Mr. J. Hoare, Dr. G. Britovsek and Mr. A. Ecke.

I gratefully acknowledge the Commonwealth of Australia [APRA(Industry) scholarship] and ICI Australia for their financial support and DISAT (formerly DITAC) funding for the research exchange to Germany.

CONTENTS

CHAPTER 3 : Synthesis

ABSTRACT

This thesis describes the development of a model and subsequent new catalyst systems for zirconium catalysed ethylene oligomerisation. The developed model predicts that conditions which favour transition states for β-hydrogen elimination, (i.e. coordinatively unsaturated metal centre, a low lying metal orbital and high Lewis acidity), would lead to better oligomerisation catalysts. This led to the *in situ* catalytic testing of hemi-labile, bidentate, chelate ligands containing atoms of varying donor ability, i.e. thioacetylacetones, Schiff's bases, picolinic acid and β-aminoketones.

In situ catalytic tests using β-aminoketones (**I**), the primary ligands in this study, have shown them to be particularly effective in promoting oligomerisation and catalytic testing has shown for the first time the ability to control reactivity and oligomer distribution in zirconium based catalyst systems by variation of ligand substituents. Bulky substituents, R^2 & R^3, reduce catalytic activities. Electron withdrawing groups on the amine (imine in complexes) or ligand backbone increase reactivity. The use of bis-β-aminoketone zirconium complexes (**II**) resulted in catalytic systems with the highest activity and average oligomer weight. Activity variations between the *in situ* catalytic testing of free β-aminoketones and preformed complexes have been explained through complex ligand-cocatalyst interactions. It is proposed that a decreased amine basicity reduces the tendency for amine coordination which increases metal centre Lewis acidity thereby resulting in lower average oligomer weight.

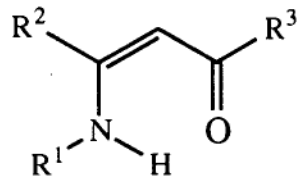

I. β-aminoketone
R^1-HR^2NacR^3ac

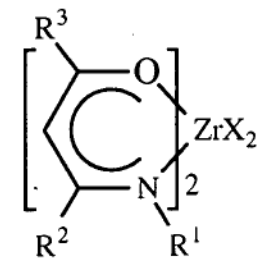

II. Bis-Ligand Complex
(R^1-R^2NacR^3ac)$_2$ZrX_2

Synthetic work has led to the isolation and characterisation of a number of new co-ordination, organometallic and cationic zirconium complexes containing β-

aminoketones. Alkyl-zirconium complexes were synthesised by the reaction of free β-aminoketones with the homoleptic tetraalkyl, $ZrBz_4$. Cationic complexes were synthesised by partial protolysis of the alkyl complexes using $PhNMe_2H^+BPh_4^-$. This work introduces a new area of ligand stabilised, highly Lewis acidic, alkyl zirconium chemistry.

VT-NMR studies have led to the identification of stability regimes for alkylated, bis-ligand complexes and indicated that β-aminoketones function as bidentate chelate ligands in most complexes. Electron withdrawing groups on or near the imine led to hemi-labile systems with nitrogen dissociation. Cis-benzyl ligands are found to have an average bonding environment somewhat between a true sigma or dihapto bond with a stronger dihapto character at lower temperatures. Benzyl bonding reflects variations in metal centre Lewis acidity. Cationic, bis-β-aminoketone zirconium complexes contain η^2-bound benzyl.

In situ NMR catalysis experiments have shown complex cocatalyst/ligand interactions which depend on the relative basicity of β-aminoketone protons. β-Aminoketones remain bonded to zirconium via oxygen during catalysis and ethylene insertion occurs at zirconium. The new catalytic systems oligomerise ethylene under very mild conditions, RT and 1 atm ethylene.

Interestingly this work has clearly demonstrated that many of the features and catalytic controls currently being developed in zirconium metallocene (and related systems) based catalysts may be achieved more simply from zirconium coordination complexes and their organometallic derivatives.

Chapter 1

Introduction

Worldwide production of linear α-olefin runs currently at around 1.4 million tonnes leading to increased activity in research to find more efficient catalytic systems for their production[1]. Since the 1950's when Ziegler and co-workers using alkyl aluminiums oligomerised ethylene to form linear α-olefins the chemistry has grown to include titanium, zirconium and nickel containing catalysts, both Ziegler-Natta and single component systems. More recently, zirconium based ethylene oligomerisation systems have increased in importance and the current study is aimed at extending the knowledge base of this new chemistry.

1.1.0. Oligomerisation : Producing Linear α-Olefins

Linear α-olefins find wide use, depending on chain length and subsequent functionalisation, as speciality chemicals, surfactants and comonomers. Linear α-olefins with four to eight carbons are used as comonomers in the production of high density polyethylene (HDPE) or linear low density polyethylene (LLDPE) where their use allows control of polymer characteristics. Longer chain linear α-olefins with fourteen to eighteen carbons can be functionalised to give a range of surfactants, i.e. alkyl sulphates, sulphonates, tertiary amines or phenyl sulphonates[2a]. The requirement for biodegradability in detergents has lead to and facilitated the availability of large supplies of linear α-olefins. Smaller amounts of other speciality chemicals are also derived from linear α-olefins including alcohols and acids, some of which are used as plasticisers in the polymer industry.

Olefin oligomerisation, the coupling together of three to thirty α-olefins, can be considered to be part of a continuum between dimerisation on the one hand and polymerisation on the other. Oligomerisation chemistry is generally considered to be similar to these chemistries but, being a fine balance in the middle of these extremes, is much more difficult to control. It is a part of the growing field of carbon-carbon coupling chemistry.

The most generally accepted oligomerisation mechanism involves olefin coordination followed by its insertion into a metal hydride bond, while termination is via β-hydride elimination. If k_p is the propagation(insertion) rate and k_e the elimination rate, then the relative rates of propagation versus elimination, k_p vs. k_e, determine the overall chain length, with dimerisation when $k_e >> k_p$ and

polymerisation when $k_p >> k_e$. Only when $k_p \cong k_e$ or $k_p > k_e$ is it possible to generate an oligomerisation system (Figure 1.1).

Figure 1.1.

General Reaction Mechanism for Olefin Coupling Reactions

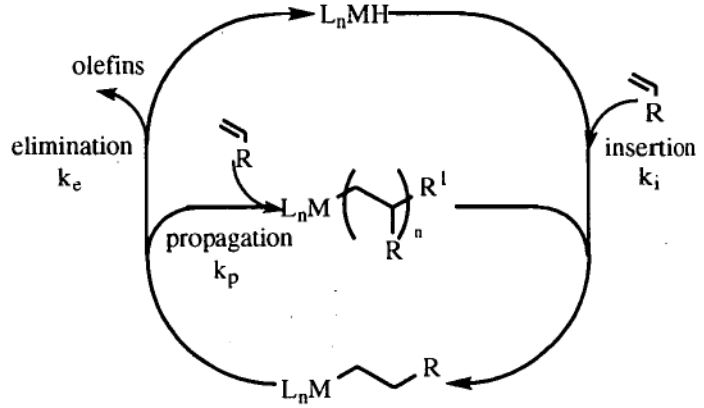

$k_p >> k_e$: Polymerisation

$k_p \cong k_e$: Oligomerisation

$k_e >> k_p$: Dimerisation

It is not surprising that when the steric or electronic environment at the metal centre is changed a range of products can be obtained from a catalytic system. Often changing temperature or pressure is enough to promote dimerisation over oligomerisation, e.g. for a Ziegler type system butenes are generated at 130-220°C and 1-9 bar of ethylene while at 176-287°C and 140-275 bar of ethylene, C_4-C_{10} oligomers are generated[2a]. A Cossee[2] type mechanism (Figure 1.2) is generally assumed but other mechanisms have been proposed.

Figure 1.2.

Cossee Mechanism for Olefin Insertion.

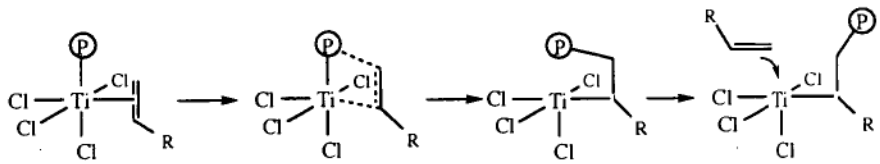

1.2.0. Industrial Oligomerisation Processes

Commercial operations have grown in size and sophistication as oligomerisation chemistry has been developed. Older thermal cracking process have been replaced by Ziegler type processes. Initially linear α-olefins were generated by wax cracking or paraffin dehydrogenation giving, as is normal with cracking processes, a wide range of products with associated separation problems to recover the required linear α-olefins. The introduction of Ziegler type systems allowed direct access in high yields to the required α-olefin from simple starting materials and gave the ability to control product distributions. These have been followed more recently by the introduction of the Shell Higher Olefins Process (SHOP) using a single component catalyst system.

1.2.1. Ziegler Based Methods

Using triethylaluminium (Et_3Al) as the catalyst, Chevron introduced a one step Ziegler process to give C_4-C_{10} oligomers with a Schultz-Flory type distribution. Chain growth is by ethylene insertion into the aluminium-alkyl bond while displacement of the growing alkyl, chain by a lower olefin, leads to termination. Reaction conditions are around 200°C and 138-276 bar with termination (displacement) favoured at high temperatures and chain growth (insertion) by an increased ethylene pressure.

A two stage variation of this process is used by the Ethyl Corporation to control more precisely the molecular weight of the resulting linear α-olefins. In this process the C_6-C_{10} oligomers are used to displace the C_{12}-C_{18} oligomers, therefore leading to a narrower Poisson product distribution (Figure 1.3.).

Figure 1.3.

Ziegler Based Oligomerisation Systems

Chain Propagation

$$Et_3Al + 3n\ CH_2{=}CH_2 \longrightarrow (Et\text{-}(CH_2\text{-}CH_2)_n)_3Al$$

Chain Termination

$$(R'\text{-}CH_2\text{-}CH_2)_3Al + 3\ R\text{-}CH{=}CH_2 \longrightarrow 3\ R'\text{-}CH{=}CH_2 + (R\text{-}CH_2\text{-}CH_2)_3Al$$

$R = H$: one step process

$R = C_4$-C_{10} : two step process

1.2.2. Shell Higher Olefin Process

The introduction of the Shell Higher Olefin Process (SHOP) led to a new era in oligomerisation chemistry by use of non-Ziegler chemistry. It has been proposed that the SHOP process utilises a single component catalyst containing a bidentate phosphorous-oxygen ligand. The catalyst is generated *in situ*[3]. The success of the SHOP lies not only in the introduction of an excellent catalytic system for the formation of linear α-olefins, which follow a Schultz-Flory distribution, but in modifying or reforming unwanted oligomers to give an excess of the favoured products by the coupling of a number of technologies. In this way long or short oligomers, which are of no great value, are modified by isomerisation and metathesis catalysts to generate new olefins in the desired product range.

Figure 1.4.

Hydride Mechanism for Nickel Based Olefin Oligomerisation.

(Two possible Precursor Complexes A & B are shown)

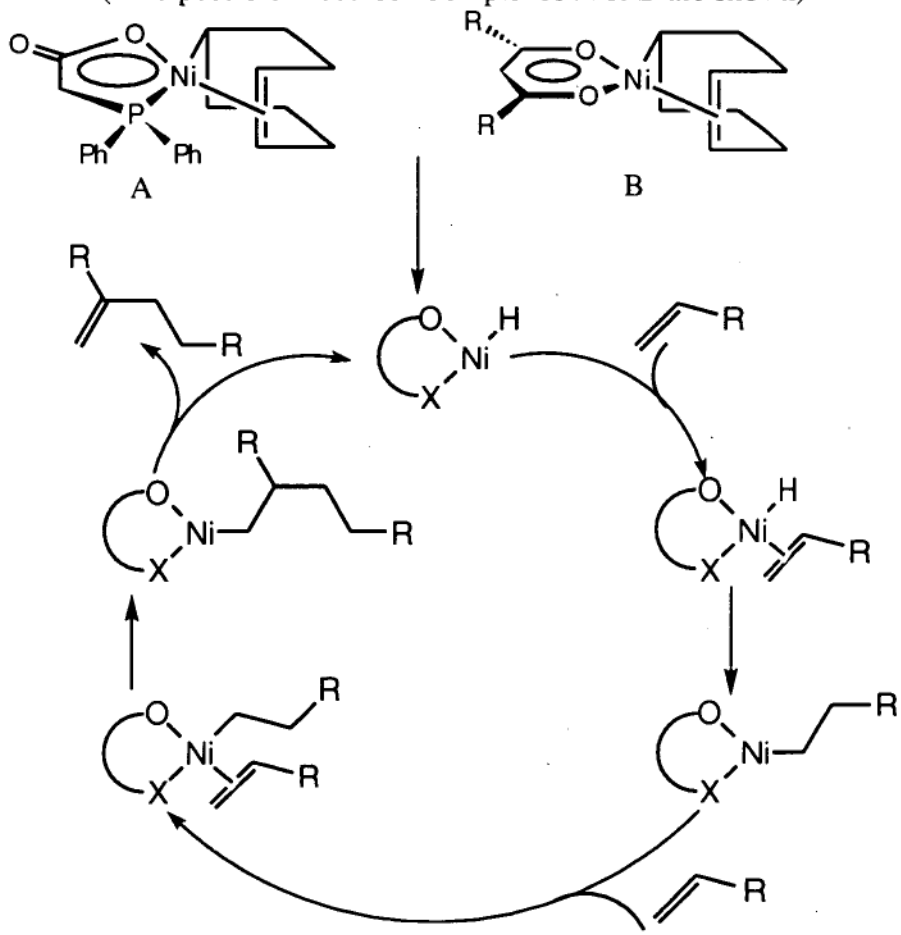

SHOP type chemistry has been thoroughly investigated and a hydride based oligomerisation mechanism has been proposed, with the hydride being derived from any number of precursor complexes[4]. Two such precursor complexes are shown in Figure 1.4. where complex A is thought to be similar to the SHOP catalyst.

1.2.3. Ziegler-Natta Systems

Oligomerisation catalysts can be formed from titanium tetrachloride, where care is taken not to reduce the titanium by the use of mono- or dialkyl aluminium chlorides, rather than the typical polymerisation catalysts based on reduced titanium(III) species. In these systems, it is believed that, the addition of a strong Lewis acid improves oligomerisation activities by supporting the formation of the proposed ion pairs in solution[5].

The use of zirconium containing systems has also been shown to lead to oligomerisation catalysts . This will be discussed in detail in Chapter 2 of this thesis. Zirconium based systems have been shown, in general, to have higher activities than corresponding titanium systems. Recently Idemitsu has commissioned a pilot plant in which zirconium based system is used in the production of linear α-olefins. In patents covering this process an oligomerisation catalyst is generated by mixing zirconium tetrachloride with an alkylaluminium cocatalyst in the presence of a weak Lewis base.

With the introduction, at an industrial scale, of zirconium based ethylene oligomerisation better fundamental knowledge of the chemistry behind this process, which is not yet available, is required. There are few papers dealing with mechanistic aspects of this chemistry even at a superficial level. The role of the ligands, or the cocatalyst, remains vague with only assumptions on possible mechanisms.

1.3.0. Problem Definition

It has been the purpose of this study to examine the processes and chemistry involved in zirconium based ethylene oligomerisation so as to enable the design of better oligomerisation catalysts. It has been assumed, as with most research in this field, that a mechanism similar to other oligomerisation or polymerisation systems is

followed. In this mechanism ligands modify the steric or electronic environment at the metal centre in what is a transition metal based carbon-carbon coupling reaction. The added cocatalyst functions as an alkylation agent and a strong Lewis acid to form, *in situ*, a tight ion pair. It is this ion pair or the cation which is the active species[6].

This study has been designed to examine the role of ligands in this reaction and to isolate potential intermediates in the mechanistic pathway thus leading to a better understanding of zirconium based oligomerisation reactions. Chapter 2 of this thesis presents a critical survey of the literature, leading to the development of a model predicting conditions under which oligomerisation is most likely to be promoted. *In situ* formation of catalytic species and the examination of the role of the ligand is covered in Chapter 3 leading to the first evidence of the ability to control, through ligand substituent variation, the oligomer product distribution and activity. Synthesis of complexes which are potentially part of the catalytic cycle is covered in Chapter 4. A number of new zirconium complexes are described including complexes leading to a new area of zirconium chemistry, that is bidentate, chelate ligand stabilised alkyl zirconium complexes. Finally, variable temperature NMR studies, Chapter 5, have lead to an understanding of the properties of these new complexes an well as *in situ* reactions occurring on addition of alkylaluminium cocatalysts to oligomerisation precursor complexes.

Figure 1.5.

Hydride Based Oligomerisation Mechanism for Cationic bis-Cp' Zirconium Species.
(for clarity two ethylene insertions shown)

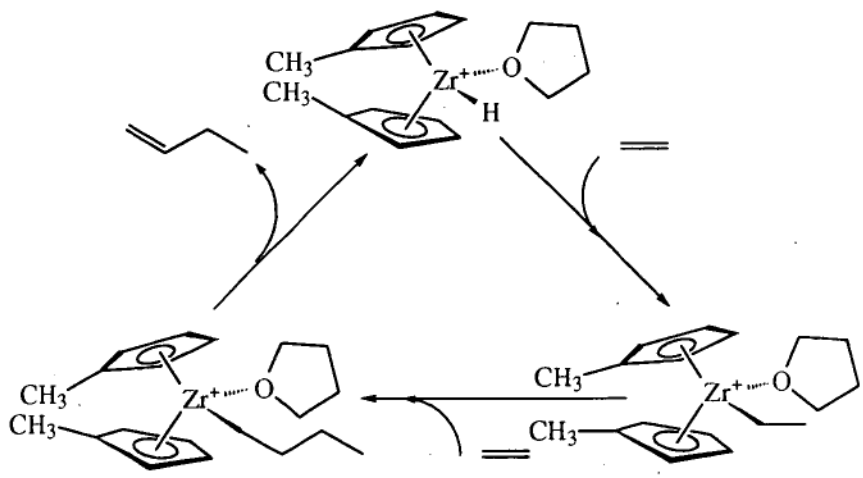

The assumption of a common mechanism for polymerisation and oligomerisation is supported by the recent appearance of cationic zirconium species which oligomerise olefins under certain conditions. The oligomerisation of ethylene by a cationic bis-methylcyclopentadienyl zirconium hydride complex was described by Jordan et al. during studies into cationic zirconium catalysts for the polymerisation of olefins[7]. Jordan proposed a zirconium hydride based mechanism for these reactions (Figure 1.5).

1 General References

a. Al-Jarallah, A.M.; Anabtawi, J.A.; Siddiqui, M.A.B.; Aitani, A.M., *Catalysis Today* 14(1), **1992**, 42-104.

b. Demianiw, D.G., *Kirk-Othmer, Encyclopedia of Chemical Technology* 3rd Ed., Vol. 16, **1981**, John Wiley & Sons, inc. 480-499.

c. Skupinska,J., *Chem. Rev.* 91, **1991**, 613-648.

2 Cotton, F.A.; Wilkinson, G., *Advanced Inorganic Chemisty* 5th Ed., John Wiley & Sons, Inc., **1980**; pg 1259.

3 Reuben, B.; Wittcoff, H. *J. Chem. Ed.* 65(7), **1988**, 605-605.

4 a. Behr, A.; Keim, W., *Arab. J. of Sci. & Eng.* 10, **1985**, 377.

b. Peukert, M.; Keim, W., *Organometallics* 2, **1983**, 594.

5 Henrici-Olivé, G.; Olivé, S., *Adv. Polym. Sci.* 15(4), **1974**, 4-30.

6 Eisch, J.J.; Cadwell, K.R., in *Homogeneous Transition Metal catalysed Reactins* Editors : Moser, W.R.; Slocum, D.W., American Chemical Society **1992**, 575-602.

7 Jordan, R.F.; La Pointe, R.E.; Bradley, P.K.; Baenziger, N., *Organometallics* 8, **1989**, 2892-2903.

Chapter 2

Literature Review and Model Development

In this chapter a critical review of zirconium based oligomerisation systems is given. Relevant information is extracted to allow development of a general model to describe conditions most likely to lead to active oligomerisation systems. Due to a limited number of theoretical studies the majority of information comes not from examining literature on oligomerisation but from the related polymerisation systems, assuming a common mechanism for the two reactions. Attention has been focused on gaining information about reaction mechanisms, reactive intermediates and synthetic methods. The effects of variations to the steric and electronic environment of the metal centre on polymerisation activity are examined in relation to their effect on rates of β-hydride elimination.

2.2.0. Summary of Oligomerisation Studies

Although zirconium based oligomerisation systems have been industrialised, the theoretical and mechanistic basis for zirconium based oligomerisation systems as opposed to polymerisation is not well understood or developed. An examination of the patent and scientific literature revealed a number of conflicting viewpoints. There is little agreement on the role of added ligands, active species, metal oxidation state or even the active metal. It is however generally assumed that active species similar to those found in polymerisation systems are present. The control of activity or oligomer product distribution through systematic ligand substituent variations has not been demonstrated. It has been suggested that the role of the ligand in zirconium based oligomerisation processes is to act as a solubilising agent to aid formation of the active species.

With this in mind the following is a review of zirconium based oligomerisation systems. Active species, activities, mechanisms and ligand influences are noted where mentioned in the original literature. A direct comparison of numbers was, however, impossible due to changes in the scale of reaction and whether batch or continuous reactors were used (units have been converted to those used in this study).

2.2.1. Early Mechanisms for Oligomerisation

The study of zirconium based oligomerisation systems[1] began in earnest following work carried out by Attridge[2]. For the first time a possible mechanism for the

oligomerisation reaction was proposed and the ability of alkyl-zirconium compounds to effectively promote oligomerisation in the presence of a cocatalyst was indicated. The co-catalyst was required for oligomerisation, with ethylene being polymerised in the absence of any added alkylaluminium reagent[3].

Attridge reported ethylene oligomerisation after activation of homoleptic zirconium tetra-alkyl or aryl with an alkylaluminium co-catalyst. On examining a number of possible co-catalysts, studies indicated that ethylaluminium sesquichloride (EASC) gave the best catalytic results.

Successive replacement of the zirconium alkyl or allyl groups by a halide to give a more acidic metal centre, with the concurrent formation of a polar-binuclear species, were proposed by Attridge as possible steps leading to the formation of the active catalytic species. Attridge[1a] then demonstrated similar results, when a mono-alkylated zirconium species was used in the catalyst mix. Turn over numbers (TONs) were of the order of 13000 (moles ethylene consumed/ mole of Zr complex per hour) with >80% linear α-olefins.

2.2.2. The Addition of Ligands, Formation of Ternary Systems

The choice of ligands is crucial to most catalytic processes and extensive effort is expended in finding the optimum ligand for the catalytic system under study. The same is true for zirconium based oligomerisation systems.

2.2.3. Phosphorous Containing Ligands

A number of phosphorus containing ligands have been examined by Motier[4] who reports propylene oligomerisation using a ternary Zr-P-Al system. A soluble zirconium source is desirable with $Zr(acac)_4$ preferred, however $ZrCl_4$, $Zr(OR)_4$ or a variety of compounds with weak field ligands are described, i.e. other β-diketones or β-ketocarboxylic esters. A trialkyl phosphine (a Lewis base) and an alkylaluminium compound complete the ternary system. Motier proposed a reduced zirconium-phosphine complex, which was formed on the addition of a Lewis acid and a reducing agent to a zirconium-phosphine precursor complex, to be the active species. The Lewis acid and reducing agent may be separate or derived from the same alkylaluminium. A TON of 1900 for the combined C_6-C_9 oligomers was reported with a number of isomers being formed ($Zr(acac)_4$:Ph_3P:EASC of 2:10:25 at 68°C and 10-31 bar). .

The role of the bidentate chelate ligand was not discussed by Motier except in the role as a solubilising agent to aid phosphine complex formation. The use of bidentate phosphines was reported to lead to no catalytic activity.

In a similar system Dzhemilev[5] dimerised and trimerised 1,3-butadienes in the presence of $Zr(OBu)_4$ and triphenylphosphine (TPP).

2.2.4. Sulfur Containing Ligands

Shiraki[6] improved the activity and product distribution of previous binary and ternary catalytic systems and showed that very active catalysts were obtained when the Lewis base contained a sulfur donor atom. In this study various phosphines, amines, sulfur containing ethers and urea were examined. Using thiophene as the preferred Lewis base, linearity of the produced α-olefins increased to >95% with a reduced yield of unwanted waxes ($>C_{30}$ oligomers). The composition and order of mixing of the various components was claimed to be important. TONs of up to 49,000 were reported at 100-120°C and 35 bar of ethylene. A slurry was formed in this system and therefore it is unknown if the active system was homogeneous or heterogeneous.

The importance of the order of mixing and the combination of alkylaluminiums was further examined and extended in a series of patents by Shiraki [7] and co-workers. Altered mixing procedures led to reported TONs of up to 139,000 under the same conditions as indicated above. In a deactivation reaction, it was proposed that excess moisture reacted with $ZrCl_4$ forming Zr-O bonds which decreased the activity of the system. Initially, reacting alkylaluminiums with trace moisture would result in C-Al bond hydrolysis and formation of small amounts of partially hydrolysed alkylaluminiums which were found to be effective co-catalysts (Section 2.5.0). A second effect that was claimed was the formation of zirconium tetrachloride-alkylaluminium coordination species. It was proposed that such species exert an influence on catalytic activity. A mixture of triethylaluminium and diethylaluminium chloride (TEA/DEAC) was reported to give optimum results with initial contact of $ZrCl_4$ with TEA preferred.

Presumably the HCl produced in the deactivation reaction of $ZrCl_4$ with water would further react with alkylaluminiums and produced oligomers in Friedel-Crafts type reactions thereby decreasing product purity, as discussed by Langer (Section 2.2.13), although this was not mentioned.

Further patents by Shiraki[8] and co-workers discuss refinements in the process with regard to wax or ash removal. This process has been commercialised.

2.2.5. Oxygen Containing Ligands

Although soluble zirconium alkoxides or diketonates had previously been used as a zirconium source the role of the alkoxide, diketonate or other deprotonated ligands had not been examined[9] . This is surprising when considering, for example the effect of ligand substituents on catalytic activity in nickel based oligomerisation systems containing β-diketones[10].

In a recent Idemitsu patent Shiraki[11] reported the replacement of thiophene, a soft Lewis base, in favour of an alcohol as the donor ligand. It is claimed that the replacement avoids contamination of the produced oligomers with the added Lewis base. TONs of up to 243,000 are reported at 120°C and 63.7 bar of ethylene. The order of mixing is again regarded as important; a catalyst formed on reacting the alkylaluminium with the $ZrCl_4$ was added to a solvent presaturated with ethylene containing the alcohol. An alkylaluminium mix of EASC:TEA in the ratio of 2:1, with Zr:Al and Zr:alcohol ratios of 1:5 and 2:1 respectively were used. Using this catalytic system the percentage of linear α-olefins was lowered by around 4% compared with thiophene containing catalytic systems. There is no discussion of possible reactive intermediates and therefore it is unknown what reactions occur or if the catalyst is heterogeneous or homogeneous. The addition of the catalyst to a solution containing an alcohol would result in the formation of an ethoxide (aluminium or zirconium) and HCl. The presence of HCl and its effect were not discussed.

Non-protic, oxygen containing donor ligands have been examined by Young[12] who investigated the use of soluble ester adducts of zirconium in catalytic systems. C_6-C_{16} esters of acetic acid were preferred. Young also examined zirconium adducts formed with ketones, ethers, amides, acid chlorides, nitriles and anhydrides.

The reactions were carried out in a continuous flow reactor at 130°C and 70 bar ethylene. Optimised conditions gave TONs for a 1:1 adduct of up to 80,000, at an Zr:Al ratio of 1:14.2 using DEAC as the cocatalyst. Moisture was reported to increase polymer formation and the percentage of linear α-olefins formed was greater than 90%.

Young[13], in a separate paper, reported TONs of 40-80,000 in a continuous flow reactor using catalytic systems containing the above $ZrCl_4$:ester adducts or $Zr(O\text{-}iPr)_4$. DEAC was used as the co-catalyst. When $Zr(O\text{-}iPr)_4$ was the zirconium source, extra DEAC was required to achieve similar activities to those of the ester adducts.

The similar activities of the two systems lead Young to conclude that the ester or the isopropoxide helps to solubilise the zirconium and therefore aid further reactions with the co-catalyst. It was proposed that the ester or isopropoxide were exchanged from the zirconium leaving a complex, possibly polynuclear, of $ZrCl_4$ and the added co-catalyst. The active species contained no added ligand. This suggests a parallel with the work of Attridge (Section 2.2.1) where formation of an ion pair or polar binuclear type species was postulated. Adventitious water reacts with the added co-catalyst (DEAC) to form methylaluminoxane (MAO) type analogues giving a greater charge separation in the active species and therefore, according to Young, a higher Lewis acidity at the metal centre promoting polymerisation. It was claimed by Young that this concurs with work reported by Eisch and Jordan, discussed in detail in Section 2.4.2. In this proposed mechanism there is no role for the added ligand in the active species.

A later patent by Young[14] has extended this work to include higher olefins, such as propylene, 1-decene, 1-tetradecene and 1-hexadecene.

Mathys[15], using the same catalytic systems as Young, showed that the inclusion of small amounts of oxygen in the feed stream led to increased yields of linear α-olefins, with the percentage of non-linear olefins reduced by up to 50%. However the overall reactivities are reduced, with TONs decreasing from 731,000 to 305,000 at 170°C and 180 bar.

The addition of a second oxygen donor ligand to these systems lead to reduced activity, as has been investigated by Chauvin[16] using $Zr(O\text{-}R)_4$, R=C_2-C_8, in the presence of THF. Ethylene was oligomerised at 75°C and 4 MPa with TONs of up to 7,051 at a Zr:Al:THF of 1:5:2.

2.2.6. Nitrogen Containing Ligands

In addition to the inclusion and examination of nitrogen containing ligands in the above studies, an active nitrogen containing oligomerisation system containing MCl_4 /EASC, M = Zr or Hf, has been described by Doyle[17]. Oligomerisation occurs in the presence of an electron rich N-substituted olefin such as a tetra-substituted biimidazolidinylidene (Figure 2.1). TONs of up to 33,000 were achieved at 100°C and 30 bar with >90% linear α-olefins.

Figure 2.1.
Tetra-Substituted Biimidazolidinylidene

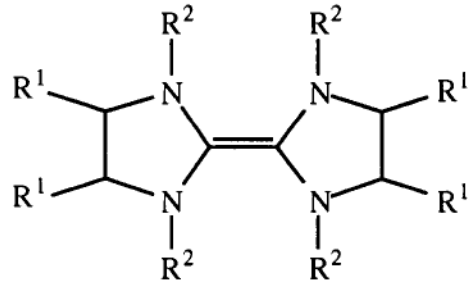

R^1, R^2 = alkyl, H, Phenyl

2.2.7. Effect of Side Reactions on Product Purity

Langer[9] in a series of patents examined complexes of the form $M(OR)_{4-n}Cl_n$, where M= Ti, Zr or Hf (Zr was preferred), n=0-4 and -OR= alkoxide, phenoxide, carboxylate or diketonate, in the oligomerisation of ethylene. TONs of up to 15,250 were reported in the presence of a cocatalyst; R_2AlOR', $R_2AlNR_2"$, R_2Zn or other alkylaluminium chlorides. No third component was present.

In these patents Langer discussed the role of side reactions in decreasing product purity, especially reactions which arose whilst deactivating the oligomerisation catalyst. Langer stated that it was essential to deactivate not only the oligomerisation catalyst, but also to remove any Friedel-Crafts activity. Due to the strong Lewis acidity of the cocatalyst, the addition of any protic reagent can promote Friedel-Crafts type reactions, such as alkylation, cationic polymerisation or isomerisation.

These side reactions decrease the purity of the produced oligomers and are therefore unwanted (Reactions 2.1-3).

Initiation

$ZrCl_4 + ROH \longrightarrow ZrCl_3OR + HCl$ [2.1a.]

$R_nAlCl_{3-n} + HCl \longrightarrow R_nAlCl_{4-n}^- + H^+$ [2.1b.]

Deactivation

$R_nAlCl_{3-n} + HCl \longrightarrow R_{n-1}AlCl_{4-n} + R\text{-}H$ [2.2a.]

$R_nAlCl_{3-n} + HL \longrightarrow R_{n-1}LAlCl_{3-n} + H\text{-}R$ [2.2b.]

Isomerisation

$R'\text{-}CH{=}CH_2 + H^+ \longrightarrow R'CH^+\text{-}CH_3$ [2.3a.]

Friedel-Crafts Alkylation

$R^+ + C_6H_5CH_3 \longrightarrow R\text{-}C_6H_4CH_3 + H^+$ [2.3b.]

In the presence of an olefin the reactions [2.2a] and [2.3a.] would be competing. Reaction [2.3a] results in the formation of a carbocation and therefore isomerisation. Cationic polymerisation and Friedel-Crafts alkylation [2.3b.] are also possible[18]. These side reactions can be avoided by reacting any protic reagent with the alkylaluminium before oligomerisation, thereby forming an alkane [2.2b.][19], or by an appropriate pre-conditioning time to allow reaction [2.2a] to go to completion. On deactivating the catalytic system it is important to use conditions, low temperature and an aqueous or alcoholic alkali solution, that do not promote these Lewis acid catalysed side reactions. Langer claimed that if a catalytic solution was exposed to air at room temperature after catalysis, there was almost complete isomerisation to internal olefins after 1 hour. If an aromatic solvent was used then Friedel-Crafts alkylation of an aromatic solvent occurred.

The addition of salts of long chain fatty acids to $ZrCl_4$/EASC catalyst solutions has been shown by Fries[20] to give oligomerisation without the deactivation problems mentioned above; calcium stearate was preferred. Fries claims that the system was effective due to the formation of a homogeneous catalytic system and that any generated chloride ions were complexed by calcium. This avoided HCl formation and therefore the formation of Friedel-Crafts type catalysts with associated side reactions as described by Langer[9]. TONs of up to 2,880 at 75°C and 11.2 bar were achieved for a Zr:Al of 1:10 and Zr:L of 1:2. Fries has also shown that a titanium

catalyst can be directly added to this system allowing copolymerisation without prior product separation in the same autoclave; ethylene and propylene were studied.

2.2.8. Bis-Cyclopentadienylzirconium based Oligomerisation Systems

Recently two new systems have been reported which oligomerise olefins. These are best described as being atypical or novel and their examination may indicate mechanistic pathways for oligomerisation reactions.

In a recent patent Watanabe[21] at Idemitsu has examined the oligomerisation of propylene with bis-Cp* zirconium and hafnium complexes, Cp* = pentamethyl-cyclopentadienyl, in the presence of MAO giving TONs of up to 104,000. In the presence of H_2, TONs of up to 323,000 were reported. In this example hydro-oligomerisation did not occur and the added H_2 did not become incorporated into the produced terminal olefins. The activity was improved by the addition of an electron donating ligand, such as ethyl-benzoate. Less substituted cyclopentadienyl rings, such as tetramethyl- or tetraethylcyclopentadienyl, led to polymerisation. The patent made no reference to ethylene reactivity or a possible mechanism.

A patent with exciting implications by Slaugh[22] described the oligomerisation of ethylene or co-oligomerisation of ethylene with C_3-C_{10} α-olefins in the presence of Cp_2ZrCl_2 and a mixed MAO/EAO cocatalyst. Since Kaminsky's pioneering work into the formation of methylaluminoxanes (MAO), and their use as cocatalysts with bis Cp-zirconium catalysts in the polymerisation of olefins, an intensive effort has been directed into understanding this polymerisation chemistry, especially in regard to stereospecific synthesis (discussed in detail in Section 2.5.0). Although this work by Slaugh was the first example of ethylene oligomerisation, Watanabe had previously oligomerised propylene using a similar catalytic system. .

Slaugh reported TONs of about 100 at 100-120^{o}C and 14 bar of ethylene with this novel system which was significantly less than those for non-Cp based systems. The Zr:Al ratio of 1:1 is considerably less than the typical 1:>1000 ratios used in polymerisation chemistry. An optimum mix of 2:1 EAO:MAO was indicated. Possible reasons for the change in behaviour will be addressed in the discussion (Section 2.8.0). Slaugh did not discuss possible active species or mechanism. Addition of a small excess of MAO-EAO rapidly leads to the formation of higher oligomers, higher activities and an increase in isomerisation (Table 2.1).

Table 2.1.
Ethylene Oligomerisation using a Cp_2ZrCl_2 / MAO/EAO System
Effect of Higher Zr:Al Ratio.

Ratio Zr:Al	Zr mmol	Yield g	C_4-C_{18} %	$>C_{20}$ %	% Linear α-olefin
3:2	3	13.2	80.3	19.7	91.0
1:8	1	13.9	69.0	31.0	58.4

2.3.0. Discussion

In all the previously presented work on zirconium catalysed ethylene oligomerisation, with *in situ* catalyst formation, there has been no detailed discussion of reaction mechanisms or formation of active species except for the initial work by Attridge, in which an ion pair or polar binuclear species was postulated. Young supported this proposed species and also discussed the relevant role of titanium(IV) in titanium based oligomerisation chemistry (only soluble, unreduced titanium(IV) species oligomerise olefins). Motier, on the other hand, has indicated that a combined Lewis acid/reducing agent is required for oligomerisation but does not indicate the oxidation state of zirconium in these systems or show that it is not zirconium IV.

The role of the added ligand is uncertain with a vast number of ligands having been used in active oligomerisation systems but without mention, except by Young, of their role. According to Young the ligands act only as solubilising agents allowing rapid interaction of the $ZrCl_4$ with the added cocatalyst, a proposal based on the similar reactivities of his $ZrCl_4$:ester adducts and $Zr(O\text{-}iPr)_4$ with Attridge's $ZrBz_4$ systems. Presumably complexed ligands are lost through ligand transfer with the cocatalyst to form the required active intermediate. Under such circumstances the reasons for not investigating the role of ligands further, especially those that can act as bidentate chelate ligands (i.e. acac-(active) and a diphosphine(inactive)) can easily be understood as they would play no role in the active species.

Only one study has attempted to clarify the understanding of zirconium based oligomerisation systems. In a series of papers, Sigwalt[23] investigated parameters

affecting the oligomerisation of 1-hexene. Mechanistic aspects are also discussed. From a restricted range of starting materials M = Ti, Zr; M-R(R=-Cp, -Me, -Bz, -O-nPr or -O*i*Pr); $AlEt_2X$(X=Et, -Cl, -OR, $-OCOCH_3$), a system comprising $Zr(O\text{-}nPr)_4$ and $AlEt_2Cl$ was found to give the best activated catalyst for 1-hexene oligomerisation. An optimal Zr:Al ratio of 1:12-15 was found with no reactivity for values less than 1:4.

The unidentified active species, formed on mixing $Zr(O\text{-}nPr)_4$ and $AlEt_2Cl$, degrades quickly in the absence of monomer showing 35% drop in activity after 1.5 hours. Solvent polarity has a dramatic effect on reactivity with faster rates in polar solvents, although the product distribution remains the same. Increased rates are also observed at higher temperatures, again with no change in product distribution.

In contrast to the prevailing thoughts for Ziegler-Natta polymerisation / oligomerisation systems, Sigwalt proposed a greater role for aluminium in "zirconium mediated aluminium oligomerisation reactions" (Figure 2.2).

Figure 2.2.

a. insertion into a Zr-alkyl bond

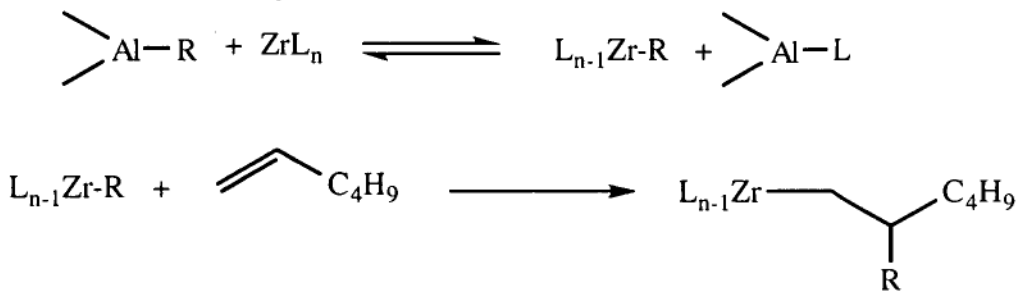

b. insertion into a zirconium activated Al-alkyl

Based on detailed product analysis, deactivation product analysis, NMR, cryometric and EPR studies, Sigwalt proposed that aluminium could be the active centre at which olefin insertion occurs. The transition metal modifies this environment to allow these reactions to occur under mild conditions. Results indicated:

i. all the aluminium alkyl groups are transferred to product olefins;
ii. long chain alkanes produced on catalyst deactivation (methanolysis) are in excess of the maximum 4:1 ratio possible for alkylated zirconium species indicating at least some alkanes originate from R-Al bonds;
iii. stability of oligomerisation intermediates in the absence of monomer indicating that β-H elimination is not a prominent decomposition pathway;
iv. NMR indicates complete interaction of the Zr and Al species up to the 1:10 ratio when all peaks are shifted upfield in the proton spectra;
v. EPR indicates the possibility of a reduced zirconium species at an Zr:Al ratio of greater than 1:5, i.e. when the species is active for oligomerisation.

The indication of a reduced species is consistent with Motier's need for a reducing agent while alkyl group transfer to aluminium is known (Section 2.4.11). The possible role of aluminium as the central metal is interesting as alkylaluminiums are themselves active oligomerisation catalysts under more severe conditions[24] and their behaviour could be modified by the interactions with a second metal.

It is seen that there is no commonly accepted theory for the zirconium catalysed oligomerisation of ethylene, although it is often assumed that a Ziegler type mechanism is valid. There is no agreement on the central metal, its oxidation state or the role of the added ligands in these catalytic systems. With this in mind it is difficult to develop better oligomerisation catalysts without a better understanding of the basic processes involved. Assuming a parallel in chemistry between oligomerisation and polymerisation chemistry, the latter has been examined in an effort to propose possible intermediates and examine possible steric and electronic effects in oligomerisation chemistry.

2.4.0. Steric and Electronic Effects in Ethylene Polymerisation

2.4.1. Active Species for Olefin Polymerisation

Since the initial work by Ziegler and Natta[25] the active species directly responsible for catalysis has been sought. In the presence of an alkyl aluminium or alkyl aluminium chloride the transition metal halide was thought to be alkylated with subsequent formation of an ion pair or polar binuclear species, the proposed active species. Solvent effects[26], faster polymerisation in polar solvents, and

electrodialysis[27] supported this theory. The isolation of catalytically active cationic species was therefore a major focus in fundamental studies into polymerisation mechanisms.

2.4.2. Isolation of Catalytically Active Cationic Complexes

It was found that on reaction of Cp_2TiCl_2 with an alkyl aluminium a binuclear complex was formed[28] (Figure 2.3a). Long[29] and Fink[30] have shown, by UV and kinetic studies respectively, that **2** is not the active catalyst and that two equilibria are required to explain the kinetic results. Evidence for the existence of the ion pair / polar binuclear species **3** was supplied by Eisch[28] who used trimethyl(phenyl-ethynyl)silane to trap the cationic intermediate with the subsequent isolation of a single product, **4**, (Figure 2.3b).

Figure 2.3a.

Proposed Interactions of Cp_2TiCl_2 and CH_3AlCl_2

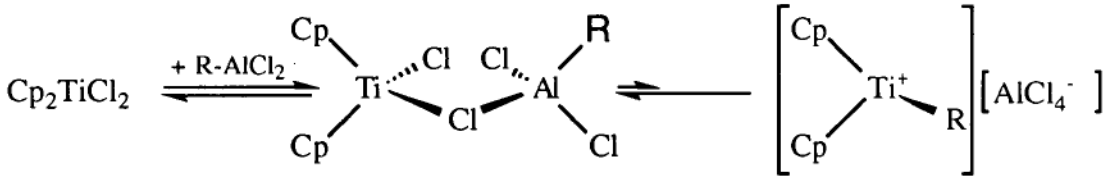

1 **2** **3**

Figure 2.3b.

Trapping of Cationic Titanium Intermediate.

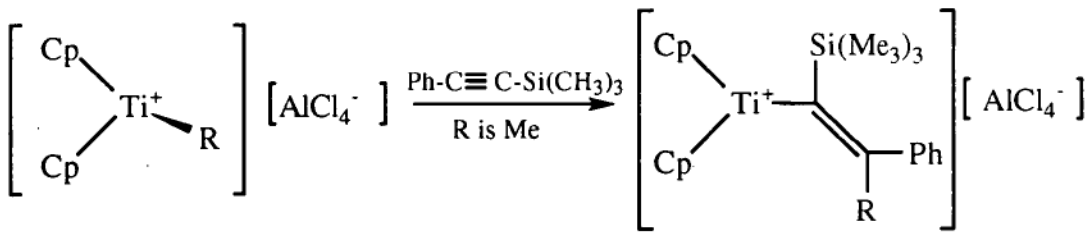

3 **4**

For the complex **4** the Ti-C-Si atoms lie in the same plane indicating possible hyper-conjugation.

Later ^{1}H-NMR studies by Eisch[31] gave the first spectral evidence for ion pairs in the $Cp_2TiCl(CH_2CMe_3)$ /$AlCl_3$ system (Figure 2.4). ^{1}H-NMR signals for the methylene CH_2 group shift downfield as would be expected for an increase in Lewis acidity at

the metal centre and hyperconjugation. This effect is dependent on solvent polarity and in donor solvents the NMR peaks are shifted upfield. When R = Cl, the formation of $AlCl_4^-$ was observed in solution (^{27}Al-NMR in 1,2-dichloroethane).

Figure 2.4.
Formation of Cationic Titanium Polymerisation Catalysts.

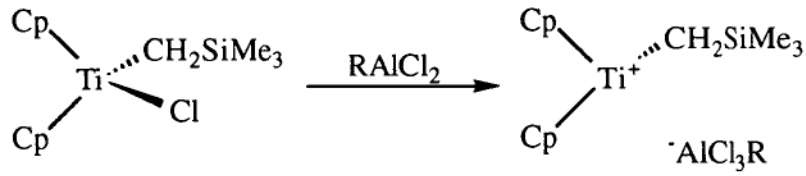

Where R = Me, Cl

The cationic species formed (Figure 2.4.) gave a homogeneous catalyst for ethylene polymerisation in 1,2-dichloroethane with $AlCl_3$ or $MeAlCl_2$. The silyl groups are incorporated into the polymer chain giving direct evidence for cationic titanium species as active ethylene polymerisation catalysts.

Concurrently, Gaudet[32] isolated the analogous zirconium complex, $[Cp_2ZrCl][AlCl_4]$. The crystal structure was determined but the complex was not tested for catalytic activity.

2.4.3. Cationic Zirconium Complexes

Concurrently with advances in the theory of polymerisation, Jordan[33] generated cationic zirconium complexes for the polymerisation of olefins which were active in the absence of cocatalysts. Although the Cp_2ZrMe^+ fragment was previously known[34], Jordan[33a] was interested in this mononuclear, cationic species with non-coordinating anions for catalysis. Initial complexes, synthesised in the presence of strong coordinating ligands, such as CH_3CN, by halide abstraction were found to be unstable (Reaction 2.5). Decomposition occurred in solution by fluoride abstraction from the counter ion, PF_6^- (Reaction 2.6). Stable complexes were formed in the presence of tetraphenyl borate, a non-coordinating anion.

These cationic complexes readily insert unsaturated molecules, i.e. CO, nitriles or ketones, into the Zr-Me bond at rates far exceeding those of dimethylzirconocene, Cp_2ZrMe_2. The cationic complex was described as a hard, strong Lewis acid. The

THF adduct (Figure 2.5.) has been shown to polymerise ethylene under mild conditions in NMR experiments. The presence of a Lewis base competes with ethylene slowing down reaction rates, as indicated by NMR experiments with excess THF.

$$Cp_2ZrMeX + M[PF_6] \longrightarrow Cp_2ZrMeL]^+ PF_6]^- + MX \qquad [2.5]$$

M=Ag, X=Cl, L= CH_3CN
M=Tl, X=I, L= CH_3CN

$$Cp_2ZrMe^+ PF_6^- \longrightarrow Cp_2ZrMeF + PF_5 \qquad [2.6]$$

Lewis base free, cationic complexes generated *in situ* by Jordan are very active polymerisation catalysts, as indicated by NMR studies in CD_2Cl_2. In the absence of a coordinating ligand (or another Lewis base), the transient cationic species decomposed to $Cp_2ZrMeCl$, presumably via halide abstraction from the solvent.

Figure 2.5.
Jordan's Cationic Complex.

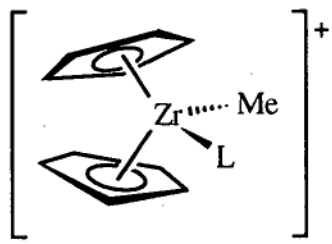

$[BPh_4]^-$

L = THF, CH_3CN, PMe_3

The benzyl group, Bz, due to its ability to coordinate in a η^2- fashion[35], allowed the free cationic species to be observed in solution by ^{1}H-NMR in CD_2Cl_2[33c,d]. When the coordinating ligand (L) is CH_3CN, no ethylene polymerisation was observed but in the presence of THF ethylene was polymerised. It was proposed that ligand dissociation was a prerequisite for ethylene insertion and the presence of the η^2-bound benzyl group allowed a greater concentration of the cationic complex free of Lewis base. Two competing reactions then could occur, ethylene insertion or ligand complexation. The rate determining step was thought to be the η^2- to η^1-benzyl group rearrangement (Figure 2.6.) as no intermediate was observed in NMR experiments. When CH_3CN is present a stable complex forms irreversibly and the

η^2-bound species is not observed in the NMR. In these studies Cp analogues, such as Cp' (C_5H_4Me-), have been used due to their higher solubility.

Figure 2.6.
Cationic Zr-Bz Complexes as Ethylene Polymerisation Catalysts

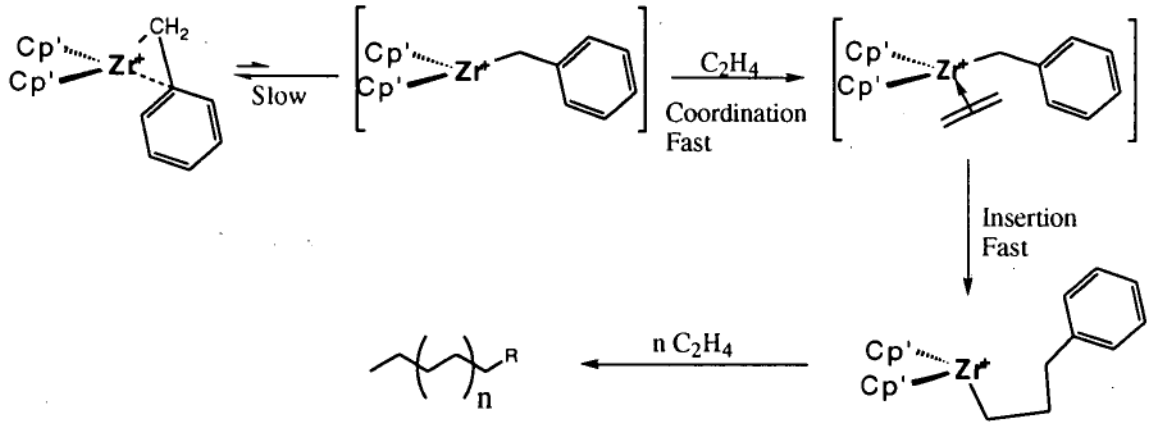

Hydrogen addition allowed control of polymer weight, i.e. hydro-oligomerisation. Jordan[33d] proposed that hydrogen reacted with the active complex cleaving the bond between the metal and the growing polymer. The hydride thus formed was then active in further polymerisation reactions. There was no reaction of hydrogen with eighteen electron complexes of zirconium with chelating ligands or the cationic complexes, $Cp_2ZrMe(dmpe)]^+$ or $Cp_2ZrMe(NCCH_3)]^+$. Hydrogen reacts slowly with $Cp_2ZrMe(THF)]^+$ in THF but much more rapidly in CH_2Cl_2. With PMe_3 as the ligand, the reaction rate with hydrogen is approximately 10^5-fold faster.

Jordan interpreted these results as indicating the need for a low lying empty metal orbital with which the H_2 can interact. When two low lying orbitals are available the reaction rate is much faster, i.e. after ligand dissociation to give a base free cationic zirconium complex, $Cp_2ZrMe]^+$ in CH_2Cl_2 or when the coordinating ligand has no available p-orbitals for Zr-L π-interactions, as for PMe_3. The cationic metal hydrides, which have been characterised, are also polymerisation catalysts and readily insert alkenes, alkynes or nitriles[33e]. The presence of these LUMO's are important for β-agostic interactions which will be discussed in Section 2.7.0.

Jordan[33f,g] has examined in detail the insertion chemistry of cationic bis-Cp zirconium complexes (cationic zirconocenes) and more recently cationic mono-Cp

zirconium complexes, $CpZrR_2L]^+$, although polymerisation has not been reported to date for these more recent complexes. Jordan has also replaced one Cp ligand in the bis-Cp complex with a divalent dicarbollide ligand resulting in a neutral, isostructural analogue of a cationic bis-Cp zirconium complex (Figure 2.7). The dicarbollide complex is an active polymerisation catalyst.

Figure 2.7.
Dicarbollide Analogues of bis-Cp Zirconium Complexes.

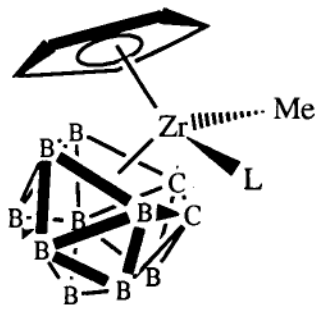

The restricting factor in the majority of Jordan's work has been the influence of the coordinating solvent. Jordan has shown that in the absence of coordinating solvent catalyst reaction rates are much higher, but without such solvents the catalyst was unstable[33]. The nature of the coordinating ligand or solvent dominates, with strongly coordinating ligands or π-bonding ligands increasing complex stability but decreasing catalysis rates.

Figure 2.8.
Comparison of work by Jordan and Taube.

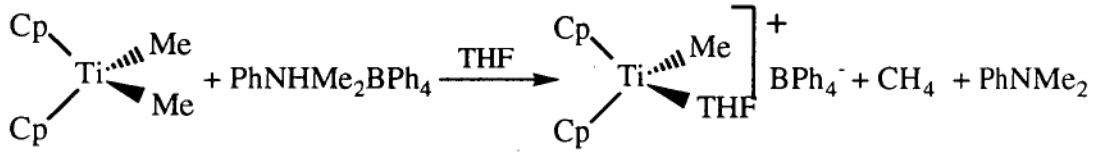

Taube

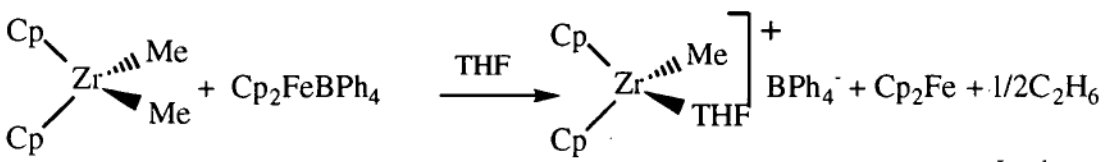

Jordan

Taube[36] has also shown that the analogous titanium complexes, $Cp_2TiMe(THF)]^+$, prepared by partial protolysis of dimethyltitanocene with N,N-dimethylanilinium tetraphenylborate, are active polymerisation catalysts (Figure 2.8). Previously prepared complexes with a coordinating nitrile or pyridine had not reacted with ethylene.

2.4.4. Coordinated Lewis Base Influences on Polymerisation Activity

The nature of the coordinating ligand was further examined by Teuben[37] who examined THF and THT in cationic mono-methylated metallocene complexes of titanium, zirconium and hafnium, $Cp^*_2MMeL]^+$ (L=THF, THT; M=Ti, Zr, Hf; Cp^*=-C_5Me_5). As found by Jordan and Bochmann[38], hard Lewis bases tended to coordinate strongly and catalysis was slow or was not observed. It was claimed that THT, being a soft weak Lewis base, allowed for easier dissociation to give *in situ* the Lewis base free cationic d^0,14-electron species and increased catalytic rates. Similar solubility and decomposition pathways were found, as already stated by Jordan, for the THF analogues. N,N-dimethylaniline and anisole were acceptable solvents for catalytic work. Strong Lewis bases, such as THF, PMe_3 or 2-Me-THF, rapidly replace coordinated THT.

The bis-Cp* titanium complexes prepared by Teuben were found to have no catalytic activity under the conditions tested or for the olefins tested (ethylene, propylene, butene, hexene, styrene and 1,3-butadiene) by comparison to Taube's cationic bis-Cp titanium d^0, 14-electron complexes. The difference in activity was explained in terms of weaker Lewis acidity at the metal centre due to the two Cp* ligands, which increase electron density at the metal centre[39], as shown in previous studies. However, steric factors due to the bulky Cp*, limiting monomer approach, could not be excluded.

Teuben reported that the cationic Zr/Hf-THT complexes, both having similar activities, polymerised ethylene under the mild conditions of room temperature and 1 bar of ethylene with a TON of 1900. This was considerably more active than TONs reported by Jordan from NMR studies, and equally as active as other propylene oligomerisation catalysts, discussed in the next Section. It is proposed that under the test conditions the complex was essentially fully dissociated.

In one of the few reports of olefin oligomerisation with cationic bis-Cp metallocene complexes Teuben, using this catalyst system, oligomerised propylene. The hafnium complex had a slightly higher activity and simpler product distribution (Table 2.2).

Table 2.2.
Propylene Oligomerisation with $Cp^*_2MMe(THT)]^+ BPh_4]^-$

Metal	M=Zr	M=Hf
Activity (TON)	150	370
Distribution		
4-methyl-1-pentene	36%	72%
4,6-dimethyl-1-heptene	28%	24%
C_{12}-C_{24}	31%	
minor products (isobutene,1-pentene)	05%	04%

Figure 2.9
Proposed Catalytic Cycle for Propylene Oligomerisation
with $[Cp_2MMe(THT)][BPh_4]$, M = Zr, Hf
(Product distribution for double insertion shown.)

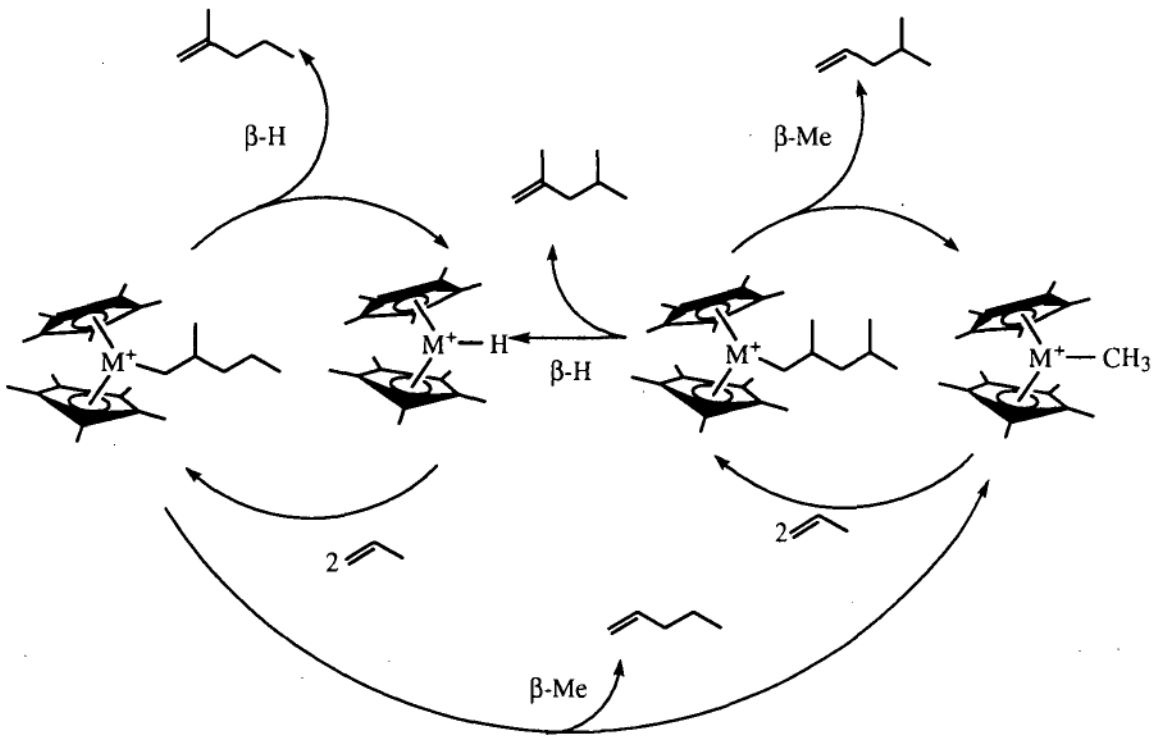

The results indicated a regular 1,2 olefin insertion but that the dominant termination mechanism was β-methyl transfer (Figure 2.9). This was the same mechanism as suggested by Watanabe[21] (Section 2.2.16) and can be explained purely on steric grounds, where the lowest energy elimination pathway has the oligomer β-methyl lying between the two Cp*'s . Trace amounts of product formed by β-hydrogen elimination were also observed.

For higher olefins CH_4 was generated, indicating C–H activation, however no oligomers were formed. Teuben postulated formation of a zwitterionic complex through metallation of one phenyl of the $BPh_4]^-$ counter-ion.

2.4.5. Effect of the Anion.

While the above research was being carried out, the role of the anion was also under investigation due to its observed influence on catalytic rates[40]. Bochmann reacted tetrabenzyl zirconium, $ZrBz_4$, with N,N-dimethylanilinium tetraphenylborate, $[PhNHMe_2][BPh_4]$, to form a cationic zirconium complex. ^1H and ^{13}C-NMR studies indicated a zwitterionic complex, with η^6-arene bonding of one of the borate phenyl groups (Figure 2.10). At room temperature the phenyls freely exchange whereas at low temperature, <-50°C, a single isomer is observed by NMR. This complex was reported to be inactive for ethylene polymerisation under mild conditions, room temperature and 1 bar ethylene in NMR studies.

Figure 2.10.

Reaction to Form the Zwitterionic Bochmann complex.

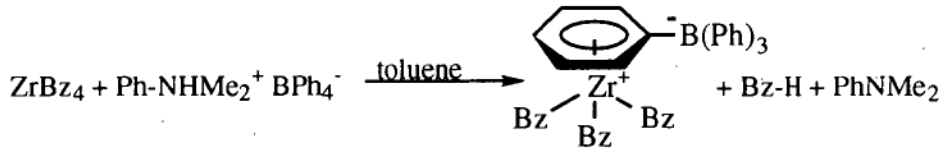

The corresponding titanium complex could not be isolated under similar conditions however the Lewis base adduct of the methylated mono-Cp analogue, $CpMMe_3$, (M=Ti, Zr, Hf), reacted to form $[CpMMe_2(L)][BPh_4]$ (L=THF).

In studying the bis-Cp versions of this chemistry Bochmann had argued for complex interactions between anion, ligand (amine) and solvent (Figure 2.11). The relative equilibrium positions are therefore determined by metal centre Lewis acidity,

solvent, anion and ligand (Lewis base). In the presence of an olefin the equilibria would be even more complicated.

Figure 2.11.
Equilibria in the $CpMMe_2(L)]^+BPh_4]^-$/solvent/olefin system

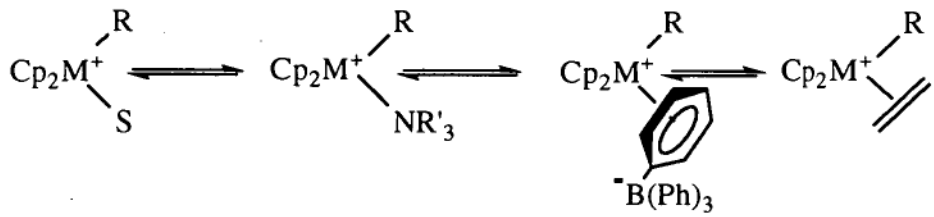

1 **2** **3** **4**

When any complex **1** to **3** predominates in solution the catalytic activity will be effected, as has been shown by Jordan in the presence of THF (Section 2.4.10). Bochmann stated that anion coordination led to competing reactions with alternate decomposition pathways. Alternative η^3- and η^6- π-arene interactions or metallation of the phenyl ring have also been reported in the literature[41,42].

2.4.6. Cationic, Base-Free Complexes with Non-Coordinating Anions

Interactions of the added anion with the highly Lewis acidic metal centre led to unwanted reactions or reduction of the catalytic activity, such as halide abstraction with PF_6^- (Jordan) or π-arene complexation (Bochmann). The preparative method has influenced possible approaches, for example, Jordan has concentrated on 1 electron reducing agents or halide abstraction reagents which necessitated the use of polar solvents, resulting in ligand coordination to the Lewis acidic metal centre.

A number of solutions have been put forward to reduce unwanted interactions. Bochmann decreased problems due to amine coordination from ammonium salts by the use of trityl tetraphenylborate, $[Ph_3C][BPh_4]$. Anion coordination problems have been decreased by the use of perfluorinated analogues of tetraphenylborate. Some examples include $[Ph_3C][B(C_6F_5)_4]$ and $[PhNEt_2H][B(C_6F_5)_4]$ (Bochman[33c,e]), $[Ph_3C][B(C_6F_5)_4]$ (Chien[43]), $[PhNEt_2H][B(4\text{-}FC_6H_4)_4]$ which coordinates through F (Horton[44]), $[Ph_3C][B(3,5\text{-}CF_3C_6H_3)_4]$ (Bahr[45]), $B(C_6F_5)_3$ (Pellecchia[46] and Marks[47]), or with metallocarboranes $(C_2B_9H_{11})_2M]^-$ (M=Fe, Co, Ni) (Hlatky[48]).

2.4.7. Polymerisation Activity of Cationic Base-Free Complexes with Non-Coordinating Anions

The use of 'non-coordinating' anions has lead to polymerisation systems which are highly active under mild conditions. Hlatky[48] polymerised ethylene and copolymerised an ethylene/1-butene mix at 6.2 bar and 60°C with TONs of up to 14,000.

Bochmann[40e] compared ethylene polymerisation activities of $[Cp_2ZrBz][B(C_6F_5)_4]$, $[CpZrBz_2][B(C_6F_5)_4]$ and $[ZrBz_3][B(C_6F_5)_4]$ formed by the reaction of the alkylated zirconium complex with $[Ph_3C][B(C_6F_5)_4]$ (Reaction 2.7). Substituted Cp ligands or *ansa*-metallocenes (bridged Cp ligands) were also tested. The reactivity was dependent on the ligand substitution pattern with bis-Cp > mono-Cp > Cp-free, giving TONs of 1393; 821; 3.5 at 60°C and 1 bar ethylene. The highest activities however were reported for the *ansa*-metallocenes (i.e. Cp_2 = ethylene-bis-(tetrahydoindenyl)- or fluorenyl benzene) with TONs up to 607,142. These reactivities are similar to the Cp_2ZrX_2/MAO systems and will be discussed more fully in Section 2.5.0.

Reaction 7

Formation of Cationic Zirconium Complexes with Perfluorinated Anions.

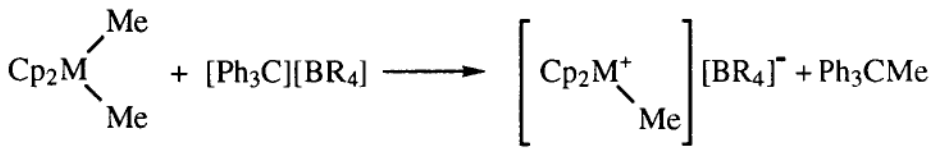

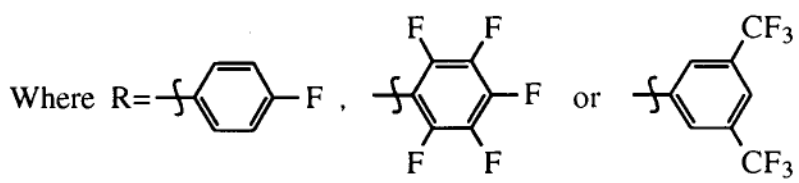

Using the same catalytic systems, temperature related variations in the relative rates of propylene polymerisation were observed for ethylene-bis(tetrahydroindenyl)-zirconium complexes, $(EBTHI)ZrR^{]+}$, where R=Me or Bz. Maximum activity occurs for $(EBTHI)ZrMe^{]+}$ at -20°C, for $(EBTHI)ZrBz^{]+}$ at 60°C and for the $(EBTHI)ZrCl_2$/MAO system at 60°C. Respective activities are 0.82, 21.53 and 12.5×10^6g of polypropylene/[(mole of Zr^+).(C_3H_6).h)],. The increased stability (lower activity) of the Zr-Bz complex is explained by η^2- bonding of the benzyl

ligand to the electron deficient metal centre. Polymerisation is only possible after a η^2- to η^1- rearrangement as previously discussed in Section 2.4.5.

A novel reaction in the synthesis of cationic zirconium complexes for olefin polymerisation is the direct reaction of a substituted zirconium complex with trialkyl/phenylborine. Alkyl transfer takes place to give the required cationic complex[46] (Reaction 2.8). The cationic species are active polymerisation catalysts. However when n=0 and R=Bz it has been shown that after alkyl transfer the benzyl ligand remains η^6-, π-arene coordinated, as in the systems already described by Bochmann[40]. When n=2 and R=H then a weak anion coordination is seen through two neighbouring fluorine atoms on one of the anion's phenyl groups. The lack of interaction through the transferred hydrogen atom is due to unfavourable steric interactions.

Reaction 2.8.

Formation of Cationic Zirconium Complexes through Alkyl Transfer

$$Cp_nZrR_{4-n} + B(C_6H_5)_3 \longrightarrow [Cp_nZrR_{3-n}][RB(C_6H_5)_3]$$

n=0-2, R=H, Me, Bz

The role of cationic zirconium complexes in the polymerisation of olefins has been strongly supported by this recent work with cocatalyst free cationic zirconium systems. They can now be synthesised free of coordinating ligands and relatively free of anion interactions. These complexes have also been shown to reversibly insert olefins and single insertion products have been isolated[49]. The versatility of these systems is shown not only in their polymerisation chemistry but also through their use in organic synthesis[50] with recent examples of stereoselective synthesis[51].

2.5.0. Aluminoxane Systems

In the early eighties Kaminsky[52] developed extremely active polymerisation catalysts using Cp_2ZrX_2/methylaluminoxane(MAO) systems. The field quickly became the centre of intense research interest when it was found that the use of chiral zirconocene type complexes could lead to highly stereospecific polymerisation of propylene or higher olefins at very high activities (TONs up to 183,000 at 60°C and 1 bar)[53]. These activities have only recently been equalled or bettered with the

cationic, base free zirconium complexes discussed in the previous section. Polymer molecular weights were controlled by temperature variation, shorter chain length at higher temperature or by addition of hydrogen[53b]. Typical precursor complexes are shown in Figure 2.12.

Figure 2.12.
Zirconocene Complexes
used in Zirconocene/MAO Polymerisation Systems.

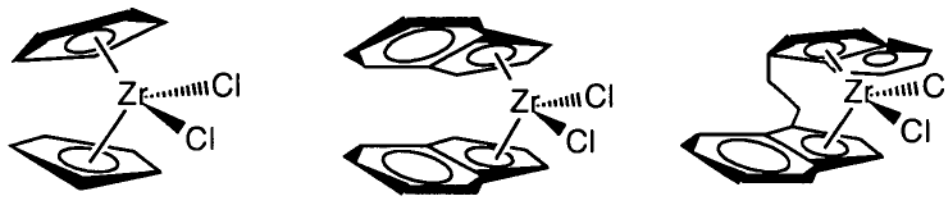

Recent focus has been on developing these new catalytic systems and has been paralleled by the development of new cationic species. It is only recently that the two areas of research have crossed paths with the development of cationic, cocatalyst free complexes to be used in applications developed from the Cp_2ZrX_2/MAO research. The assumption of a common, but as yet unidentified, active species appears to have been born out and is thought to be the cationic metal hydride.

Commercialisation of zirconocene based polymerisation systems has been reported. It is believed that these processes are based on substituted-Cp or bis-Cp-zirconium chloride/MAO type systems[54], or chiral analogues for the stereospecific synthesis of polypropylene.

A number of studies using these Cp_2ZrX_2/MAO systems have examined the effect on polymerisation activities and polymer molecular weights via changes to the steric and electronic nature of the ligands. Assuming a common mechanism for polymerisation and oligomerisation, these studies are considered to be directly relevant to the formation of active species in zirconium based oligomerisation chemistry and are discussed in this section. The oligomerisation of ethylene and propylene by Watanabe[21] and Slaugh[22], using Cp_2ZrX_2/MAO/EAO systems, has already been mentioned.

2.5.1. Nature of Methylaluminoxane (MAO)

The structure of MAO, formed by the controlled hydrolysis of trimethylaluminium, is not fully known. It is believed to be a complex mixture of linear and cyclic oligomers of the general form shown in Figure 2.13[55].

Figure 2.13.
Proposed Structure of MAO.

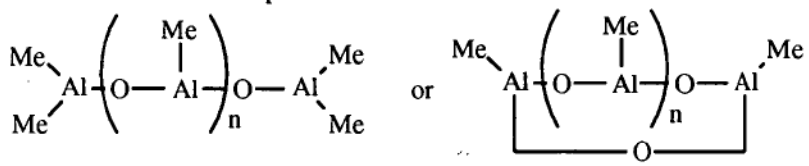

In polymerisation reactions a large excess of MAO is generally required with a Zr:Al ratio between 1:2,000 and 1:4,000. It is believed that the produced active species is a cationic, 14-electron, d^0 zirconium complex similar to those discussed in the previous section. The role of MAO is then similar to that of an alkylaluminium, with initial complexation, halide abstraction and metal alkylation. The improved activity of MAO systems over Cp_2ZrX_2/alkylaluminium systems then resulted from the ability of MAO to solvate and support the resulting ion pair, especially in non polar solvents, resulting in a high concentration of the free cationic zirconium species. In extensive NMR studies Kaminsky has followed the complicated series of reactions resulting from mixing Cp_2ZrX_2 with MAO, consequently proposing a zirconium-oxygen ion pair (Figure 2.14.) as the dominant species before the introduction of an olefin. The Zr-O-Al bond is either highly polar or forms an ion pair resulting in a high Lewis acidity at the metal centre.

Figure 2.14.
Proposed Species formed on mixing
$Cp_2ZrX_2$and MAO

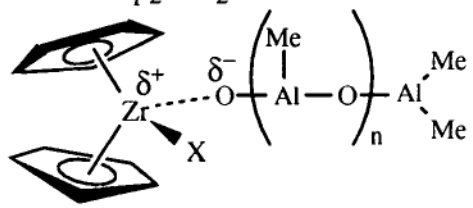

Kaminsky also states that this is a simplified picture. EXAFS measurements indicated that, when using an excess of MAO, the active species appears to be at the centre of a cluster containing one or more MAO chains[55,56].

Kaminsky[57] has oligomerised ethylene and 1-butene using (EBTHI)ZrX_2 (X=0-acetyl-(R)mandelate) with MAO. The mandelate complex was used because it was more easily purified and was shown to have a similar activity to the dichloride. The resulting oligomers were formed by 1,2 insertion into the Zr-R bond with termination by β-H elimination. This work is comparable to that of Teuben[37] (Section 2.4.10.) using the cationic zirconium complex, $[Cp^*_2ZrMe(THT)][BPh_4]$, where the dominant termination path was via β-Me transfer. Kaminsky uses, as did Slaugh and Watanabe, a low Zr:Al ratio of around 1:1, a high catalyst concentration and low monomer concentration to promote oligomerisation.

In these papers the termination step (β-hydride elimination or β-methyl transfer) appears to be dependent on the degree of cyclopentadienyl or indenyl substitution and therefore on the electrophilicity of the metal centre or on steric factors. Mise[58] has investigated this effect and shown that the number and substitution pattern of the Cp substituents, $C_5H_{5-n}Me_n$, determines the catalyst activity and polymer molecular weight. Decreasing the Zr:Al ratio from 1:4,000 to 1:40 induced oligomerisation with β-hydride elimination if n=0 and β-methyl transfer with n=5. End group analysis of the produced oligomers indicated only β-methyl transfer when Zr:Al was 1:20 for the $Cp^*_2ZrX_2$/MAO system (Cp^*=-C_5Me_5) and mixed β-methyl transfer and β-hydride elimination for the $(C_5HMe_4)_2ZrX_2$/MAO polymerisation system, with Zr:Al of 1:2. Mise remained unsure as to whether a steric or electronic effect was responsible, stating only that a large steric interaction would result if β-hydride elimination occurred between the β-methyl and one of the Cp-methyl groups. Resconi[58] states that the effect is only relevant for propylene reactions and is therefore most likely due to steric interactions.

It must be stated that the oligomerisation reactions discussed above are separate and distinct from hydro-oligomerisation reactions, where hydrogen is added to control oligomer/polymer molecular weight[59].

2.6.0. Stereoselective Synthesis with Cp_2ZrX_2/MAO Systems

A further advance in the polymerisation chemistry of Cp_2ZrX_2/MAO systems came when the stereoselective synthetic methods, using chiral *ansa*-metallocenes, were coupled with the polymerisation work being developed by Kaminsky and Brintzinger[53] . This work highlights the development of catalysts capable of the stereoselective cyclo-polymerisation of dienes to give optically active polymers[60] (Figure 2.15). Ligand substituents can be placed to control possible transition states, thereby reducing rates of β-hydride elimination or controlling the stereochemistry. Also, increased Cp ligand basicity, and hence lower metal centre Lewis acidity, increase polymer molecular weights. These concepts are of prime importance when considering oligomerisation systems.

Figure 2.15.
Stereoselective Cyclopolymerisation of 1,5-hexadiene.

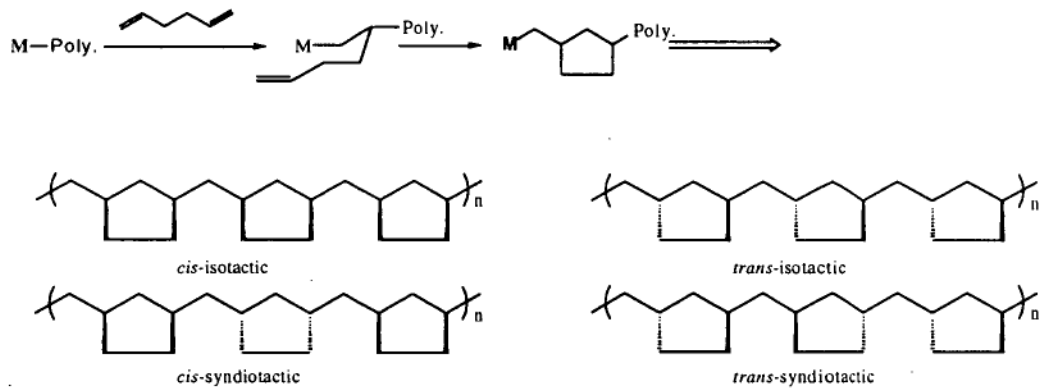

Stereoselective polymerisation requires the availability of chiral metal complexes or complexes of varying symmetries. The majority of which at present are substituted *ansa*-metallocenes[61] or achiral substituted metallocenes[62] (Figure 2.16).

For the substituted metallocene systems the bulky nature of the substituents prevents unrestricted rotation of the Cp moiety, effectively resulting in a chiral system. A number of studies have been completed examining the effect on reactivity and stereochemistry using the above zirconium complexes.

Figure 2.16.

Metallocenes used in Stereoselective Polymerisation.

(R-Groups shown are typical but not all inclusive)

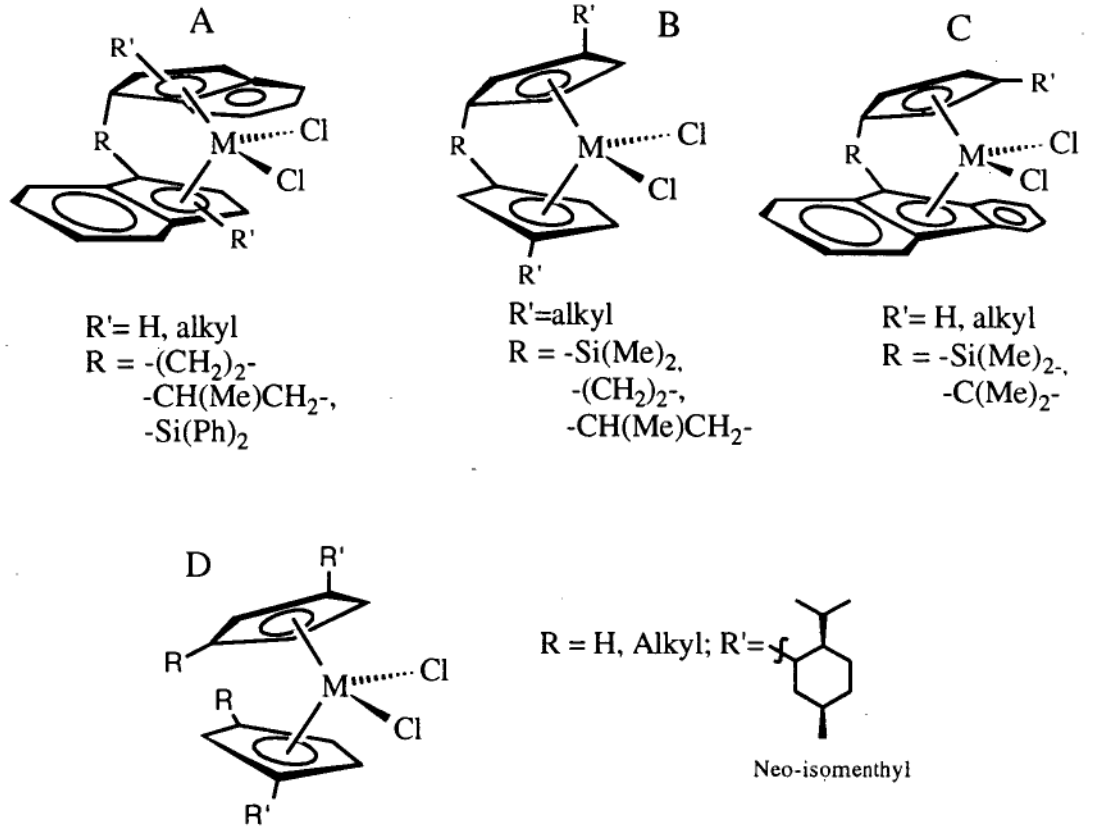

2.6.1. Structure/Reactivity Relationship

Kaminsky[63] has examined the effect of bridged (*ansa*) and non-bridged metallocenes, M=Ti, Zr, Hf, on the polymerisation of ethylene and propylene. Steric and electronic factors are found to play important roles. *Ansa*-metallocene complexes with C_2 symmetry are highly isospecific catalysts, while the fluorenyl complex (Figure 2.16-C) is syndiospecific. Bis-Cp systems where R'=R=H produce atactic polymers while if R=H, R'=bulky and chiral (neomenthyl) an isotactic polymer is produced. It was observed that the less substituted complexes are the most active ethylene polymerisation catalysts and hafnocene complexes are the least active. Some relative activities for ethylene polymerisation are, Cp_2ZrCl_2 : rac-[En(Ind)$_2$]$ZrCl_2$: rac-[Me_2Si(Ind)$_2$]$ZrCl_2$: rac-[EBTHI]$ZrCl_2$: rac-[En(Ind)$_2$]$HfCl_2$ are 60,900 : 41,100 : 36,900 : 22,200 : 2,900 kg PE/Mol Zr/h.

The stereocontrol in these reactions can be ascribed to site specific control of the orientation of the incoming monomer, i.e. enantiomorphic control of the stereochemistry.

Electron releasing groups on the Cp ring appeared to increase average polymer molecular weights, while a shorter bridge length, $-C_2H_2-$ vs. $-SiMe_2-$, did not increase activity, as may be expected with the increase in bite angle and hence less steric hindrance for monomer access. The rates of propylene polymerisation are often very different when other steric factors are included, Cp_2ZrCl_2 having the lowest activity.

Ansa-metallocenes, bridged systems, with C_2 symmetry have the highest activities, which are maximum with short bridge lengths. Changing from C_2 to C_S symmetry changes the polymer from being isospecific to syndiospecific, while shortened bridge lengths again increase reactivities.

Chien[64] discussed the effects of a number of structural parameters on polymerisation activities using non-symmetrical chiral catalysts of titanium or zirconium (Figure 2.17). The complexes can exist as anti and syn diastereomers which have different activities, both producing hemiisotactic polymer. Each diastereomer however has a bimodal product distribution not accounted for by conventional theories. Chien suggests in these non symmetric complexes conformational isomers are possible leading to observed variations in polymer properties and catalytic activities, one leads to a more stereoregular polymer. It was suggested that this effect is possible in other complexes.

Figure 2.17.

Non-Symmetric Chiral Metallocenes

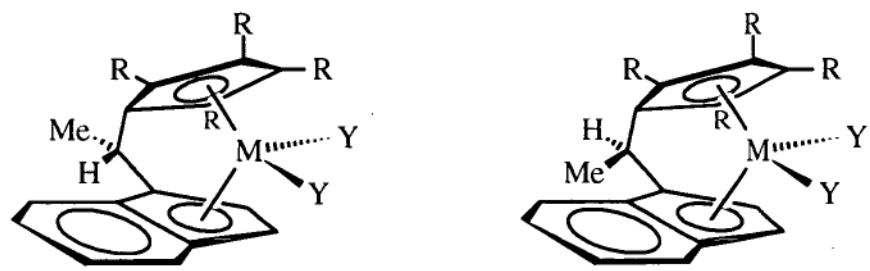

Anti. Syn.

R=Me ; Y=Cl & Me ; M = Ti & Zr

The shorter bridge length for this ligand reduced the ability to hold the zirconium deeply within the complex. This led to poor polymerisation stereocontrol and a greater susceptibility to deactivation through the formation of bimetallic ethyl bridged species[53b], -Zr-CH_2CH_2-Zr-. Activities were even lower than the titanium species, where titanium is located deep within the wedge, and 4 orders of magnitude lower than the Cp_2ZrCl_2/MAO system.

Polar solvents promote formation of the catalytic species allowing a linear increase in activity with increasing solvent polarity[65] (increasing dielectric constant). Solvent effect on polymer stereochemistry is dependent upon the catalyst symmetry. C_2 symmetric catalysts showed no variation. C_S symmetric catalysts show a reduced level of stereospecificity in polar solvents. In C_S symmetry systems the growing chain can migrate before monomer insertion altering the stereochemistry between insertions as polar solvents aid the ion pair separation and hence migration.

Erker[66] has examined non-bridged, chiral metallocenes and has shown excellent stereocontrol is possible with appropriate substitution on the metallocene (Figure 2.18). Isotactic propylene is produced with enantiomorphic site control for the *racem*-like α-A and α-B diastereomers. Reactivities are somewhat lower than the *ansa*-metallocenes/MAO systems.

Erker also warns of simplistic structure-reactivity relationships before examination of all parameters[66d]. Propylene polymerisation with a $(C_5H_4iPr)_2TiPh_2$/MAO system lead to isotactic polypropylene at -50°C, atactic polypropylene at -10°C, and slightly syndiotactic polypropylene at 10°C. The difference is said to be due to the influence of entropy and enthalpy effects in the transition state on two possible conformational isomers at various temperatures.

The influence of *ansa*-metallocene alkyl group substitution pattern on activity has been examined by Brintzinger[67]. When alkyl groups are placed to decrease possible misinsertion of monomer or to decrease β-agostic interactions for β-hydride elimination reactions, polypropylene molecular weights are dramatically increased. The favoured substitutions then allow for α-agostic interactions and easier alignment of the incoming monomer.

Figure 2.18.
Chiral Non-Bridged Metallocenes.

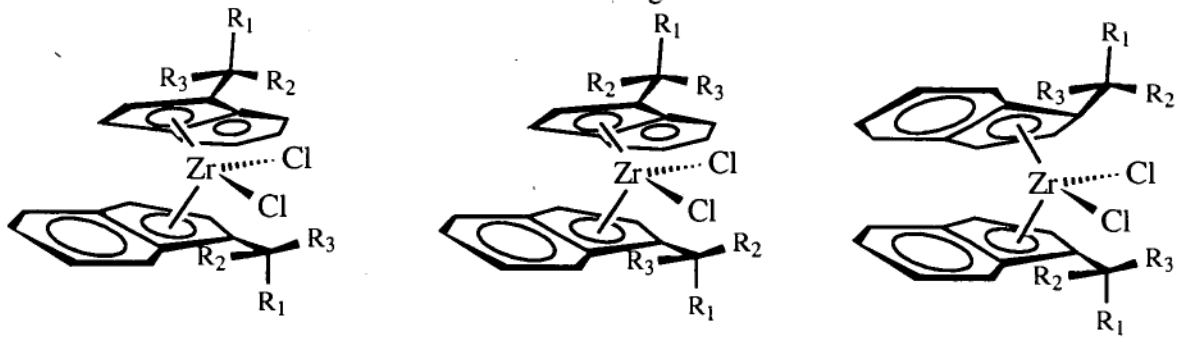

R_1=H ; R_2=Me ; R_3=Cy, Ph, -CH2-(9-BBN)

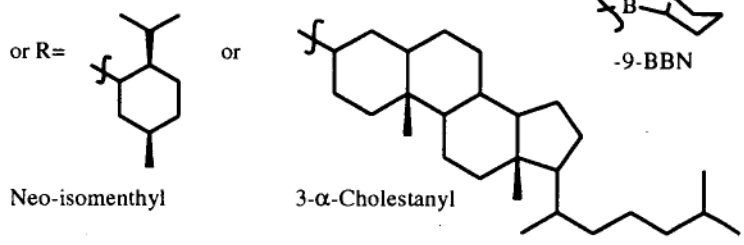

The presence of β-agostic interactions has been indicated by Brintzinger[68] in the hydrodimerisation of 1-deuterohexene with the chiral R-(EBTHI)$ZrCl_2$/MAO. A consistent excess of the threo or erythreo dimer, dependent on starting hexene, indicates preferred insertion with the opposite enantioface orientation. For the achiral Cp_2ZrCl_2/MAO system, unexpectedly, an excess product was also observed. Hydrodimerisation of (Z)-1-deutero-1-hexene led to an excess of the erythreo dimer. The presence of a preferred α-agostic interaction in a pure isotopic effect would, together with the normally preferred trans-oriented alkyl group on the incipient C-C bond, result in the reported product (Figure 2.19). The excess of the erythreo product is in agreement with that expected from calculations.

The role of α-agostic interactions in transition states had previously been proposed by Green[69]. A mechanism between that of Cossee-Arlman and Green-Rooney, as part of a continuous series of possible intermediates, dependant on the steric and electronic environment of the central metal should be considered for zirconium based systems (Figure 2.20). This shows a marked difference from the chemistry of titanium where such α-agostic interactions where shown not to be present[70].

Figure 2.18.
Hydrodimerisation of 1-Deuterohexene
Using Achiral Zirconocene Polymerisation Systems

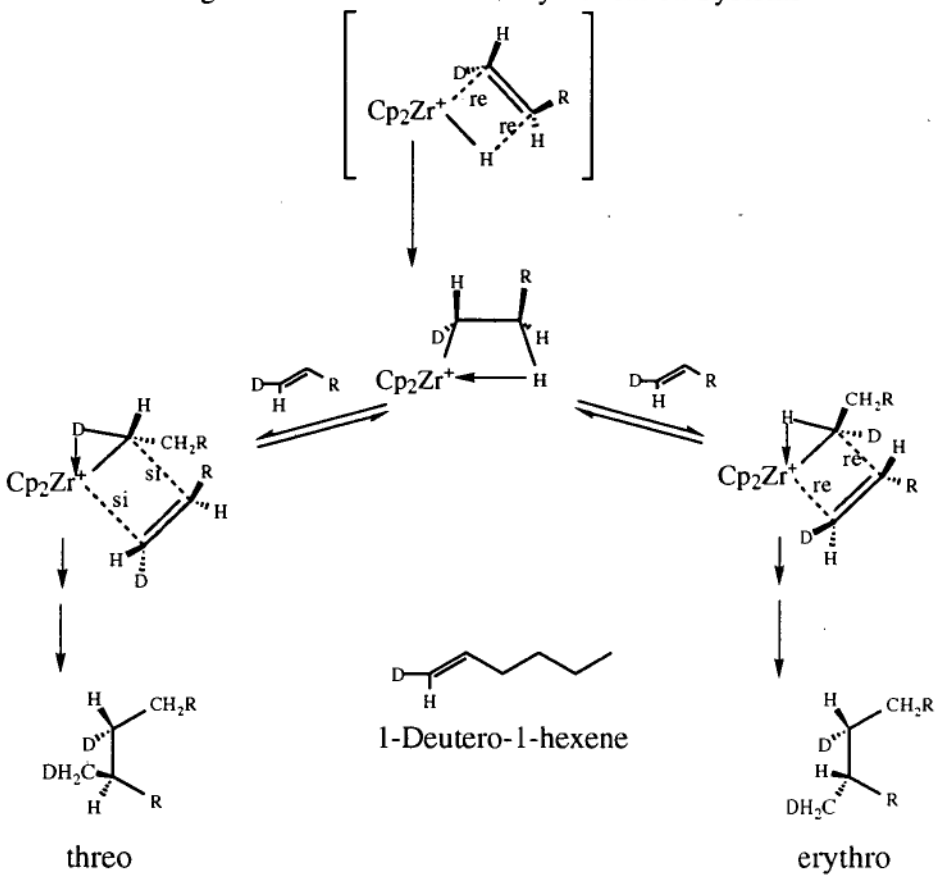

Figure 2.20.
Proposed Polymerisation Mechanism
for Zirconium Based Polymerisation Systems

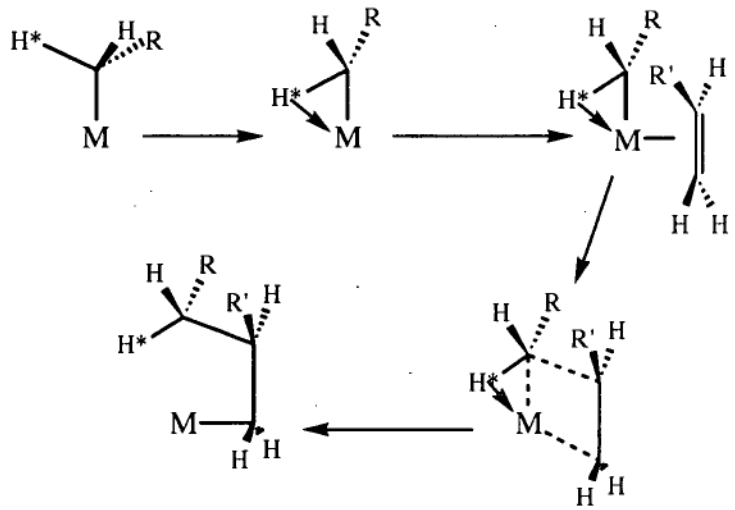

Modified Green-Rooney Polymerisation Mechanism

Brintzinger[71] has tried to formalise structure-reactivity relationships in ring substituted C_2 symmetric *ansa*-metallocenes in an analogous way to that of Tolman's cone angle concept[72]. In this model two parameters are defined; the wedge angle and an obliquity or twist angle. The wedge angle is the angle between two planes bisecting the metal centre and tangential to the Van der Waals surface of the Cp alkyl groups, positioned to give the maximum angle of the bisecting planes. The obliquity or twist angle is defined as the rotation of the wedge intersection line away from the line through the metal centre, perpendicular to the Cp-M-Cp plane where a clockwise rotation is defined as positive (Figure 2.21).

Figure 2.21.
Brintzinger's Model of Wedge and Obliquity Angle
for C_2 Symmetric *Ansa*-metallocenes

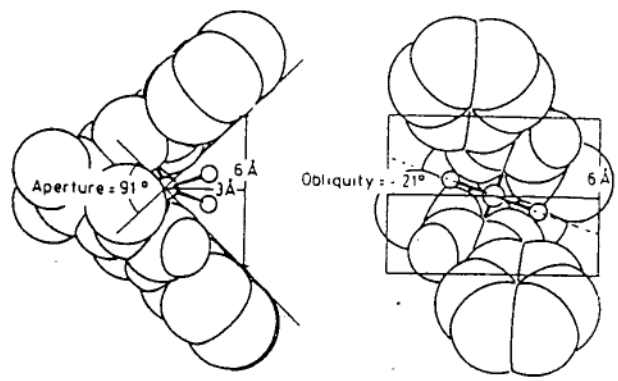

As reported by Hortman, K., Brintzinger, H-H., *New J. Chem.*, 16, **1992**, 51-55.

The two parameters in effect define a gap size and chirality. The degree of twist can be positive or negative and activities are related to the "degree of fit" of the transition state complex into this gap. The actual transition state can be defined using similar wedge and obliquity angles and if the wedge angle of the transition state is less than or equal to that of the complex and the obliquity angles are similar, then reactivities are high. The described transition state for stereospecific propylene polymerisation includes *trans*-orientation of the growing polymer to the incoming monomer across the incipient C-C bond and an α-agostic interaction to the polymer chain. In such cases Brintzinger shows a significant correlation between structure and reactivity.

2.6.2. Metal Centre Lewis Acidity/Reactivity Relationship

A detailed investigation into structure and electronic effects on reactivities using substituted bis-indenyl zirconium complexes (Figure 2.22.) reveals some very interesting effects[73] in ethylene and propylene polymerisation reactions.

Figure 2.22.

Substitution Patterns for Bis-Indenyl Zirconium Complexes

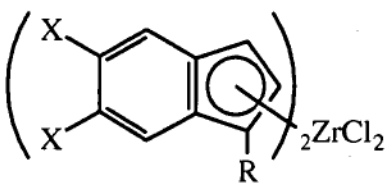

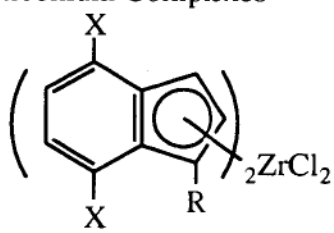

1a R=H ; X=H
1b R=H ; X=Me
1c R=H ; X=OMe
1d R=H ; X=Cl, F

1e R=H ; X=Me

2a R=-$(CH_2)_2$- ; X=H
2b R=-$(CH_2)_2$- ; X=Me
2c R=-$(CH_2)_2$- ; X=OMe

2e R=-$(CH_2)_2$- ; X=Me

In this study it has been indicated for ethylene polymerisation (Zr:Al of 1:2000 at 25°C and 0.75 bar) that electron withdrawing groups decrease activities and result in lower polymer molecular weights. No catalysis is observed with X=-OMe. The methyl substituted indenyls, 1b and 2b, are twice as active as the non-substituted indenyls; TONs $8.93x10^5/7.85x10^5$ compared to $5.00x10^5/3.57x10^5$ respectively. The 4,7-dimethyl substituted indenyls have similar activities to the non-substituted indenyls; TONs of $4.92x10^5$ and $4.64x10^5$ respectively, however, despite the similar electronic environments polymer molecular weights are greatly increased, M_n non-bridged $2.78x10^5$ and $3.52x10^5$ respectively and bridged M_n of $1.25x10^5$ and $2.05x10^5$.

Propylene polymerisation using the *ansa*-metallocenes shows similar trends with little or no reactivity when X=OMe, higher polymerisation rates for the 5,6-dimethyl substituted complex compared to the non-substituted complex, TONs of $7.44x10^5$ and $6.28x10^5$ respectively, and the 4,7-dimethylsubstituted complex having lower reactivity (TON of $1.81x10^5$) but the highest stereoselectivity.

The difference between the 5,6- and 4,7- dimethylsubstituted indenyls would appear to be steric in nature as the electronic environments are similar. The difference has been explained by steric interactions between the indenyl methyl and the inserting monomer for the 4,7-dimethyl substituted indenyl. It was also found that the polymer formed with the 5,6-dimethyl substituted complex was less stereoregular than the parent, non-substituted indenyl, opposite to what could be expected on steric grounds. This was ascribed to an electronic effect, with the electron releasing methyl groups reducing the Lewis acidity of the metal centre and therefore the degree of α-agostic stabilisation in the transition state.

2.7.0. Metal Centre Lewis Acidity and β-Hydride Elimination

A decrease in the Lewis acidity of the metal centre has been proposed to increase polymerisation reactivities and decrease β-hydride elimination reaction rates, as indicated above, generating so called living catalysts. Such systems have been shown to have very low rates for β-hydride elimination compared to insertion and can be generated by increasing the number of Lewis basic Cp groups attached to the zirconium metal centre[74], i.e. Cp_3ZrH/Et_3Al system.

The increase in activity indicated above can be correlated to electron donating alkyl side chains on the Cp (or indenyl) group, making the Cp moiety more Lewis basic and hence the metal centre less Lewis acidic[75]. Similar living catalysts are generated for the neutral permethylscandocenes[76] which are in general less Lewis acidic[77].

However, studies examining the steric and electronic effects on rates of β-hydride elimination are limited. Bercaw[76] has examined the effects of alkyl-β-substituents on β-hydride elimination rates for permethylscandocenes. Electron releasing groups on the β-carbon increase rates while electron withdrawing groups have the opposite effect. Elimination rates measured over a range of temperatures indicate a positive energy of activation.

A relatively tight, four-centre transition state was proposed with a positive charge build up on the β-carbon (Figure 2.23). Bercaw states that steric interactions are also important in this sterically hindered system leading to changes in expected orders of reactivity, i.e. *n*-butyl eliminates more slowly than *n*-propyl, due to greater interaction of the β-alkyl substituent with the Cp methyls in the transition state.

Effects of changes to the metal centre Lewis acidity through changes to the Cp substituents on β-hydride elimination rates were not examined.

Figure 2.23.
Proposed β-Hydride Elimination Transition State

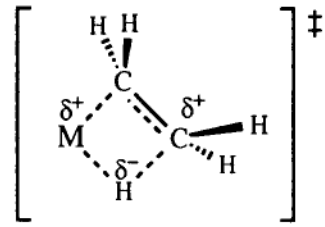

Jordan[78] working with methyl substituted zirconocenes observed similar effects on β-hydride elimination rates for zirconium complexes. Again variations to the metal centre Lewis acidity were not examined.

It can, however, be quite clearly seen from Jordan's work that for β-hydride elimination to occur or at least initial transition states to form, a vacant, low lying metal orbital must be present. The complex $Cp^*_2Zr(CH_2CH_3)(L)^+$, L=CH_3CN, undergoes β-hydride elimination while $Cp^*_2Zr(CH_2CH_3)(L)_n^+$ is stable. This is also seen by the adoption of β-agostic bonding for this type of complex where L = CH_3CN or PMe_3 while for L = THF, which is able to effectively occupy the vacant metal orbital through π interactions[33b], a normal σ-bound ethyl is observed. The related rates of reaction with H_2 for these complexes has already been mentioned[33d].

Theoretical studies into Ziegler-Natta type polymerisation systems, examining steric and electronic effects, have supported the above considerations, especially a positive activation energy for the reverse, β-hydride elimination, process and tight four-centred transition states[79].

2.8.0. Discussion

There is no major discussion of reaction mechanisms in the early reports of zirconium based oligomerisation processes. The assumption being that the reaction followed a Cossee-Arlman mechanism, the predominantly accepted mechanism for olefin polymerisation. The role of the added ligand in these oligomerisation systems is undefined and appears to function only as a solubilising agent in the formation of the preferred homogeneous system. Direct comparisons between activities for ligand solubilised systems and ligand free homoleptic tetraalkyl systems lead Young to the same conclusion. Attridge postulates an ion pair system generated after successive alkyl transfers to the cocatalyst. The nature of the produced ion pair or precursor species is not discussed. No further discussions of this species have been given.

2.8.1. Oligomerisation Model Development

From the examination of the literature a general model can be drawn up to give, in general terms, systems most likely to oligomerise α-olefins. Such a catalytic system must contain:

i. vacant, low lying metal orbitals for the formation of required transition states.
ii. a sterically unsaturated metal centre to allow the formation of the required transition state.
iii. a highly Lewis acidic metal centre.

The work by Jordan shows directly the need for vacant, low lying metal orbitals for the formation of required transition states. Lewis bases used to stabilise such complexes must have little or no π-bonding ability thus leaving non-bonding or vacant orbitals free for agostic/transition state interactions.

The large body of work on improving stereoselective synthesis in propylene polymerisation systems indicated the ability to block formation of β-hydride elimination transition states by the careful placement of ligand substituents. The ability to freely form such intermediates in a sterically unhindered metal centre should aid β-hydride elimination.

Although not directly addressed in any of the above work it can be proposed that an increased metal centre Lewis acidity is required. This is based on three observations:

i. increased Lewis basicity of Cp ligands leads to an increase in polymer molecular weight and a decrease in termination rates. In some instances this leads to the formation of living catalysts, where the rate of β-hydride elimination is negligible. If the mechanisms for oligomerisation and polymerisation are assumed to be the same, a metal centre with greater Lewis acidity should decrease oligomer weights.

ii. an increase in Cp Lewis basicity leads to a slight loss of stereocontrol for propylene polymerisation systems possibly due to the weaker α-agostic interactions resulting from a decreased metal centre Lewis acidity.

iii. electron releasing groups on the β-carbon of a metal alkyl group promote β-hydride elimination transition states leading to increased elimination rates. In oligomerisation systems the electronic properties of such R-groups cannot be influenced or controlled, however it is proposed that a higher metal centre Lewis acidity would increase the chance of β-agostic interactions and β-hydride transfer.

Other process conditions can be altered to increase rates of β-hydride elimination as mentioned previously. As the transition state involves a positive energy of activation, higher temperatures will increase the rate of β-hydride elimination. Also an increased catalyst concentration can increase the possibility of elimination reactions.

In summary, conditions which support the formation of β-hydride elimination transition states should lead to more effective oligomerisation systems.

Such complexes where a high metal centre Lewis acidity is desired are bound to be unstable and therefore bidentate, chelating ligands containing both hard and soft donor atoms may be used to aid in stabilisation. The hard donor atom provides the primary bonding and the soft donor atom provides stabilisation. It may then be possible by varying the electronic nature of the labile, soft donor atom to increase lability to a point where the complex is stabilised but in the presence of ethylene does not interact with the metal centre, allowing an appropriate transition state form without hindrance by ligand coordination.

The ability of R-Cp_2ZrCl_2/MAO/EAO or [Cp^*_2ZrMe(THT)][BPh4] systems to oligomerise propylene and in one case ethylene, may then be explained by such a

model. In these cases the Zr:Al ratio is low, 1:1 compared to polymerisation systems at 1:2000, the catalyst concentration is high and monomer concentration low to promote elimination reactions. Kaminsky inferred that the active species in oligomerisation reactions was similar to that of polymerisation systems. The low Zr:Al ratio would prevent any secondary supporting interactions from the excess MAO or EAO through oxygen, thereby decreasing the effective metal centre Lewis acidity by adduct formation or similar reactions. The MAO or EAO present can only be involved in primary reactions of halide abstraction and metal alkylation. This is supported by the observation that increased MAO or EAO additions rapidly led to increased oligomer weights and higher reactivities.

1 Langer, A.W., *J. Macromol. Sci. Chem.* A4,**1970**, 775

2 a. Attridge, C.J. *J. Chem. Soc., Chem. Comm.* **1973**, 132-133
b. Attridge, C.J., Jones, E., Pioli, A.J.P., Wilkinson, P.J., Runcorn, C., Ger. Offen., DE 2 219 049, 20pp,**1973.**

3 a. Zucchini, U.; Albizzati, E.; Giannini, U., *J. Organometallic Chem.* 26,**1971**, 357-372.
b. Giannini, U.; Zucchini, U.; Albizzati, E., *J. Pol. Sci., Part B* 8, **1970**, 405.

4 a. Motier, J.F.; Yoo, J.S., US Patent US 3,855,341 1969.
b. Motier, J.F.; Yoo, J.S., US Patent US 4,026,822 **1977.**

5 Dzhemilev, U.M.; Ibragimov, A.G.; Tolstikov, G.A.; Vostrikova, O.S.; Zelenova, L.M., *Zh. Org. Khim.* 17(11), **1981**, 2313-2319. Eng. Trans., **1982**, XXXX

6 Shiraki, Y.; Kawano, S.; Takouchi, K., Eur. Pat. Appl. Ep 0 241 596(Cl. C 07 C2/30), 31.10.1990.

7 a. Shiraki, Y.; Tamura, T., Eur., Pat Appl. EP 0 328 728 A1(Cl. CO7C 2/30), 17.8.1988.
b. Shiraki, Y.; Tamura, T., Eur., Pat Appl. EP 0 481 435 A2(Cl. CO7C 2/22), 15.10.1991.

8 a. Shiraki, Y.; Ueda, K.; Takeuchi, K., Eur., Pat Appl. EP 0 444 505 A2(Cl. CO7C 2/32), 20.02.1991.
b. Nakashima, Y.; Takeuci, K.; Fujita, N., Eur. Pat. Appl. Ep 0 320 571 A2(Cl. C07C 2/30) 17. 08.1988.

9 for example see,
a. Langer, A.W., US. Pat. Appl., US 4,409,414 (Cl. CO7C 2/34) 11. 10.1983.
b. Langer, A.W., US. Pat. Appl., US 4,442,309 (Cl. CO7C 2/22) 10. 04.1984.
c. Langer, A.W., US. Pat. Appl., US 4,486,615 (Cl. CO7C 2/22) 04.12.1984.

10 Keim, W.; Hoffman, B.; Lodewick, R.; Peuckert, M.; Schmitt, G.; Fleischhauer, J.; Meier, U.. *Journal of Molecular Catalysis* 6, **1979**, 79.

11 Shiraki, Y.; Tamura, T.; Eur., Pat Appl. EP 0 481 435 A2(Cl. CO7C 2/22), 15.10.1991.

12 Young, D.A.; Jones, L.O.; Campione, T.J., Eu.Pat.Appl., EU 0 295 960 (Cl. C 07 C 2/30), 21.12.1988.

13 Young, D.A., *Journal of Molecular Catalysis* 53, **1989**, 433-442.

14 Young, D.A.; Jones, L.O.; CAmpione, T.J., PCT Int.Appl., WO 9216477(Cl.C07C 2/30), 01.10.1992.

15 Mathys, G.M.K., PCT Int.Appl., WO 9102707(Cl. C07C 2/30), 07.03.1991.

16 Chauvin, Y., Fr. Demande, FR 2 669 921(Cl. C 07 C 11/02, 2/30), 05.06.1992.

17 Doyle, M.J.; Clark, J.M.T., Eu.Pat.Appl., EU 0 435 367 A1(Cl. C07C 2/30), 03.07.1991.

18 Morrison, R.T.; Boyd, R.N., *Organic Chenistry*, 5th Ed., Allyn and Bacon, 1987, pg540-541.

19 Cotton, F.A.; Wilkinson, G., *Advanced Inorganic Chemisty*, 4 th Ed., John Wiley & Sons, Inc., 1980, pg 344.

20 Fries, R,W., SU Pat.Appl., US 5,116,795(C08F 4/652), 26.05.1992.

21 Watanabe, M.; Kuramoto, M., Eur.Pat.Appl. EU 0 268 214 B1(Cl. CO7C 2/34) 21.08.1991.

22 Slaugh, L.H., Eu.Pat.Appl., EU 0 366 212 A1(Cl. C07C 2/34), 02.05.1990.

23 a. Sigwalt, P.; Liu, H.Q.; Deffieux, A., *Makromol. Chem.* 192, **1991**, 2111-2123.

b. Sigwalt, P.; Liu, H.Q.; Deffieux, A., *Makromol. Chem.* 192, **1991**, 2125-2140.

24 a. Al-Jarallah, A.M.; Anabtawi, J.A.; Siddiqui, M.A.B.; Aitani, A.M., *Catalysis Today* 14(1), **1992**, 42-104.

25 Masters, C., *Homogeneous Transition-Metal Catalysis-A Gentle Art*, Chapman and Hall 1981, pg159.

26 Babkina, O.N.; Grigorian, E.A.; Dyachkovskii, F.S.; Shilov, A.E.; Shuvalova, N.H., *Zh.Fiz.Chim.* 43, **1969**,7.

27 Dyachkovskii, F.S., *Visn.Mol.Soedin.* 7, **1965**,114.

28 Eisch, J.J.; Piotrowski, A.M.; Brownstein, S.K.; Gabe, E.J.; Lee, F.L., *J. Am. Chem. Soc.* 107, **1985**, 7219-7221.

29 Long, J.A., *J. Am. Chem. Soc.* 81, **1959**, 5312.

30 Fink, G.; Zoller, W., *Makromol. Chem.*, 182, **1981**, 3265.

31 Eisch, J.J.; Caldwell, K.R.; Werner, S.; Krüger, C., *Organometallics* 10, **1991**, 3417-3419.

32 Gaudet, M.V.; Zaworotko, M.J.; Cameron, T.S.; Linden, A., *J. Organometallic Chem.* 367, **1989**, 267-273.

33 a. Jordan, R.F.; Dasher, W.E.; Echols, S.F., *J. Am. Chem. Soc.* 108, **1986**, 1718-1719.

b. Jordan, R.F.; Bajur, C.S.; Willett, R.; Scott, B., *J. Am. Chem. Soc.* 108, **1986**, 7410-7411.

c. Jordan, R.F.; La Pointe, R.E.; Bajur, C.S.; Echols, S.F.; Willett, R., *J. Am. Chem. Soc.* 109, **1987**, 4111-4113.

d. Jordan, R.F., *J. Chem. Ed* 65(4), **1988**, 285-289

e. Jordan, R.F.; La Pointe, R.E.; Bradley, P.K.; Baenziger, N., *Organometallics* 8, **1989**, 2892-2903.

f. Jordan, R.F., *Adv. in Organomettalic Chem.* 32, **1991**, 325-382.

g. Crowther, D.J.; Jordan, R.F.; Baenziger, N.; Verma, A., *Organometallics* 9, **1990**, 2574-2580.
h. Borkowsky, S.L.; Jordan, R.F.; Hinch,G.D., *Organometallics* 10, **1991**, 1268-1274.
i. Alelyunas,Y.W.; Jordan, R.F.; Echols, S.F.; Borkowsky, S.L.; Bradley, P.K., *Organometallics* 10, **1991**, 1406-1416.
j. Crowther, D.J.; Baenziger, N.C.; Jordan, R.F, *J. Am. Chem. Soc.* 113, **1991**, 1455-1457.

34 a. Casey, C.P.; Jordan, R.F.; Rheingold, A.L., *J. Am. Chem. Soc.* 105, **1983**, 665.
b. Longato, B.; Martin, B.D.; Norton, J.R.; Anderson, O.P., *Inorg. Chem.* 24, **1985**, 1389.

35 Scholz, J.; Rehbaum, F.; Thiele, K-H.; Goddard, R.; Betz, P.; Krüger, C., *J. Organometallic Chem.* 443, **1993**, 93-99.

36 Taube, R.; Krukowka, L., *J. Organometallic Chem.* 347, **1988**, C9-C11.

37 Eshuis, J.J.; Tan, Y.Y.; Teuben, J.H., *J. Molecular Catalysis* 62, **1990**, 277-287.

38 Bochman, L.M.; Wilson, L.M., *J. Chem. Soc., Chem. Commun.* **1986**, 1610.

39 Andrea, R.R.; Terpstra, A.; Oskam, A., *J. Organometallic Chem.* 307, **1986**, 307-317.

40 a. Bochman, M.; Karger, G.; Jagger, A.J., *J. Chem. Soc., Chem. Commun.* **1990**, 1038-1039.
b. Bochman, M.; Jagger, A.J.; Nicholls, J.C., *Angew. Chem., Int. Ed. Engl.* 29(7), **1990**, 780-782.
c. Bochman, M.; Lancaster, S.J., *J. Organometallic Chem.* 434, **1992**, C1-C5.
d. Bochman, M., *Angew. Chem., Int. Ed. Engl.* 31(9), **1992**, 1181-1182.
e. Bochman, M.; Lancaster, S.J., *Organometallics* 12, **1993**, 633-640.

41 Horton, A.D.; Frijins, J.H.J., *Angew. Chem., Int. Ed. Engl.* 30(9), **1991**, 1152.

42 Hlatky, G.G.; Turner, H.W.; Eckman, R.R., *J. Am. Chem. Soc.* 111, **1989**, 2728-2729.

43 Chien, J.C.W.; Tsai, W-M.; Rausch, M.D., *J. Am. Chem. Soc.* 113, **1991**, 8570-8571.

44 Horton, A.D.; Orpen, A.G., *J. Am. Chem. Soc.* 10, **1991**, 3910-3918.

45 Bahr, S.R.; Boudjouk, P., *J. Org. Chem.* 57, **1992**, 5545-5547.

46 a. Pellecchia, C.; Longo, P.; Proto, A.; Zambelli, A., *Makromol. Chem., Rapid Commun.* 13, **1992**, 265-268.
b. Pellecchia, C.; Longo, P.; Proto, A.; Zambelli, A., *Makromol. Chem., Rapid Commun.* 13, **1992**, 277-281.
c. Pellecchia, P.; Proto, C.; Longo, A.; Zambelli, A., *Makromol. Chem., Rapid Commun.* 12, **1991**, 663-637.
d. Pellecchia, C.; Grassi, A.; Immirzi, A., *J. Am. Chem. Soc.* 115, **1993**, 1160-1162.
e. Pellecchia, C.; Grassi, A.; Zambelli, A., *J. Mol. Catal.* 82, **1993**, 57-65.
f. Pellecchia, C.; Grassi, A.; Zambelli, A., *Organometallics* 12, **1993**, 4473-4478.
g. Bochman, M., Lancaster, S.J., *Organometallics* 13, **1994**, 2235-2243.
h. Crowther, D.J.; Borkowsky, S.L.; Swenson, D.; Meyer, T.Y.; Jordan, R.F, *Organometallics* 12, **1993**, 2897-2903.

47 a. Yang, X.; Stern, C.L.; Marks, T.J., *Angew. Chem., Int. Ed. Engl.* 31(10), **1992**, 1375-1377.
b. Yang, X.; Stern, C.L.; Marks, T.J., *J. Am. Chem. Soc.* 113, **1991**, 3623-3625.

48 Hlatky, G.G.; Eckman, R.R.; Turner, H.W., *Organometallics* 11, **1992**, 1413-1416.

49 Pellecchia, C.; Grassi, A.; Zambelli, A., *Organometallics* 13, **1994**, 298-302.

50 a. Maeta, H.; Hashimoto, T.; Hasegawa, T.; Suzuki, K., *Tetrahedron Letters* 33(40), **1992**, 5965-5968.
b. Guram, A.S.; Swenson, D.C.; Jordan, R.F., *J. Am. Chem. Soc.* 114, **1992**, 8991-8996.
c. Corey, J.Y.; Zhu, X-H., *J. Organometallic Chem.* 439, **1992**, 1-17.

d. Guo, Z-Y.; Bradley, P.K.; Jordan, R.F., *Organometallics* 11, **1992** ,2690-2693.
e. Horten, A.D.; Orpen, A.G.; *Angew. Chem., Int. Ed. Engl.* 31(7), **1992**, 876-878.
f. Collins, S.; Ward, D.G., *J.Am. Chem. Soc.* 114, **1992**, 5460-5462.
g. Guram, A.S.; Jordan, R.F., *J. Org. Chem.* 57, **1992**, 5994-5999.
h. Horten, A.D., *Organometallics* 11, **1992**, 3271-3275.
i. Spence, R.E.v.H.; Buchwald. S.L.; Richardson, J.F., *Acta Chemica Scandinavica* 47, **1993**, 326-329.
j. Sinnema, P-J.; Meetsma, A.; Teuben, J.H., *Organometallics* 12, **1993**, 184-189.
k. Guram, A.S; Guo, Z.; Jordan, R.F., *J. Am. Chem. Soc.* 115, **1993**, 4902-4903.

51 Rodewald, S.; Jordan, R.F., *J. Am. Chem. Soc.* 116, **1994**, 4491-4492.

52 a. Kaminsky, W.; Sinn, H., *Angew. Chem., Int. Ed. Engl.* 19, **1980**, 390.
b. Kaminsky, W.; Sinn, H., *Adv. Organometallic Chem.* 18, **1980**, 99.

53 a. Kaminsky, W.; Külper, Brintzinger, H-H.; Wild, F.R.W.P., *Angew. Chem., Int. Ed. Engl.* 24, **1985**, 507-508.
b. Kaminsky, W.; Steiger, R., *Polyhedron* 7(22/23), **1988**, 2375-2381.

54 Rotman, D.; Wood, A., *ChemicalWeek* Sept. 15, **1993**, 5.

55 Kaminsky, W.; Steiger, R., *Polyhedron* 7(22/23), **1988**, 2375-2381.

56 Kaminsky, W.; Bark, A.; Steiger, R., *J. Molecular Catal.* 74, **1992**, 109-119.

57 Kaminsky, W.; Ahlers, A.; Möller-Lindenhof, N., *Angew. Chem., Int. Ed. Engl.* 28(9), **1989**, 1216-1218.

58 a. Mise, T.; Kageyama, A.; Miya, S.; Yamazaki, H., *Chem. Letters* 9, **1991**, 1525-1528.
b. Resconi, L.; Piemontesi, F.; Franciscono, G.; Abis, L.; Fiorani, T., *J. Am. Chem. Soc.* 114, **1992**, 1025-1032.

59 a. Pino, P.; Galimberti, M.; Prada, P.; Consiglio, G., *Makromol. Chem.* 191, **1990**, 1677-1688.

b. Pino, P.; Galimberti, M., *J. Organometallic Chem.* 370, **1989**, 1-7.
c. Pino, P.; Cioni, P.; Wei, J., *J. Am. Chem. Soc.* 109, **1987**, 6189-6191.

60 a. Mogstad, A-L.; Waymouth, R.M., *Macromolecules* 25, **1992**, 2282-2284.
b. Coates, G.W.; Waymouth, R.M., *J. Am. Chem. Soc.* 115, **1993**, 91-98.
a. Okuda, J., *Nachr. Chem. Tech. Lab.* 41(1), **1993**, 8-14.
b. Coates, G.W.; Waymouth, R.M., *J. Am. Chem. Soc.* 113, **1991**, 6270-6271.
c. Mogstad, A-L.; Waymouth, R.M., *Macromolecules* 25, **1992**, 2282-2284.

61 a. Wiesenfeldt, H.; Reinmut, A.; Barsties, E.; Evertz, K.; Brintzinger, H-H., *J. Organometallic Chem.* 369, **1989**, 359-370.
b. Erker, G.; Wilker, S.; Krüger, C.; Goddard, R., *J. Am. Chem. Soc.* 114, **1992**, 10983-10984.
c. Razavi, A.; Ferrara, J., *J. Organometallic Chem.* 435, **1992**, 299-310.
d. Ewan, J.A.; Jones, R.L.; Razavi, A.; Ferrara, J.D., *J. Am. Chem. Soc.* 110, **1988**, 6255-6256.

62 a. Troyanov S.I.; Rybakov, V.B.; Thewalt, U.; Varga, V.; Mach, K., *J. Organometallic Chem.* 447, **1993**, 221-225.
b. Ewan, J.A., *J. Am. Chem. Soc.* 106, **1984**, 6355-6364.

63 a. Heiland, K.; Kaminsky, W., *Makromol. Chem.* 193, **1992**, 601-610.
b. Kaminsky, W.; Engehausen, R.; Zoumis, K.; Spaleck, W.; Rohrmann, J., *Makromol. Chem.* 193, **1992**, 1643-1651.

64 a. Llinas, G.H.; Day, R.O.; Rausch, M.D.; Chien, J.C.W., *Organometallics* 12, **1993**, 1283-1288.
b. Chien, J.C.W.; Llinas, G.H.; Rausch, M.D.; Lin, Y-G.; Winter, H.H.; Atwood, J.L.; Bott, S.G., *J. Polym. Sci. Part A: Polym. Chem.* 30, **1992**, 2601-2617.
c. Chien, J.C.W.; Llinas, G.H.; Rausch, M.D.; Lin, Y-G.; Winter, H.H.; Atwood, J.L.; Bott, S.G., *J. Am. Chem. Soc.* 113, **1991**, 8569-8570.

65 Herfert, N.; Fink, G., *Macromol. Chem.* 193, **1992**, 773-778.

66 a. Erker, G.; Nolte, R.; Aul, R.; Wilker, S.; Krüger, C.; Noe, R., *J. Am. Chem. Soc.* 113, **1991**, 7594-7602.
b. Erker, G.; Temme, B., *J. Am. Chem. Soc.* 114, **1992**, 4004-4006.
c. Erker, G., *Pure & Appl. Chem.* 64(3), **1992**, 393-401.
d. Erker, G.; Fritze, C., *Angew. Chem., Int. Ed. Engl.* 31(2), **1992**, 199-202.

67 a. Röll, W.; Brintzinger, H-H.; Rieger, B.; Zolk, R., *Angew. Chem., Int. Ed. Engl.* 29, **1990**, 279-280.
b. Krauledat, H.; Brintzinger, H-H., *Angew. Chem., Int. Ed. Engl.* 29, **1990**, 1412-1413.

69 a. Brookhart, M.; Green, M.L.H.; Wong, L-L., *Prog. Inorg. Chem.* 36, **1988**, 1-124.
b. Brookhart, M.; Green, M.L.H., *J. Organometallic Chem.* 250, **1983**, 395-408.

70 Clawson, L.; Soto, J.; Buchwald, S.L.; Steigerwald, M.L.; Grubbs, R.H., *J. Am. Chem. Soc.* 107, **1985**, 3377-3378.

71 Hortmann, K.; Brintzinger, H-H., *New J. Chem.* 16, **1992**, 51-55.

72 a. Tolman, C., *Chem. Reviews* 77(3), **1977**, 313-348.
b. Ferguson, G.; Roberts, P.J.; Alyea, E.C.; Khan, M., *Inorg. Chem.* 17(10), **1978**, 2965-2967.

73 a. Lee, I-M.; Geuthier, W.J.; Ball, J.M.; Iyengar, B.; Collins, S., *Organometallics* 11, **1992**, 2115-2122.
b. Piccolrovazzi, N.; Pino, P.; Consiglio, G.; Sironi, A.; Moret, M., *Organometallics* 9, **1990**, 3098-3105.

74 Sinn, H.; Kaminsky, W.; Vollmer, H.-J.; Woldt, R., *Angew. Chem., Int. Ed. Engl.* 19, **1980**, 390-392.

75 a. Gassman, P.G.; Macomber, D.W.; Hershberger, J.W., *Organometallics* 2, **1983**, 1470-1472.
b. Andrea, R.R.; Terpstra, A.; Oskam, A., *J. Organometallic Chem.* 307, **1986**, 307-317.
c. Bordwell, F.G.; Bausch, M.J., *J. Am. Chem. Soc.* 105, **1983**, 6188-6189.

d. Longato, B.; Martin, B.D.; Norton, J.R.; Anderson, O.P., *Inorg. Chem.* 24, **1985**, 1389-1394.

[76] Burger, B.J.; Thompson, M.E.; Cotter, W.D.; Bercaw, J.E., *J. Am. Chem. Soc.* 112, **1990**, 1566-1577.

[77] Mashima, K.; Nakamura, A., *J. Organometallic Chem.* 428, **1992**, 49-58.

[78] a. Alelyunas, Y.W.; Guo, Z.; LaPointe, R.E.; Jordan, R.F., *Organometallics* 12, **1993**, 544-553.
b. Guo, Z.; Swenson, D.C.; Jordan, R.F, *Organometallics* 13, **1994**, 1424-1432.

[79] a. Mohr, R.; Berke, H.; Erker, G., *Helvetica Chimica Acta* 76, **1993**, 1389-1409.
b. Castonguy, L.A.; Rappe, A.K., *J. Am. Chem. Soc.* 114, **1992**, 5832-5842.
c. Gleiter, R.; Hylakryspin, I.; Niu, S.Q.; Erker, G., *Organometallics* 12, **1993**, 3828-3836.
d. Woo, T.K.; Fan, L.; Ziegler, T., *Organometallics* 13, **1994**, 2252-2261.

Chapter 3

Synthesis

Based on an examination of literature data for zirconium oligomerisation and polymerisation systems in Chapter 2 a model has been proposed in which conditions that favour the formation of β-hydride elimination transition states should lead to more effective oligomerisation systems. As the electronic or steric nature of the growing oligomer cannot be influenced, changes must occur through the selected ligand system. According to this model the formation of a sterically unsaturated, highly Lewis acidic metal centre is required. It could be expected that such a system would be highly unstable and therefore, the use of hemi-labile ligands, common in catalytic systems for other metals, to aid stabilisation and allow flexibility in coordination number (via dissociation of the labile end group to generate the sterically unsaturated metal centre) was examined. As zirconium is a strong, hard Lewis acid and very oxophilic, oxygen appeared to be an obvious choice for the hard, fixed donor atom while sulfur, nitrogen or phosphorous were potential labile donor atoms.

3.1.0. Ligand Selection

As β-diketones have been shown to be effective ligands in oligomerisation systems and have been extensively used with other metals, β-diketonate derivatives have been targeted. In particular nitrogen containing analogues of the β-diketones, the β-aminoketones, have been the focus of this study (Figure 3.1). Three major reasons leading to the selection of the tetra-substituted β-aminoketones were:

i. Electronic; the electronic nature of both donor atoms could be significantly altered through variation of the four substituents. In particular the nucleophilicity of the nitrogen could be controlled by ligand backbone substituent variations and directly through nitrogen substituents.

ii. Steric; assuming the nitrogen co-ordinates to the metal centre, the nitrogen substituent could be used to directly influence nitrogen-metal interactions through the close proximity of the ligand to the metal centre. Where propylene or higher olefins were used as a feed gas, chiral information could be placed close to the metal centre.

iii. Ligand Flexibility; β-aminoketones are flexible ligands forming de localised electronic systems on complex formation, aiding in the formation and stabilisation of the required active species.

Sulfur, a soft weak base, plays a less important role in the chemistry of zirconium, a strong hard acid, with only a few groups of sulfur containing inorganic zirconium complexes reported: adducts of thioethers or dithioethers, mono- or dithioxanthates and trisdithiolenes. Due to small bite angles, ligand rigidity and the inability to easily modify ligands sterically or electronically these complexes have not been included in this study.[1]

It is perhaps because of the increased lability of sulfur containing ligands in zirconium complexes that such ligands are effective in the oligomerisation chemistry of zirconium being the donor atom of choice, as described in Idemitsu's patented process (Chapter 2.2.4). In other studies replacement of THF by the sulfur analogue, THT, has been shown to increase catalytic rates significantly (Chapter 2.4.10). In light of these observations it was decided that where possible sulfur analogues of oxygen containing ligands in active oligomerisation systems would also be tested.

Figure 3.1.
Bidentate, Chelate Ligands used in this Oligomerisation Study

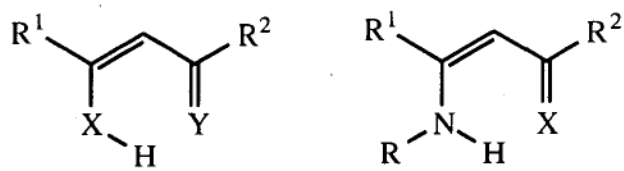

X=Y=O; acetylacetone
X=Y=S; dithioacetylacetone
X=O,Y=S; monothioacetylacetone

X=O; aminoketone
X=S; aminothioketone

Hemilabile systems can be formed from β-diketones by changing the backbone substitution pattern or by thiolation to give a sulfur-oxygen analogues. Some of these ligands and sulfur analogues of the β-aminoketones have been examined for comparison to β-aminoketone containing systems. Alternative nitrogen-oxygen containing ligand systems, which are sterically rigid and which have significantly different electronic properties to β-aminoketones, such as Schiff's bases and picolinic acid, were also examined.

3.1.1. Nomenclature

The frequently used β-diketones are referred to in this study by well known abbreviations, i.e. acetylacetone (Hacac), hexafluoroacetylacetone (Hhfac) or dibenzoylmethane (Hbzbz). No standard nomenclature has been found for β-

aminoketones in the literature, where reference was made to ketenamines in chromatographic studies or β-aminoketones in spectroscopic studies. In this study the β-aminoketone nomenclature is used and abbreviations are derived from that used for β-diketones or their thiolated analogues, with the basic description R-HNacac, or for more complicated ligands R-HR^{1}acR^{2}ac. Therefore on reacting *iso*-propylamine with acetylacetone, the product 4-(*iso*-propylamino)-3-penten-2-one or *i*-Pr-HNacac is formed. More complicated ligands follow the same pattern, i.e. reacting dibenzoylmethane with cyclohexylamine gives 1,3-diphenyl-2-(cyclohexylamino)-acrolein or Cy-HNbzbz. Deprotonated ligands are then simply described as for acetylacetonate, acac$^-$, that is deprotonating *i*-Pr-HNacac gives *i*-Pr-Nacac$^-$ or deprotonating Cy-HNbzbz gives Cy-Nbzbz$^-$ (Figure 3.2). Thiolated β-aminoketones are described similarly to thiolated acetylacetones, e.g. monothioacetylacetone, HSacac, and a β-aminothioketone as R-HNacSac.

Figure 3.2.
Nomenclature for Ligand Abbreviations

β-diketone

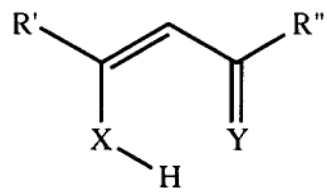

β-aminoketone

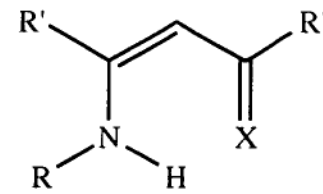

Nomenclature

X=Y=O; HR'acR"ac
X=Y=S; HR'SacR"Sac
X=O,Y=S; HR'SacR"ac

X=O; R-HR'NacR"ac
X=S; R-HR'NacR"Sac

Deprotonated Ligands

X=Y=O; R'acR"ac$^-$
X=O,Y=S; R'SacR"ac$^-$

X=O; R-R'NacR"ac$^-$
X=S; R-R'NacR"Sac$^-$

3.1.2. Tautomers

Like their β-diketone precursors, β-aminoketones may be present in solution as any one of three possible tautomers (Figure 3.3). NMR and IR studies have indicated that the aminoketone was present to the exclusion of all other tautomers in solution for reported β-aminoketones[2]. This tautomer is easily observed for β-aminoketones containing an α-hydrogen on the amino-R group, which coupled with the amine

proton giving appropriate splitting patterns for the α-proton. The coupling disappears upon ligand deuteration.

Figure 3.3.
Possible β-Aminoketone Tautomers.

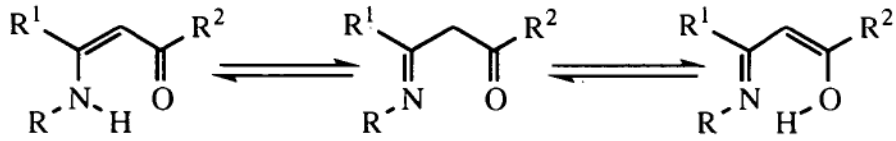

Based on this NMR and structural data, ligands have been drawn as β-aminoketones rather than ene-imines or imino-ketones and will be referred to as such in this study. Complexed ligands undergo electronic rearrangement forming ene-imines with σ-bonded oxygen or 6 member chelate rings and are referred to in general as bis-ligand complexes. The actual species remains unknown in certain cases Section 3.5.2. In the catalysis section (Chapter 4), where the active species in solution is unknown, the ligands will be referred to in their free form, i.e. β-diketones, β-aminoketones or Schiff's bases. Actual species which may be present and reactions in solution are discussed in Chapter 5.3.0.

3.2.0. Catalyst Design

Synthesis has been directed toward isolating possible catalytic precursors or intermediates in the oligomerisation process. Assuming that oligomerisation has similar activation and propagation mechanisms to polymerisation, oligomerisation differing only in the relative rates of the insertion and β-hydrogen elimination reactions, then similar catalytic intermediates could be expected for both processes. The proposed activation mechanism for ethylene or propylene polymerisation with a metal-chloride/EASC system is shown in Figure 3.4. Metal alkylation followed by halide abstraction leads to the formation of the proposed cationic precursor complex. The catalytic activity of recently synthesised cationic, 14-electron, d^0 zirconium species, in the absence of a cocatalyst, has strongly supported this mechanism (Chapter 2.4.3).

Figure 3.4.
Mechanism for Polymerisation Activation
in a Metal-Chloride/EASC System

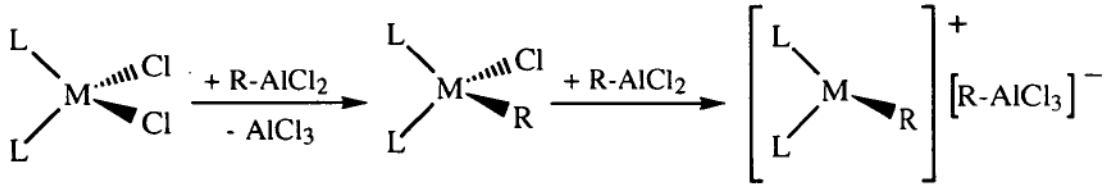

Therefore synthesis was directed toward formation of zirconium complexes of the ligands in Figure 3.1, their alkylated analogues and finally cationic species (Figure 3.5). Synthetic work was also closely coupled to a catalytic test program. Where catalytic testing of new complexes indicated low or no activity, ethylene polymerisation or the same activity as *in situ* tests, synthesis was not continued. Many possible complexes or adducts therefore were not isolated.

Figure 3.5.
Synthetic Target Molecules

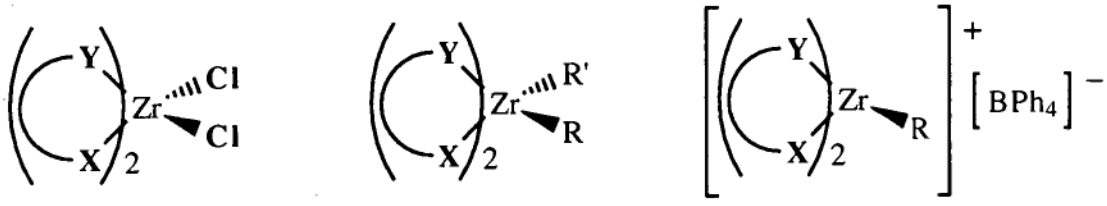

Bis-Ligand Complex | Mono/Di-alkylated Bis-Ligand Complex | Cationic, Bis-Ligand Complex

The coordination chemistry of zirconium is extensive, and a number of zirconium complexes containing bidentate, chelate ligands containing nitrogen, oxygen or sulfur donor atoms have been reported. Of these β-diketone containing systems predominate with a number of Schiff's base containing complexes also found. No zirconium complexes of bidentate β-aminoketones have been reported.

3.3.0. Bidentate $\widehat{OO}$ and $\widehat{OS}$ Complexes of Zirconium

Zirconium is an oxophilic metal readily forming adducts or complexes with oxygen donor ligands, e.g. alcohols, diketones, esters, ethers etc[1]. The alkoxides were first

reported in 1904[3] and have been extensively studied. A range of zirconium β-diketone complexes have since been reported[1].

3.3.1. β-Diketone Containing Complexes of Zirconium

Acetylacetone (Hacac), as discussed in Chapter 2.2.6, has previously been reported as a ligand in active zirconium catalysed ethylene oligomerisation systems and synthetic routes to zirconium-β-diketone complexes are well known. The most common synthetic routes are listed below and no detailed discussion of this chemistry is included here[1], (Reactions 3.1-4).

$$ZrX_4 + nHdik \longrightarrow Zr(dik)_nX_{4-n} + nHX \quad [3.1]$$

$$Zr(dik)_4 + nHdik' \longrightarrow Zr(dik')_4 + nHdik \quad [3.2]$$

$$ZrX_4 + Zr(dik)_4 \longrightarrow 2Zr(dik)_2X_2 \quad [3.3]$$

$$Zr(O\text{-}i\text{-}Pr)_4.HOi\text{-}Pr + nHdik \longrightarrow Zr(dik)_4 + 5HOi\text{-}Pr \quad [3.4]$$

$Zr(acac)_4$ is commercially available and therefore other required β-diketone complexes were prepared by following Reaction 3.3 above or direct reaction of acetylacetone with $ZrCl_4$ (Reaction 3.1).

3.3.2. Monothio-β-Diketone Ligand Synthesis

The thiolated diketones used in the above preparations and for *in situ* catalytic testing can be prepared by acid catalysed thiolation of the appropriate β-diketone with H_2S in acetonitrile at low temperature, -40°C, Reaction 3.5[4]. Alternative base catalysed thiolations have been reported[5]. The ligands were stored as lead salts after reaction with lead acetate. Reaction of the lead salt with H_2S in ether or hexane released the free ligand.

With the acid catalysed syntheses of monothio-β-diketones no control over the placement of the sulfur in non symmetric diketones was possible. This problem was overcome by using a base promoted Claisen condensation of a ketone and a thioester[6] (Reaction 3.6). The ligands were converted to lead salts for storage.

Acid Catalysed Thiolation of β-Diketones

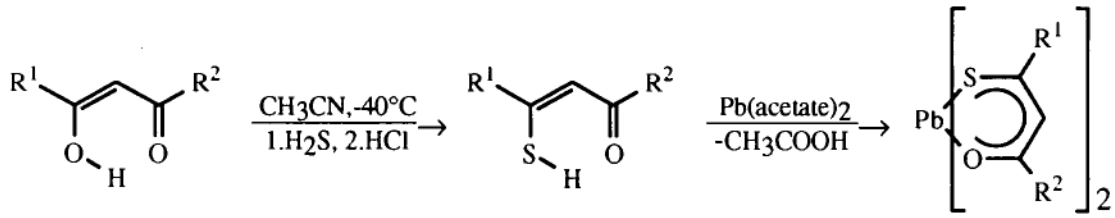

[3.5]

Claisen Condensation Synthesis of Monothio-β-Diketones

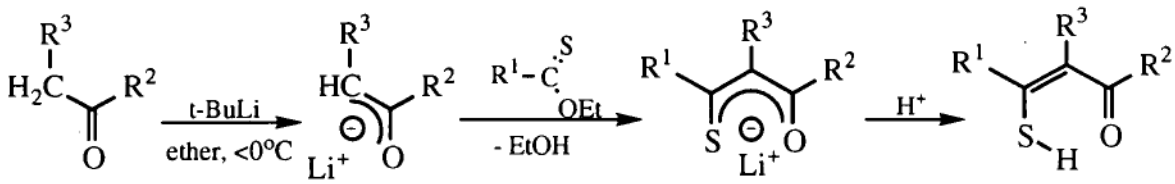

[3.6]

The thioesters for the Claisen condensation could be formed from the appropriate ester by reaction with a thiolating agent, such as P_4S_{10} or Lawesson's Reagent, however incomplete reaction and formation of disulphides led to problems with product purification[7,8]. The most convenient method for the formation of thioesters was found to be the hydrosulfurisation of the appropriate ethyl alkyl or arylimidate hydrochloride under anhydrous conditions[9]. Yields were above 80% and separation problems were decreased by careful selection of base (Reaction 3.7). The imidate hydrochlorides were purchased or generated from the appropriate nitrile[10].

Synthesis of O-Ethyl Thioesters

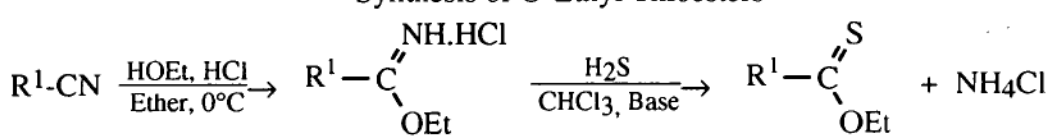

[3.7]

3.3.3. Monothio-β-Diketone Containing Complexes of Zirconium

At the beginning of this study only one zirconium-monothio-β-diketone had been reported[11], tetrakis(thioacetylacetonato)zirconium(IV), ($Zr(Sacac)_4$). The yellow, thermally stable solid has been prepared by reaction of stoicheiometric amounts of $ZrCl_4$ and sodium thioacetylacetonate in DCM (Reaction 3.8).

This synthesis has been repeated in this study using the lead salt of the thioacetylacetonate. The synthesis of the related series of compounds, $Zr(Sacac)_3Cl$, $Zr(Sacac)_2Cl_2$ and $Zr(Sacac)Cl_3$, has been attempted in a similar manner or by a metathetical exchange reaction between stoicheiometric amounts of $Zr(Sacac)_4$ and $ZrCl_4$ (Reactions 3.9 & 10).

$$ZrCl_4 + 4NaSacac \longrightarrow Zr(Sacac)_4 + 4NaCl \qquad [3.8]$$

$$ZrCl_4 + 2Pb(Sacac)_2 \longrightarrow Zr(Sacac)_4 + 2PbCl_2 \qquad [3.9]$$

$$ZrCl_4 + Zr(Sacac)_4 \longrightarrow 2Zr(Sacac)_2Cl_2 \qquad [3.10]$$

Only the bis ligand complex, $Zr(Sacac)_2Cl_2$, has been isolated and found to be relatively stable in solution, it decomposed slowly in DCM above 0°C. When THF was used as the solvent, the bis THF adduct, $Zr(Sacac)_2Cl_2.2THF$, was formed. In solution $Zr(Sacac)Cl_3$ disproportionated to give $Zr(Sacac)_2Cl_2$ and presumably $ZrCl_4$, as indicated by a slight cloudiness in the solution. Solids isolated in the attempted preparation of $Zr(Sacac)_3Cl$ disproportionate in solution to give a mixture of $Zr(Sacac)_4$ and $Zr(Sacac)_2Cl_2$, as indicated by proton NMR. These complexes did not react with added phosphorus or nitrogen containing ligands, e.g. dppe, TPP or pyridine, although addition of THF or pyridine to a solution containing $Zr(Sacac)Cl_3$ lead to the isolation of the bis-THF or pyridine-$ZrCl_4$ adduct.

3.3.4. Dithio-β-Diketone Complexes of Zirconium

No zirconium dithio-β-diketones have been reported in the literature and attempts to form such complexes in this study were not successful. Synthesis was complicated by the instability of most dithio-β-diketones, which readily dimerise[12], and the incompatibility of known synthetic methods with reactive $ZrCl_4$[13], i.e. reported high temperature reactions with H_2S in acidic ethanol.

A number of attempts were made to generate the required dithio-β-diketone zirconium species *in situ* by reacting reduced zirconium species with a dithio-β-diketone precursor, dithiolium salts[14], in a redox reaction. The reduction of

zirconium was initially completed in the presence of dithiolium iodide in THF over a sodium amalgam (Reaction 3.11).

Reduction of Zr over Na/amalgam.

$$ZrCl_4 + 4 \text{ [dithiolium]}^+ I^- \xrightarrow[THF]{Na/Hg} Zr(SacSac)_4 + 4NaCl + 4Na \qquad [3.11]$$

The range of reaction conditions was, however, limited due to the presence of the amalgam (low temperature reactions were not possible). Attempts were therefore made to generate stable reduced zirconium species in solution[15] so that they could be separated from the amalgam. The second stage of reaction, the oxidative addition, was then carried out under different conditions, i.e. < -10°C (Reactions 3.12-17).

Synthesis of Soluble Reduced Zirconium Species

$$ZrCl_4.2THF + 3bpy \xrightarrow[THF]{Na/Hg} Zr(bpy)_3 + 4NaCl \qquad [3.12]$$

$$ZrCl_4.2THF + 3PBu_3 \xrightarrow[THF]{Na/Hg} 1/2[ZrCl_3(PBu_3)_2]_2 + 4NaCl \qquad [3.13]$$

$$ZrCl_4.2THF + 3dppe \xrightarrow[THF]{Na/Hg} Zr(dppe)_3 + 4NaCl \qquad [3.14]$$

$$Zr(bpy)_3 + 2 \text{ [dithiolium]}^+ I^- \xrightarrow[<0°C]{THF} Zr(SacSac)_2I_2 + 3bpy \qquad [3.15]$$

$$2[ZrCl_3(PBu_3)_2]_2 + 2 \text{ [dithiolium]}^+ I^- \xrightarrow[<0°C]{THF} Zr(SacSac)Cl_3 + 4PBu_3 + ZrCl_2I_2 \qquad [3.16]$$

$$Zr(dppe)_3 + 2 \text{ [dithiolium]}^+ I^- \xrightarrow[<0°C]{THF} Zr(SacSac)_2I_2 + 3dppe \qquad [3.17]$$

Unfortunately the $SacSac^-$ complexes could not be prepared even in the presence of a coordinating solvent or other donor ligands.

3.4.0. $\widehat{NO}$ and $\widehat{NS}$ Containing Ligand Systems

In view of the model developed in Chapter 2, where conditions which favour the formation of β-hydride elimination transition states should promote oligomerisation

over polymerisation, it was thought that β-aminoketones were the most likely ligands to lead to active oligomerisation systems. Hence this ligand system was originally chosen to be the prime focus of this study.

3.4.1. β-Aminoketone Ligand Synthesis

Synthesis of β-aminoketones was achieved relatively simply by condensing a primary amine with an appropriate diketone at elevated temperatures[2] (Reaction 3.18). Water generated from the reaction can be collected by the addition of a drying agent for low boiling amines, or with a water trap (Dean Stark apparatus) when refluxing toluene is used. An acid catalyst was required for less favourable reactions. Microwave irradiation[16] was a useful alternative method.

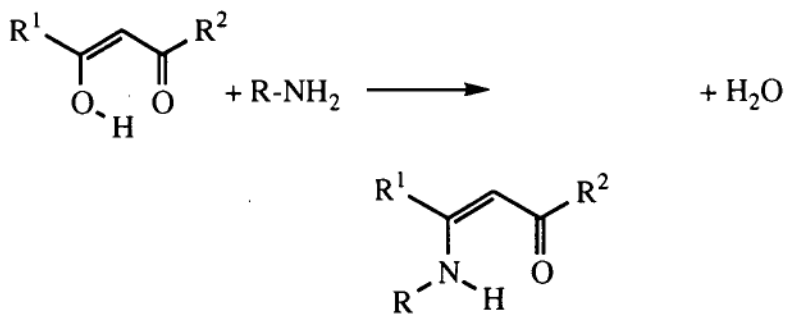

[3.18]

The restricting factor in this reaction was the acidity of the β-diketone. In the presence of strongly electron withdrawing groups, e.g. $-CF_3$, the acidity became too high with acid-base chemistry dominating, leading to the formation of ammonium salts of the β-diketonate. Formation of an appropriate silyl ether from the β-diketone (i.e. the introduction of a better leaving group) overcame this problem allowing the formation of a large range of β-aminoketones with varying steric and donor properties[17], Reaction 3.19.

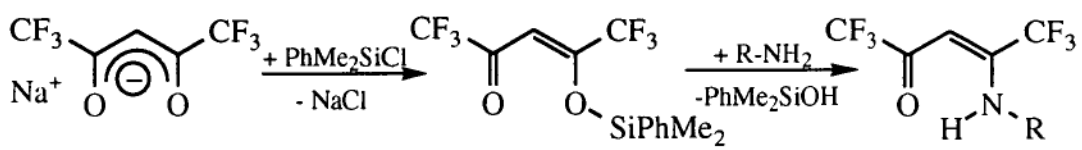

[3.19]

A list of β-aminoketones prepared in this work is shown in Table 3.1.

Table 3.1.

β-Aminoketones Synthesised in this Study

Ligand	R	R^1	R^2	
[1] *i*-Pr-HNacac	*i*-Pr-	Me	Me	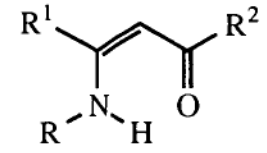
Hex-HNacac	Hex-	Me	Me	
[1] Cy-HNacac	Cy-	Me	Me	
t-Bu-HNacac	*t*-Bu-	Me	Me	
tmp-HNacac	tmp-*	Me	Me	
ClPh-HNacac	ClPh-*	Me	Me	
MeOPh-HNacac	MeOPh-*	Me	Me	
[1] Ph-HNacac	Ph-	Me	Me	
[1] Hex-HNacbz	Hex-	Me	Ph	
Hex-Hbzbz	Hex-	Ph	Ph	
[2] Ph-HNacbz	Ph-	Me	Ph	
[2] Ph-Hbzbz	Ph-	Ph	Ph	
i-Pr-HNtfac	*i*-Pr-	Me	CF_3	

*tmp-:2,4,6-trimethylphenyl-, ClPh-:*p*-chlorophenyl-, MeOPh-:*p*-methoxyphenyl-

[1] reported in Everett, G.W., Jr., Holm, R.H., *J. Am. Chem. Soc.* 87, **1965**, 2117-2127

[2] reported in Martin, D.F., Janusonis, G.A., Martin, B.B., *J. Am. Chem. Soc.* 83, **1961**, 73-75.

Reacting a β-diketone with a secondary amine results in the formation of a β-aminoketone that can only act as a neutral analogue of the above described ligands. These secondary-β-aminoketone are more sterically crowded around the amine functionality and are constrained to adopt an aminoketone structure. The diphenyl and diethyl examples have been prepared and employed in catalytic testing for comparison with the above ligands. Their use results in catalytic systems with low activity and no further syntheses were attempted.

3.5.0. Bis-$\widehat{NO}$ or $\widehat{NS}$ Containing Ligand Complexes of Zirconium

In situ catalytic testing of a range of β-aminoketones has shown, for the first time in the oligomerisation chemistry of zirconium, the ability to control oligomer product distributions through ligand substituent variation, (discussed fully in Chapter 4.3.2). An extensive literature search indicated no previously reported zirconium-β-aminoketone complexes and therefore no synthetic methods were available for their formation. In light of the initial results from catalytic testing and the desire to isolate

potential intermediates in the oligomerisation process extensive development of this chemistry was pursued.

Very recently the synthesis of the related tetradentate N_4-macrocyclic complexes was reported[18]. The macrocycles, formed by the reaction of β-diketones with diamines, readily form L_4ZrCl_2, L_4ZrR_2 or cationic L_4ZrR^+ species (L_4 = divalent N_4-tetradentade macrocycle). The synthetic methods reported are similar to those developed during this study.

3.5.1. β-Aminoketone-$ZrCl_4$ Adducts

β-Aminoketones form 1:1 or 2:1 adducts with $ZrCl_4$. With a large excess of the ligand, only a 2:1 adduct is formed. Even under forcing conditions, such as refluxing in toluene, no further reaction occurs. This is not unexpected as Schiff's bases, such as N-bonded salicylaldimines containing a more acidic proton, only react further in refluxing toluene (Section 3.8.0).

The adducts, which are sparingly soluble in polar solvents and insoluble in non-polar solvents, were purified by continuous extraction into refluxing DCM during periods of 8-24 hours. As solids they are stable toward moisture, showing only slight decomposition after 3 months storage in plastic capped vials. The adducts have been characterised by elemental analysis, NMR and IR (in KBr disks). IR spectra show the movement of a strong band at 1620cm^{-1} (due to C=O in the free ligand) upon adduct formation to overlap with a band at 1560cm^{-1} (C=C stretch) and the appearance of a relatively sharp peak of medium intensity at around 3280cm^{-1}. This peak has been assigned to a N-H stretching band after loss of strong intramolecular hydrogen bonding on adduct formation.

^{1}H-NMR spectral data indicated chemical shifts for the amine functionality slightly downfield compared to the free ligand shifts, and somewhat broadened (Table 3.2). Splitting is observed for the *i*-Pr-group α-hydrogen peak due to coupling with the amine proton.

This indicates an oxygen bonded ligand which maintains the aminoketone type structure in solution, as indicated by the loss of the C=O stretching band in the IR (or

movement to lower energy and hidden by other intense bands) and the splitting of the α-proton in the proton NMR.

Table 3.2

Comparative Summary of NMR Data for β-Aminoketones as Free Ligands and bis-Ligand Adducts with $ZrCl_4$

Ligand	Methyls	=CH-	N-H	Amine R-group
Free ligand				
i-Pr-HNacac	1.96, 1.92	4.88	10.80	1.20(d, 6H, Me), 3.68(m, 1H, CH)
Ph-HNacac	2.04,1.97	5.18	12.50	7.33(m,2H), 7.17(m, 1H), 7.10(m, 2H)
Adduct				
i-Pr-HNacac	2.44,2.10	5.07	10.50	1.43(d, 6H, Me), 3.90(m, 1H)
Ph-HNacac	2.54,2.14	5.40	15.60	7.32-7.42(m, 5H)

NMR shifts are against TMS in $CDCl_3$ at RT.

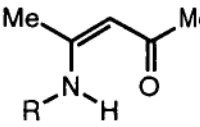

3.5.2. Crystal structure of $ZrCl_4$.2(*i*-Pr-HNacac)

To clarify the unexpected structure of the adducts, as suggested by spectroscopic data, a crystal structure analysis was carried out on the compound $ZrCl_4$.2(*i*-Pr-HNacac). Crystals suitable for structure determination were grown by the slow cooling of a saturated DCM solution. The structure is shown in Figure 3.6, and relevant bond lengths are shown in Table 3.3. The structure, with *cis*-O-bonded ligands, shows that a significant rearrangement of electron density has occurred to give what could be called an en-imine structure in the solid state. The N-C3 bond length of 1.307(2) Å approaches that of a C-N double bond (1.30 Å). The C1-C2 bond at 1.363(3) Å can be considered olefinic (1.34 Å) and the O-C1 bond at 1.303(2) Å is considerably longer than expected for a C-O double bond (1.24 Å[19]). The position of the hydrogen is therefore uncertain with nitrogen approaching a triply coordinated structure without the hydrogen (a single bond to the iso-propyl group and a double bond C3-N). Thus tautomeric structures are suggested, in which the hydrogen may be associated with the oxygen in the solid state (en-imine

structure), whereas the ^{1}H-NMR spectrum of this compound indicates significant N-H interactions in solution (amino-ketone structure).

Table 3.3.

Important Bond Lengths for the $ZrCl_4$.2(*i*-Pr-HNacac) Adduct.

Bond	O-C1	C1-C2	C2-C3	C3-N
Length Å	1.303(2)	1.363(3)	1.425(3)	1.307(3)

Figure 3.6.

Crystal Structure of $ZrCl_4$.2(*i*-Pr-HNacac)

(measured by Dr. U. Englert, Institut für Anorganische Chemie der RWTH, Aachen)

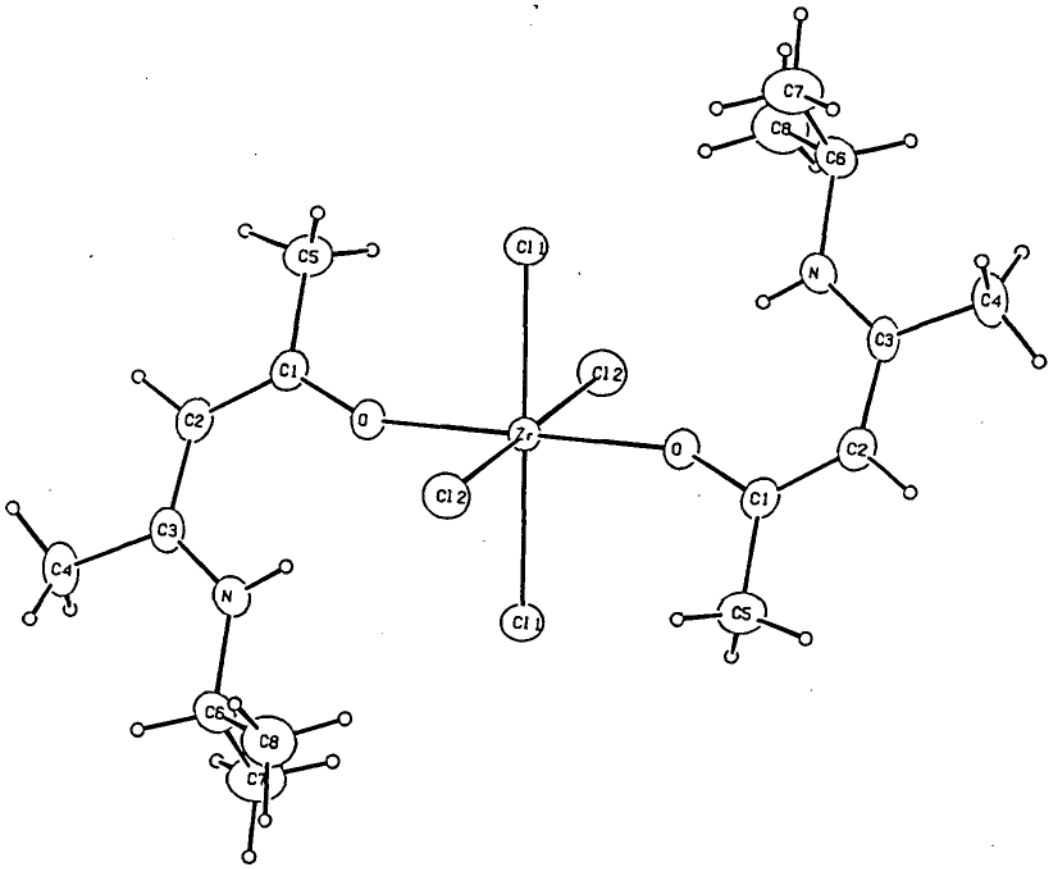

In situ catalytic testing of $ZrCl_4$ plus the free ligand and of the isolated adducts gave similar reactivities and product distributions, within experimental error, and therefore isolation of further β-aminoketone-$ZrCl_4$ adducts was not considered important for the purpose of catalysis.

3.5.3. Bis-β-Aminoketone-Zirconium Complexes

As synthesis was to be directed toward isolating possible intermediates in the oligomerisation process it was first necessary to suggest possible reactions occurring in the catalytic solution which lead to the formation of the active species so that target molecules could be defined. It was assumed that zirconium was the active metal and that a similar activation mechanism to that discussed in Chapter 2 for polymerisation reactions occurred; that is metal alkylation and halide abstraction to form the active species.

In the presence of a β-aminoketone it was assumed, that ligand deprotonation on reacting with the cocatalyst, followed by halide abstraction from $ZrCl_4$ to form an intermediate β-aminoketone/$ZrCl_{n-4}$ complex occurred. Whether adduct formation occurred before or after ligand deprotonation was not clear with complexes of the type $(R\text{-Nacac})_nZrCl_{4-n}$ being generated in solution. The complex would then be alkylated and undergo halide abstraction in line with normal mechanisms for Ziegler-Natta polymerisation.

For this reaction path it would be expected, that in the presence of a cocatalyst, the catalytic species formed *in situ* from bis-ligand adducts or complexes, would be identical. An alternative activation mechanism for the reaction, leading to the formation of bis-β-diketonate zirconium complexes could be envisaged, such as cocatalyst induced metal alkylation with subsequent reaction of the ligand via alkane elimination to form the above intermediate complex. However the form of the intermediate complex remains the same and therefore would have the same catalytic activity and product distribution.

Consequently the initial target species were bis-β-aminoketonate zirconium complexes. A literature search failed to reveal any known examples of these complexes.

3.5.4. β-Aminoketone Complexes of other Metals

Some work has been reported on developing synthetic routes for the formation of β-aminoketone complexes of other, mainly divalent, 1st row transition metals. These ligands have been of special interest in studies on the steric and electronic effects on equilibria between square planar and tetrahedral complexes of Ni(II)[20]. In these

studies complexes have been formed by direct reaction of the β-aminoketone with an appropriate metal halide or salt, via amine exchange or by *in situ* preparation of the complex from the amine, β-diketone and metal salt. A more general method applicable to moisture or oxygen sensitive complexes involves the *in situ* formation of a potassium β-aminoketonate by reaction of the free ligand with KO*t*-Bu in HO*t*-Bu followed by reaction of the resultant solution with the appropriate metal salt[20c].

Protic solvents used in these methods however do not allow for more reactive metal salts like $ZrCl_4$ to be used. Recent work investigating volatile fluorinated β-aminoketones in chemical vapour deposition of thin copper layers has shown that the sodium salts of highly fluorinated β-aminoketones can be isolated by reaction with NaOMe in ether[17]. Metal complexes could then be formed by salt elimination. It has been found in this study that this reaction is not possible for the majority of β-aminoketones which are either not acidic enough for the sodium salt to form on reaction with NaOMe or that an equilibrium exists leading to low yields.

One cationic β-aminoketone titanium complex has recently been prepared by the *in situ* enolate migration to a coordinated nitrile forming a cationic bis-Cp-titanium complex[21]. Due to the requirement of initially forming a cationic bis-Cp titanium complex, this route was not considered to be synthetically useful to the target complexes in this study.

3.5.5. Formation of Potassium/Sodium β-Aminoketonates

Potassium β-aminoketonates have been isolated for the first time by reaction of a slight excess of the free β-aminoketones with potassium tertiary butoxide in THF at 60°C. The salts are precipitated by the addition of toluene, filtered and washed with toluene and hexane to remove the excess β-aminoketone and tertiary butyl alcohol. The white or pale yellow, moisture sensitive salts were sufficiently pure, as indicated by ^{1}H-NMR, to be used directly. They reacted with chlorinated or protic solvents and decomposed in THF solutions over 1-2 hours.

^{1}H-NMR spectra of these salts in methanol-d_4 showed salt-solvent interactions affecting one methyl peak, as indicated by complicated splitting patterns (Figure 3.7). It is thought that a rearrangement occurs in solution with the formation of a potassium enolate from the potassium amide/aminoketonate as indicated by the

increase in relative area of the methine peak (δ 5.3ppm) to 2 and the corresponding decrease of the methyl area (δ 2.085 multiplet) from 3 to 2. It is thought that an equilibrium is then set up between the enolate salt and the solvent. The same spectra are generated by adding sodium methoxide to the free ligands in methanol-d_4. The interactions disappear upon the addition of H_2O.

Figure 3.7.
NMR Spectra of Potassium Enolate Salt derived from
4-Phenylamino-3-penten-2-one

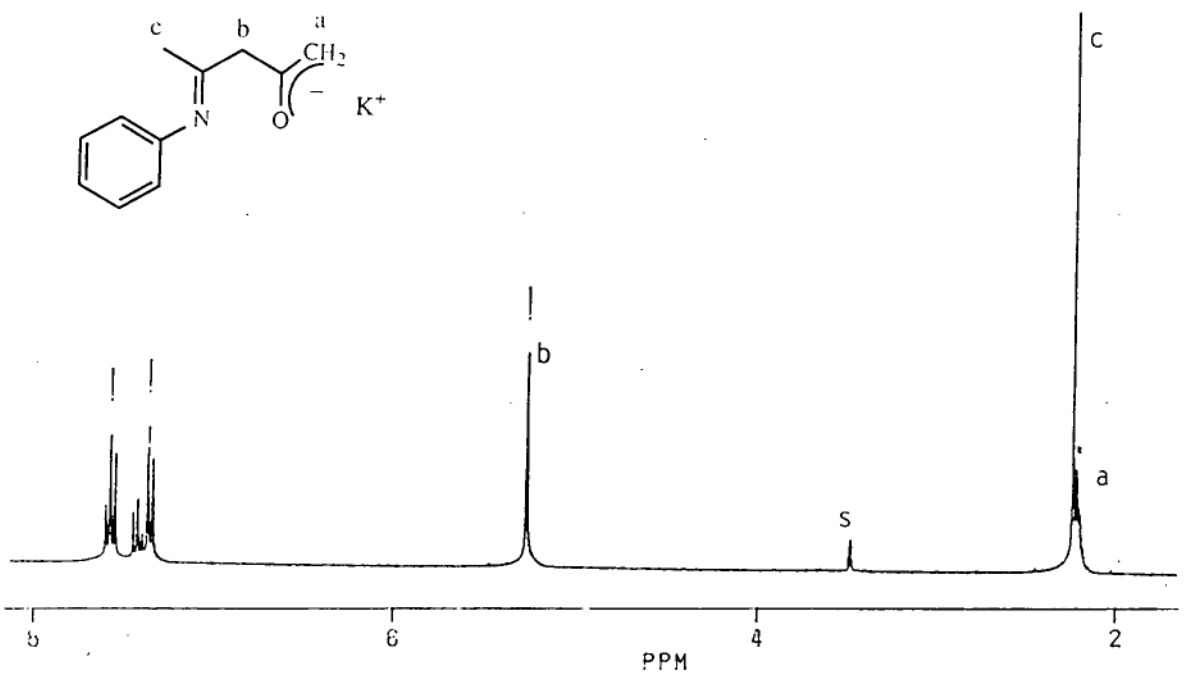

The analogous sodium salts can be generated by reaction of the free ligands with sodium hydride in an appropriate solvent, such as ether, hexane or THF. For ligands of low acidity (e.g. Ph-HNbzbz) heating and longer reaction times were required. If the sodium hydride is relatively pure the sodium β-aminoketonate can be formed *in situ* and then reacted directly with $ZrCl_4$ to give the appropriate bis-ligand complex.

3.5.6. Synthesis of β-Aminoketone Complexes of Zirconium

New synthetic methods had to be developed for the formation of the required bis-ligand zirconium complexes. A number of general methods are available for the synthesis of other zirconium bis-ligand complexes.

1. direct reaction of a metal salt with the ligand,

$$ZrCl_4 + 2R\text{-}HNacac \longrightarrow (R\text{-}Nacac)_2ZrCl_2 + 2HCl \quad [3.20]$$

2. salt elimination,

$$ZrCl_4 + 2R\text{-}MNacac \longrightarrow (R\text{-}Nacac)_2ZrCl_2 + 2MCl \quad [3.21]$$

3. alkane elimination

$$Zr(R')_2Cl_2 + 2R\text{-}HNacac \longrightarrow (R\text{-}Nacac)_2ZrCl_2 + 2H\text{-}R' \quad [3.22]$$

4. metathetical exchange (ligand redistribution reaction),

$$ZrCl_4 + Zr(R\text{-}Nacac)_4 \longrightarrow 2(R\text{-}Nacac)_2ZrCl_2 \quad [3.23]$$

5. reaction of an amide or alkoxide with a protic ligand,

$$Zr(NMe_2)_4 + 2R\text{-}HNacac \longrightarrow (R\text{-}Nacac)_2Zr(NMe_2)_2 + 2HNMe_2 \quad [3.24]$$

Other reactions, such as electrochemical formation, are possible but are less common and are not mentioned here. Reaction 3.24 depends on the acidity of the ligand proton and requires a second transformation to remove amines (or butoxides) before catalysis.

In choosing a synthetic route, one major consideration was, that Lewis base adducts of the bis-ligand complexes would be unsuitable for catalysis and therefore strongly coordinating solvents were to be avoided if possible. To avoid formation of Lewis base adducts would mean alternative synthetic routes would be required.

A salt elimination reaction in a non-coordinating solvent was the preferred synthetic route.

3.5.7. 1. Direct Reaction with a β-Aminoketone

As previously mentioned the addition of the free ligand to $ZrCl_4$ results in adduct formation. This reaction occurs even in the presence of a Lewis base, i.e. triethylamine. Attempted extraction of these adducts in refluxing toluene or THF, i.e. reaction under forcing conditions, did not induce further reaction to form the complexes although some decomposition was noted.

3.5.8. 2. Salt Elimination

Bis-ligand complexes of zirconium chloride could be successfully synthesised by salt elimination after the initial problems of solvent choice and complex stability were overcome (Reaction 3.25).

Synthesis of $(R\text{-}R^1NacR^2ac)_2ZrCl_2$ Complexes

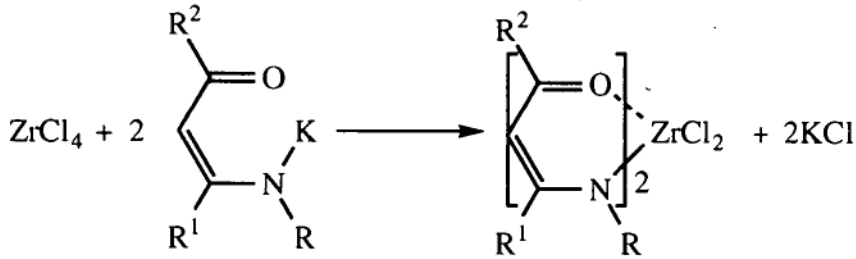

[3.25]

The bis-β-aminoketonate-zirconium complexes are in general pale yellow, moisture and temperature sensitive solids, soluble in coordinating or polar solvents and have been characterised by ^1H-, ^{13}C-NMR and elemental analysis. They are relatively unstable in solution, slowly decomposing above RT in non-coordinating solvents. N-phenyl substituted complexes are significantly more stable than N-alkyl substituted complexes. A CD_2Cl_2 solution of $(Ph\text{-}Nacac)_2ZrCl_2$ under nitrogen showed no significant decomposition at RT after 3-4 days while a solution of $(i\text{-}Pr\text{-}Nacac)_2ZrCl_2$ showed 10-15% decomposition after 24 hours at RT (^1H-NMR data).

3.5.9. 3. Alkane Elimination

It is theoretically possible to generate the required bis-ligand complexes by reaction of a free ligand with an appropriate alkyl/aryl zirconium chloride complex (Reaction 3.26). Although many alkyl- or arylzirconium chloride complexes have been reported[22], this reaction has not been attempted in this study. However, reaction of a free β-aminoketone with a homoleptic zirconium tetraalkyl has been used with great success in generating the related alkylated bis-ligand zirconium complexes (Section 3.7.5).

This reaction was, however, attempted *in situ*, where a zirconium bis-ligand adduct was reacted with an alkyl or aryl lithium reagent to form the required bis-ligand complex. Two alternative mechanisms are possible for this reaction: either alkylation of the metal followed by alkane elimination as the coordinated ligand

reacts, or deprotonation of the coordinated ligand followed by salt elimination to form the required bis-ligand complex. Initial attempts using MeLi, nBuLi or PhLi did not lead to the formation of the required complex when using the *i*-Pr-β-aminoketone adduct. After a number of bis-ligand complexes were isolated using Reaction 3.26 and an understanding of this chemistry had been developed the reaction was repeated and appropriate bis-ligand complexes were formed

Alkane Elimination Reactions for The Generation of $(R\text{-}Nacac)_2ZrCl_2$ type Complexes of Zirconium

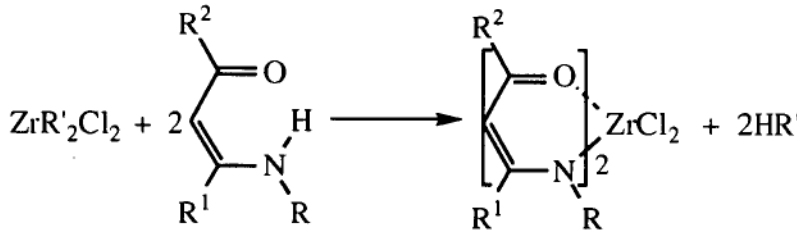

[4.26]

3.5.10. VT-NMR Studies of Bis-β-Aminoketone-Zirconium Dichloride Complexes

Variable temperature ^1H- and ^{13}C-NMR studies indicate that the β-aminoketonate ligands in bis-ligand complexes are clearly bonded through nitrogen and oxygen with no indication of significant line broadening for the backbone methyl groups (^1H δ 1.70 & 1.32ppm) up to 40°C in CD_2Cl_2 (Figure 3.8a & b). The complexes contain a highly delocalised chelate ring as indicated by similar shifts of the amino and carbonyl carbons (^{13}C δ 175.5 & 174.3ppm), which are widely separated in the free ligands (Table 3.4). The amino-phenyl group in the $(Ph\text{-}Nacac)_2ZrCl_2$ complex shows a very dynamic behaviour with a broad resonance for the *meta*-proton (^1H δ 7.34ppm) and split broad resonances for the *ortho*-protons (^1H δ 6.69 & 7.11ppm) which resolve and sharpen with decreasing temperature. The VT-^{13}C-NMR spectra show similar changes.

The reason for the splitting patterns was only indicated when the crystal structure for the $(Ph\text{-}Nacac)_2ZrCl_2$ complex was determined and will be discussed in Section 3.5.11.

All bis-ligand complexes isolated to date have similar NMR spectra with splitting of phenyl resonances or separate environments for alkyl substituted β-aminoketones (see collected spectra in Appendix A.1.0). The NMR data for these new complexes

have been summarised in Table 3.5a & b. It is proposed that the NMR shift of the β-aminoketone backbone methine proton (^{1}H δ ≈5.2ppm) or carbon (^{13}C δ ≈107ppm)) is a good relative indicator of metal centre Lewis acidity reflecting the strength of the chelate ring current. In this case a downfield shift indicates a decreased ring current and therefore an increased Lewis acidity[23]. The amino-phenyl appears to be electron donating in these complexes and phenyl substituents caused only a small variation in metal centre Lewis acidity, i.e. *p*-chlorophenyl increased the metal centre Lewis acidity slightly compared to phenyl substitution. In these complexes the phenyl substituent is a more effective electron donating group than the *iso*-propyl group.

Table 3.4.
Comparative NMR Data for a Free and Complexed β-Aminoketone
Ph-HNacac and $(Ph\text{-}Nacac)_2ZrCl_2$

	Ligand Backbone				Amine Substituent			
	Me's	CH	C-O	C-N	*i*-Ph	*o*-Ph	*m*-Ph	*p*-Ph
^{1}H NMR								
Ph-HNacac	1.978 2.050	5.191				7.135	7.335	7.174
$(Ph\text{-}Nacac)_2ZrCl_2$	1.698 1.322	5.294				6.689, 7.114	7.336	7.192
^{13}C-NMR								
Ph-HNacac	20.35, 29.62	98.19	196.5	160.6	139.6	125.2	129.8	126.0
$(Ph\text{-}Nacac)_2ZrCl_2$	23.38, 25.17	107.2	175.5	174.3	149.3	121.3, 126.6	129.6	126.6

shifts(ppm) in CD_2Cl_2 at RT

Figure 3.8a.

Variable Temperature ^{1}H-NMR Spectra for $(Ph\text{-}Nacac)_2ZrCl_2$

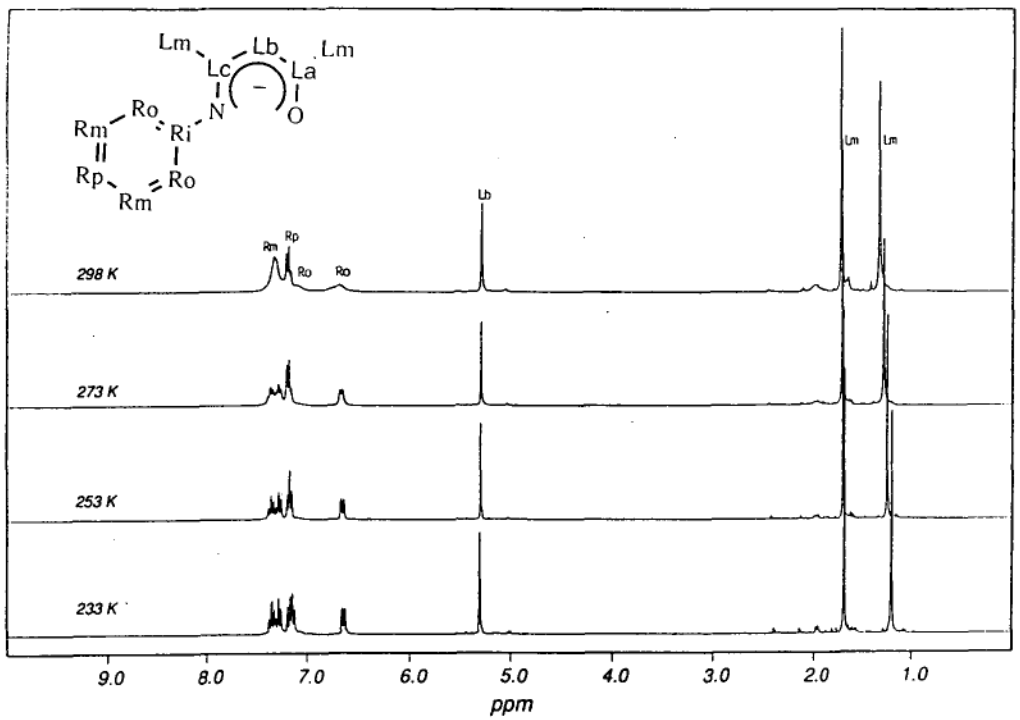

Figure 3.8b.

Variable Temperature ^{13}C-NMR Spectra for $(Ph\text{-}Nacac)_2ZrCl_2$

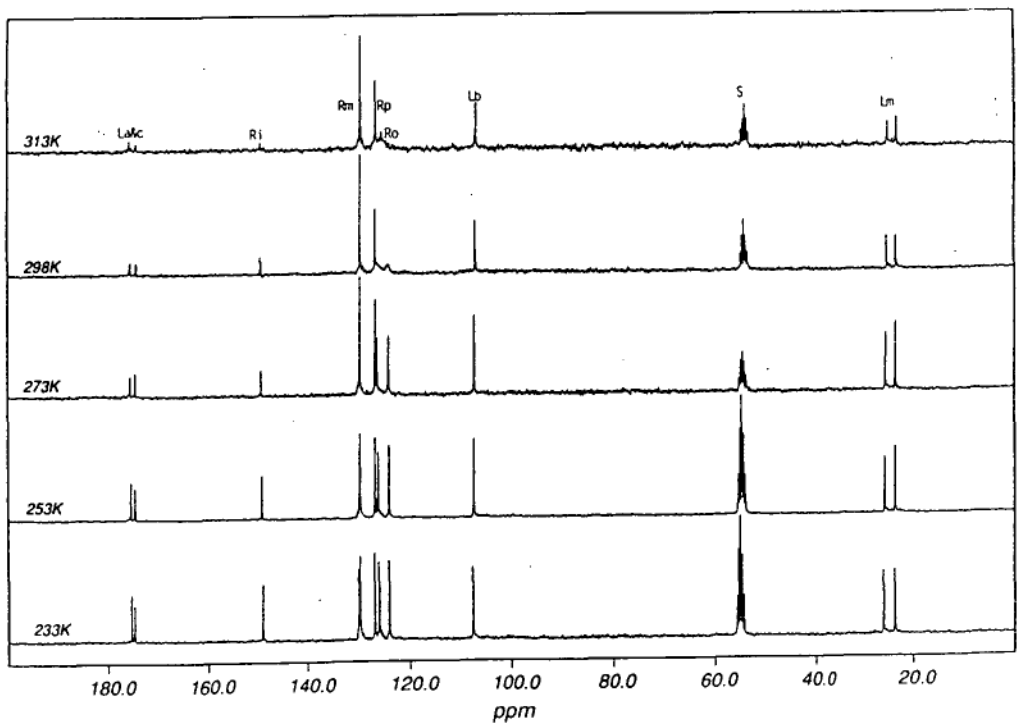

Table 3.5a.

Summary of NMR Data for the Bis-Ligand Complexes, $(R\text{-Nacac})_2ZrCl_2$

	β-Aminoketone Backbone			
	C-O	C-N	Me's	CH
^1H NMR				
$(i\text{-Pr-Nacac})_2ZrCl_2$			2.154 & 1.909	5.398
$(MeOPh\text{-Nacac})_2ZrCl_2$			1.687 & 1.359	5.305
$(Ph\text{-Nacac})_2ZrCl_2$			1.681 & 1.248	5.309
$(ClPh\text{-Nacac})_2ZrCl_2$			1.690 & 1.327	5.341
^{13}C NMR				
$(i\text{-Pr-Nacac})_2ZrCl_2$	173.9 or 172.6	172.6 or 173.9	25.0 & 24.1	109.0
$(MeOPh\text{-Nacac})_2ZrCl_2$	174.7	174.7	25.0 & 23.2	107.2
$(Ph\text{-Nacac})_2ZrCl_2$	174.6 or 174.0	174.0 or 174.6	25.1 & 22.9	107.1
$(ClPh\text{-Nacac})_2ZrCl_2$	175.2 or 174.6	174.6 or 175.2	25.3 & 23.1	107.2

* shifts(ppm) in CD_2Cl_2 at -20°C

Table 3.5b.

Summary of NMR Data for the Bis-Ligand Complexes, $(R\text{-Nacac})_2ZrCl_2$

	Aminoketone Substituent				
^1H NMR			N-CH(CH3)2	N-CH(CH3)2	
$(i\text{-Pr-Nacac})_2ZrCl_2$			4.497(sept)	1.392(d)	
	-OMe		*o*-Ph	*m-Ph*	*p*-Ph
$(MeOPh\text{-Nacac})_2ZrCl_2$	3.755(s)		6.566 & 7.098	6.796 & 6.876	
$(Ph\text{-Nacac})_2ZrCl_2$			6.662 & 7.201	7.295 & 7.373	7.189
$(ClPh\text{-Nacac})_2ZrCl_2$			6.566 & 7.260	7.157 & 7.348	
^{13}C NMR					
			N-CH(CH3)2	N-CH(CH3)2	
$(i\text{-Pr-Nacac})_2ZrCl_2$			52.6	22.2.	
	-OMe	*i*-Ph	*o*-Ph	*m*-Ph	*p*-Ph
$(MeOPh\text{-Nacac})_2ZrCl_2$	55.8	140.9	126.4 & 124.5	114.7& 113.5	157.6.
$(Ph\text{-Nacac})_2ZrCl_2$		148.3	126.1 & 123.3	129.3 & 129.1	125.2.
$(ClPh\text{-Nacac})_2ZrCl_2$		147.0	127.3 & 125.0	129.4	131.6.

* shifts(ppm) in CD_2Cl_2 at -20°C

3.5.11. Crystal Structure of $(Ph\text{-}Nacac)_2ZrCl_2$

Crystals of the bis-ligand complex, $(Ph\text{-}Nacac)_2ZrCl_2$, suitable for structural analysis were obtained by slow cooling of a saturated toluene/DCM solution. The monomeric complex contains zirconium in a slightly distorted octahedral environment with a chloride channel chain running through the structure (see Figure 3.9). This channel lies in the plane of the page running from left to right. All chloride atoms lie above the plane while all ligand atoms lie on or below the plane (crystal structure data and a diagram of the unit cell are shown in Appendix IV).

Figure 3.9.

Crystal Structure of the Bis-Ligand Complex $(Ph\text{-}Nacac)_2ZrCl_2$

(measured by Dr. A. White, University of Western Australia, Perth.)

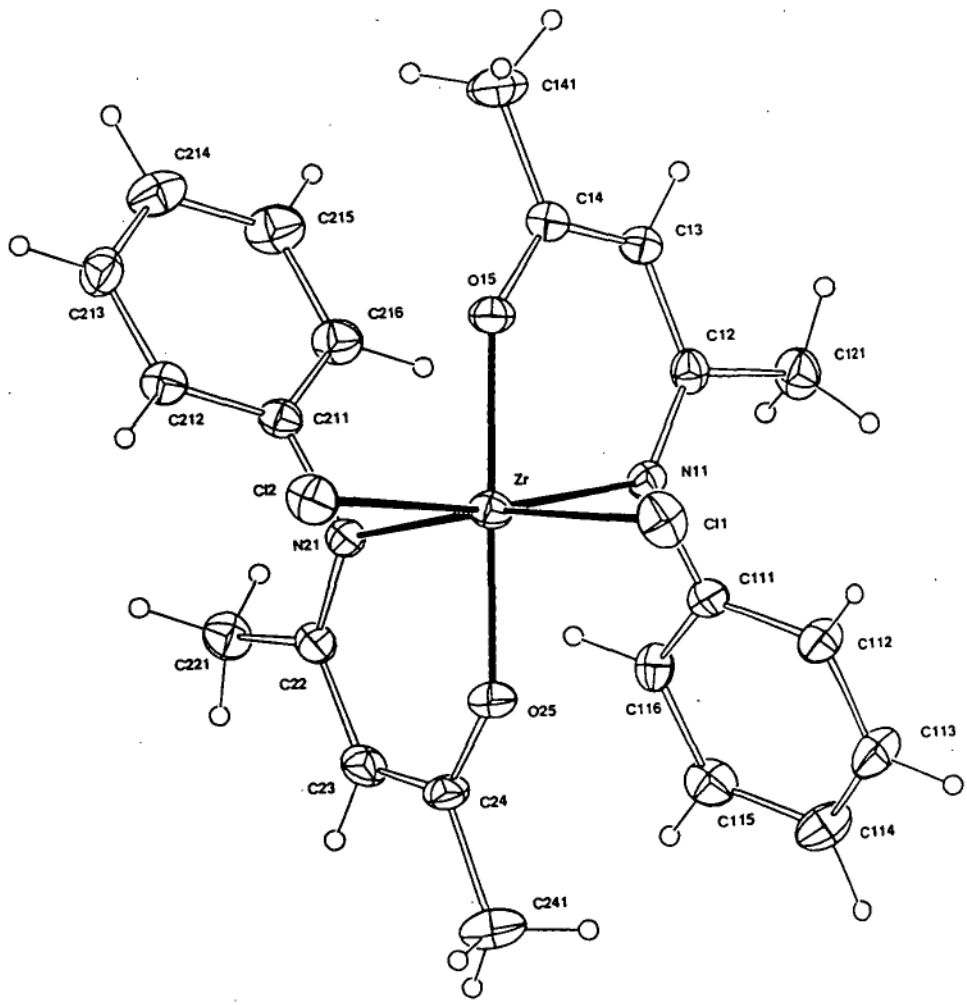

The oxygen atoms are trans to each other while, unexpectedly, the nitrogen atoms are *cis* , presumably due to unfavourable steric interactions between the amino-substituent and the carbonyl methyl on the second ligand if the nitrogen atoms were *trans*. In this orientation the amino-phenyl substituents can align roughly parallel with the chelate ring formed by the second ligand, but being offset, thereby bringing one *ortho*-carbon in line with the centre of the chelate ring while the other approaches one of the chlorides leading to significantly different environments for the two ortho protons. The VT-NMR data indicates that this structure is maintained in solution although the degree of association is unknown.

Ligand deprotonation to form the ligand chelate is accompanied by an electronic redistribution as expected. The C-N and C-O bond lengths increase slightly compared with the adduct and the C1-C2 carbon double bond is shortened but an en-imine structure is assigned(Table 3.6). The presence of the highly Lewis acidic metal centre appears to remove electron density from the chelate ring keeping all distances shorter than in a similar palladium complex, (π-methallyl)(2-(R,S)-α-2-Ph-Et-Nacac)Pd(II) where an imine type structure is more apparent. This is compared directly with the cationic titanium complex where the C-O and C-N distances are considerably shorter, due to the higher Lewis acidity of the cationic titanium centre.

Table 3.6.

Important Bond Lengths for R-Nacac Containing Species

	Bond			
	O(1)-C(1)1	C(1)1-C(1)2	C(1)2-C(1)3	C(1)3-N(1)
Typical	1.24	1.34		1.30
ZrCl4:2*i*-Pr-HNacac	1.303(2)	1.363(3)	1.425(3)	1.307(3)
(Ph-Nacac)$_2$ZrCl$_2$	1.323(6)	1.337(7)	1.430(7)	1.321(5)
Cp$_2$Ti(H-Nac(tmpPh)ac)$^+$ [a]	1.266(13)	1.342(17)	1.431(18)	1.271(15)
(π-methallyl)(2-(R,S)-α-(2-Ph)-Et-Nacac)Pd [b]	1.34(2)	1.38(2)	1.51(3)	1.28(3)

[a]Claverini, R.; Ganis, P.; Pedone, C., *J. Organometallic Chem.* 50, **1973**, 327-332, counter ion $CF_3CO_3^-$.

[b]Veya, P.; Floriani, C.; Chesi-Villa, A.; Rizzoli, C., *Organometallics* 12, **1993**, 4892-4898.

Metal-oxygen and metal-nitrogen distances appear to be short compared to other reported distances, although values for directly comparable complexes are difficult to find. A selection of values is presented in Table 3.7.

Table 3.7.

Important Bond Lengths for R-Nacac Containing Species

	Zr-O	Zr-S	Zr-N
$(Ph\text{-}Nacac)_2ZrCl_2$	2.009		2.306
ZrCl4:2*i*-Pr-HNacac			
$Zr(acac)_4$	2.198		
$Zr(Sacac)_4$	2.185, 2.132	2.724, 2.665	
$Zr(8\text{-}O\text{-}Quin)_4$ *	2.106		2.405
$Zr(Et\text{-}NPhO)_4$ *	2.055		2.539
$Zr(acac)_2(NO_3)_2$ *	2.096		

* Wilkinson, G., Comprehensive Coordination Chemistry, Vol.3, Main Group and Early Transition Metals, Pergamon Press **1987**, (32) 363-451; 8-O-Quin = 8-quinolinato and Et-NPhO = N-ethylsalicylaldiminato

Catalytic testing of bis-ligand zirconium complexes indicated a significant increase in reactivity and a higher average oligomer weight compared to *in situ* testing of free ligands or adducts. The assumption that the active species derived from all these systems would be identical appears to be incorrect. The proposed reason, discussed in detail in Chapter 5.3.0, is that under the test conditions the amino proton is not acidic enough in all cases to react with the added cocatalyst, forming instead a N-Al adduct which leads to a significantly different environment around the metal centre during catalysis. Also it is believed that where deprotonation occurs ligand exchange reactions are slow or do not proceed leading to different species in solution.

3.5.12. Synthesis of β-Aminothioketones Complexes of Zirconium

β-Aminothioketones, the sulfur analogues of the β-aminoketones, are readily obtained from the respective β-aminoketone by thiolation[24] (Reaction 3.27). They are also accessible from dithiolium salts by reaction with a primary amine[25] or by thiolation with Lawesson's reagent[26]. Initial *in situ* catalytic testing indicated that β-aminothioketones were not as effective as the β-aminoketones in promoting the zirconium based oligomerisation reaction and consequently only a small number of the thiolated analogues have been generated.

Potassium β-aminothioketonates can be formed using the same synthetic method as for potassium β-aminoketonates and one bis-β-aminothioketone complex has been isolated, $(i\text{-Pr-NacSac})_2ZrCl_2$. This complex appears to be less stable than the β-aminoketone analogue.

Thiolation of β-Aminoketones

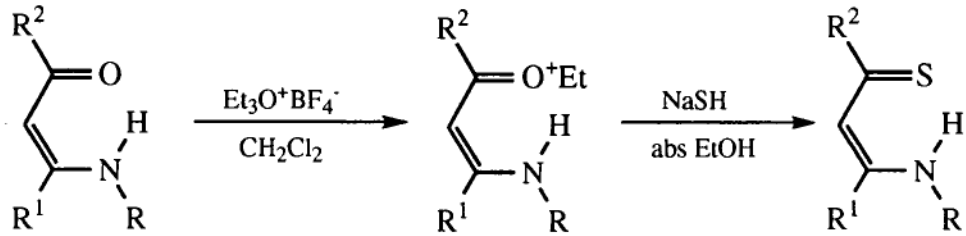

[3.27]

3.6.0. Bis-Ligand Alkyl Zirconium Complexes

Proposed intermediates in the polymerisation/oligomerisation process include alkylated metal centres formed through interactions with added cocatalyst. The preparation of alkylzirconium β-aminoketonates was therefore considered important. Three general methods have been tried for the formation of alkylated zirconium species;

1. Salt elimination, i.e. direct alkylation of the metal.

$$(R\text{-Nacac})_2ZrCl_2 + nMR' \longrightarrow (R\text{-Nacac})_2ZrR'_nCl_{2-n} + nMCl \qquad [3.28]$$

2. Metathetical exchange (ligand redistribution reaction).

$$ZrR'_4 + ZrL_4 \longrightarrow 2L_2ZrR'_2 \qquad [3.29]$$

3. Alkane elimination,

$$ZrR'_4 + nR\text{-HNacac} \longrightarrow (R\text{-Nacac})_nZrR'_{4-n} + nHR' \qquad [3.30]$$

Very few complexes of the type ZrL_nR_{4-n}, where L is a monovalent, bidentate, chelate ligand, have been reported[27]. Bulky R-groups or groups which do not undergo β-elimination are required to stabilise the complexes (i.e. $Zr(acac)(CH_2SiMe_3)_3$ and $Zr(acac)_2(CH_2SiMe_3)_2$). These complexes[28] were formed via alkane elimination from the homoleptic alkyl during an NMR experiment at

-70°C and no comment was made about their stability above -20°C, although disproportionation of the $Zr(acac)(CH_2SiMe_3)_3$ complex was noted at this temperature.

i. Salt Elimination Reactions

Complex stability appears to be a significant problem with alkylated bis-ligand zirconium complexes and initial attempts to form species of this type via salt elimination reactions (where L= acac-) did not lead to an isolable product (Reaction 3.31). This was later found to be due to the instability of these complexes under the reaction conditions used.

Alkylated Zirconium Complexes via Salt Elimination Reactions

$$Zr(acac)_2Cl_2 + nMR \xrightarrow[<0°C]{ether} Zr(acac)_2R_nCl_{2-n} + MCl \qquad [3.31]$$

(or RMgCl) where R=Ph, Me, Bz M=Li
R=Bz M=K,Mg

ii. Metathetical Exchange Reactions

Attempts to isolate hydrocarbyl complexes using ligand redistribution reactions were also unsuccessful (Reaction 3.32). During reaction gold coloured solutions, possibly containing the desired complexes, were generated below -40°C but the colour was slowly lost at -20°C or above.

$$ZrL_4 + ZrBz_4 \xrightarrow[<-40°C]{toluene} 2ZrL_2Bz_2 \quad L= acac^-, hfacac^- \qquad [3.32]$$

iii. Alkane Elimination Reactions

Alkylated bis-ligand zirconium complexes were readily synthesised by alkane elimination reactions. The homoleptic tetraalkyl complex, $ZrBz_4$, has been employed in this study. The method also allows easy monitoring of preliminary reactions on an NMR scale to determine approximate complex stabilities. In these small scale tests the reactants were mixed in the appropriate molar ratio at ~-70°C to -80°C in deuterated DCM or toluene and the reaction monitored as the temperature was slowly increased to RT or above.

In these tests it was easy to determine stability regimes for the majority of target complexes in this study. It was shown that benzylzirconium-acac's are not stable above -40°C, confirming previously reported results, discussed above. This also confirmed that the attempted salt elimination reactions would not give products under the conditions used. The complexes decompose by ligand coupling forming benzyl-acac or dibenzyl species, as confirmed by MS after hydrolysis and workup. In general, benzyl complexes were significantly more stable if N-phenyl-β-aminoketones were employed. Approximate stabilities for a number of benzyl bis-ligand complexes of zirconium are shown in Table 3.8.

Table 3.8.
Approximate Stabilities of Benzylated Zirconium Complexes
Determined from VT-NMR Experiments*

Ligand	Ratio L:Zr	Initial Reaction °C	Complex Decomposes °C
i-Pr-HNacac	2:1	-60	≈0
t-Bu-HNacac	2:1	-60	≈-10
Cy-HNacac	2:1	-30	>20
i-Pr-HNtfac	2:1	-20	>40
i-Pr-HNacSac	2:1	-20	>20
Ph-HNacac	2:1	-60	>20
Picolinic Acid	2:1	<-60	≈-50
i-Pr-NPhOH	2:1	<-60	≈0
HOPh-HNacac	1:1	<-60	<-60
Hacac	2:1	<-60	≈-40

*Reactions completed in CD_2Cl_2 at -60 to 30°C with 10-20μmoles of $ZrBz_4$ over 4-6 hours.

Data in Table 3.8 indicate that the phenyl substituted β-aminoketone formed a relatively stable benzyl zirconium complex as does the CF_3-substituted *iso*-propyl-β-aminoketone (*i*-Pr-HNtfac). Alkyl substituted β-aminoketones and the Schiff's base (*i*-Pr-NPhOH) have lower stabilities but could probably still be isolated. Benzyl complexes of picolinic acid, the phenol substituted β-aminoketone and Hacac, with decomposition temperatures of less than -40°C, are not stable enough for isolation.

The relative stability of the β-aminothioketone is of interest, indicating that the sulfur analogues of the isolated β-aminoketone species may also be isolable.

A typical set of spectra from one VT-^{1}H-NMR experiment is shown in Figure 3.10. Reaction is indicated by the loss of the broad amino-proton resonance of the free ligand (δ 9.5ppm), the presence of toluene resonances (δ 2.3 & 7.1-7.3ppm) and the formation of a single set of ligand resonances at 273K (ligand δ 2.00 & 1.89, Me's; 5.21, CH; 1.08,*i*-Pr-Me; 3.6, *i*-Pr-CH; benzyl δ 1.84, CH_2; 6.6-7.0, Ph).

Figure 3.10.
In situ Generation of (*i*-Pr-Nacac)$_2$ZrBz$_2$
VT-NMR Experiment

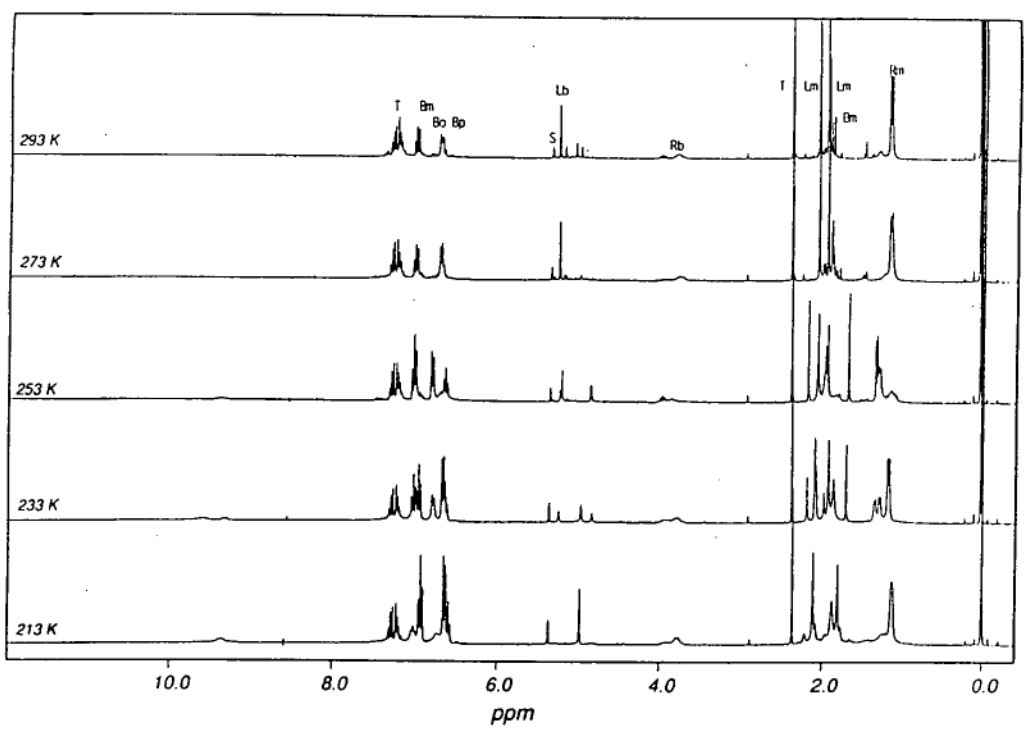

$ZrBz_4$ + 2*i*-Pr-HNacac --> (*i*-Pr-Nacac)$_2$$ZrBz_2$ + 2 Toluene
Where s=solvent (CD_2Cl_2); T=toluene; b=benzyl; CH=ligand methine; Me=ligand methyl; iPr=*i*-Pr methine; iPr-Me=*i*-Pr methyl.

It is proposed that the reaction mechanism involves ligand coordination followed by rapid deprotonation of one ligand followed by slow reaction of the second ligand at above -40°C. This is indicated by the presence of toluene, non-deprotonated ligand and by the large downfield shift of the benzyl methylene peak, from 1.35ppm

($ZrBz_4$) to 1.80ppm on ligand coordination, at -60°C. Decomposition is indicated by the formation of a number of ligand environments at higher temperatures (20°C) with time.

3.6.1. Synthesis of Bis-Ligand Alkyl Zirconium Complexes

The data in Table 3.8 allowed selection of those complexes most likely to be stable under working conditions and therefore isolable on a larger scale. All β-aminoketone complexes listed in Table 3.8, which had a decomposition temperature above 0°C, have been isolated as dark burgundy or orange coloured solids. They are extremely air and moisture sensitive and due to the presence of the benzyl group are light sensitive (as is $ZrBz_4$[29]). Complexes have been examined by ^1H- and ^{13}C-NMR. Their extreme air and moisture sensitivity led to difficulties in obtaining acceptable MS or microanalytical data in most cases, i.e. analysis calculated for (*i*-Pr-Nacac)$_2ZrBz_2$ ($C_{30}H_{40}N_2O_2Zr$), C, 65.05; H, 7.64; N, 5.06: Found C, 63.67; H, 7.75; N, 5.36. The NMR spectra of these complexes and detailed discussion of ligand bonding modes is covered in Chapter 5.2.0.

These complexes represent an exiting and new area of organometallic chemistry, i.e. "stable" alkyl zirconium complexes containing monovalent, bidentate, chelate ligands.

3.7.0 Cationic Zirconium Complexes

Important research by Jordan, Bochmann, Hlatky etc., discussed in Chapter 2.4.4, indicated that cationic species may play a central role in zirconium based polymerisation chemistry. Any study comparing oligomerisation and polymerisation mechanisms would need to include such important species.

In this study new reactive cationic zirconium complexes have been isolated. Significantly, these are non-Cp containing, alkyl zirconium complexes with monovalent, bidentate, chelate ligands. These complexes, in the absence of a cocatalyst, polymerise rather than oligomerise ethylene (Chapter 4.3.6).

3.7.1. Synthetic Routes

Two general synthetic routes have been reported for the preparation of cationic, d^0, 14-electron zirconium species. Jordan has used a one electron oxidation of dialkyl zirconocenes with ferricinium tetraphenylborate[30] (Reaction 3.33).

Formation of Cationic, 14-electron, d^0 Zirconocene Complexes
by a One Electron Oxidation Dimethylzirconocene

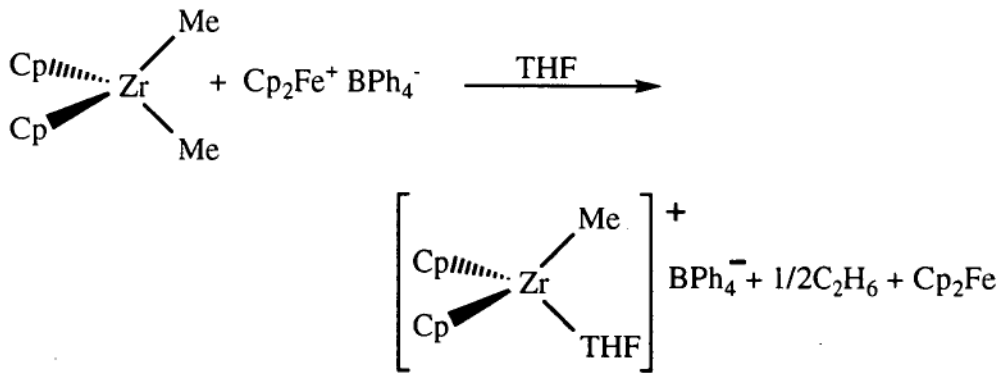

[3.33]

Bochmann initiated the use of tertiary ammonium salts of tetraphenylborate for the partial protolysis of alkyl zirconium species[31] (Reaction 3.34). To decrease the strong cation-anion interactions described by Bochmann (i.e. π-arene interaction of one phenyl of the tetraphenylborate due to formation of a highly Lewis acidic metal centre) a number of fluorinated tetraphenylborates are now commonly used[32]. Also, to decrease possible interaction due to the tertiary amines non-coordinating alkyl trapping groups are used (i.e. the trityl cation).

Formation of Cationic, 14-electron, d^0 Zirconium Complexes
by the Partial Protolysis of Homoleptic Alkyl Zirconium Species

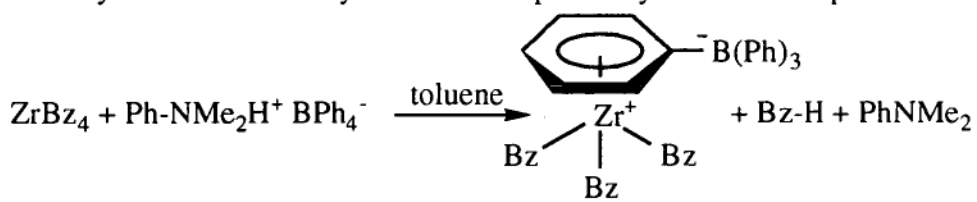

[3.34]

An alternative but related synthesis to that of Bochmann involves an alkyl transfer from the zirconium species to a fluorinated triphenylborine[33] (Reaction 3.35).

However, due to the high Lewis acidity of the metal centre, anion-cation interactions are still possible and a π-arene interaction is present in the final product if R=Bz.

Formation of Cationic, 14-electron, d^0 Zirconocene Complexes by Alkyl Transfer

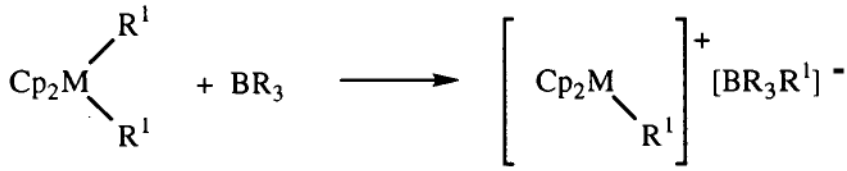

R^1=H, Me, Bz [3.35]

3.7.2. Synthesis of [(R-Nacac)$_2$ZrBz][BPh$_4$] Complexes

Cationic, bis-β-aminoketone complexes of zirconium have been prepared in this work by partial protolysis of bis-alkylzirconium-bis-β-aminoketonates with dimethyl-analinium tetraphenylborate (Reaction 3.36) or by reaction of the free ligand with the cationic tris-benzylzirconium species in DCM at low temperature (Reaction 3.37). The very moisture and air sensitive complexes are difficult to obtain pure (as has been reported for other cationic zirconium species[34]) and have been characterised by ^{1}H and ^{13}C-NMR.

Formation of Cationic, bis-β-aminoketone Complexes of Zirconium

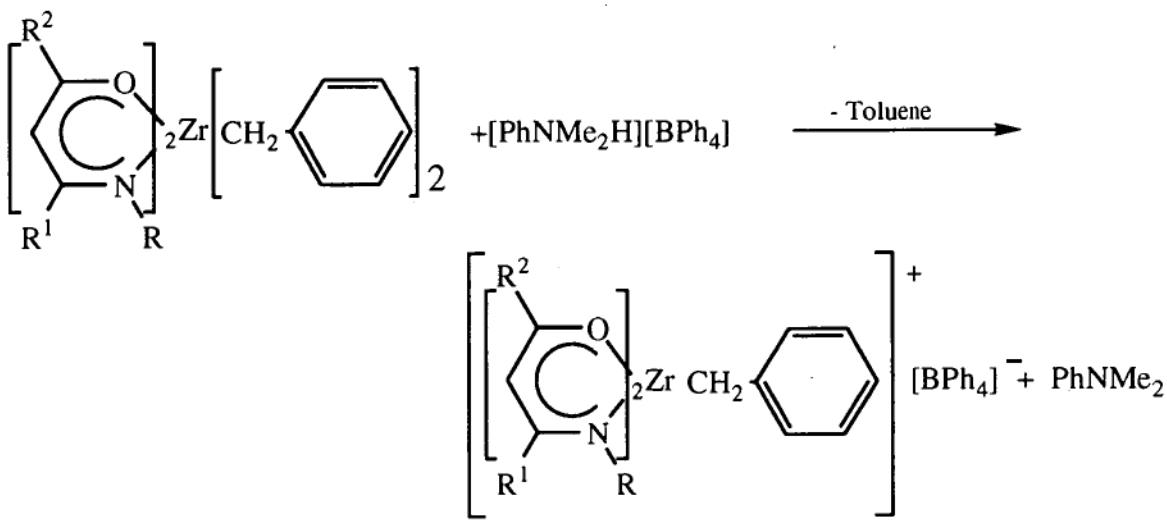

[3.36]

The formation of cationic species is dependent on the β-aminoketone substituents. For simple N-alkyl substituted β-aminoketones the cationic species form. In the case of N-phenyl substituted β-aminoketones or trifluoro-substituted β-aminoketones, the required bis-ligand cationic species are not generated. Ligand redistribution is believed to occur with formation of the tris-ligand species, $[(Ph\text{-}Nacac)_3ZrBz][BPh_4]$ and unreacted $[ZrBz_3][BPh_4]$. Unreacted $[ZrBz_3][BPh_4]$ was isolated from the reaction mixture. The VT-NMR data is presented in the next chapter.

$$[ZrBz_3][BPh_4] + 2\ R\text{-}HNacac \xrightarrow[-20°C]{DCM} [(R\text{-}Nacac)_2ZrBz][BPh_4] + Toluene \qquad [3.37]$$

The use of tri-*n*-butylammonium tetraphenylborate lead to the formation of cationic complexes with coordinated tri-n-butylamine which could not be removed by drying under vacuum.

3.8.0. Schiff's Base Complexes of Zirconium

A number of zirconium adducts and complexes of semicarbazides, semicarbazones, aminophenols and ethanolamines have been reported in which the ligands show monodentate N, O(S) or bidentate coordination. By far the largest group of potentially bidentate, or higher coordination nitrogen and oxygen containing ligands, are the Schiff's bases providing mono-, bi-, tri- or tetradentate ligands of varying valency[1]. Bidentate Schiff's bases fall within the selection criteria for ligands in this study and, although they are relatively rigid and the potential for substituent variation was limited, were of sufficient interest to be compared to other selected ligand systems.

It has been reported that under mild conditions $ZrCl_4.2L$ (L=Schiff's base) adducts are formed, with the Schiff's base acting as a N-bonded monodentate ligand, based on IR investigations[1].

The monovalent, bidentate ligand complexes, $Zr(L)_nX_{4-n}$, can be formed by a number of methods, heating the adducts in refluxing toluene (Reaction 3.38), reacting the primary amine with salicylaldehydato-zirconium complexes, reaction of the free ligand with $Zr(NMe_2)_4$ or reaction of a Schiff's base salt with $ZrCl_4$. The

$Zr(L)_2Cl_2$ complexes (L=Schiff's base) are insoluble in all solvents tested, even under reflux (i.e. toluene, THF, DCM and chloroform). Due to the poor solubilities of the complexes, thought to be due to polymeric chloride bridged structures[1], purification was a problem and satisfactory elemental analyses were not obtained.

[3.38]

Concurrent catalytic test work indicated poor catalytic reactivities for systems containing these Schiff's bases, therefore further test work was restricted to VT-NMR experiments reacting $ZrBz_4$ with Schiff's bases to examine the stability of related alkylated complexes (discussed in Section 3.7.0).

3.9.0. Picolinic Acid Complexes of Zirconium

Picolinic acid is an alternative monovalent, potentially bidentate chelate ligand which, as with the Schiff's bases, has been found in this study to form insoluble bis-ligand zirconium complexes which, due to a proposed polymeric structure, are difficult to purify and characterise[1].

Concurrent catalytic testing indicated that systems containing picolinic acid showed poor activity and therefore synthetic work was terminated except for examination of thermal stabilities of benzyl zirconium complexes in VT ^{1}H-NMR experiments. Such experiments showed that these complexes had very poor stabilities and decomposed at ≈-50°C (Section 3.7.4).

3.10.0. Discussion

In this study examples of all the required target molecules containing β-aminoketones have been synthesised, or at least synthesis has been attempted, with the concurrent development of suitable synthetic methods. These species include the new fundamentally and catalytically interesting complexes: $ZrCl_4$:bis ligand adducts,

bis-β-aminoketone zirconium complexes, bis-β-aminoketone alkylzirconium complexes and cationic bis-β-aminoketone alkylzirconium complexes.

β-Aminoketone ligands have proved to be effective in stabilising new alkylzirconium complexes. The β-aminoketone amino substituents, in the new bis-ligand complexes, exhibit unusual fluxional behaviour on the NMR time scale due to a non-symmetric ligand environments. β-Aminoketone ligands appear to act as bidentate chelate ligands in these complexes and it is proposed that the NMR shift of the methine proton or carbon acts as a relative measure of metal centre Lewis acidity, a downfield shift indicates an increased metal centre Lewis acidity. Ligand bonding modes for the alkylzirconium complexes are discussed in Chapter 5.

A number of general synthetic methods have been developed for the synthesis of β-aminoketone containing complexes. The bis-ligand complexes are accessible via salt elimination reactions or via the *in situ* reaction of bis-ligand adducts with an alkyl lithium reagent. It has not been possible to react the free ligand directly with $ZrCl_4$. This synthetic route may be possible for β-aminoketones which, due to strongly electron withdrawing groups on the amine or ligand backbone, should be more acidic.

Alkylzirconium complexes containing β-aminoketones are readily accessible from homoleptic tetraalkyls by direct reaction with the free ligand. These complexes represent an exiting and new area of organometallic chemistry, i.e. stable alkyl zirconium complexes containing monovalent, bidentate, chelate ligands.

1 Wilkinson, G., *Comprehensive Coordination Chemistry*, Vol.3, Main Group and Early Transition Metals, Pergamon Press **1987**, (32) 363-451.

2 Dudek, G.O.; Holm, R.H., *J. Am. Chem. Soc.* 84, **1962**, 2961-2969.

3 Blitz, W.; Clinch, J.A., *Z. Anorg. Allg. Chem. I* 40, **1904**, 218.

4 a. Duus, F.; Anthonson, J.W., *Acta Chim. Scand.* B31, **1977**, 40-46.
b. Chaston, S.H.H.; Livingston, S.E.; Lokyer, T.N.; Pickles, V.A., *Aust. J. Chem.* 18, **1965**, 673-689.
c. Duus, F., *J. Org. Chem.* 42(19), **1977**, 3123-3127.

5 Mayer, K.; Hiller, G.; Nitzschke, M.; Jentsch, J., Agnew. Chem. 75(21), 1963, 1011-1014.

6 a. Duus, F., *Synthesis* **1985**, 672-674.
b. Carlsen, L.; Duus, F., *Synthesis* **1977**, 256-258.
c. Uhlemann, E.; Müller, H., *Angew. Chem.* 77(4), **1965**, 172.

7 a. Scheeren, J.W.; Ooms, P.H.J.; Nivard, R.J.F., *Synthesis* **1973**, 149-151.
b. Trebaul, C., *Bull. Soc. Chem. France* 3, **1973**, 1102-1103.

8 a. Pederson, B.S.; Scheibye, S.; Clausen, K.; Lawesson, S.-O., *Bull, Soc. Chim. Belg.* 87(4), **1978**, 293-297.
b. Pederson, B.S.; Scheibye, S.; Nilsson, N.H.; Lawesson, S.-O., *Bull, Soc. Chim. Belg.* 87(3), **1978**, 223-228.
c. Scheibye, S.; Pederson, B.S.; Lawesson, S.-O., *Bull, Soc. Chim. Belg.* 87(3), **1978**, 229-238.
d. Scheibye, S.; Pederson, B.S.; Lawesson, S.-O., *Bull, Soc. Chim. Belg.* 87(4), **1978**, 299-306.

9 Mayer, R.; Scheithauer, S., *Methoden der organische Chemie* vierte Auflage;Band E5, Falbe, J. (Ed.); Houben-Weyl, Stuttgart **1985**, 785-799.

10 Henecka, H.; Kurtz, P., *Methoden der organische Chemie* vierte Auflage; Sauerstoffverbindungen III, Falbe, J. (Ed.), Eugen Müller, Tübingen **1952**, 697-699.

11 Silver, M.E.; Chun, H.K.; Fay, R.C., *Inorg. Chem.* 21, **1982**, 3765-3771.

12 Siimann, O.; Fresco, J., *Spectrochimica Acta* 27A, **1971**, 673-682.

13 a. Barraclough, C.G.; Martin, R.L.; Stewart, I.M., *Aust. J. Chem.* 22, **1969**, 891-904.
b. Hendrickson, A.R.; Martin, R.L., *Aust. J. Chem.* 25, **1972**, 251-271.
c. Bond, A.M.; Hendrickson, A.R.; Martin, R.L., *J. Am. Chem. Soc.* 95(5), **1973**, 1449-1456.

14 Klingsberg, E., *J. Am. Chem. Soc* 83, **1961**, 2934-2937.

15 $ZrCl_4.2THF$
a. Manzer, L.E., *Inorg. Synth.* 21, **1982**, 135.
$Zr(bpy)_3$
b. Fowles, G.W.A.; Willey, G.R., *J. Chem. Soc.* A **1968**, 1435-1438.
$[ZrCl_3(PBu_3)_2]_2$
c. Wengrovis, J.H.; Schrock, R.R.; Day, C.S., *Inorg. Chem.* 20, **1981**, 1844-1849.
d. Wengrovis, J.H.; Schrock, R.R., *J. Organometallic Chem.* 205, **1981**, 319-327.
$[ZrCl_3dppe]_4$
e. Cotton, F.A.; Diebold, M.P.; Kibala, P.A., *Inorg. Chem.* 27, **1988**, 799-804.
f. Cotton, F.A.; Kibala, P.A., *Inorg. Chem.* 29, **1990**, 3192-3196.

16 Rechsteiner, B.; Texier-Boullet, F.; Hamelin, J., *Tettrhedron Letters* 34(32), **1993**, 5071-5074.

17 Shin, H.K.; Hampden-Smith, M.J.; Kodas, T.T.; Rheingold, A.L., *J. Chem. Soc., Chem. Comm.* **1992**, 217-219.

18 Uhrhammer, R.; Black, D.J.; Gardner, T.G.; Olsen, J.D.; Jordan, R.F., *J. Am. Chem. Soc.* 115, **1993**, 8493-8494.

19 Weast, R.C.; Editor in Chief *CRC Handbook of Chemistry and Physics, 66th ed.*; CRC Press, Inc.; Boca Raton, Florida, **1985**.

20 a. Martin, D.F.; Janusonis, G.A.; Martin, B.B., *J. Am. Chem. Soc.* 83, **1961**, 73-75.
b. Everett, G.W.; Holm, R.H., *J. Am. Chem. Soc.* 87, **1965**, 2117-2127.
c. Holm, R.H.; Röhrscheid, F.; Everett, G.W., *Inorg. Synthesis* 11, **1968**, 72-82.

21 Veya, P.; Floriani, C.; Chesi-Villa, A.; Rizzoli, C., *Organometallics* 12, **1993**, 4892-4898.

22 a. Thiele, K.H., *Pure & Applied Chemistry* 30, **1975**, 575-585.
b. Clarke, J.F.; Fowles, W.A.; Rice, D.A., *J. Organometallic Chem.* 76, **1974**, 349-353.
c. Razuvaev, G.A.; Latyaeva, V.N.; Vishinskya, L.I.; Rabinovitch, A.M., *J. Organometallic Chem.* 49, **1973**, 441-444.
d. Thiele, K.H.; Krüger, J., *Z. Anorg. Allg. Chem.* 383, **1971**, 272-278.
e. Clarke, J.F.; Fowles, W.A.; Rice, D.A., *J. Organometallic Chem.* 74, **1974**, 417-422.

23 A range of similar complexes synthesised during a catalyst optimisation program for a later patent application has confirmed this. These complexes include a larger range of ligands with electron withdrawing or releasing substituents on the ligand backbone and amino-phenyl substituent.

24 Blum, P.R.; Wei, R.M.C.; Cummings, S.C., *Inorg. Chem.*. 13(2), **1974**, 450.

25 a. Gerlach, D.H.; Holm, R.H., *J. Am. Chem. Soc.* 91(13), **1965**, 3457-3467.
b. Klingsberg, E., *J. Am. Chem. Soc.* 83, **1961**, 2934-2937.
c. Leaver, D.; McKinnon, D.M.; Robertson, W.A.H., *J. Chem. Soc.* **1965**, 32-40.
d. Leaver, D.; McKinnon, D.M.; Robertson, W.A.H., *J. Chem. Soc.* **1962**, 5104.

26 Walter, W.; Proll, T., *Synthesis, Comm.* **1979**, 941.

27 Cardin, D.J.; Lappert, M.F.; Raston, C.L., *Chemistry of Organo-Zirconium and -Hafnium Compounds*, Ellis Horwood Limited,Chichester, **1986**, 373-388.

28 Collier, M.R.; Lappert, M.F.; Pearce, R., *J. Chem. Soc. Dalton* **1973**, 445-451.

29 Zucchini, U.; Albizzati, E.; Giannini, U., *J. Organometallic Chem.* 26, **1970**, 1491.

30 a. Jordan, R.F.; Dasher, W.E.; Echols, S.F., *J. Am. Chem. Soc.* 108, **1986**, 1718-1719.
b. Jordan, R.F.; La Pointe, R.E.; Bajur, C.S.; Echols, S.F.; Willett, R., *J. Am. Chem. Soc.* 109, **1987**, 4111-4113.

31 Bochman, M.; Karger, G.; Jagger, A.J., *J. Chem. Soc., Chem. Commun.* **1990**, 1038-1039.

32 Strauss, S.H., *Chem. Rev.* 93, **1993**, 927-942.

33 a. Pellecchia, C.; Grassi, A.; Zambelli, A., *J. Mol. Catal.* 82, **1993**, 57-65.
b. Pellecchia, C.; Grassi, A.; Zambelli, A., *Organometallics* 13, **1994**, 298-302.
c. Pellecchia, C.; Grassi, A.; Zambelli, A., *Organometallics* 12, **1993**, 4473-4478.

34 Bochman, M., Lancaster, S.J., *Organometallics* 13, **1994**, 2235-2243.

Chapter 4

Catalysis

4.0.0. Introduction

As the broad goal of this research project was to provide a general base upon which further studies could be conducted, a general overview of active catalytic systems was planned. During this phase of the work a number of ligand systems, selected using knowledge and expertise available in this research group, were to be examined in zirconium based oligomerisation systems . General trends and relative activities then allowed selection of target groups of complexes for further synthetic, catalytic or NMR studies.

Zirconium based oligomerisation catalysts can be broadly divided into two groups; those using preformed adducts or complexes or those prepared *in situ* by mixing the required chemicals in the required stoicheiometry. The first group is typified by the work of Young[1] who examined alkyl acetate adducts of zirconium in the presence of an alkylaluminium (Reaction 4.1). *In situ* catalyst formation is typified by the work of Shiraki[2] who used active catalysts formed by the stepwise addition of components (Reaction 4.2). Often, the order of reagent mixing and cocatalyst selection play an important role and for zirconium based oligomerisation systems the most frequently used cocatalyst is ethylaluminium sesquichloride (EASC), $Et_3Al_2Cl_3$.

$$ZrCl_4.(CH_3COO(CH_2)_nCH_3) + Et_3Al_2Cl_3 \longrightarrow \text{Active Species} \qquad [4.1.]$$

Step 1

$$ZrCl_4 + Et_3Al_2Cl_3 \longrightarrow \{\text{Precursor Complex}\} \qquad [4.2a.]$$

Step 2

$$\{\text{Precursor Complex}\} + \text{Ligand} \longrightarrow \text{Active Species} \qquad [4.2b.]$$

4.1.0. Ligand Selection

Ligand selection (based on the proposed model for promoting oligomerisation) for examination in this study and the synthesis of possible reactive intermediates was discussed Chapter 3. Bidentate, chelate ligands have played an important role in the catalytic chemistry of transition metals (such as catalysts for asymmetric synthesis[3]), especially ligands having end groups with varying donor abilities. The role of such bidentate, chelate ligands in the oligomerisation chemistry of zirconium has been examined in this study. As the coordination chemistry of zirconium with bidentate

or possibly bidentate ligands is potentially vast the following restraints, as discussed in Chapter 3, have been placed on ligand selection:

1. the ability to vary the electronic and steric environment around the metal centre through variations in ligand substituents.

2. ligand coordination must leave the complex coordinatively unsaturated to allow for activation reactions.

3. ligands capable of forming 5 or 6 member metallocycles

These preconditions are easily met by a number of ligands which currently find application in nickel based oligomerisation systems[4]. Based on examination of active zirconium oligomerisation systems the choice of ligands in this study has been further constrained by restriction to bidentate ligands containing O, N or S donor groups (Chapter 2.2.0). Examples of possible ligand types are shown in Figure 4.2. β-Aminoketones are of particular interest and have been the focus of this study.

Figure 4.2.
Bidentate, Chelate Ligand Systems

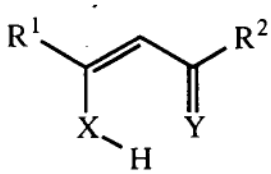

X=Y=O; acetylacetone
X=Y=S; dithioacetylacetone
X=O,Y=S; monothioacetylacetone

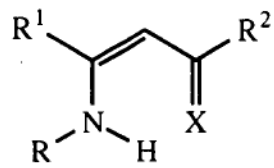

X=O; aminoketone
X=S; aminothioketone

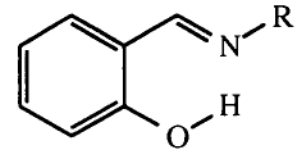

salicylaldimine

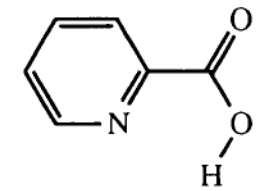

picolinic acid

The *in situ* catalytic testing of these ligands, including testing for catalytic activity of intermediates and derived organo-zirconium complexes is discussed in this Chapter. Catalytic activities significantly greater than those previously reported are presented for catalytic systems containing β-aminoketones. The mechanism for this reaction will be more fully discussed in Chapter 5 where results from NMR studies are presented.

The *in situ* preparation of active catalytic species used by Shiraki and test conditions leading to the best activity and product distribution have been examined and used in

this study as a standard. Test conditions for other experiments were kept as close as possible to those for the standard test and changes were only made when necessary, i.e. when intermediate complexes or alkylzirconium species were tested. For this reason none of the test conditions have been optimised to date and later experiments indicate that milder conditions may favour catalysis.

4.2.0. Standard Procedures

Idemitsu has recently commissioned an oligomerisation plant based on zirconium chemistry. Test conditions giving the high activity, highest percentage linear α-olefins and a high C_4-C_{16} product distribution were chosen from recent patent applications by Idemitsu and used as standard test conditions in this study[2b]. After selection of standard conditions an initial test program was set up, based on the Idemitsu approach, to examine reproducibility, influence of cocatalyst and alternative zirconium sources. These tests were designed to repeat what has been presented in the literature, to gain a better feel for zirconium based oligomerisation systems and to develop analytical methods on known active systems.

4.2.1. Standard Test Conditions

In the standard test used in this study, $ZrCl_4$ is contacted at 60°C with EASC for 20 minutes to form a precursor solution. This precursor solution is cooled to 25°C and the appropriate ligand added to obtain a desired zirconium:EASC:ligand ratio. An aliquot of the catalyst solution is then transferred to an autoclave. With thiophene, the preferred ligand, a clear solution is not present and a slurry is formed. Oligomerisation is carried out at 100°C and 35 bar of ethylene for 1 hour.

By repeating the standard test the typical variation in catalytic activity could be examined (Table 4.1). Large variations in catalytic behaviour are not unusual for this type of catalytic system where 20 μmoles of catalyst is charged and all reagents are sensitive to moisture and air. Further variation can be expected due to problems encountered when transferring small amounts of a slurry rather than a homogeneous solution. Later tests where only homogeneous solutions are present show smaller variations in activity (Table 4.5).

The best of these tests (Test 1.4) has been selected as a comparison to other tests in his study. Blank tests, Tests 1.1 and 1.2, show no reactivity in the absence of ligand or $ZrCl_4$.

Table 4.1.
Summary of Catalytic Test Results
Activity Variation in Standard Test

Test	Ligand	L:Zr	TON	Yield g/g $ZrCl_4$	-Ln(α)	C_4-C_{10}	Wax (%)	α-Olefin (%)
1.1	no Ligand		nc[d]					
1.2	[a]Thiophene		nc					
1.3	Thiophene	2	20760	2499	0.277	75.1	1.3	94.8
1.4	Thiophene	2	23053	2775	0.318	81.3	0.8	80.4
1.5	Thiophene	2	14907	1794	0.305	79.6	1.0	88.0
1.6	Thiophene	2	8218	989	0.322	81.8	1.1	90.1
1.7	[b]Thiophene	2	7907	951	0.356	85.0	1.1	≥95
1.8	[b]Thiophene	2	9194	1104	0.351	84.4	1.7	90.6
1.9	Thiophene	2	10252	1234	0.354	84.5	1.9	97.8
1.10	Thiophene	2	7253	873	0.319	80.5	2.2	95.9
1.11	Thiophene	2	5971	719	0.333	80.6	3.9	≥95
1.12	Thiophene	2	6469	779	0.327	80.2	3.6	96.8
1.13	[c]Thiophene	2	nc					

[a]no $ZrCl_4$, [b] same catalyst solution used in the two tests, [c] 20 ml of air introduced into autoclave [d] no catalysis ; Reaction Conditions: 50 ml autoclave, $ZrCl_4$ 0.02 mmoles, Al:Zr 10:1, Zr:L 1:2, T=100°C, Ethylene 30-35 Bar, t = 60 minutes, solvent toluene (20 ml)

The parameters used in Table 4.1 to describe catalyst activity and product distribution are defined and discussed here. They are used in all following tables.

L:Zr Ratio of added ligand to $ZrCl_4$.

Al:Zr Ratio of the aluminium in the added cocatalyst to $ZrCl_4$.added

TON The Turn Over Number (TON) is the number of moles of ethylene used per mole of zirconium charged per hour. The total weight of oligomer produced (ethylene consumed) is calculated from the measured oligomer

distribution using a Schultz-Flory plot to allow for losses in the lighter oligomer fractions

Yield — The yield is quoted in terms of grams of oligomer produced per gram of $ZrCl_4$ charged per hour. If a complex or adduct is used then the equivalent weight of $ZrCl_4$ charged is calculated.

Ln(α) — Slope of the Schultz-Flory plot. This figure gives a measure of the product distribution and is related to the relative rates of monomer insertion and β-hydride elimination. The closer the number is to zero the broader the oligomer distribution and therefore the higher the average molecular weight.

C_4-C_{10} — Weight % of produced oligomers having chain lengths of 4-10 carbons.

Wax — Weight % of higher molecular weight oligomers, assumed to be C≥40, which precipitate upon cooling the catalyst solution after deactivation and which are collected by filtration.

α-olefin — The weight % of C_{14} oligomers which are linear α-olefins. There is no consistent measure of linearity quoted in the literature with various workers quoting linearity values for the C_{14} or C_{16} fractions, a combined C_{14} to C_{20} fraction or other groupings. A figure of >95 means that the GC detection limits have been surpassed for catalysts with low activity.

4.2.2. Product Identification and Distribution

Catalyst products were found to be predominantly linear α-olefin as characterised by GC, GC-MS and NMR. A typical GC trace (for Test 10.1: (*i*-Pr-Nacac)$_2ZrCl_2$ + EASC + Ethylene) is shown in Figure 4.3. GC-MS fragmentation patterns were typical of linear alkanes with successive CH_2 loss[5], GC-MS spectral data appears in Appendix A.1.0. Minor peaks were identified as isomers (branched chain or internal olefins, labelled A&B in Figure 4.3) or alkylated toluene (labelled X in Figure 4.3) as a minor side reaction (Section 4.7.0). A NMR spectrum of the high boiling fraction, >120°C to remove the toluene, gave typical resonances for long chain linear α-olefins[6] (Figure 4.4).

Figure 4.3.
GC Trace of Produced Oligomers

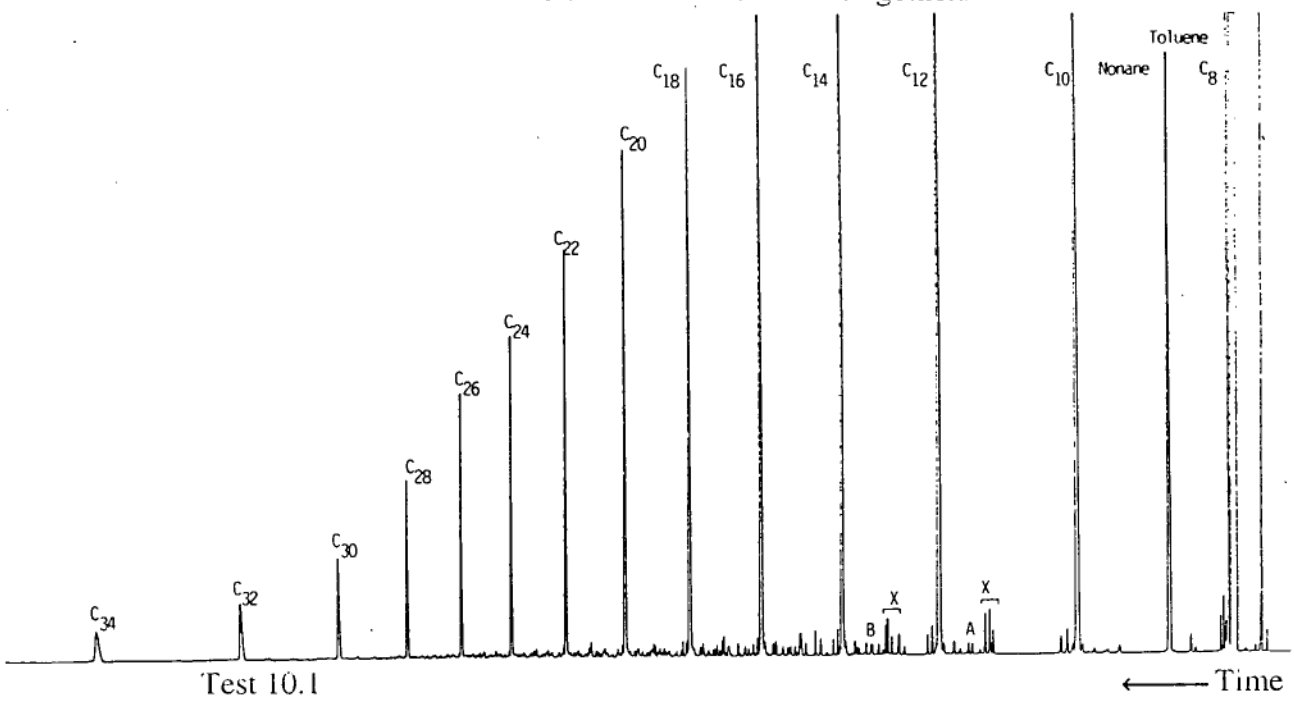

Figure 4.4.
^{1}H NMR Spectrum of High Boiling Oligomers, ≥ 120°C

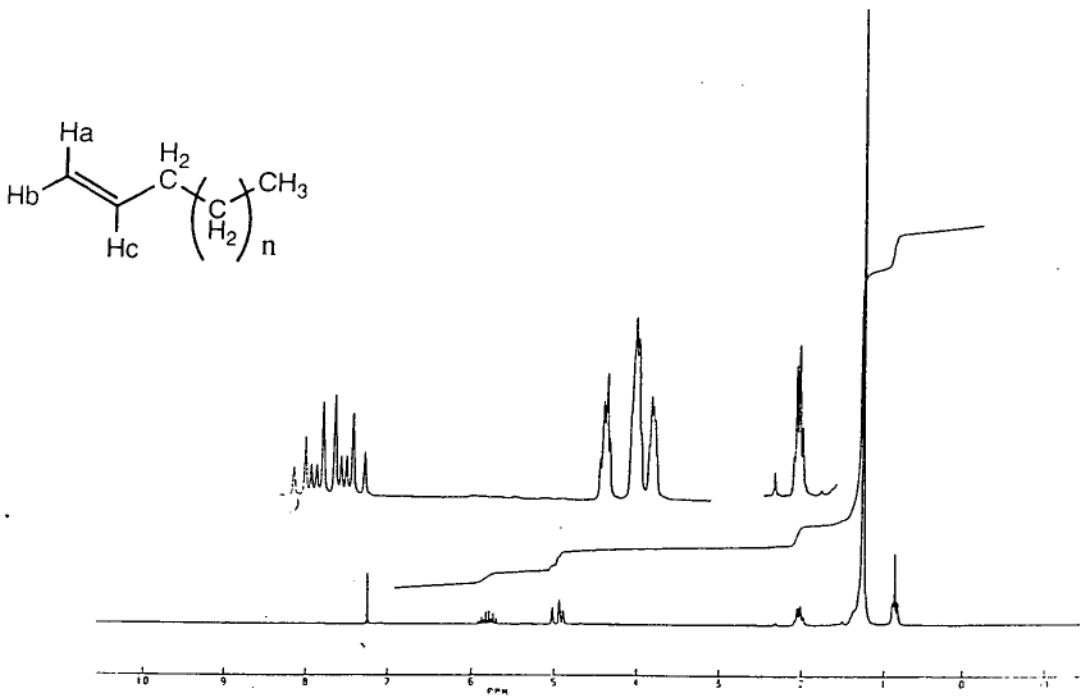

^{1}H-NMR of high boiling oligomers after the removal of toluene, in $CDCl_3$ 25°C

The oligomers produced in this work have been found to follow a Schultz-Flory distribution (Figure 4.5). Correlation coefficients for the majority of tests are generally between 0.98-0.99. For tests with low activity, GC detection limits lead to lower accuracy. Peak discrimination becomes difficult at higher carbon numbers especially for low activity systems, therefore data for the Schultz-Flory plot was generally taken from oligomer fractions with carbon numbers in the range from 10-30. The good fit allowed a theoretical product distribution to be calculated, enabling TON and yield calculations to be completed, as no attempt was made to collect or prevent the loss of lighter oligomer fractions on depressurising the autoclave.

Figure 4.5.
Typical Schultz-Flory Plot Showing
Actual Data and Theoretical Data Fit

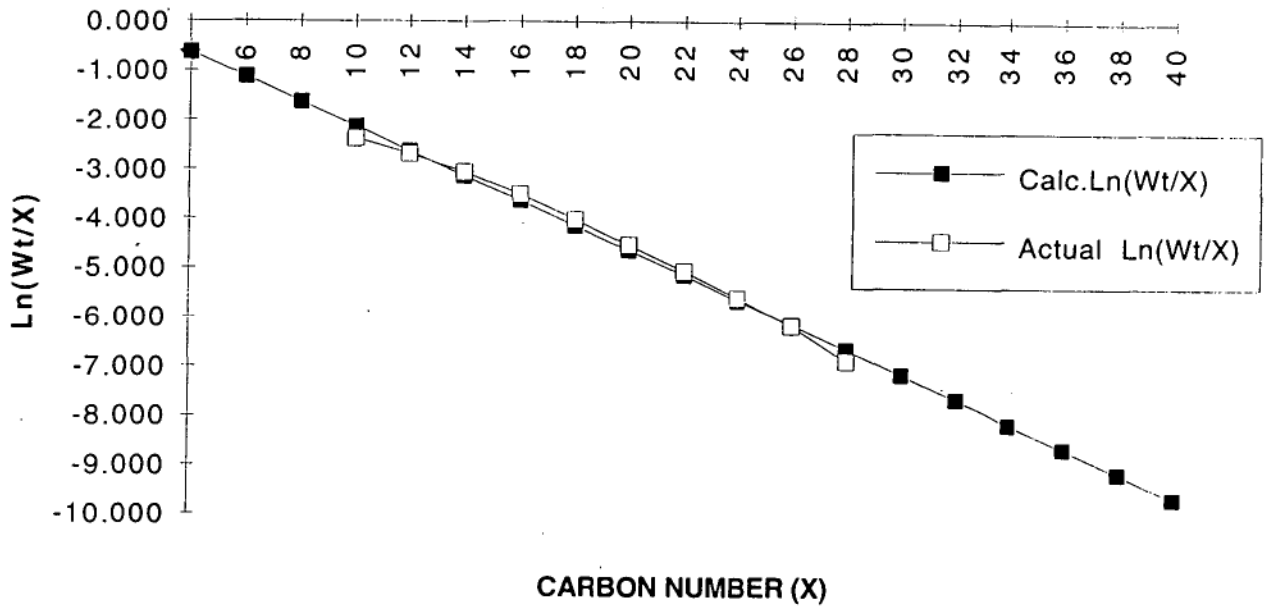

The Schultz-Flory plot assumes constant relative rates for the propagation and termination reactions[7]. The percentage of oligomers with a certain carbon number will be related to the percentage of oligomers with 2 less carbons (for ethylene insertion) by a constant ratio α, which is given by:

$$\alpha = \frac{k_p}{k_p + k_t}$$

where k_p and k_t are the rates of the propagation and termination respectively. It can also be shown in such a case that:

$$\text{Log}\left(\frac{M_x}{x}\right) = x\text{Log}(\alpha) + c \text{ , where } c = \text{Log}\ \frac{(1-\alpha)^2}{\alpha}$$

where M_x is the weight percent of oligomers with carbon number x. The Schultz-Flory plot is then simply a plot of $\text{Log}(M_x/x)$ against x. The assumption of a constant rate ratio is generally good for $x \geq 6$ but there may be slight variations for small chain lengths (x=4). For initial catalytic tests, where average oligomer carbon numbers were 10-12, this was not considered to be significant.

4.2.3. Cocatalyst Influences

Dramatic changes are seen in reactivity and product distribution on varying the added cocatalyst (Table 4.2). EASC is the typical cocatalyst for zirconium based oligomerisation systems and leads to good reactivity to give linear α-olefins. The use of DEAC lead to active oligomerisation systems but with the production of a significantly lower percentage of linear α-olefins. The use of TEA did not produce an active catalytic system. MAO, the new and very effective cocatalyst for polymerisation systems, lead to the formation of polyethylene but only at significantly higher addition levels than for EASC or similar alkylaluminiums. Therefore EASC was employed consistently throughout these studies.

Table 4.2.
Summary of Standard Catalytic Test Results:
Effect of Alkylaluminium Variation

Test	Ligand	Alkyl-Alum.[a]	TON	Yield g/g $ZrCl_4$	-Ln(α)	C_4-C_{10}	Wax (%)	α-Olefin (%)
1.4	Thiophene	EASC	23053	2775	0.318	81.3	0.8	80.4
2.1	Thiophene	DEAC	16925	2037	0.213	58.1	8.1	75.1
2.2	Thiophene	DEAC	20830	2507	0.213	60.9	3.8	79.6
2.3	Thiophene	TEA		nc				
2.4	Thiophene	MAO		nc				
2.5	Thiophene	[b]MAO		polymerisation			2.28g	

[a] Alkyl aluminium EASC 97%, DEAC 97%, TEA 1.9M in toluene, MAO 10.4% in toluene. [b] Al:Zr 100:1, polymerisation. ; nc = no catalysis ; Reaction Conditions: 50 ml autoclave, $ZrCl_4$ 0.02 mmoles, Al:Zr 10:1, Zr:L 1:2, T=100°C, Ethylene 30-35 Bar, t = 60 minutes, solvent toluene (20 ml)

4.2.4. Zirconium Source

$ZrCl_4$ is the most commonly used zirconium source material however the zirconium complexes $Zr(acac)_4$ and $Zr(O\textit{i}\text{-}Pr)_4.HO\textit{i}\text{-}Pr$ have also been used (Chapter 2, Section 2.2.6) and the ester adducts mentioned previously. As found by Young, catalysis was very good when using alternative zirconium complexes but an excess of cocatalyst was required (Table 4.3). Young[1] has suggested that this excess cocatalyst acted as a sponge mopping up excess ligand before the active species was formed. Due to the possible interference from other ligands or Lewis bases and the desire to introduce synthesised intermediates into the catalytic system, $ZrCl_4$ remained as the primary starting material.

Table 4.3.
Summary of Catalytic Test Results
Alternative Zirconium Sources

Test	Ligand/Complex	Al:Zr	TON	Yield g/g $ZrCl_4$	-Ln(α)	C_4-C_{10}	Wax (%)	α-Olefin (%)
1.4	$ZrCl_4$+2Thiophene	10	23053	2775	0.318	81.3	0.8	80.4
3.1	$Zr(O\textit{i}\text{-}Pr)_4.HO\textit{i}\text{-}Pr$	20	15312	1843	0.312	81.1	2.6	89.0
3.2	$ZrCl_4$+2Hacac	10	12081	1454	0.324	80.6	2.6	95.8

Reaction Conditions: 50ml autoclave, Zr = 0.02 mmoles, L:Zr = 2:1, T=100°C, Ethylene at 30-35bar, t = 60 minutes, solvent = toluene (20 ml)

4.3.0. Preliminary Catalytic Testing

4.3.1. Catalysis with β-Aminoketones

Initial catalytic testing was carried out using *iso*-propyl-β-aminoketone (*i*-Pr-HNacac) to examine the effect of a number of cocatalysts (Table 4.4). EASC again proves to be the most effective cocatalyst under the conditions tested and was used in all further tests. Although the activities, TON's of 5-8,000 compared to 20,700, were somewhat less than the standard test, the results were encouraging and certainly a number of variations were possible to improve activities. For this ligand a desirable shorter average oligomer weight was produced. A point to note is that reproducibility with these homogeneous systems was significantly improved over the standard test.

Table 4.4.

Summary of Catalytic Test Results

Activity of *i*-Pr-HNacac Containing Systems

Test	Ligand/ Complex	Alkyl-Alum.[a]	TON	Yield g/g $ZrCl_4$	-Ln(α)	C_4-C_{10}	Wax (%)	α-Olefin (%)
1.4	Thiophene	EASC	23053	2775	0.318	81.3	0.8	80.4
5.1	*i*-Pr-HNacac	EASC	5684	683	0.395	88.4	1.6	≥95.0
5.2	*i*-Pr-HNacac	EASC	4678	526	0.348	83.8	2.0	≥95.0
5.3	*i*-Pr-HNacac	EASC	4952	595	0.385	87.4	1.8	94.1
5.4	*i*-Pr-HNacac	EASC	8106	974	0.459	92.2	1.5	96.9
5.5	*i*-Pr-HNacac	[b]EASC	3970	477	0.182	-	-	
5.6	*i*-Pr-HNacac	MAO					0.59[c]	
5.7	*i*-Pr-HNacac	MAO					0.50[c]	
5.8	*i*-Pr-HNacac	DEAC		<250				
5.9	*i*-Pr-HNacac	DEAC		<250				

[a] Alkyl aluminium = EASC 97%, DEAC 97%, TEA 1.9M in toluene, MAO 10.4% in toluene. [b] L:Zr 1:1, significant solvent alkylation ; [c] polymerisation-autoclave filled within 1 minute ; Reaction Conditions: 50 ml autoclave, $ZrCl_4$ 0.02 mmoles, Al:Zr = 10:1, L:Zr = 2:1 ;T=100°C, Ethylene at 30-35bar, t = 60 minutes, solvent = toluene (20 ml)

4.3.2. β-Aminoketone Substituent Variations

Three of the four possible substituents on the β-aminoketones were varied leading to significant modification of catalytic activity (Table 4.5). This work is the first time that systematic ligand substituent variations have been shown to alter catalyst activity and product distributions for zirconium based oligomerisation systems, indicating the importance of the ligand in the active species.

Although the results presented in Table 4.6 are from a series of single tests two general observations can be made; electron withdrawing groups on the amine increase catalyst activity at a slightly higher average oligomer weight (Tests 6.2-9) and increased phenyl substitution on the β-aminoketone backbone decreases catalyst activity (Tests 6.3.1-3 and 6.7.1-3). It was predicted that the substitution of electron withdrawing groups would lead to better catalysis. The poor activity for the trifluoro substituted β-aminoketone (Test 6.1) is thought to be due to electronic factors with no ligand deprotonation taking place (Chapter 5.3.0).

Table 4.5.
Summary of Catalytic Test Results
Effect of β-Aminoketone Substituent Variation

Test	Ligand/Complex	TON	Yield g/g $ZrCl_4$	-Ln(α)	C_4-C_{10}	Wax (%)	α-Olefin (%)
1.4	Thiophene	23053	2775	0.318	81.3	0.8	80.4
5.1	*i*-Pr-HNacac	5684	683	0.395	88.4	1.6	≥95.0
6.1	*i*-Pr-HNtfac	2580	311	0.354	84.9	1.4	91.3
6.2	*i*-Pr-HNacac	8106	974	0.459	92.2	1.5	96.9
6.3	hex-HNacac	7527	906	0.415	89.7	1.7	95.9
6.4	Cy-HNacac	3956	476	0.472	93.4	0.9	94.0
6.5	*t*-Bu-HNacac	8345	1005	0.368	86.7	0.9	99.0
6.6	tmp-HNacac	5315	640	0.391	88.3	1.3	99.5
6.7	Ph-HNacac	15959	1921	0.329	82.2	1.4	95.0
6.8	ClPh-HNacac	16203	1950	0.338	83.5	1.1	97.6
6.9	MeOPh-HNacac	29455	3546	0.304	79.4	1.0	98.4
6.3.1	hex-HNacac	7527	906	0.415	89.7	1.7	95.9
6.3.2	hex-HNacPhac	5442	605	0.445	91.1	2.0	>95.0
6.3.3	hex-HNbzbz		nc				
6.7.1	Ph-HNacac	15959	1921	0.329	82.2	1.4	>95.0
6.7.2	Ph-HNacPhac	12212	1470	0.309	79.9	1.5	93.3
6.7.3	Ph-HNbzbz		nc				

Reaction Conditions: 50 ml autoclave, $ZrCl_4$ = 0.02 mmoles, Al:Zr = 10:1, L:Zr = 2:1 ;T=100°C, Ethylene at 30-35bar, t = 60 minutes, solvent = toluene (20 ml)

Catalyst activity appears to be related to the basicity of the amino proton. The amine basicity, indicated by relative proton NMR shifts, was to some extent determined by the nature of the amino R-group. A general correlation between ^{1}H-NMR proton shifts (hence basicity) and reactivity was observed (Table 4.5). This comparison does not include any account of steric effects or *in situ* reactions which are believed to occur (the extensive reactions and interactions of the cocatalyst and ligands and their relationship to possible active intermediates are discussed in Chapter 5.3.0). The higher activities were associated with higher average oligomer weights.

Table 4.6.

Catalyst Activity vs. Amine Basicity

	Amino R-Group Substituent							
	Hex-	*i*-Pr-	Cy-	*t*-Bu-	tmp-	Ph-	ClPh-	MeOPh-
^{1}H Shift (ppm)	10.8	10.8	11.0	11.4	11.8	12.4	12.3	12.3
TON ($*10^3$)	7.5	8.1	4.0	8.4	5.3	16.0	16.2	29.4

Whether the backbone substituent effects on catalytic activity are steric or electronic is not known and due to the poor recorded activities no further work has been undertaken with phenyl substitution of the ligand backbone.

4.3.3. Catalytic Activity of $ZrCl_4$.β-Aminoketone Adducts

It was found that β-aminoketones readily form 1:1 or 1:2 adducts on mixing with $ZrCl_4$, however the formation of all possible adducts has not been attempted. No ligand has been found to react directly via ligand deprotonation with $ZrCl_4$ (Chapter 4.) It is to be expected that the lower basicity of ligands with strongly electron withdrawing groups may lead to reaction of the ligand with $ZrCl_4$ to form complexes with the displacement of chloride (formation of bis-ligand complexes). Typical results for catalytic tests on two isolated adducts compared to the *in situ* addition of the free ligand show no essential variation in activity or product distribution (Table 4.7). With regard to these observations the *in situ* addition of the free ligand was used for most of these tests.

4.3.4. Effect of Zr:Al Ratio

For *in situ* testing and testing of isolated adducts, it could be expected that the presence of a potentially reactive amine proton may lead to the consumption of some of the added cocatalyst and therefore an excess may be needed to achieve optimum activities, as indicated by Young when $Zr(O$*i*$-Pr)_4HO$*i*$-Pr$ was used (Chapter 2.2.5). Lower additions of EASC did not lead to the formation of active catalytic systems The addition of a large excess EASC did not lead to significant improvements in performance, although a slight increase in activity was noted (Table 4.8). Later NMR studies indicated that in the case where *i*-Pr-HNacac was used ligand deprotonation did not occur. Formation of cocatalyst-amine adducts, however, may

remove some of the available cocatalyst leading to the slight increase in reactivity on addition of an excess of cocatalyst.

Table 4.7.
Summary of Catalytic Results
Activity of $ZrCl_4$ -bis-β-Aminoketone Adducts

Test	Ligand/Adduct	TON	Yield g/g $ZrCl_4$	-Ln(α)	C_4-C_{10}	Wax (%)	α-Olefin (%)
6.2	* *i*-Pr-HNacac	8106	974	0.459	92.2	1.5	96.9
8.1	$ZrCl_4$.2*i*-Pr-HNacac	5301	637	0.499	92.5	2.7	90.9
8.2	* Ph-HNacac	17245	2076	0.251	70.7	0.8	98.6
8.3	$ZrCl_4$.2Ph-HNacac	18863	2271	0.259	72.6	0.4	99.4

* free ligand added *in situ* in the same proportion as for the adduct ; Reaction Conditions: 50 ml autoclave, $ZrCl_4$ 0.02 mmoles, Al:Zr = 10:1, L:Zr = 2:1 ;T=100°C, Ethylene at 30-35bar, t = 60 minutes, solvent = toluene (20 ml)

Table 4.8.
Summary of Catalytic Test Results
Effect of Al:Zr ratio on Catalytic Activity

Test	Ligand	Al:Zr Ratio	TON	Yield g/g $ZrCl_4$	-Ln(α)	C_4-C_{10}	Wax (%)	α-Olefin (%)
9.1	*i*-Pr-HNacac	5		<250				
6.2	*i*-Pr-HNacac	10	8106	974	0.457	92.2	1.5	96.9
9.2	*i*-Pr-HNacac	20	11481	1382	0.459	92.5	1.1	87.1

Reaction Conditions: 50 ml autoclave, $ZrCl_4$ = 0.02 mmoles, L:Zr = 2:1 ;T=100°C, Ethylene at 30-35bar, t = 60 minutes, solvent = toluene (20 ml)

4.3.5. Activity of bis-Ligand Complexes, $(R\text{-}Nacac)_2ZrCl_2$

It has been shown that β-aminoketones effectively promote zirconium based oligomerisation of ethylene and that activities and product distributions can be altered through ligand substituent variations. Reactions occurring in solution and the nature of the active species were, however, unknown.

The first step in understanding the catalytic process was to isolate probable intermediates in the catalytic process and test these for catalytic activity. It was

assumed that the first *in situ* reaction would be ligand deprotonation and bis-ligand complex formation . The first sign that this may not be happening came from the comparison between the catalytic testing of the bis-ligand complexes and the *in situ* addition of free ligand (Table 4.9). The activity differences, especially for the initial tests where R = *i*-Pr, were considerable. The activity of the bis-ligand complex was considerably higher, e.g. TONs of 29,510 compared to 8,106 for the *iso*-propyl-β-aminoketone containing systems. Associated with this dramatic increase in activity was a significant change in product distribution with oligomers of higher average molecular weight being formed.

Table 4.9.
Summary of Catalytic Test Results
Activity of Bis-Ligand-Complexes of Zirconium

Test	Ligand/ Complex	TON	Yield g/g $ZrCl_4$	-Ln(α)	C_4-C_{10}	Wax (%)	α-Olefin (%)
6.2	* *i*-Pr-HNacac	8106	974	0.459	92.2	1.5	96.9
8.1	$ZrCl_4$.2*i*-Pr-HNacac	5301	637	0.499	92.5	2.7	90.9
10.1	(*i*-Pr-Nacac)$_2ZrCl_2$	29510	3552	0.204	60.1	1.4	99.4
8.3	* Ph-HNacac	17245	2076	0.251	70.7	0.8	98.6
10.2	(Ph-Nacac)$_2ZrCl_2$	33726	4060	0.206	60.0	2.4	99.1
6.9	* ClPh-HNacac	16203	1950	0.338	83.5	1.1	97.6
10.3	(ClPh-Nacac)$_2ZrCl_2$	32078	3859	0.153	41.5	1.1	94.5
6.10	* MeOPh-HNacac	29455	3546	0.304	79.4	1.0	98.4
10.4	(MeOPh-Nacac)$_2ZrCl_2$	54420	6551	0.152	46.0	1.0	95.3

* free ligand added *in situ* in the same L:Zr ratio as for the complex ; Reaction Conditions: 50 ml autoclave, $ZrCl_4$ = 0.02 mmoles, Al:Zr = 10:1, L:Zr = 2:1 ;T=100°C, Ethylene at 30-35bar, t = 60 minutes, solvent = toluene (20 ml)

It was also observed that there was a greatly reduced or no induction time before ethylene consumption started when preformed complexes were used by comparison to *in situ* testing of ligands or adducts. This indicated that species formed from these complexes may be active at a much lower temperature, i.e. catalysis occurred at or near 50°C, the initial temperature of the autoclave.

4.3.6. Cationic and Alkylated-bis-Ligand Complexes

The work of Jordan, Kaminsky, Bochmann, Teuben, Eshuis and others (discussed in Chapter 2) indicated that cationic, 14-electron d^0, alkyl zirconium complexes were active polymerisation catalysts. Consequently it was important to know if similar cationic complexes could be generated with bidentate, chelate ligands giving rise to active oligomerisation catalysts in the absence of a cocatalyst.

Alkylated-bis-ligand complexes as well as cationic bis-ligand alkyl-complexes were prepared, which in the presence of EASC, oligomerise ethylene (Table 4.10). The synthesis and characterisation of these new and very interesting complexes are discussed in Chapters 3 and 5. The cationic complexes in the absence of a cocatalyst polymerise ethylene. These are the first bidentate, chelate ligand containing cationic zirconium complexes to be formed and also the first time such complexes have been shown to polymerise ethylene. The ionic complex, $[ZrBz_3][BPh_4]$, has not before been previously reported to polymerise ethylene, although the conditions used for ethylene oligomerisation in this study are much more severe that those for typical polymerisation studies.

The catalytic activities for these systems are very low but no optimisation was attempted. It is known from complex characterisation that these species are not stable at higher temperatures.

It is believed that in the presence of the cocatalyst, secondary interactions between the amine end of the ligand occurred reducing the ability of the ligand to act effectively as a bidentate ligand thereby increasing the metal centre Lewis acidity and decreasing the metal centre coordination number, in line with the developed model. This increased the β-hydride elimination rate and induced oligomerisation. In the absence of a cocatalyst, the β-aminoketone acted as a bidentate, chelate ligand. This effectively decreased the metal centre Lewis acidity, through the interaction of the second donor atom of the ligand with the metal centre. In line with the model the rate of β-hydride elimination decreased leading to polymerisation. This idea is fully explored in light of NMR studies in Chapter 5, where reactive intermediates are proposed and the consequences of this model are explored with regard to predictions for the generation of cationic, cocatalyst free oligomerisation catalysts.

Table 4.10.
Summary of Catalytic Test Results
Catalytic Activity of Alkylated Bis-Ligand Complexes
and Cationic Complexes

Test	Complex	TON	-Ln(α)	C_4-C_{10}	Wax (%)	α-Olefin (%)
Alkylzirconium Complexes + EASC						
11.1	$ZrBz_4$	2265	0.210	46.2	25.8	69.7
11.2	(*i*-Pr-Nacac)$_2ZrBz_2$	5442	0.375	86.2	2.1	97.0
Cationic Alkylzirconium Complexes + EASC						
11.3	$[ZrBz_3][BPh_4]$	1607	0.145	34.4	22.0	96.5
11.4	[(*i*-Pr-Nacac)$_2$ZrBz][BPh_4][a,c]	5437	0.191	45.4	21.1	99.2
Cationic Alkylzirconium Complexes						
11.5	$[ZrBz_3][BPh_4]$	[b]polyethylene				
11.6	[(*i*-Pr-Nacac)$_2$ZrBz][BPh_4][c]	[b]polyethylene				

[a] at 60°C ; [b] polymerisation-autoclave filled within 1 minute ; [c] analytically impure product, see Chapter 4.8.2. ; Reaction Conditions: 50 ml autoclave, $ZrCl_4$ = 0.02 mmoles;T=100°C, Ethylene at 30-35bar, t = 60 minutes, solvent = toluene (20 ml)

4.4.0. Catalysis with β-aminothioketones

Substitution of the hard donor atom, oxygen, by the soft donor, sulfur, was expected to increase ligand lability. The effect on complex stability through such a change was unknown but as sulfur plays a significant role in the oligomerisation chemistry of zirconium it was of interest to explore what effect such a substitution would have.

The use of β-aminothioketones resulted in the formation of active catalytic systems with similar or slightly lower activities compared to those of the β-aminoketone containing systems (Table 4.11). As in previous tests, EASC was the most effective cocatalyst with MAO resulting in polymerisation. Activities were similar to those of the β-aminoketones so no further testing was undertaken.

4.5.0. Catalysis with Monothioketones

The substitution of a hard donor atom with a soft donor atom has been shown to be very effective in promoting catalysis, especially in nickel based oligomerisation

chemistry[8]. As there appears to be an advantage in using soft donor atoms in zirconium based oligomerisation systems (Chapter 2.2.4. & 2.4.3.), a number of monothio-β-diketones have been tested catalytically (Table 4.12). Results indicated effective catalysis but without significant improvements or benefits. Consequently no further work was undertaken.

Table 4.11.

Summary of Catalytic Results

Catalytic Activity of β-Aminothioketone Containing Systems

Test	Ligand	Alkyl-Alum.[a]	TON	Yield g/g $ZrCl_4$	-Ln(α)	C_4-C_{10}	Wax (%)	α-Olefin (%)
5.4	*i*-Pr-HNacac	EASC	8106	974	0.459	92.2	1.5	96.9
12.1	*i*-Pr-HNacSac	EASC	8374	1008	0.51	83.5	1.5	92.3
12.3	Ph-HNacSac	EASC	11780	1418	0.187	56.0	0.9	89.3
12.4	Ph-HNacSac	EASC	7252	873	0.178	47.5	11.8	97.8
12.5	Hex-HNacSac	EASC	1919	231	0.228	59.8	10.2	94.0
12.6	*i*-Pr-HNacSac	EADC	5392	649	0.484		2.3	>95.0
12.7	*i*-Pr-HNacSac	DEAC		<250				
12.8	*i*-Pr-HNacSac	[b]MAO					0.6g	

[a] EASC 97%, DEAC 97%, TEA 1.9M in toluene, MAO 10.4% in toluene.; [b] polymerisation-autoclave filled within 1 minute ; Reaction Conditions: 50 ml autoclave, $ZrCl_4$ = 0.02 mmoles, Al:Zr = 10:1, L:Zr = 2:1 ;T=100°C, Ethylene at 30-35bar, t = 60 minutes, solvent = toluene (20 ml)

Table 4.12.

Summary of Catalytic Test Results

Activity of Monothio-β-diketone Containing Systems

Test	Ligand/Complex	L:Zr	TON	Yield g/g $ZrCl_4$	-Ln(α)	C_4-C_{10}	Wax (%)	α-Olefin (%)
3.3	$ZrCl_4$+2Hacac	2	12081	1454	0.324	80.6	2.6	95.8
4.1	$Zr(Sacac)_2Cl_2$	2	12484	1500	0.428	90.5	1.3	≥95.0
4.2	$Zr(Sacac)_3Cl$	3	15521	1865	0.546	92.6	4.0	≥95.0
4.3	$ZrCl_4$+2HPhacSac	2	3474	418	0.259	71.8	1.5	≥95.0
4.4	$ZrCl_4$+2PhacPhSac	2	4985	600	0.304	77.3	3.5	≥95.0

Reaction Conditions: 50 ml autoclave, $ZrCl_4$ 0.02 mmoles, Al:Zr 10:1, T=100°C, Ethylene 30-35 Bar, t = 60 minutes, solvent toluene (20 ml)

4.6.0. Catalysis with Alternative Ligand Systems

As mentioned at the start of this chapter a number of ligand systems have been examined other than the β-aminoketones, β-diketones and their thiolated analogues. Doyle had shown that electron rich nitrogen containing olefins effectively promote oligomerisation while Shiraki, although he has examined an extensive number of ligands, has not examined bidentate sulfur containing ligands. Two such ligands, the phenyl substituted bissulpidophosphinomethane and the *iso*-propyl substituted 1,4-diazabutadiene (Figure 4.6), were examined but promoted little or no catalytic activity (TON's≤500), hence were not further examined. This was also the case with picolinic acid and dialkyl- or diaryl-β-aminoketones (neutral, aprotic analogues of the β-aminoketones, R_2-Nacac's, R = Ph and Et).

Figure 4.6.
Neutral Bidentate, Chelate Ligands

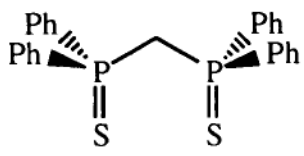

Bissulphidophosphinomethane

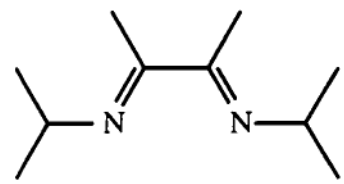

1,4-diazabutadiene

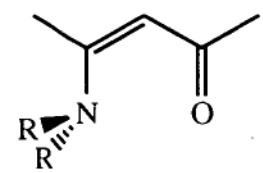

β-Aminoketone

4.7.0. Side Reactions: Friedel-Crafts Alkylation

Schiff's bases were also examined as bidentate chelate ligands with soft and hard donor atoms. A major difference of the β-aminoketone from these Schiff's base containing systems was the lack of side reactions and the consistent formation of predominantly linear-α-olefins. During the *in situ* testing of Schiff's base ligands or acetylacetone significant alkylation of the solvent (toluene) occurred (Peaks labelled A-J in Figure 4.7). From GC-MS data it was determined that not only mono-, di- and triethyltoluene were formed but also higher homologues, butly-, hexyl-, octly- etc., as well as mixed products. Alkylation and oligomerisation were occurring at the same time. Alkylation did not occur in every test and the relative rates of alkylation varied for unknown reasons (Table 4.13).

Two causes for this behaviour were considered, Friedel-Crafts type alkylation or electrophilic attack by the highly Lewis acidic metal centre on the solvent.

Figure 4.7.
Catalysis GC-Trace with High Levels of Alkylated Toluene

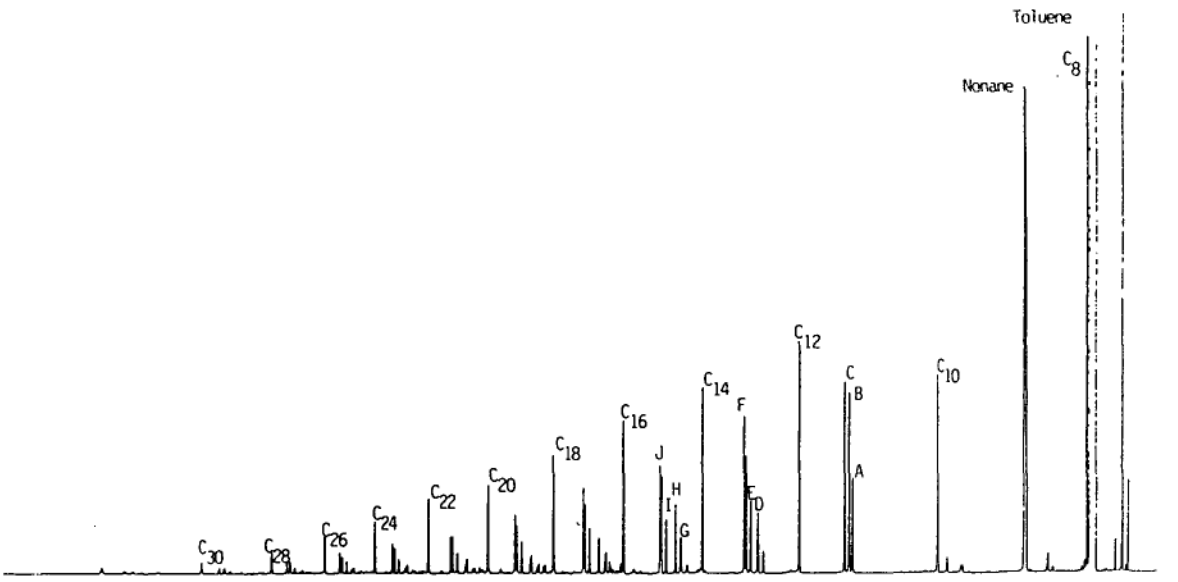

Test 13.8 ← Time

Table 4.13.
Summary of Catalytic Results
Tests With High Levels of Solvent Alkylation

Test	Ligand	L:Zr Ratio	TON	Yield g/g $ZrCl_4$	-Ln(α)	C_4-C_{10}	Wax (%)	α-Olefin (%)
13.1	*i*-Pr-NPhOH	2.0	6672	803	0.328	81.6	2.1	95.5
13.2	*i*-Pr-NPhOH	2.0	14565	1735	alkylated tol., 44% monoethylated			
13.3	*i*-Pr-NPhOH	2.5	7054	849	0.299	77.4	2.5	98.4
13.4	*i*-Pr-NPhOH	1.5	1969	237	0.311	76.7	7.2	95.0
13.5	Hacac	2.0	12081	1454	0.324	80.6	2.6	95.8
13.6	Hacac	2.0	18288	2201	alkylated tol.		6.4	-
13.7	Hacac	2.0	22068	2656	alkylated tol.		5.0	-
13.8	*i*-Pr-HNacac	2.0	8093	974	0.459	92.2	1.5	96.9
13.9	*i*-Pr-HNacac	2.0			alkylated tol.			

Reaction Conditions: 50 ml autoclave, $ZrCl_4$ 0.02 mmoles, Al:Zr 10:1, L:Zr 2:1 ;T=100°C, Ethylene 30-35 Bar, t = 60 minutes, solvent toluene (20 ml)

The first, a solvent metallation process, is well known for the early transition metals[9]. Termination would then be via a hydride shift or C-H bond metathesis leaving a saturated alkane and metallated solvent. However this would require zirconium acting in two different modes simultaneously, oligomerisation and solvent metallation. Also as the oligomerisation product distributions for these ligand systems are similar to other systems where no solvent alkylation occurs but a metal centre of similar reactivity would be expected it was considered that Friedel-Crafts alkylation was more likely. However detailed work would be required to determine if zirconium played a role in the alkylation of toluene in these systems.

It is well known that oligomerisation systems are susceptible to Friedel-Crafts alkylation reactions on deactivation (Reaction 4.3.) and steps are taken to minimise these reactions[10]. These are cooling the reaction mix before deactivation and destroying the Lewis acidity of the reaction mix as well as the oligomerisation reactivity. However in these cases the Friedel-Crafts activity was present after oligomerisation on exposing the catalyst solution to atmospheric moisture or incorrect deactivation.

Activation

$$ZrCl_4 + HL \longrightarrow ZrCl_3L + HCl \qquad [4.3a]$$

Alkylation

$$H^+ \; R'\text{-}CH{=}CH_2 \longrightarrow R'\text{-}CH^+\text{-}CH_3 \qquad [4.3b]$$

$$R'\text{-}CH^+\text{-}CH_3 \; Ar\text{-}H \longrightarrow Ar\text{-}CH(R')CH_3 + H^+ \qquad [4.3c]$$

Deactivation

$$HL + RAlCl_2 \longrightarrow H\text{-}R + LAlCl_2 \qquad [4.3d]$$

$$HCl + RAlCl_2 \longrightarrow H\text{-}R + AlCl_3 \qquad [4.3e]$$

In the previous studies, where zirconium complexes of protic ligands were used, the ligand had already been deprotonated or could only react with the added cocatalyst releasing an alkane, e.g. $Zr(acac)_4$ or $Zr(O\textit{i}\text{-}Pr)_4.HO\textit{i}\text{-}Pr$. Where a protic ligand was used *in situ* a significant contact time between the cocatalyst and the ligand ensured complete reaction. In these previous studies the proton was relatively acidic reacting readily with the cocatalyst or $ZrCl_4$.

In this study solvent alkylation has been found to be dependent on mixing and ligand acidity which is quite variable but in most cases much lower than that of previously

used ligands, e.g. β-aminoketones or Schiff's bases do not react at RT with $ZrCl_4$ to form complexes releasing HCl. Even under mild heating, normally used to form the precursor complexes, reaction may not occur (Chapter 5.3.1). Therefore conditions for the addition of free protic ligands to precursor solutions in this study were not sufficient to completely deactivate Friedel-Craft activity, i.e. reaction of HCl or HL with the cocatalyst forming an alkane and Al-Cl or Al-L bonds. In fact reaction may occur under oligomerisation conditions.

The method was altered to stop the majority of Friedel-Crafts alkylation in future tests by precontacting ligands with EASC, use of preformed complexes or longer conditioning times.

4.7.1. Friedel-Crafts Alkylation with Dienes

The high activity of these alkylation reactions (Table 4.13, Test 13.2) was however of interest, especially where monoethylation occurred. If these systems could also be used for dienes and the tendency to form branched products could be controlled then an interesting area of chemistry would be opened up, such as the formation of Ibuprofen type precursors in a one step, catalytic process (Figure 4.8). It is assumed that zirconium takes no part in these reactions and that typical Friedel-Crafts chemistry is present[11], although this has not been clearly demonstrated.

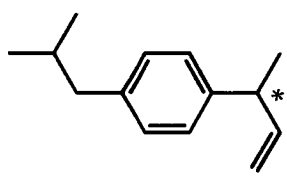

Ibuprofen Precursor

The introduction of butadiene into an active catalyst solution, optimised to Friedel-Crafts alkylation, led to the catalytic alkylation of toluene with butadiene (Peaks labelled A-C, Figure 4.9); multiple alkylation of toluene with butadiene or alkylation with butadiene oligomers was also noted (peaks labelled D-J Figure 4.9). The first fraction (peaks labelled A-C) was isolated by distillation, identified by GC and ^{1}H-NMR and indicated that the 1-4 addition product with an internal double bond was the major component (Appendix A.3.0). Catalytic activity was low, with a TON of 108 moles butadiene/ mole zirconium/ per hour.

Figure 4.8.

Friedel-Crafts Alkylation of Toluene with Butadiene

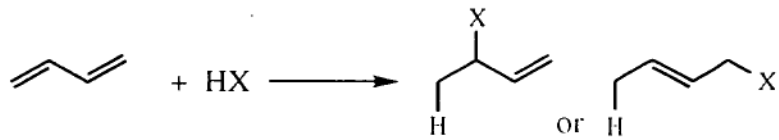

1,2-Addition 1,4-Addition

a. Possible products for the addition of HX to Butadiene.

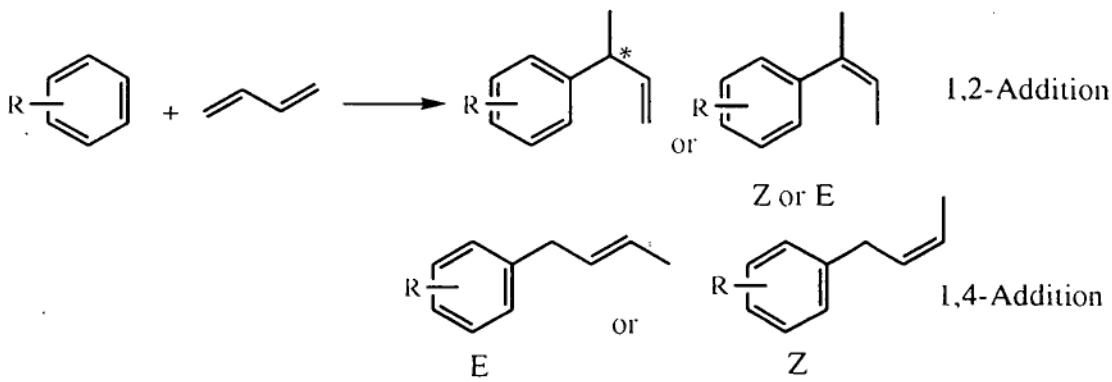

b. Possible addition products on alkylating an alkylbenzene with butadiene.

As Friedel-Crafts alkylation is not the main theme of this study no further testing of this system was carried out.

Figure 4.9.

GC Trace for the Catalytic Addition of 1,4-Butadiene to Toluene

Products have been identified by GC-MS and ^{1}H-NMR

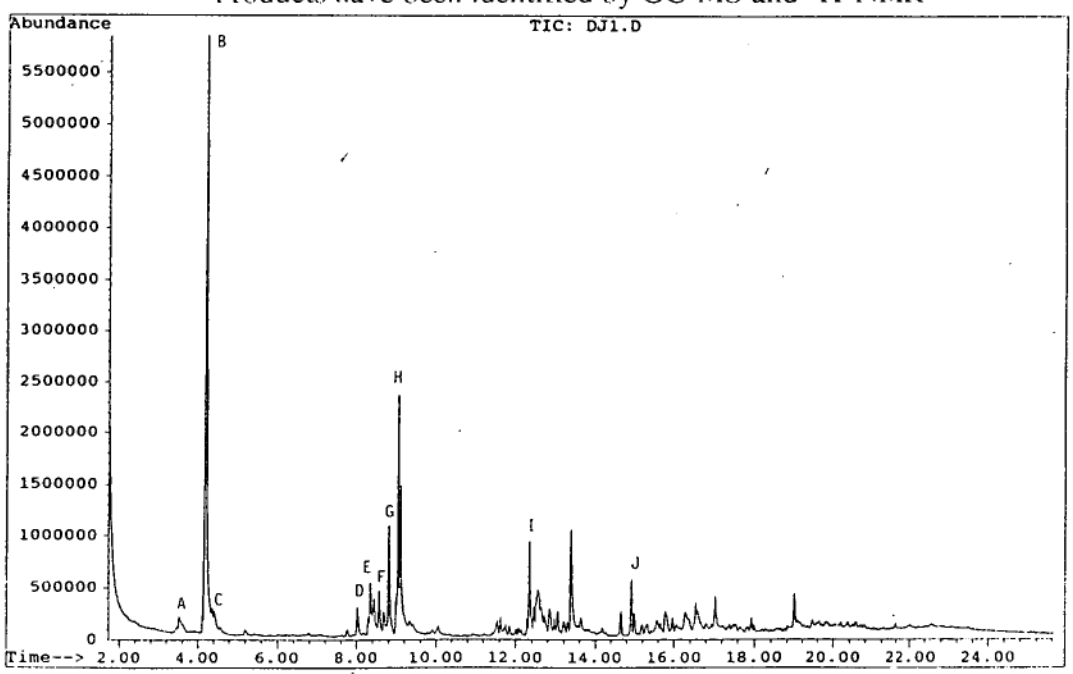

A full investigation of the alkylation process, whether acid catalysed (Friedel-Crafts alkylation) or zirconium catalysed (oligomerisation type process), is not warranted here. Such a study is peripheral to the main topic of this thesis, namely the development of catalysts for the production of linear α-olefins. Consequently, the study of the alkylation process was limited to that given in the forgoing discussion, i.e. its control or elimination. A more detailed investigation of this aspect of the work should be the subject of new studies.

4.8.0. Summary

It has been found that β-aminoketones effectively support oligomerisation in zirconium based systems. It has also been shown for the first time that the catalytic activity and product distribution can be controlled by ligand substituent variation, which allowed control of the oligomerisation process and the product distribution as required. The ability to change four substituents allowed a flexibility in altering the steric and electronic properties of the ligand and therefore at the metal centre which is not available with many other ligand systems. In line with the developed model, catalytic systems which increased metal centre Lewis acidity and decreased metal centre coordination number resulted in catalytic activities significantly higher than those previously reported. More strongly electron withdrawing substituents decreased average oligomer weight while reduced steric crowding at the metal centre increases activities significantly. The reasons for these changes will be explored more fully in Chapter 5.

Experiments with strongly electron withdrawing groups on the amine of β-aminoketone ligands need to be extended to include the β-aminothioketones.

1 a. Young, D.A.; Jones, L.O.; Campione, T.J., PCT Int.Appl., WO 9216477(Cl.C07C 2/30), 01.10.1992.
b. Young, D.A.; Jones, L.O.; Campione, T.J., Eu.Pat.Appl., EU 0 295 960 (Cl. C 07 C 2/30), 21.12.1988.
c. Young, D.A., *Journal of Molecular Catalysis* 53, **1989**, 433-442.

2 a. Shiraki, Y.; Kawano, S.; Takouchi, K., Eur. Pat. Appl. Ep 0 241 596(Cl. C 07 C2/30), 31.10.1990.
b. Shiraki, Y.; Tamura, T., Eur., Pat. Appl. EP 0 328 728 A1(Cl. CO7C 2/30), 17.8.1988.
c. Shiraki, Y.; Tamura, T., Eur., Pat Appl. EP 0 481 435 A2(Cl. CO7C 2/22), 15.10.1991.
d. Shiraki, Y.; Tamura, T., Eur., Pat Appl. EP 0 481 435 A2(Cl. CO7C 2/22), 15.10.1991.

3 Moser, W.R.; Slocum, D.W, *Homogeneous Transition Metal Catalysed Reactions* American Chemical Society, Boston, **1992**, Ch. 8-15.

4 Mehlhorn, A., PhD Thesis, RWTH Aachen, Germany, **1991.**

5 Silverstein, R.M.; Clayton Bassler, G.; Morill, T.C., *Spectrometric Identification of Organic Copound 4th Ed.*, John Wiley & Sons, Inc., Singapore, **1981**, 16-18.

6 Pouchert, C.J., *The Aldrich Library of NMR Spectra* 2nd Ed., Aldrich Chemical Company, Inc., Milwakee 1, **1983**, 20-22.

7 Bond, G.C., *Heterogeneous Catalysis, Principles and Applications* 2nd Ed., Clarendon Press, Oxford, **1987**, 98-99.

8 a. Abeywickrema, R.; Bennett, M.A.; Cavell, K.J;, Koney, M; Masters, A.; Webb, A.G., *J. Chem. Soc. Dalt. Trans.* **1993**, 59-68.
b. Foulds, G.A.; Bennett, A.M.A.; Thornton, D.A.; Brown, S.J.; Clutterbuck, L.M.; Hinton, C.; Humphreys, G.B., *Polyhedron* 11(11), **1992**, 1285-1293.

9 a. Thompson, M.E; Hoff, C.D; Stoutland, P.O; Newman, L.J.; Buchanan, J.M; Bergman, R.g; Yang, G.K; Peters, K.S., *J. Am. Chem. Soc.* 109, **1987**, 3143-3145.
b. Thompson, M.E; Baxter, S.M; Bulls, A.R; Burger, B.J; Nolan, M.C; Santarsiero, B.D; Schaefer, W.P; Bercaw, J.E., *J. Am. Chem. Soc.* 109, **1987**, 203-219.
c. Jones, W.D; Feher, F.J., *J. Am. Chem. Soc.* 108, **1986**, 4814-4819.
d. Desrosiers, P.J; Shinomoto, R.S; Flood, T.C., *J. Am. Chem. Soc.* 108, **1986**, 7964.
e. Crabtree, R.H., *Chem. Rev.*, 85, **1985**, 245-269.

10 a. Langer, A.W., *J. Macromol. Sci. Chem.* A4,**1970**, 775
b. Langer, A.W., US. Pat. Appl., US 4,409,414 (Cl. CO7C 2/34) 11. 10.1983.
c. Langer, A.W., US. Pat. Appl., US 4,442,309 (Cl. CO7C 2/22) 10. 04.1984.
d. Langer, A.W., US. Pat. Appl., US 4,486,615 (Cl. CO7C 2/22) 04.12.1984.

11 Weissermel, K.; Arpe, H-J., *Industrial Organic Chemistry 2nd. Ed.*, VCH Verlagsgesellschaft, Weinheim, **1993**, 333-336.

Chapter 5

Variable Temperature NMR Studies

5.1.0. Introduction

NMR experiments on isolated complexes or *in situ* complex formation has given important information on ligand bonding modes, complex stabilities and metal centre Lewis acidity for new β-aminoketone complexes of zirconium. Some of this work, such as ligand bonding modes in bis-ligand complexes, has been mentioned in the previous chapter and will be not expanded here.

It is important to be able to explain, in terms of the developed model for zirconium catalysed ethylene oligomerisation, the various observations noted during synthesis and catalysis. Synthetic work has indicated that alkylated zirconium complexes of Schiff's bases, picolinic acid or acetylacetone are not stable. Zirconium-β-aminoketone complex stability is dependent on the electronic properties of the amine substituent. Catalysis indicates, that for these β-aminoketone-zirconium systems, preformed complexes have higher activities than adducts or *in situ* generated systems and also that use of preformed complexes results in a higher average oligomer weight. Electron withdrawing amine substituents increase oligomerisation activity.

It has been proposed in Chapter 2 that conditions which favour transition states for β-hydride elimination would lead to better oligomerisation rather than polymerisation catalysts. The expected highly Lewis acidic metal centre would need to be stabilised hence the use of hemi-labile, bidentate, chelate ligands. Variation of the donor properties of the labile end group could then lead to control of the oligomerisation process while stabilising the complex. NMR techniques have proved to be sensitive tools in probing the complicated behaviour of ligands in these new systems.

Discussions included in this section focus on the *in situ* formation of alkylated, bis-ligand complexes of zirconium and ligand metal interactions. The choice of tetrabenzyl zirconium as a starting material is discussed as is the isolation of a number of new organometallic zirconium complexes showing unusual ligand bonding modes due to the high Lewis acidity of the metal centre and/or constrained steric environments.

Highly fluxional ligand environments, noted for almost all bis-ligand complexes, have been discussed in the previous chapter and will not be discussed further here.

5.1.1. Alkyl/Aryl Zirconium Complexes (Ligand Selection)

The stabilisation of highly Lewis acidic metal centres was thought to be of prime importance in this study. Alkyl or aryl zirconium complexes must therefore be intrinsically stable under these condition. Ligands capable of β-hydride elimination were immediately excluded leaving aryl, benzyl or highly substituted alkyls or methyl silanes. Stability under reasonable working conditions was also considered important, eliminating phenyl, methyl or allyl zirconium species, although these ligands will be included in later work. Tetrabenzyl zirconium, and therefore the benzyl ligand, possesses the stability requirements and the benzyl ligand has the added advantage of producing a number of stabilising bonding modes, σ–, η^2- and η^3-Bz (Figure 5.1.), which were first suggested by King & Fronzaglia[1] on the basis of NMR studies. Various workers have extended these ideas examining benzylic ligands in a number of metal complexes[2] and all these bonding modes are now well characterised.

Figure 5.1.
σ–, η^2-, η^3-Bonding Modes for the Benzyl Ligand

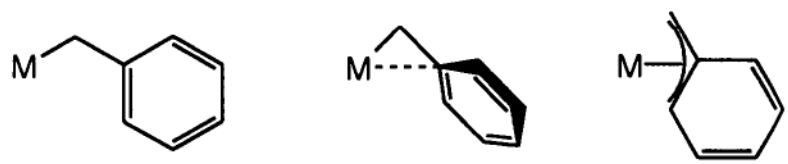

The presence of η^2-benzylic bonding is characterised by upfield ^{13}C-NMR shifts for the methylene and *ipso*-carbons, < 75 ppm and around 130 ppm respectively, as well as a large methylene carbon C-H coupling, > 130Hz. Benzylic η^3-bonding is characterised by splitting of the benzyl methylene ^{1}H-NMR peaks, a strong upfield shift in the *ortho*-protons, 6.3-6.5 ppm, splitting of the *ortho*-hydrogen peak as the two sides of the phenyl group become inequivalent, strong upfield ^{13}C-NMR shifts of the *ipso* and *ortho*-carbons, splitting of the *ortho*-carbons and large C-H coupling on the benzylic methylene.

Although strong metal centre-phenyl ring interactions are seen in most of the reported metal complexes, therefore indicating at least dihapto benzyl bonding. Definite "freezing out" of a particular η^3-benzyl bonding mode is rarely seen. NMR spectra of the majority of these complexes always showed singlets for the benzylic methyl group and no differentiation in the *ortho*-hydrogen on the phenyl group.

Therefore in solution a rapid interconversion between possible environments was seen, i.e. fast suprafacial exchange.

Figure 5.2.
Suprafacial Exchange for η^3-benzyl in η^3-MeBzMo(C_5H_5)$(CO)_2$

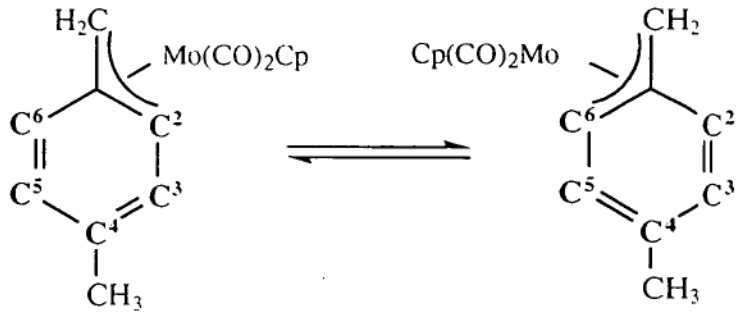

Figure 5.3.

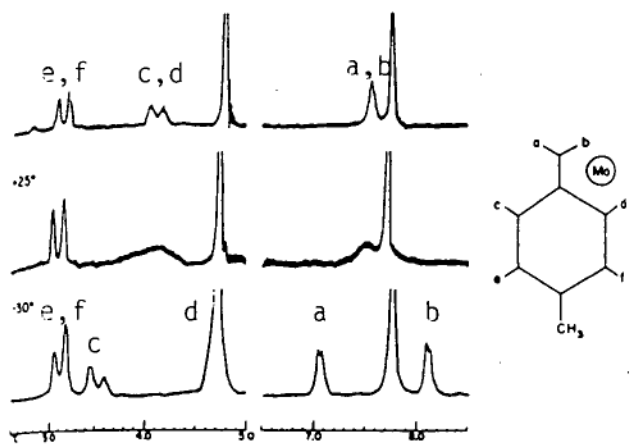

^{1}H-NMR of η^3-MeBzMo(C_5H_5)$(CO)_2$ in $CDCl_3$ as reported by Cotton, F.A., Marks, & T.J. *J. Am. Chem. Soc.* 91, **1969**, 1339-1346, shifts reported in τ

For some metal complexes this "freezing out" of η^3-bound benzyl was observed with complete resolution of the *ortho*-hydrogen in ^{1}H NMR studies. Cotton & Marks[3] have demonstrated this behaviour with the molybdenum complex, η^3-MeBzMo(C_5H_5)$(CO)_2$, (Figure 5.2). The complex was shown to undergo suprafacial and antarafacial exchange via a 14-electron, σ-benzyl intermediate. VT-^{1}H NMR studies on this complex show that on cooling to -30°C both the methylene

and *ortho*-hydrogen signals split giving distinct new environments (from τ 4.2 to 3.6 & 4.8 ppm, *o*-H; 7.6 to 7.1 & 8.2 ppm, CH_2), (Figure 5.3). X-Ray crystal structure determination confirms the assignment of η^3-bonding in this complex with Zr-C bond lengths of 2.48, 2.36 and 2.27Å for the *ortho*, *ipso* and methylene carbons respectively. In this case there is no noticeable splitting of the meta-hydrogen signals.

Similarly a VT-^{1}H NMR study on the thorium complex[4], $Th(C_5Me_5)Bz_3$, has shown "freezing out" of η^3-bound benzyl below -90°C.

5.1.2. Benzyl Zirconium Complexes

Benzyl-zirconium complexes have been shown in numerous X-Ray crystal structures[5] to have σ-, η^2- or mixed (σ-, η^2)- bound benzyl ligands[6,7] similar to that found in other metals. In these complexes the plane of the phenyl group in η^2-bound benzyl lies approximately perpendicular to the Zr-CH_2 axis with a small Zr-CH_2-*ipso*-C angle allowing interaction of the metal centre with the *ipso*-carbon and the phenyl π-system (Figure 5.1). No evidence has been presented to indicate η^3-bound benzyl ligands in zirconium systems, as detailed for the molybdenum complex above. It has been suggested that for $Zr(OAr')Bz_3$, -OAr' = 2,6-di-*tert*-butylphenol, problems in determining the solid state structure may be due to highly fluxional η^1- and η^3- bonding[7b]. The related complex, $Zr(OAr')(CH_2PhF)_3$, has one η^2- and two σ-bound benzyl ligands.

This form of benzylic bonding needs to be distinguished from a similar effect caused by inequivalent environments in chiral or prochiral zirconium complexes or zirconium complexes of low symmetry, such as *ansa*-metallocenes. In this case the methylene protons experience different steric environments causing splitting in the ^{1}H-NMR but with a typical σ- or η^2-bound benzyl[8] (Table 5.1).

The methylene signals for the complexes described in Table 5.1 are split. However, the $Et(Ind)_2Zr(CH_2Ph)_2$ complex has a typical σ-bonded benzyl while the cationic complex indicates a typical η^2-bonded benzyl, ^{13}C shifts of 68.4, 152.7 and 56.7, 125-130 respectively for the methylene and *ipso*-carbons. There is no indication, through splitting of the NMR signal, of unusual bonding involvement for *ortho*-protons or *ipso*- and *ortho*-carbon atoms. The splitting patterns can be explained entirely on steric or symmetry grounds.

Table 5.1.

Benzyl ^{1}H-NMR Splitting Patterns in Chiral Zirconium Complexes

Complex	^{1}H	Group		^{13}C
$Et(Ind)_2Zr(CH_2Ph)_2$				
in CD_2Cl_2	-0.37(d, 2H, J=11.2)	CH_2Ph		68.4(t,J_{CH}=120.5)
	0.59(d, 2H, J=11.2)	CH_2Ph		
	6.53-7.63(m)	Ph	*o*-	128.3
			i-	152.7
$Et(Ind)_2Zr(CH_2 Ph)^+B(Ph)_4^-$				
in $C_2D_2Cl_4$	0.12(d,1H J=7.8)	CH_2Ph		56.7(t, J_{CH}=132)
	3.31(d, 1H J=7.8)	CH_2Ph		
	7.07(d, 2H J=7.5)	Ph	*o*-	122.7 or 132.9
			i-	124.6 or 132.7

VT-NMR Experiments

5.2.0. Bis-β-Aminoketone, Benzyl Zirconium Complexes

All benzyl, bis-β-aminoketone complexes of zirconium, found to be stable at 0°C or above, show ^{1}H-NMR splitting patterns associated with σ-bound benzyl ligands in non symmetric environments at low temperature. The effect, observed in VT-NMR experiments, is dependent on the electron withdrawing power of the ligand substituents. The only exception being the perfluorinated complex, (*i*-Pr-Ntfac)$_2$ZrBz$_2$, which is seen to have two distinct benzyl environments and 4 distinct proton environments for the benzyl methylene group at 0°C due to β-aminoketone ligand lability. Two distinct amine environments are present, leading to inequivalent environments for the methylene protons. VT ^{1}H- & ^{13}C-NMR data for new complexes showing distinct behaviour are described below.

5.2.1. (Ph-Nacac)$_2$ZrBz$_2$

In situ formation of (Ph-Nacac)$_2$ZrBz$_2$ monitored by VT-NMR indicates that the N-phenyl substituted β-aminoketone completely reacts with ZrBz$_4$ at -60°C (Appendix B.2.4). The β-aminoketone ligand resonances for the isolated complex (δ 1.61, 5.08, 6.63, 6.98, 7.10 ppm) vary only slightly on warming to 20°C which has been taken to indicate bidentate, chelate coordination (Figure 5.4). The β-aminoketone phenyl

group *ortho*-proton (labelled Ro) shows a large upfield shift at δ 6.65 ppm. The process is completely reversible and on cooling to -60°C a spectrum identical to that shown is obtained.

The variation in the benzyl peak resonances is particularly interesting. The methylene protons (labelled Bm) appear as a doublet of doublets at -60°C which coalesce on warming and move downfield to appear as a singlet at 20°C (from δ 1.29 & 1.16 ppm to 1.77 ppm). The *ortho*-hydrogen peaks on the benzyl phenyl (labelled Bo) appear strongly shifted upfield as two doublets. The doublets also coalesce on warming appearing as a doublet at 20°C (from δ 6.60 & 6.23 ppm to 6.49 ppm). This pattern is identical in form to that discussed above for the η^3-benzylmolybdenum complex (Figure 5.3). Inequivalence of the two meta-protons is not observed in this set of spectra however the peak is seen to broaden on cooling. It was therefore important to be able to distinguish between two possible benzyl coordination modes, either benzylic or as benzyl in a non-symmetrical environment. It was thought that the presence of two bidentate, coordinate donor ligands would decrease the Lewis acidity of the metal centre and significantly decrease the possibility of η^3-benzyl ligands.

Variable Temperature ^{13}C-NMR on the (Ph-Nacac)$_2$ZrBz$_2$ complex (Figure 5.5) indicates the presence of what can be considered σ-bound benzyl ligands, a methylene shift (Bm) of 65.8 ppm with a C-H coupling of 124Hz and the *ipso*-carbon resonance (Bi) at 147.3 ppm (selected NMR data for bis-ligand benzyl complexes are summarised in Table 5.2). It is therefore believed that the splitting of the *ortho*-phenyl and methylene signals is due to loss of symmetry at low temperature as in the *ansa*-metallocenes mentioned above.

Figure 5.4.

Variable Temperature ^{1}H-NMR of (Ph-Nacac)$_2$ZrBz$_2$ in CD_2Cl_2

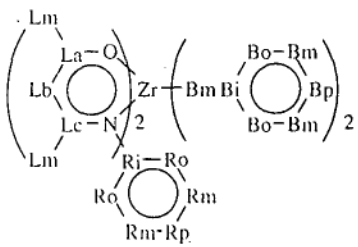

Key to Spectra Resonances

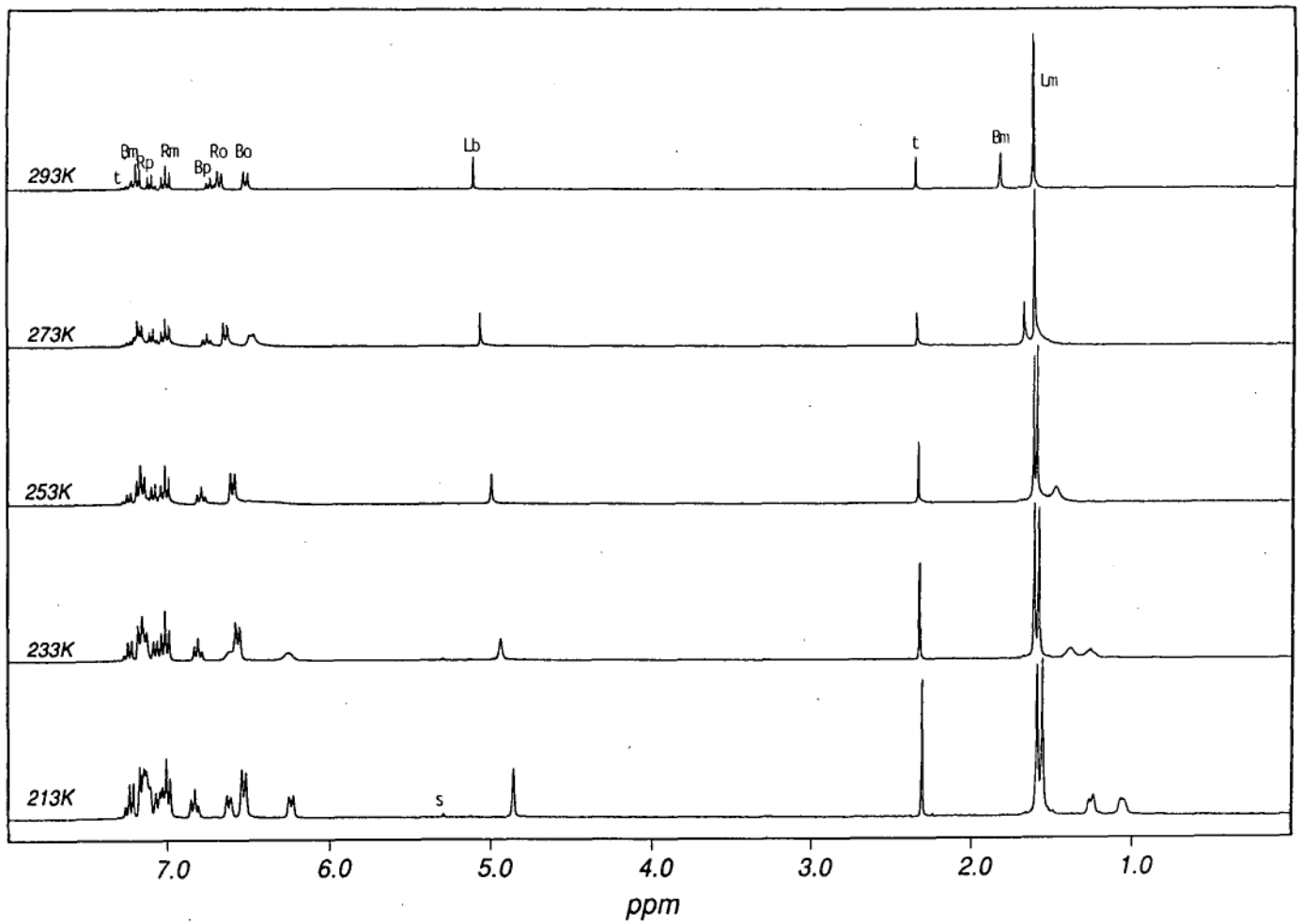

Where: Ligand backbone: Lm=methyls, Lb=methine; N-phenyl substituent: Ro=*ortho*-Ph, Rm=*meta*-Ph, Rp=*para*-Ph; Benzyl: Bm (1-2ppm)=benzyl methylene, Bo=*ortho*-Bz, Bm=*meta*-Bz, Bp=*para*-Bz; s=solvent, t=toluene.

Figure 5.5.

Variable Temperature ^{13}C-NMR of (Ph-Nacac)$_2$ZrBz$_2$ in CD_2Cl_2

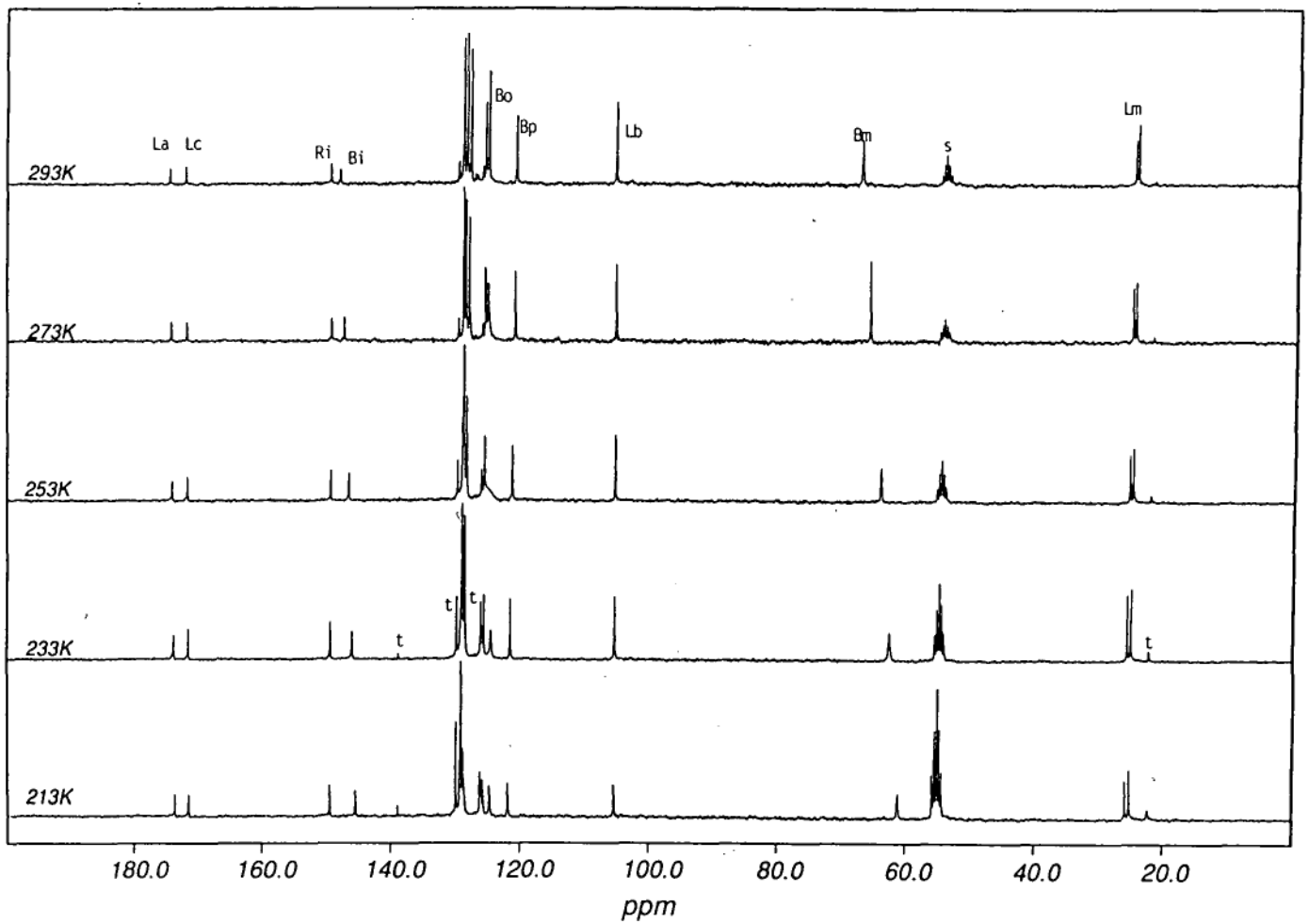

Where: Ligand backbone: Lm=methyls, La=carbonyl carbon, Lb=methine, Lc=amino carbon; N-phenyl substituent: Ri=*ipso*-Ph, Ro=*ortho*-Ph, Rm=*meta*-Ph, Rp=*para*-Ph; Benzyl: Bm (1-2ppm)=benzyl methylene, Bi=*ipso*-Bz, Bo=*ortho*-Bz, Bm=*meta*-Bz, Bp=*para*-Bz; s=solvent, t=toluene.

In these complexes however a very constrained environment must be present as no other study has reported splitting of the *ortho* and *meta* proton and carbon resonances. It is believed that a metal centre of high Lewis acidity is present causing the relatively high upfield methylene shifts compared to $ZrBz_4$ but a dihapto bonding arrangement cannot form due to steric constraints.

A complex similar to that shown for the $(Ph\text{-}Nacac)_2ZrCl_2$ complex is proposed for the alkylated bis-ligand complex with *cis*-benzyls. Upon cooling the favoured configuration involves minor interaction of the metal centre with the benzyl *ipso*-carbons, as indicated by the upfield shifts of the methylene and *ipso*-carbon resonances in the ^{1}H-NMR and ^{13}C-NMR spectra (Figure 5.4 & 5). However the interaction is not strong enough to be regarded as a true η^2-bound benzyl.

Table 5.2.
Summary of NMR Data for Benzyl Ligands in $(R\text{-}\widehat{NO})_2ZrBz_2$ Complexes in CD_2Cl_2 at -20°C

	Benzyl Group				
Complex	CH_2	*i*-Ph	*o*-Ph	*m*-Ph	*p*-Ph
Benzyl ^{1}H-NMR					
$(Ph\text{-}Nacac)_2ZrBz_2$	2.365(s)		6.523(d)	7.203(t)	6.755(t)
$(i\text{-}Pr\text{-}Ntfac)_2ZrBz_2$	1.990(d), 1.841(d), 1.647(bs), 1.543(bs)		6.478(d) & 6.652(d)	7.036(t) & 6.952(t)	6.850(t,) & 6.689(t)
$(Cy\text{-}Nacac)_2ZrBz_2$	1.9221(s)		6.641(d)	6.900(t)	6.708(t)
$(i\text{-}Pr\text{-}Nacac)_2ZrBz_2$	1.895(s)		6.654(d)	6.938(t)	6.622(t)
Benzyl ^{13}C-NMR					
$(Ph\text{-}Nacac)_2ZrBz_2$	65.8 ($J_{C,H}$ 124.0Hz)	147.3	128.5	127.9	120.8
$(i\text{-}Pr\text{-}Ntfac)_2ZrBz_2$	65.9 & 65.2 ($J_{C,H}$ 128Hz)	145.3 & 144	129.7 & 128.9	128.5	122.4 & 122.0
$(Cy\text{-}Nacac)_2ZrBz_2$	69.8	149.9	128.1	127.6	120.2
$(i\text{-}Pr\text{-}Nacac)_2ZrBz_2$	66.6(b)	148.7	128.0 or 127.7	128.0 or 127.7	120.2

5.2.2. (*i*-Pr-Nacac)$_2$ZrBz$_2$

The *in situ* formation of (*i*-Pr-Nacac)$_2$ZrBz$_2$ monitored by VT-NMR indicated that reaction between ZrBz$_4$ and the free ligand began at ≤-60°C and is not complete until ≈-20°C; as indicated by the absence of NH peak and the formation of toluene (Figure 3.8). Isolation of the pure complex allowed examination of the ligand environment down to -60°C (Figure 5.6). At 20°C one ligand environment is observed, although all peaks are slightly broadened. The benzyl *ortho*- and *para*-resonances (Bo and Bp) are shifted strongly upfield, 6.65 and 6.62 ppm respectively.

Cooling the complex does not result in major changes for the β-aminoketone ligand backbone peak positions (as is the case for all complexes isolated) which has been taken to indicate strong bidentate, chelate coordination. The broadening of the *i*-Pr peaks is associated with changes in the benzyl ligand on cooling and is thought to be steric in origin. Benzyl resonances broaden on cooling with the methylene (Bm) and *ortho*-phenyl (Bo) peaks splitting into poorly resolved doublets at -40°C (Bm from δ 1.89 to 1.36 & 1.55 ppm and Bo from δ 6.65 to 6.40 & 6.68 ppm). Variations seen in the ^{13}C-NMR spectra, are similar to those for the N-phenyl substituted complex discussed above, therefore indicating spectral changes are due to loss of symmetry at low temperature with the benzyl resonances being similar to those for σ-bound benzyl ligands (Table 5.2).

5.2.3. (Cy-Nacac)$_2$ZrBz$_2$

In situ formation of (Cy-Nacac)$_2$ZrBz$_2$ monitored by VT-NMR indicates that the free ligand has completely reacted with ZrBz$_4$ at -40°C (Appendix B.2.2). Warming the mixture to 20°C results in the formation of one predominant product which appears stable, however the aromatic region of the spectrum remains difficult to interpret showing a number of differing benzyl environments. VT-NMR spectra collected on the isolated (Cy-Nacac)$_2$ZrBz$_2$ complex allowed for better analysis (Appendix B.3.1. & B.3.2.) where cooling to -60°C results in significant variations in β-aminoketone ligand resonances, which can be explained in terms of cyclohexyl ring rearrangements as observed for the *iso*-propyl complex. A number of environments are noted on cooling the complex to -60°C reflecting the complexity in the cyclohexyl environment.

Figure 5.6.

Variable Temperature ^{1}H-NMR of (*i*-Pr-Nacac)$_2$ZrBz$_2$ in CD_2Cl_2

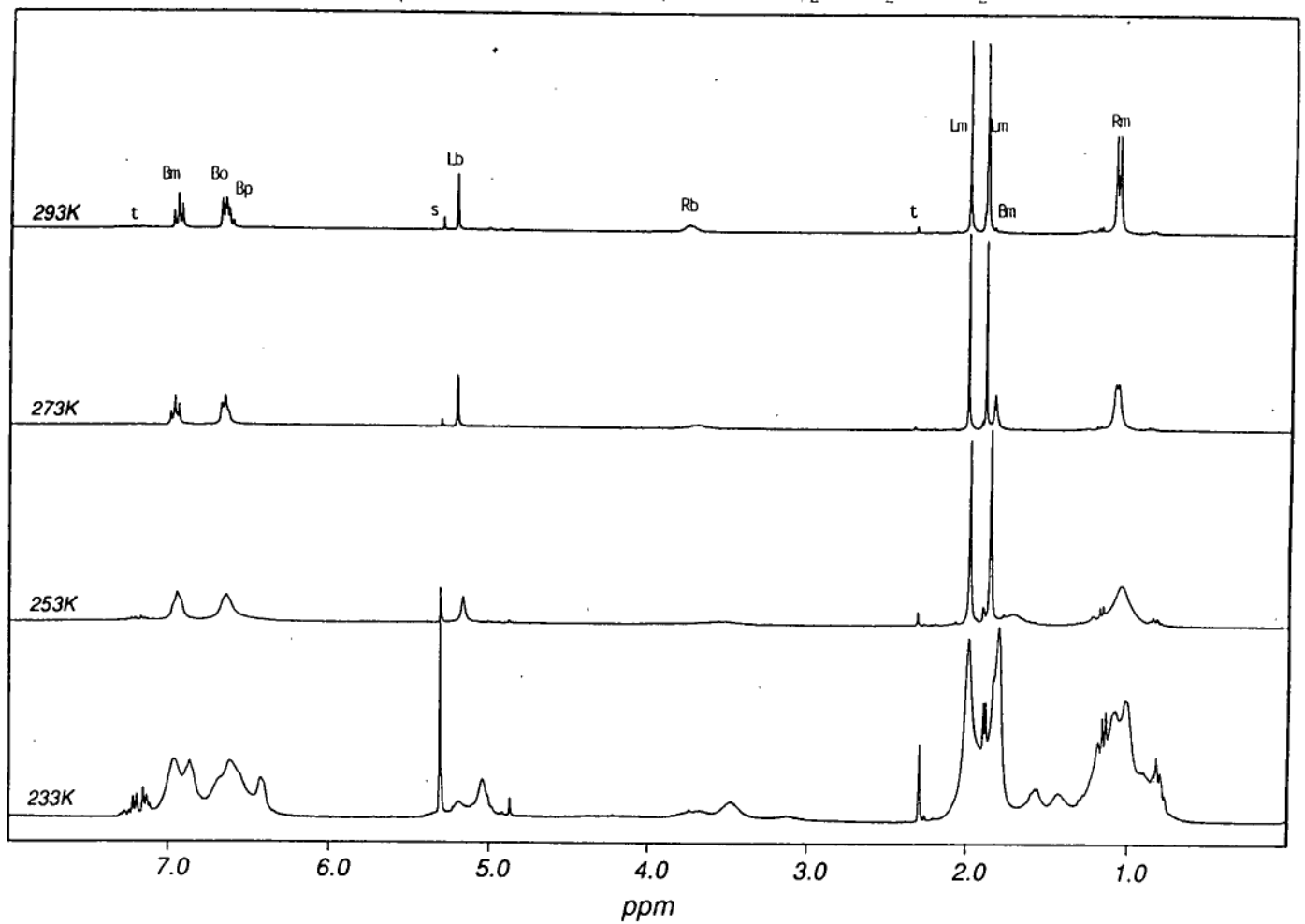

Where: N-*iso*-propyl substituent: Rb=*iso*-propyl methine, Rm=*iso*-propyl methyls; rest as in Figure 5.4.

Figure 5.7.

Variable Temperature ^{13}C-NMR of (*i*-Pr-Nacac)$_2$ZrBz$_2$ in CD_2Cl_2

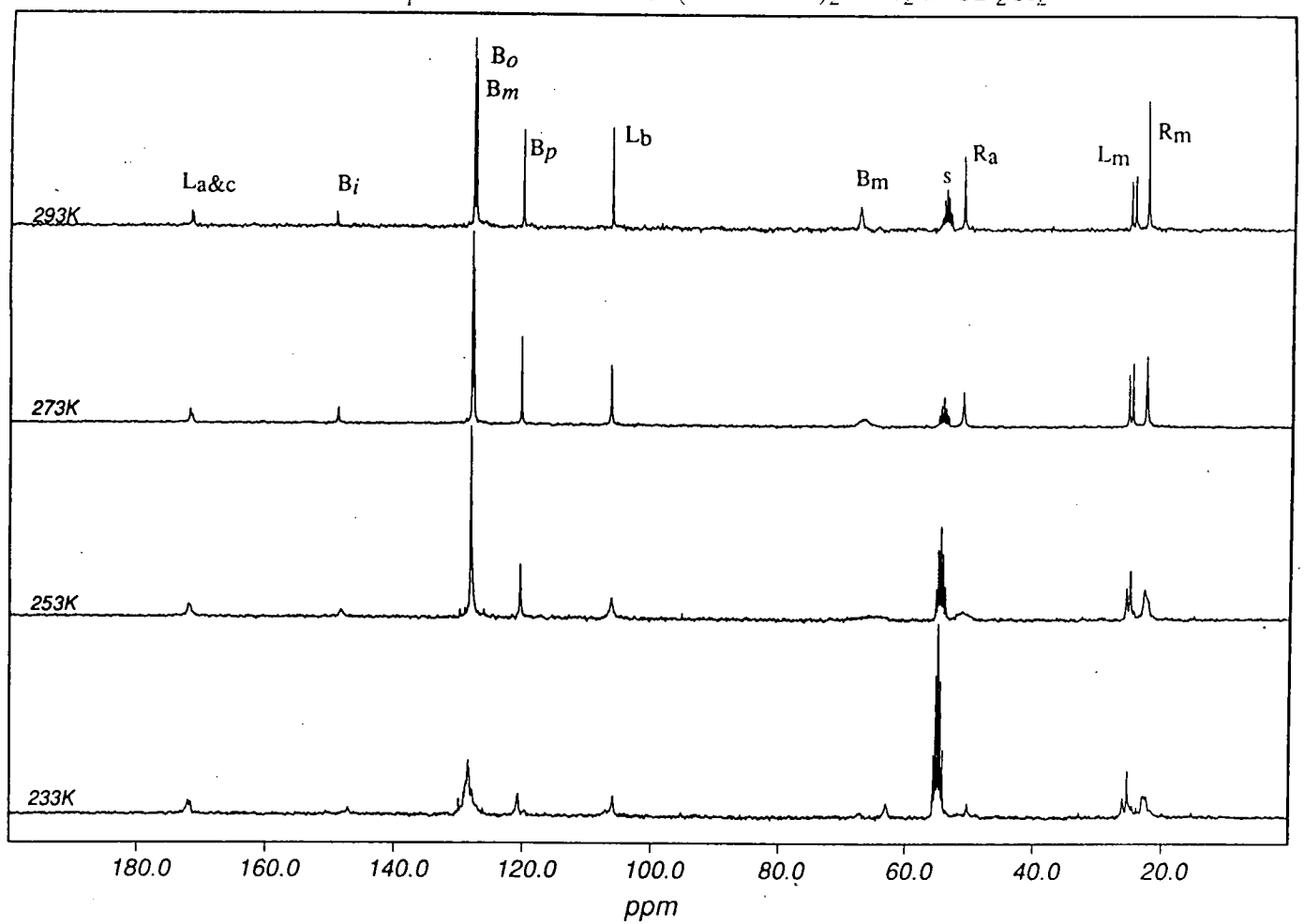

Where: N-*iso*-propyl substituent: Rh=*iso*-propyl methine, Rm=*iso*-propyl methyls; rest as in Figure 5.4.

Due to the complexity of this system and it's similarity to the *i*-Pr containing complex (with respect to the benzyl resonances) no further studies have been completed.

Table 5.3.
Comparative ^{1}H NMR Ligand Backbone Peak Shifts
for (R-Nacac)$_2$ZrCl$_2$ and (R-Nacac)$_2$ZrBz$_2$

	C-N	C-O	Me's CN-Me & CO-Me	CH
^{1}H NMR				
(*i*-Pr-Nacac)$_2$ZrCl$_2$			2.154(s) & 1.909(s)	5.398(s)
(*i*-Pr-Nacac)$_2$ZrBz$_2$			2.005(s) & 1.906(s)	5.212(s)
(Ph-Nacac)$_2$ZrCl$_2$			1.359(s) & 1.687(s)	5.305(s)
(Ph-Nacac)$_2$ZrBz$_2$			1.628(s) & 1.637(s)	5.119(s)
(*i*-Pr-Ntfac)$_2$ZrBz$_2$			2.156 & 2.120	5.737 & 5.632
(Cy-Nacac)$_2$ZrBz$_2$			2.021(s) & 1.908(s)	5.214(s)
^{13}C NMR				
(*i*-Pr-Nacac)$_2$ZrCl$_2$	173.9 or 172.6	173.9 or 172.6	24.1 & 25.0	109.0
(*i*-Pr-Nacac)$_2$ZrBz$_2$	171.5 or 171.2	171.5 or 171.2	24.7 & 25.3	106.3
(Ph-Nacac)$_2$ZrCl$_2$	174.7	174.7	23.2 & 25.0	107.2
(Ph-Nacac)$_2$ZrBz$_2$	171.7	174.2	24.6 & 25.1	105.2
(*i*-Pr-Ntfac)$_2$ZrBz$_2$ [1]	172.4 & 171?(b)	153.5 & 152(m)	26.5 & 26.3	105.8 & 104.7
(Cy-Nacac)$_2$ZrBz$_2$	171.6	171.6	25.6 & 24.9	106.8

[1] also CF_3 resonances, quartets, at 120.6 & 120.2 ppm; in CD_2Cl_2 at 20°C

5.2.4. (*i*-Pr-Ntfac)$_2$ZrBz$_2$

Addition of an electron withdrawing group to the β-aminoketone backbone for the (*i*-Pr-Ntfac)$_2$ZrBz$_2$ complex resulted in a dramatic change in the dynamic behaviour of the ligands.

In situ formation of (*i*-Pr-Ntfac)$_2$ZrBz$_2$ monitored by ^{1}H-NMR indicates complete reaction of the free ligand with ZrBz$_4$ by -40°C, Appendix B.2.3. The pure complex was isolated and VT ^{1}H-NMR and ^{13}C-NMR spectra collected (Figures 5.8 and 5.9, also Appendix B.3.3-7). At -20°C two distinct β-aminoketone ligand environments are observed in the ^{1}H-NMR spectra although the peaks are broadened. The two sets

of benzyl ligand resonances reflect the two β-aminoketone environments. Warming the solution to 20°C results in broad unresolved peaks that coalesce but do not sharpen on warming further to 40°C. As CD_2Cl_2 was used as the solvent higher temperatures were not possible.

Spectral interpretation is complicated by peak multiplicity and coincident peaks for a very labile system. The peak positions for the two sets of ligand resonances are listed in Table 5.4. For each benzyl-ligand environment a set of doublet of doublets is seen for the methylene protons between 1 and 2 ppm (labelled Bm) indicating four distinct proton environments for the four methylene protons present.

The VT ^{13}C-NMR spectra similarly indicate two dynamic β-aminoketone and benzyl environments (Figure 5.9). The benzyl methylene and *ipso*-carbon resonances are shifted slightly upfield in comparison to the other alkylated bis-ligand complexes already described, indicating a greater degree of dihapto bonding (Table 5.2). However a C-H coupling constant for the methylene carbons of 128Hz and *ipso*-carbon resonances at 145.3 and 144.0 ppm compared to that of >130Hz and around 130 ppm, required for full dihapto bonding, indicate an equilibrium structure midway between σ- and η^2-bonding.

The NMR data can best be explained through a five coordinate complex in which only one of the nitrogen donor groups is coordinated and exchange is slow on the NMR timescale. One of the benzyl groups would then participate in a strengthened interaction with the metal centre but not significant enough to be regarded as full dihapto bonding. A metal centre of low symmetry results leading to the observed inequivalence of the benzyl methylene protons. The lower coordinating power of the nitrogen is thought to be due to an inductive effect of the trifluoro group on the ligand backbone and is indicated by the significant downfield shifts of the *iso*-propyl resonances when compared to the non-fluorinated complex, Tables 5.4 & 5.5. The reduced donor ability of the nitrogen atom is sufficient to preclude a second nitrogen coordination.

Figure 5.8.

Variable Temperature ^{1}H-NMR of (*i*-Pr-Ntfac)$_2$ZrBz$_2$ in CD_2Cl_2

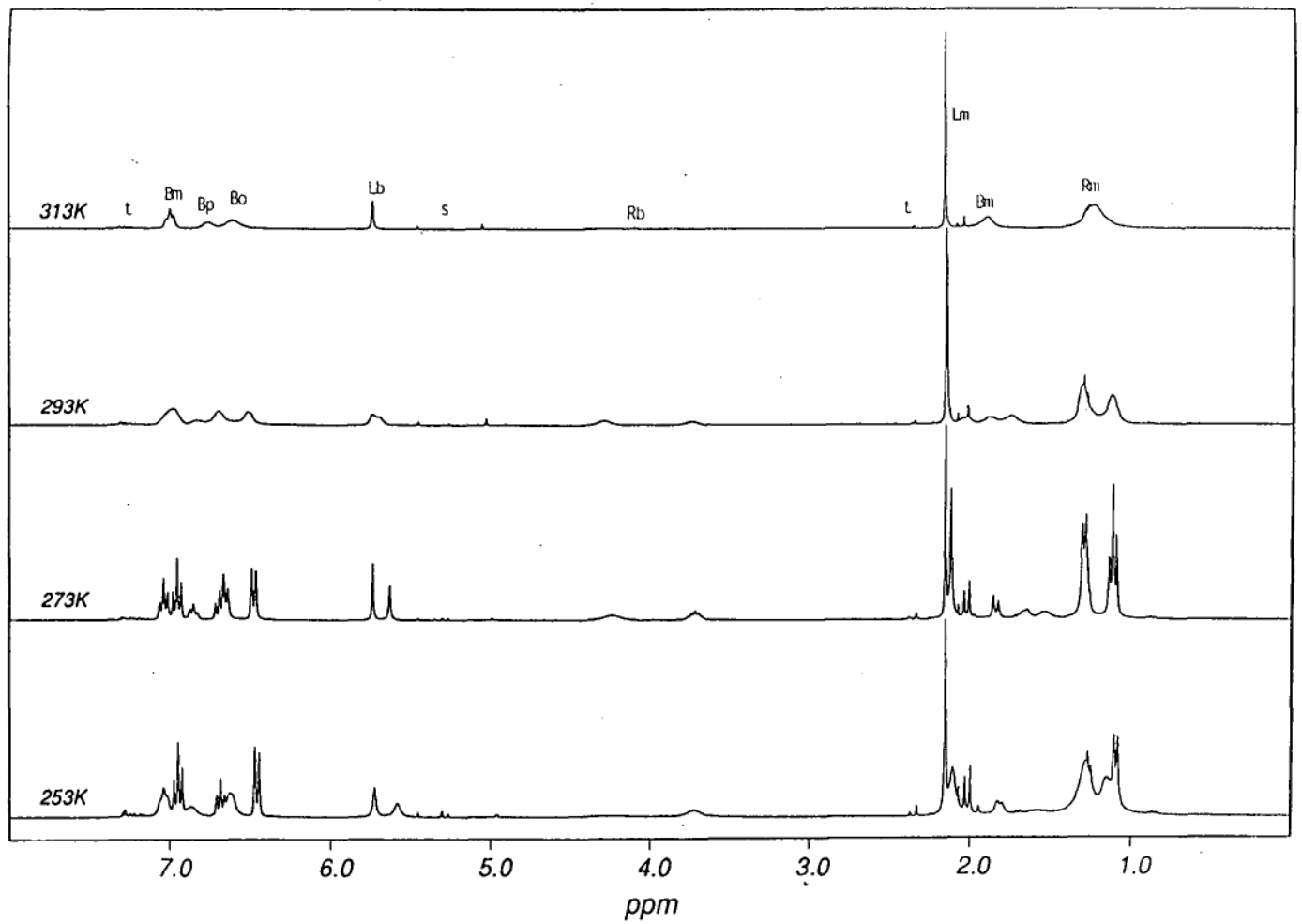

Where: N-*iso*-propyl substituent: Rb=*iso*-propyl methine, Rm=*iso*-propyl methyls; rest as in Figure 5.4.

Figure 5.9.

Variable Temperature ^{13}C-NMR of (*i*-Pr-Ntfac)$_2$ZrBz$_2$ in CD_2Cl_2

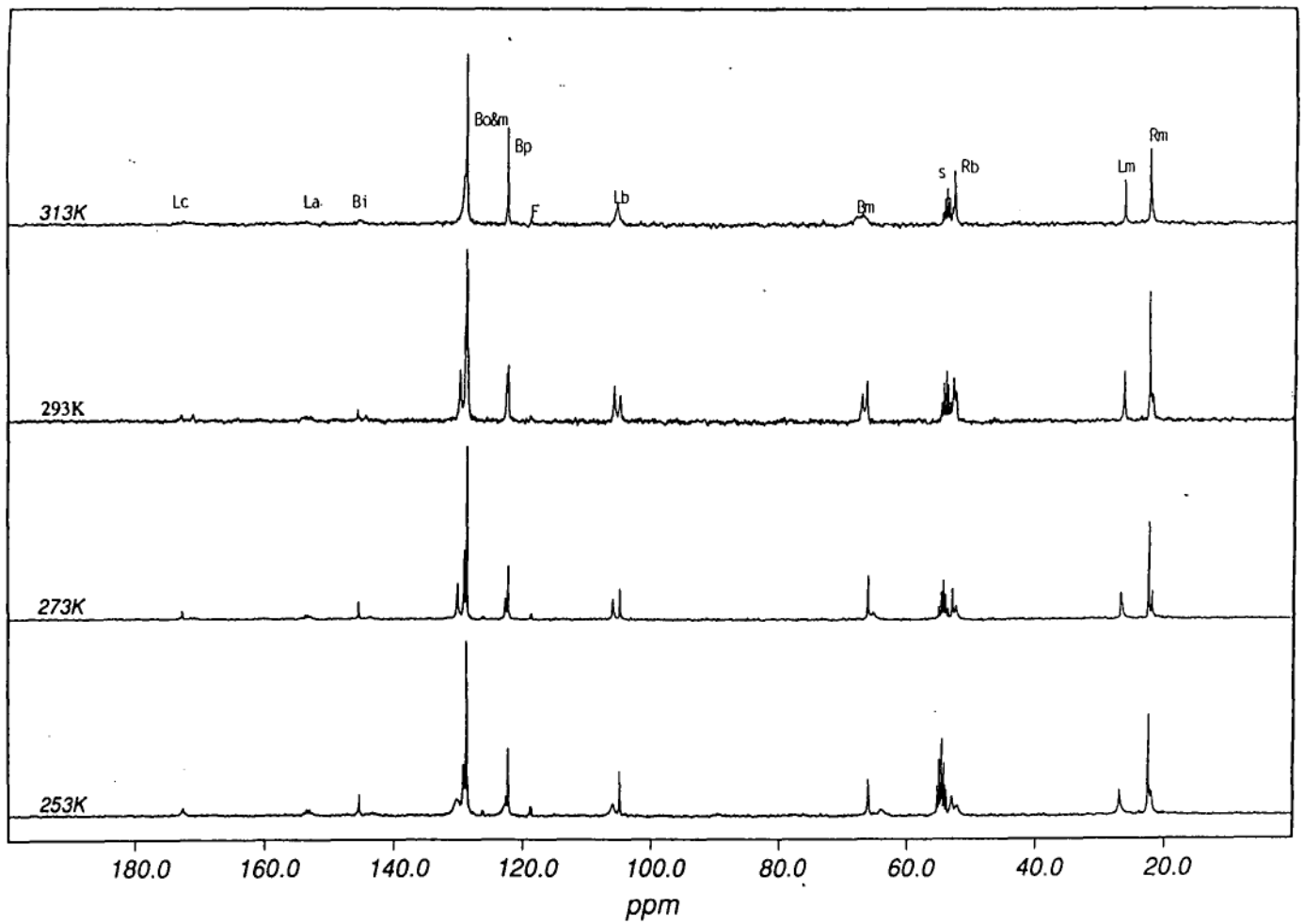

Where: Ligand backbone: F-CF_3; N-*iso*-propyl substituent: Rb=*iso*-propyl methine, Rm=*iso*-propyl methyls; rest as in Figure 5.4.

In general, an upfield shift of the ligand resonances on alkylating (R-Nacac)$_2$ZrCl$_2$ complexes, indicates a higher chelate ring current (Table 5.3 & 5.5) and therefore a lower metal centre Lewis acidity. This is as would be expected by the substitution two chloride ligands by two donor benzyl groups. The phenyl group appears to be inductively more electron donating than the *iso*-propyl group in these complexes as indicated by the upfield shift of the methylene resonances in the N-phenyl substituted complexes compared to the analogous N-*iso*-propyl substituted complexes. As expected fluorinating the ligand backbone increases the metal centre Lewis acidity (Table 5.3). Models had indicated that the amino substituent may interact with the nearest methyl group and may have explained the δ 0.15-0.25 ppm downfield shift in the CN-Methyl resonances however NOE experiments have failed to show a definite interaction.

Table 5.4.
Selected ^{1}H-NMR Data for (*i*-Pr-Ntfac)$_2$ZrBz$_2$
in comparison to (*i*-Pr-Nacac)$_2$ZrBz$_2$

	β-Aminoketone				Benzyl			
	H	H -Pr	Me *i*-Pr	Me C(N)	CH_2 Bz	*o*- Ph	*m*- Ph	*p*- Ph
Environment A	5.75	4.26	1.3	2.16	2.02, 1.88	6.50	6.96	6.70
Environment B	5.65	3.71	1.12	2.13	1.62, 1.72	6.69	7.04	6.88
(*i*-Pr-Nacac)$_2$ZrBz$_2$	5.21	3.72	1.09	2.01	1.85	6.66	6.98	6.66

in CD_2Cl_2 at 0°C.

5.2.5. Other complexes

A number of alternate ligand systems have been examined using VT-NMR techniques, as discussed in Chapter 3.6.4. For most of the systems any complexes which formed showed immediate or low temperature decomposition. A few were relatively stable and a number of interesting observations can be drawn from these sets of spectra. These data are reported in Table 3.5 while the Spectra are presented in Appendix B.2. Although it appears that these complexes may be stable under reasonable conditions no attempt has been made to isolate them to date.

i. $(SacPhac)_2ZrBz_2$

The complex formed on mixing H-SacPhac with $ZrBz_4$ in a 2:1 ratio appears to be relatively stable up to 0°C in the short term (Appendix B.2.5). The complex is mentioned because the largest variation in benzyl peak positions are seen (Table 5.5.) especially the upfield shift of the benzyl *ortho*-proton to δ 6.20 ppm. These values are significantly different to any other reported values and appear to be indicative of extensive zirconium benzyl-π interactions, however without complex isolation or further *in situ* complex formation to allow collection of VT ^{13}C-NMR data this cannot be confirmed.

Table 5.5.

Selected ^1H-NMR Data for Dibenzyl-Bis-β-Aminoketone Complexes

Complex	β-amino-ketone		Imino-R		Benzyl			
	Me	H	H *i*-Pr	Me *i*-Pr	*o*- Ph	*m*- Ph	*p*- Ph	CH_2 Bz
$(Ph\text{-}Nacac)_2ZrBz_2$	1.62, 1.61	5.09			6.49	>7	6.73	1.77
$(i\text{-}Pr\text{-}Nacac)_2ZrBz_2$	1.91, 2.00	5.21	3.76	1.08	6.65	6.93	6.62	1.90
$(i\text{-}Pr\text{-}Ntfac)_2ZrBz_2$ [1]	2.17	5.75	4.1	1.24	6.64	7.00	6.77	1.95
$(SacPhac)_2ZrBz_2$	2.62, 2.67	7.61			6.20	6.73	6.62	2.21
$ZrBz_4$					6.33	7.21	7.14	1.33
$ZrBz_4(dppe)$ [2]					6.73	7.13	6.93	1.85
$Zr(OAr')Bz_3$ [3]					6.71	>7.0	>7.0	2.32
$Zr(OAr')(CH_2PhF)_3$ [3]					6.4	>7.0	>7.0	2.08

in CD_2Cl_2 at 20°C, except [1] at 40°C

[2] Giolami, G.S., Wilkinson, G., Thornton-Pett, M., Hursthouse, M.B., *J. Chem. Soc. Dalton Trans.*, **1984**, 2789-2794, [3] Alelyunas, Y.W., Guo, Z., LaPointe, R.E., Jordan, R.F., *Organometallics* 12, **1993**, 544-553.

ii. $(i\text{-}Pr\text{-}NacSac)_2ZrBz_2$

The thiolated β-aminoketone, *i*-Pr-HNacSac, does not react with $ZrBz_4$ on mixing at low temperature. In fact on warming to 30°C no noticeable reaction has occurred, Appendix B.2.6. With prolonged storage at RT the system appears to undergo some form of slow decomposition, indicated by broad peaks formation with no structural information.

iii. $(i\text{-Pr-NPhO})_2ZrBz_2$

The *iso*-propyl substituted Schiff's base reacts cleanly with $ZrBz_4$ at low temperature giving what appears to be a stable complex with two different ligand environments (Appendix B.2.7). Due to time constraints no further work has been completed on this system.

5.3.0. Cationic Bis-Ligand Complexes of Zirconium

The formation of cationic complexes containing β-aminoketone ligands is dependant on the amino and backbone substituents. For simple alkyl substituted β-aminoketones, cationic species with η^2-bound benzyl ligands are formed.

5.3.1. Formation of $[(i\text{-Pr-Nacac})_2ZrBz][BPh_4]$

VT ^{1}H- & ^{13}C-NMR spectra for the $[(i\text{-Pr-Nacac})_2ZrBz][BPh_4]$ complex are shown in Figures 5.10 and 5.11. The ^{1}H-NMR spectra are dominated by the anion (A δ 7.32, 7.04 & 6.89 ppm, BPh_4^-) and the ligand resonances (L δ 2.15, 2.10, 3.96, 5.62, 1.34 & 1.12 ppm). The benzyl ligand resonances are obscured by the BPh_4^- and ligand methyl resonances (δ 2.15 & 2.10 ppm). The ligand resonances, except for the *iso*-propyl methyls, show no significant variation on warming which has been taken to indicate strong bidentate chelate coordination. The very large separation of the *iso*-propyl methyls (Rm δ 1.34 and 1.12 ppm) which coalesce on warming is not reflected in the methine peak (Rb δ 3.96 ppm) and indicates two significantly different steric environments. The spectrum of the $[ZrBz_3][BPh_4]$ complex (Complex A) is included for comparison.

Table 5.6.
Comparison of ^{13}C-NMR Benzyl Ligand Resonances
in Cationic Zirconium Complexes

	CH_2	*i*-Ph	*o*- & *m*-Ph	*p*-Ph
$(i\text{-Pr-Nacac})_2ZrBz_2$	66.6	148.7	128.0 & 127.7	120.2
$[(i\text{-Pr-Nacac})_2ZrBz][BPh_4]$	75.2	134.2	131.2 & 130.5	126.8
$[ZrBz_3][BPh_4]$ Complex A	74.4	136.9	130.6 & 130.2	124.4

Shifts(ppm) in CD_2Cl_2 at -20°C

The resonances due to benzyl ligand in the $[(i\text{-Pr-Nacac})_2ZrBz][BPh_4]$ complex are clearly seen in the ^{13}C-NMR spectra (Figure 5.11) where the methylene carbon is shifted slightly downfield (Bm from δ 66.6 to 75.2 ppm) and the *ipso*-carbon

resonance is shifted significantly upfield (Bi from δ 148.7 to 134.2 ppm) from their values for the bis-benzyl complex (Table 5.6). These values indicate strong dihapto bonding for the benzyl ligand. C-H coupling constants for the benzyl methylene could not be obtained so the ligand coordination cannot be confirmed.

The slight downfield shift of the benzyl methylene resonance is opposite to what would be normally expected on forming a cationic complex and may be due to steric interactions in the starting complex restricting formation of the dihapto bond.

5.3.2. Formation of $[(Ph\text{-}Nacac)_3Zr][BPh_4]$

In the case of phenyl substituted β-aminoketones or trifluoro-substituted β-aminoketones, the required bis-ligand cationic species are not generated. Data collected for the N-phenyl substituted complex is presented here. Ligand redistribution is believed to occur with formation of the tris-ligand species, $[(Ph\text{-}Nacac)_3ZrBz][BPh_4]$ and $[ZrBz_3][BPh_4]$. This is clearly observed in the ^1H & ^{13}C-NMR spectra of the reaction product (Figure 5.12 & 13). Complex A, $[ZrBz_3][BPh_4]$, was isolated from the reaction mixture and is characterised by the π-bound phenyl resonances at δ 8.2, 6.6 and 6.2 ppm and the benzyl *ortho*-proton at 6.28 ppm. These peaks are clearly identified in the reaction product and their presence is independent of the synthetic method used. Only one set of benzyl resonances is observed (B δ 1.54, 6.28 others overlap with BPh_4^- resonances).

A second set of resonances overlaps those due to $[ZrBz_3][BPh_4]$. These have been assigned to $[(Ph\text{-}Nacac)_3Zr][BPh_4]$. The free anion resonances, $[BPh_4^-]$, are seen at δ 7.3, 7.0 and 6.9 ppm. The ligand backbone resonances are clearly observed (δ 1.63, 1.71 & 5.45 ppm) while the N-phenyl resonances overlap those of free tetraphenyl borate.

The presence of the two species has also been confirmed by examination of the VT ^{13}C-NMR (Figure 5.13). The presence of only one benzyl environment is observed with one methylene resonance (Bm δ 74.4 ppm).

Figure 5.10.

VT ^{1}H-NMR Spectra of [(*i*-Pr-Nacac)$_2$ZrBz][BPh$_4$]

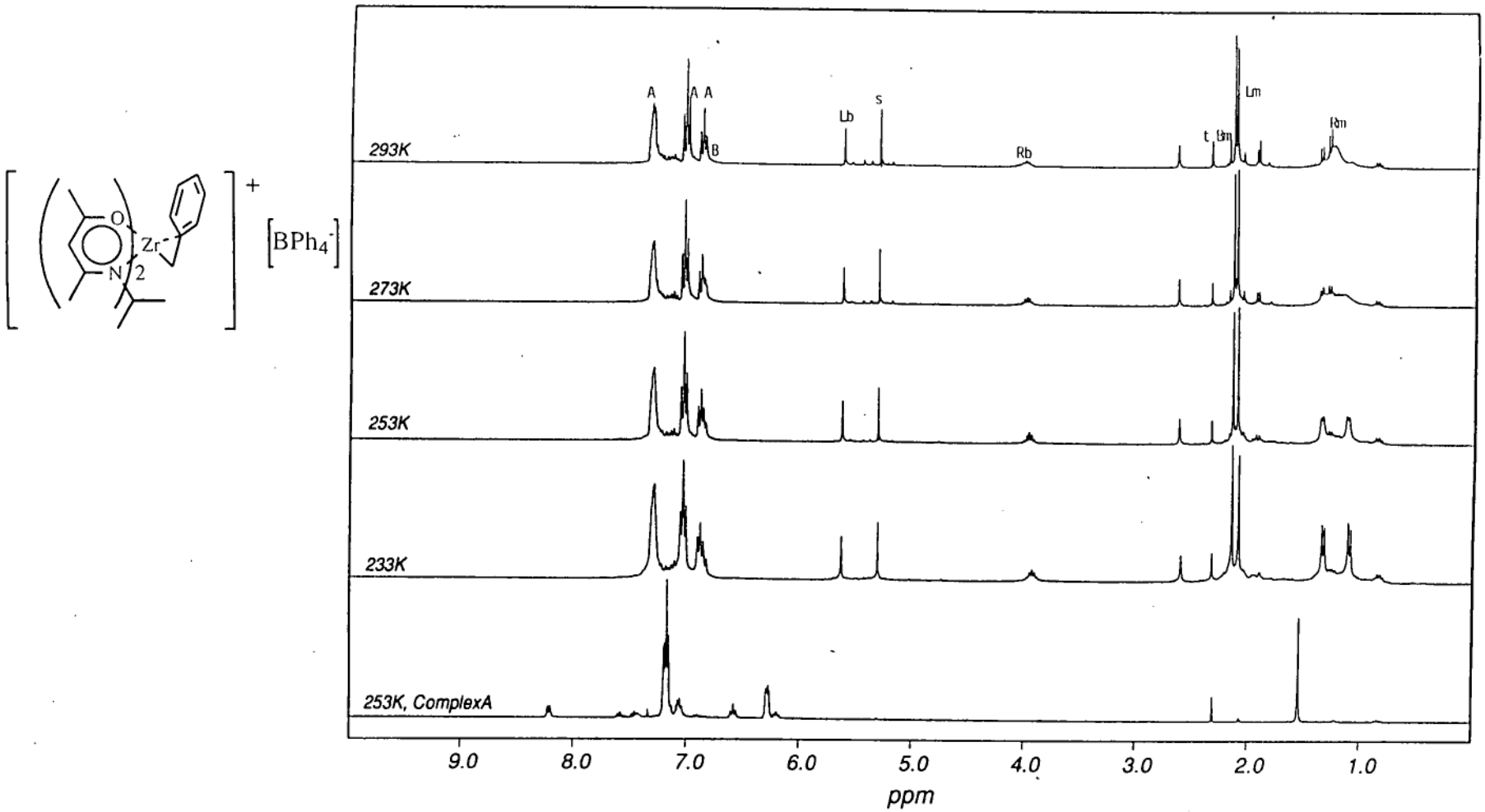

Where: Ligand backbone: Lm=methyls, Lb=methine; N-*iso*-propyl substituent: Rb=*iso*-propyl methine, Rm=*iso*-propyl methyls; Benzyl: Bm (1-2ppm)=benzyl methylene, B-Bz(peak under A); Tetraphenyl borate: A=anion phenyl; s=solvent, t=toluene.

Figure 5.11.

VT ^{13}C-NMR Spectra of [(*i*-Pr-Nacac)$_2$ZrBz][BPh_4]

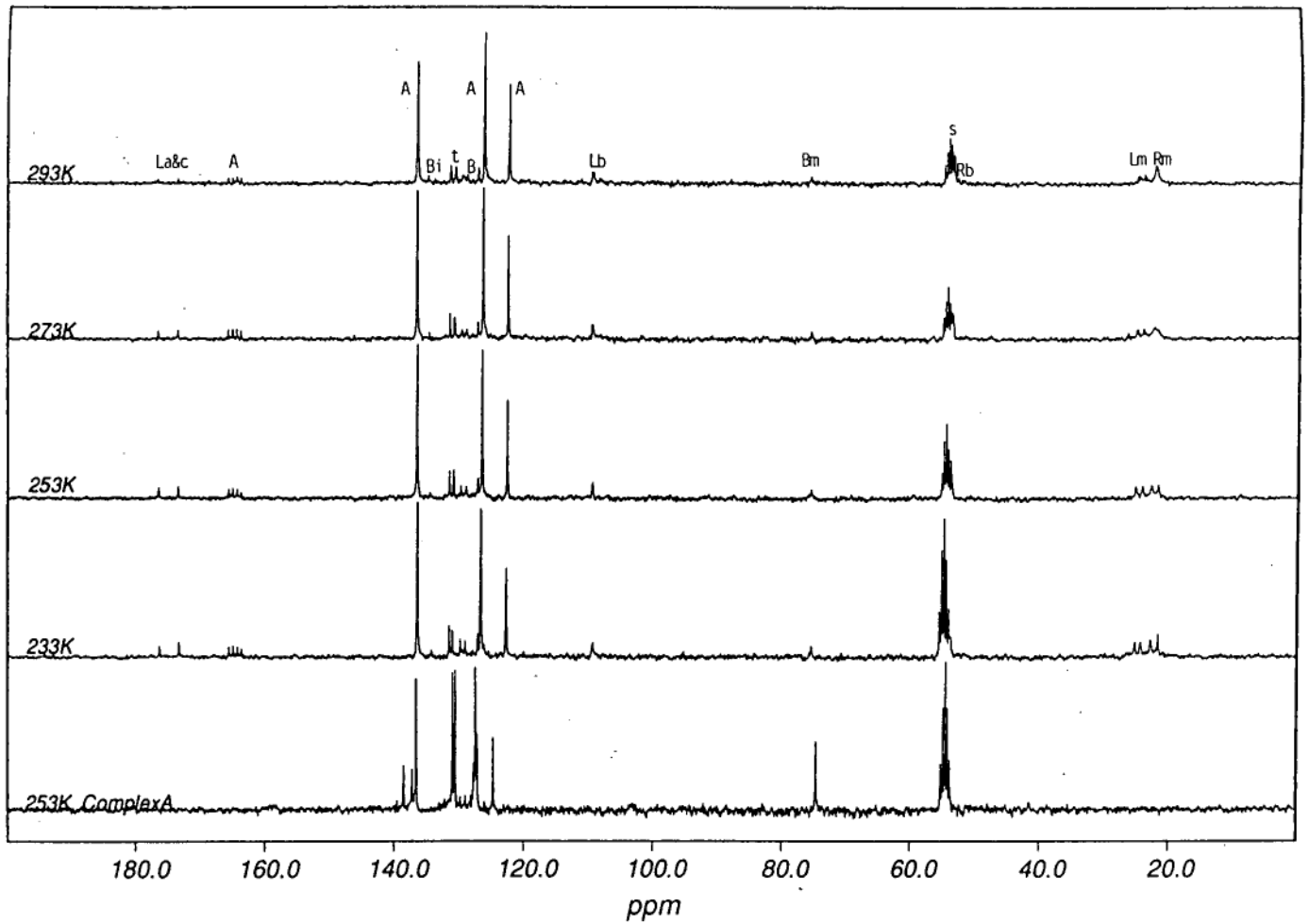

Where: Ligand backbone: Lm=methyls, La=carbonyl carbon, Lb=methine, Lc=amino carbon; N-*iso*-propyl substituent: Rb=*iso*-propyl methine, Rm=*iso*-propyl methyls; Benzyl: Bm (1-2ppm)=benzyl methylene, Bi=*ipso*-Bz, B=*ortho*-, *meta*- & *para*-Bz; s=solvent, t=toluene.

Figure 5.12.

VT ^{1}H-NMR Spectra of $[(Ph\text{-}Nacac)_3Zr][BPh_4]$ + $[ZrBz_3][BPh_4]$

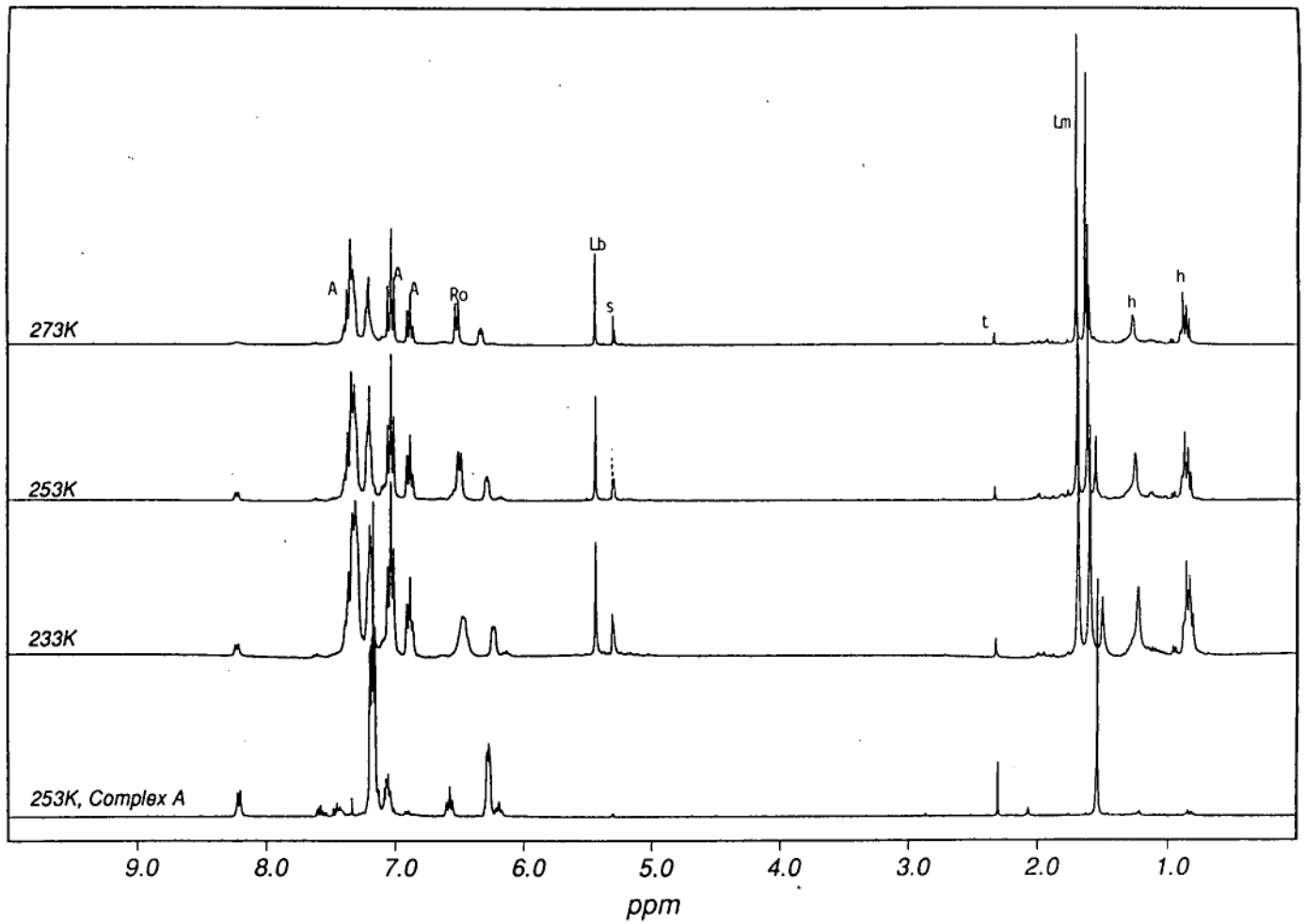

Where: Ligand backbone: Lm=methyls, La=carbonyl carbon, Lb=methine, Lc=amino carbon; N-*iso*-propyl substituent: Rb=*iso*-propyl methine, Rm=*iso*-propyl methyls; Benzyl: Bm (1-2ppm)=benzyl methylene, B=*ortho*-, *meta*- & *para*-Bz; s=solvent, t=toluene.

Figure 5.13.

VT $^{13}C\{^{1}H\}$-NMR Spectra of $[(Ph\text{-}Nacac)_3Zr][BPh_4]$ + $[ZrBz_3][BPh_4]$

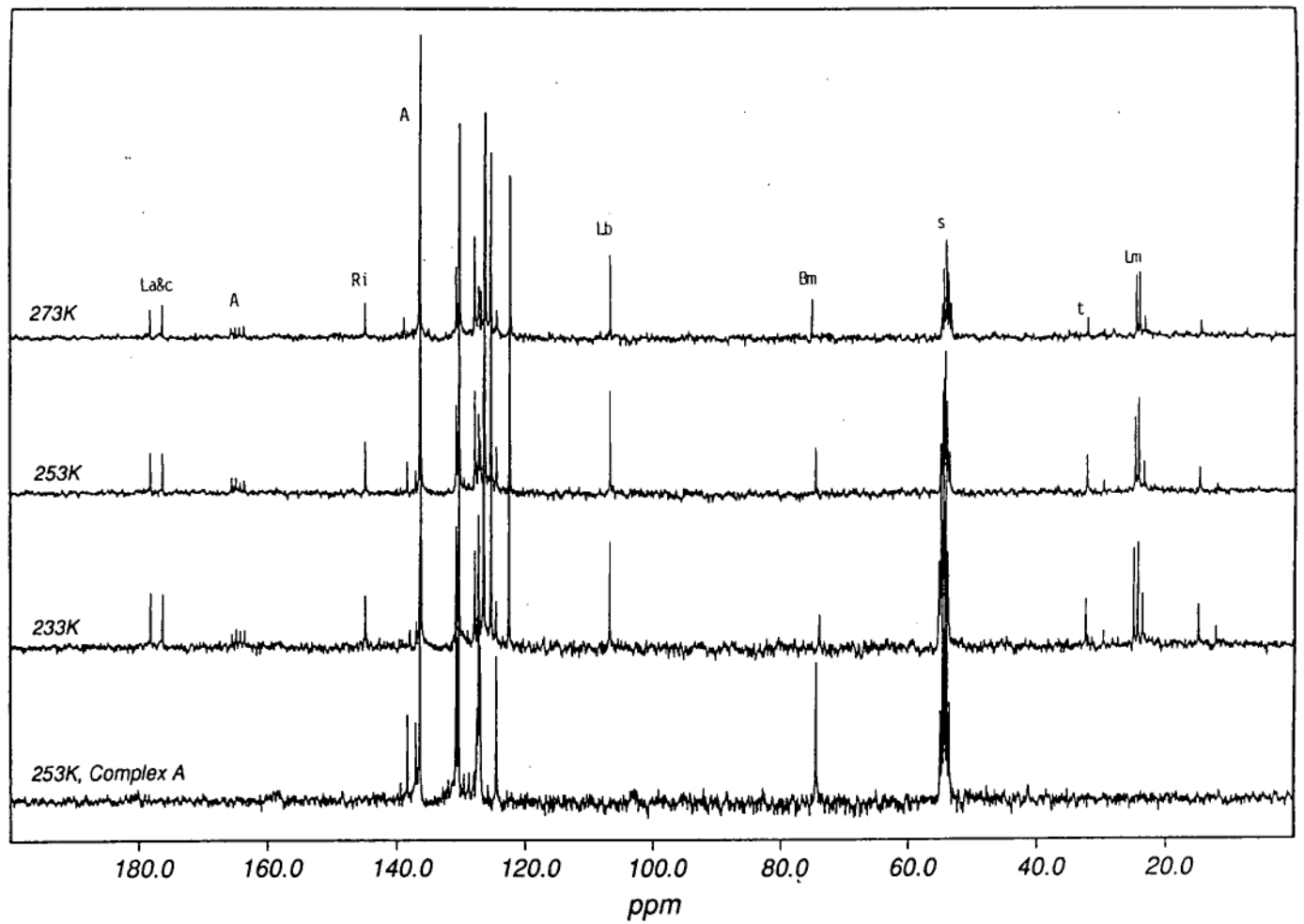

Where: Ligand backbone: Lm=methyls, La=carbonyl carbon, Lb=methine, Lc=amino carbon; N-*iso*-propyl substituent: Rb=*iso*-propyl methine, Rm=*iso*-propyl methyls; Benzyl: Bm (1-2ppm)=benzyl methylene, Bi=*ipso*-Bz, B=*ortho*-, *meta*- & *para*-Bz; s=solvent, t=toluene.

5.4.0. Discussion

β-Aminoketones form a distinct group of ligands which stabilise alkyl zirconium complexes. Other hemilabile ligands examined in this study may also lead to stable complexes however. The reason for the stability generated by these N^O ligands when compared with the instability of other bidentate systems, such as β-diketones, is unknown. It is interesting to note that even sulphur substituted β-diketones are inherently more stable than their precursors.

The high stability of these β-aminoketone stabilised benzylzirconium complexes opens up a new and exciting area of organometallic zirconium chemistry, that is non-Cp based bidentate, chelate stabilised alkyl zirconium chemistry. In these complexes, β-aminoketones generally act as bidentate ligands and only when strong electron withdrawing groups are placed on the ligand backbone is the donor power of the nitrogen donor sufficiently reduced to allow formation of hemilabile systems.

It is proposed, from NMR evidence, that the two σ-benzyl ligands in these new complexes are *cis* to each other with β-aminoketone nitrogen groups taking the other two equatorial positions in an octahedral environment around the metal centre. This results at low temperature in inequivalent environments for the benzyl groups as indicated in dynamic equilibria and peak splitting at low temperature. NMR evidence does not indicate strong interactions between the metal centre and the benzyl π-system but minor interactions are indicated at low temperature helping to form inequivalent benzyl environments.

5.5.0. *In Situ* Catalyst Formation

Interactions of alkylaluminium co-catalysts with metal complexes invariably involve a complex series of reactions resulting finally in the formation of an active catalytic species. It is commonly proposed in catalytic systems that metal hydrides, thought to be formed from metal alkyls by β-hydride elimination, are generated at some stage and that these hydrides at low concentrations are the active species[9]. Isolation of these, generally very reactive intermediates, is difficult. Hydrides have also been proposed as active species in zirconium based polymerisation systems with cationic, Lewis base stabilised, zirconium hydrides recently being isolated[10]. These zirconium hydrides have been shown to insert a range of olefins (Reaction 5.1).

$$[Cp_2ZrH(THF)]^+ + X{=}CHR \longrightarrow Cp_2Zr\text{-}X\text{-}CH_2R \qquad [5.1a]$$

where $X=CH_2$, or O

$$\text{or} \quad + RC{\equiv}CR \longrightarrow Cp_2ZrCR{=}CHR \qquad [5.1b]$$

if R=H, polymerisation.

To help explain possible causes for the variations in reactivity for zirconium adducts and complexes in the oligomerisation systems studied as well as possible cocatalyst-ligand interactions it was decided that *in situ* observation of such systems would be undertaken. Three such experiments are described here showing extremes of behaviour. Discussion is focused on cocatalyst interactions with the ligands. As active oligomerisation systems have been developed it is expected that there are also complicated metal centre:cocatalyst interactions but except in certain cases no direct evidence is available for their presence and they are not discussed in detail. To simplify later figures these interactions have been omitted.

5.5.1. EASC/Ligand Interactions

Complex interactions between β-aminoketones and alkylaluminium cocatalysts were expected due to the presence of two donor groups on the ligands. Further, major changes in these interactions could be expected in the presence of zirconium.

Alkylaluminiums react rapidly at low temperature with ligands having acidic protons[11], e.g. acetylacetones, quinols, pyridine carboxylic acids or alcohols. Reaction with amines, amides, Schiff's bases or aminoketones depend on the alkyl

aluminium used and the proton basicity. Initial adduct formation often occurs and elevated temperatures are often required to promote further reaction[12] (Reaction 5.2).

$$2Et_2AlBr{:}NH_2i\text{-}Bu \longrightarrow (EtBrAlNHi\text{-}Bu)_2 + 2C_2H_6 \qquad [5.2]$$

Amides react at RT or under mild reflux[13] (Reaction 5.3).

$$2R^1{}_3Al + 2R^2NHC(O)R^3 \longrightarrow (R^1{}_2AlNR^2C(O)R^3)_n + HR^1 \qquad [5.3]$$

The reaction of alkylaluminiums with α-aminoketones depends on ligand substitution[14]. Adduct formation or alternative reaction paths are possible (Figure 5.14). Coordination to oxygen or nitrogen in these complexes can be difficult to determine by NMR, where, for example, coordination in the 1:1 α-aminoketone : TEA adduct is unclear (Figure 5.14a). Alkylation (5.4b.) or reduction (5.4c.) can occur at or below 40°C. When adducts are the primary product at low temperature, they react further on heating to 80°C in toluene.

Figure 5.14.
Reaction Products for the Me_3Al/α-Aminoketone System

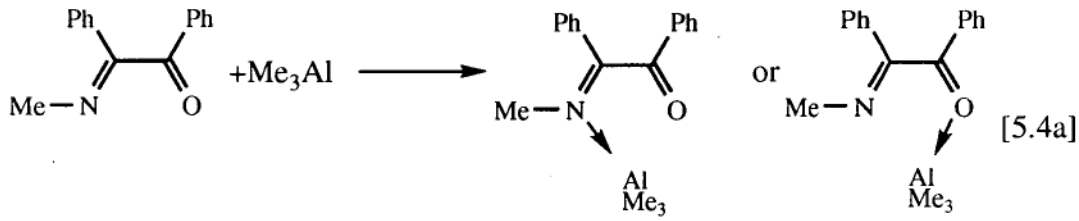

[5.4a]

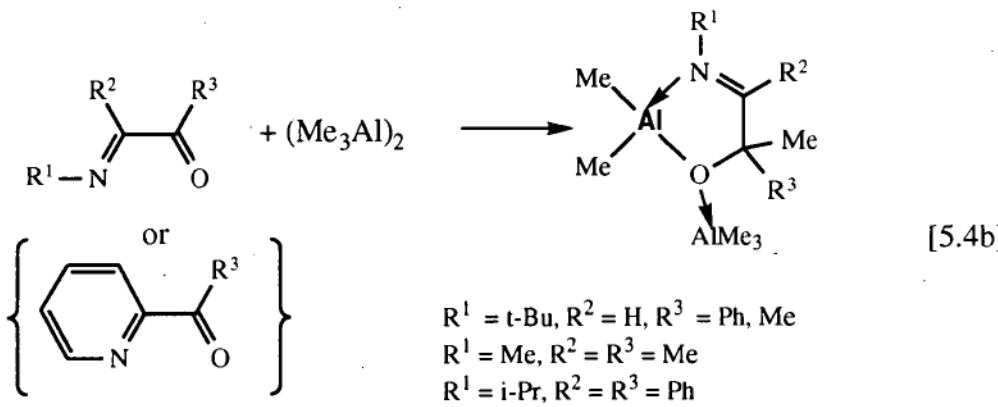

[5.4b]

R^1 = t-Bu, R^2 = H, R^3 = Ph, Me
R^1 = Me, R^2 = R^3 = Me
R^1 = i-Pr, R^2 = R^3 = Ph

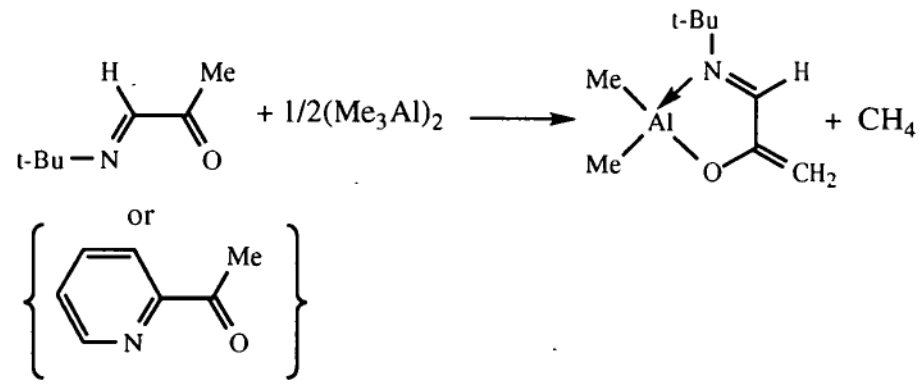

[5.4c.]

There is one reported reaction of an alkylaluminium with a β-aminoketone; the tetradentate, divalent bis-β-aminoketone formed on reaction of ethylene diamine with two moles of acetylacetone[15], Et(-HNacac)$_2$. It is reported that Et$_3$Al, added in a 1:1 ratio of TEA to ligand, reacts on contact with the ligand at room temperature to release one equivalent of ethane. On heating for several hours at 70°C further reaction occurs, releasing a second equivalent of ethane (Reaction 5.5).

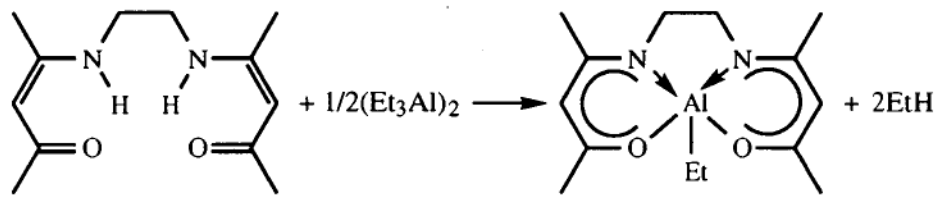

[5.5]

To further explore the full range of possible reactions and coordination modes for this system, the TEA:L ratio was varied. For a ratio of 4:1, based on NMR spectral data, a structure with two N-Al donor bonds and a four member Al-O ring was proposed (Reaction 5.6). For a TEA:L ratio of 2:1 a similar structure was proposed but lacking the N-Al bonds.

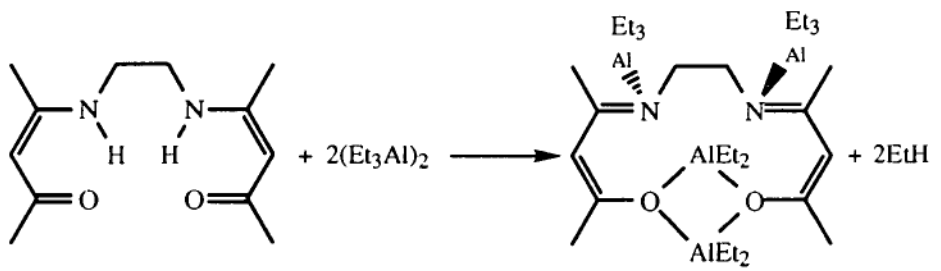

[5.6]

5.5.2. EASC/β-Aminoketone Systems

It has been found that on mixing EASC with a β-aminoketone the reaction depends on the relative basicity of the amine. Three systems will be discussed here, those for which the amino-substituent are *iso*-propyl, phenyl and *para*-methoxyphenyl. VT-NMR spectra referred to but not shown can be found in Appendix III

Changes which occur on mixing EASC and *i*-Pr-HNacac in a 5:1 ratio and heating to 75°C have been monitored by VT ^{1}H-NMR. The spectra are shown in Figure 5.15. There was no significant ligand deprotonation at 25°C or on heating the mixture to 75°C, as would be indicated by evolution of ethane (a peak at δ 1.02 ppm) and the loss of the amino proton resonance at 11.4 ppm (the minor peak at 1.02 ppm is due to a trace of moisture). Adduct formation is indicated by the downfield shifts of EASC resonances (δ 1.28 & 1.23 to 1.35 & 1.47 ppm, CH_3 protons and δ 0.40 & 0.50 to 0.48 & 0.70 ppm, CH_2) and shifts of the ligand peaks (as listed in Table 5.7), especially the amine proton from 11.4 ppm in the free ligand to 10.30 & 10.41 in the adduct. The minor EASC resonances, due to $EtAlCl_2$ in the EASC dimer ($EtAlCl_2.Et_2AlCl$), have been shifted further downfield, indicating a preferential association with the aluminium coordinating one ethyl group. In light of this, to simplify diagrams, adduct formation or reaction will be depicted with EADC. Certainly both aluminium centres take part in adduct formation, as indicated by resonance shifts, and this is only a simplify diagrams and facilitate discussion.

With an excess of the EASC only two sets of cocatalyst resonances are observed at 25°C, therefore indicating a rapid exchange of free and coordinated cocatalyst on the NMR time scale. Two β-aminoketone ligand environments reflect two EASC aluminium environments with exchange slow on the NMR time scale. Ligand methyl peak assignment is difficult but, due to results to be discussed shortly, the downfield peak at 2.2 ppm (labelled Lo) has been assigned to the methyl on the carbonyl carbon. Significant charge redistribution occurs, as seen by the upfield shift for the methine peak (from δ 5.10 in the free ligand to 4.77 ppm on reaction with EASC). Detailed examination of the spectra indicate that a proton is most likely associated with the amine, due to indications of secondary splitting of the *iso*-propyl (δ 3.56 ppm) methine peak at 75°C.

Figure 5.15.

Reaction of EASC with *i*-Pr-HNacac in C_6D_6 monitored by Variable Temperature ^{1}H-NMR (EASC:*i*-Pr-HNacac = 5:2)

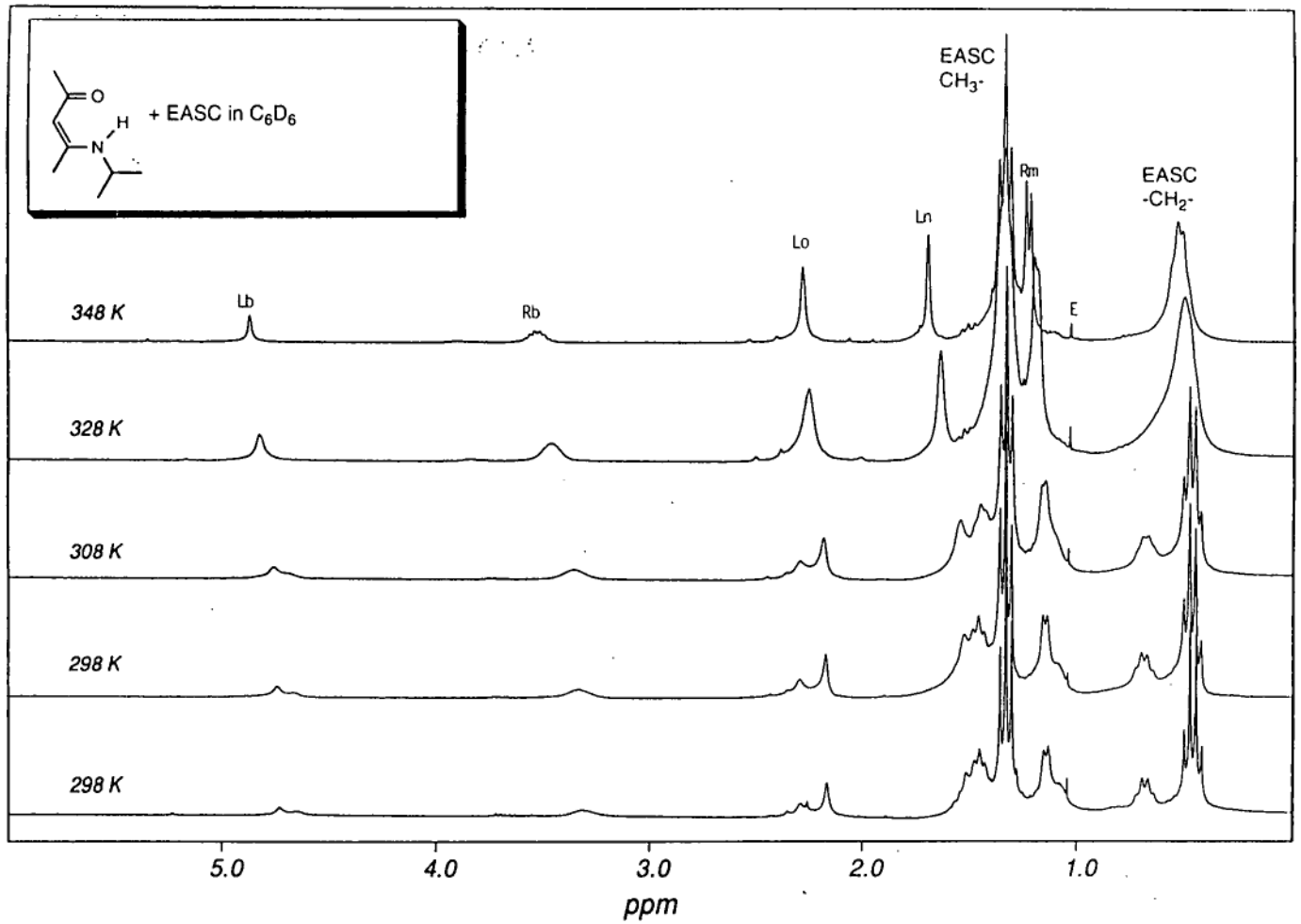

Temperature cycled from 298K to 348K before returning to starting temperature (bottom Spectrum); for clarity the NH region has not been shown (δ 10.30 & 10.41ppm, N-H). Where: Ligand backbone: Lo= carbonyl methyl; Ln=amino carbon methyl, Lb=methine; N-*iso*-propyl substituent: Rb=*iso*-propyl methine, Rm=*iso*-propyl methyls; E=ethane.

On warming to 75°C peaks coalesce giving only one ligand and one clear EASC-ethyl environment. This coalescence reflects that found with EASC only under the same conditions (Appendix B.4.1).

A proposed structure for the adduct in solution is shown in Figure 5.16. In excess EASC adducts form with both the ketone and amine. It is not possible from the NMR data obtained to say if one or more interactions between oxygen and aluminium are present.

Figure 5.16.
Proposed Structure of the *i*-Pr-HNacac/EASC Adduct

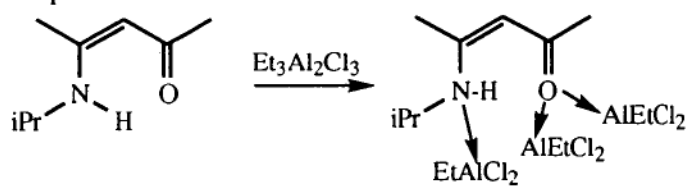

5.5.3. EASC/$ZrCl_4$:2*i*-Pr-HNacac System

The presence of $ZrCl_4$ could be expected to complicate the system with the possibility of ligand exchange reactions and competition for oxygen adduct formation from two oxophilic metals (Al and Zr). If, as was expected, ligand bonding through oxygen to zirconium is preferred then the character of the ligand may change due to this strong interaction, allowing new ligand/EASC reactions to take place. VT ^{1}H-NMR Spectra for the *in situ* reaction of EASC with $ZrCl_4$:2*i*-Pr-HNacac are shown in Figure 5.17 and selected data are presented in Table 5.7.

There is no indication of significant ethane production at any temperature, as indicated by the lack of a significant sharp peak at 1.02 ppm, affirming that adduct formation is the only ligand-EASC interaction. EASC resonances, especially the minor peaks are again shifted downfield but not to the same degree as for interactions with the free ligand. The β-aminoketone resonances show a single environment although the peaks are broad at low temperature. The peak shifts are essentially the same as for the free ligand/EASC spectra.

The spectra have been interpreted as indicating a O-bonded zirconium-ligand adduct with amine-EASC adduct formation. Due to zirconium-oxygen ligand interactions

the downfield EASC peak shift is less than for the free ligand system as fewer EASC molecules are involved in adduct formation, i.e. the average EASC-ethyl environment is closer to that of free EASC. Ligand peak broadening at low temperature is due to adduct formation with EASC and reflects changes to EASC resonances on warming. The broadening of the downfield carbonyl methyl indicates a possible continued interaction between oxygen and the cocatalyst.

Table 5.7.

Selected ^{1}H-NMR Data for in-situ VT-NMR Experiments

Containing *i*-Pr-HNacac or *i*-Pr-Nacac$^-$

System	β-Aminoketone Ligand Shifts						EASC Shifts	
	Me C(O)	H	Me C(N)	N-H	H *i*-Pr	Me *i*-Pr	EASC CH_2	EASC CH_3
in C_6D_6 at 25°C								
EASC (free)							0.40	1.28
							0.50	1.23
i-Pr-HNacac (free)	2.28	5.10	1.68	11.45	3.34	1.02		
i-Pr-HNacac	2.19	4.77	1.53	10.30	3.36	1.17	0.48	1.35
+ EASC	2.32	4.69	(?)	10.41	(?)	1.10	0.70	1.47
$ZrCl_4$:2*i*-Pr-HNacac	2.17	4.76	1.55	10.23	3.33	1.14	0.44	1.32
+ EASC							0.63	1.39
(*i*-Pr-Nacac)$_2$$ZrCl_2$	2.20	5.24	1.53		3.55	1.34	0.75	1.48
+ EASC							0.61	1.39
							0.43	1.30
in C_6D_6 at 75°C								
EASC							0.49	1.27
i-Pr-HNacac (free)	2.24	5.10	1.77	11.32	3.49	1.11	-	-
i-Pr-HNacac + EASC	2.30	4.90	1.72	10.39	3.54	1.24	0.53	1.35
$ZrCl_4$:2*i*-Pr-HNacac + EASC	2.29	4.91	1.74	10.27	3.56	1.24	0.51	1.33
(*i*-Pr-Nacac)$_2$$ZrCl_2$	2.25	5.39	1.83		3.80	1.36	0.51	1.35
+ EASC	1.98	5.07	1.75		(?)	1.49	≈0.70	≈1.43

Figure 5.17.

Reaction of EASC with $ZrCl_4$:2*i*-Pr-HNacac in C_6D_6

monitored by Variable Temperature ^{1}H-NMR

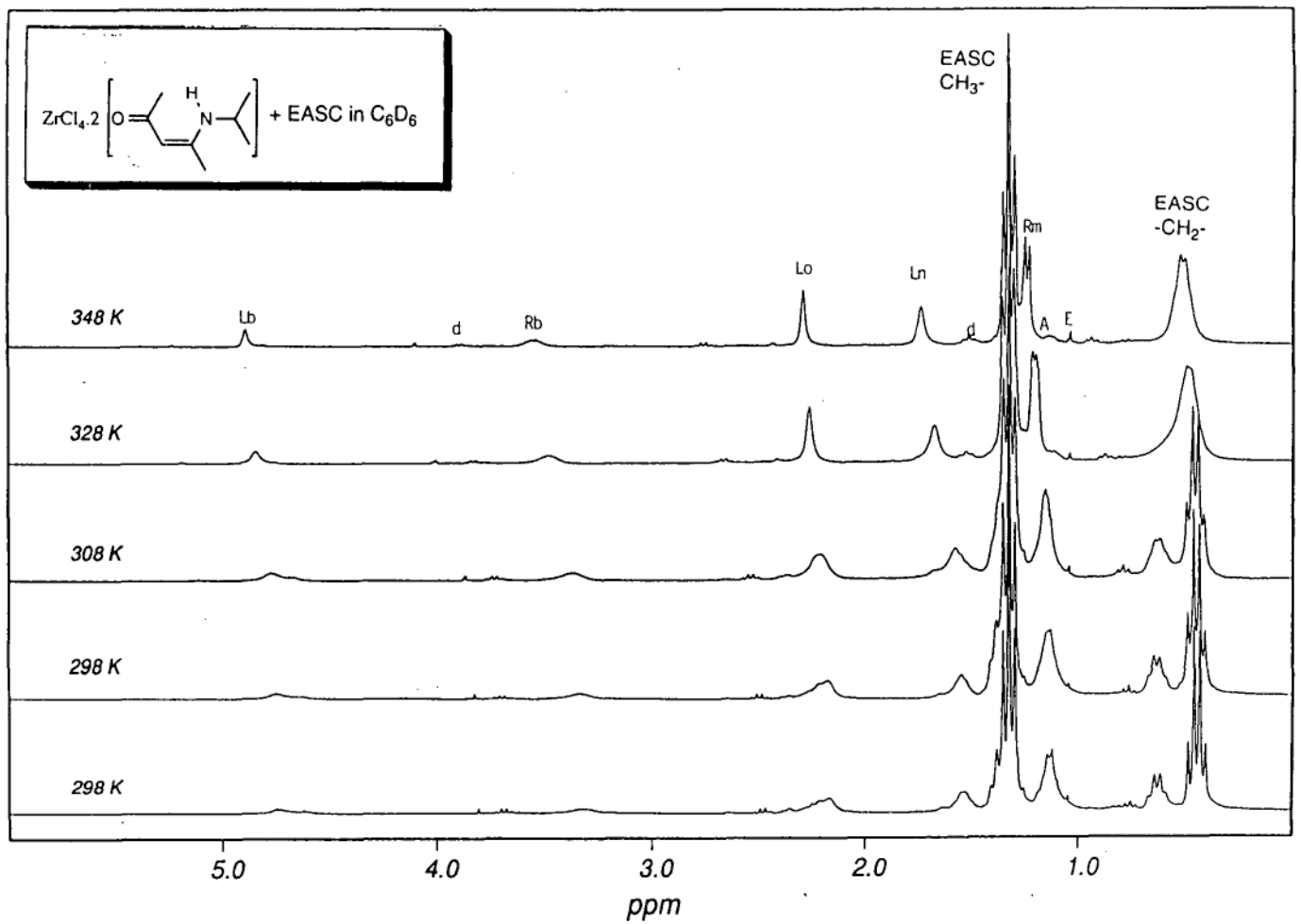

Temperature cycled from 298K to 348K before returning to starting temperature (bottom Spectrum); for clarity the NH region has not been shown (δ 10.23ppm, N-H). Where: Ligand backbone: Lo= carbonyl methyl; Ln=amino carbon methyl, Lb=methine; N-*iso*-propyl substituent: Rb=*iso*-propyl methine, Rm=*iso*-propyl methyls; E=ethane, A=metal centre alkylation, d=decomposition product.

Figure 5.19.

Reaction of EASC with $ZrCl_4$:2*i*-Pr-HNacac in the presence of Ethylene

In C_6D_6 monitored by Variable Temperature ^{1}H-NMR

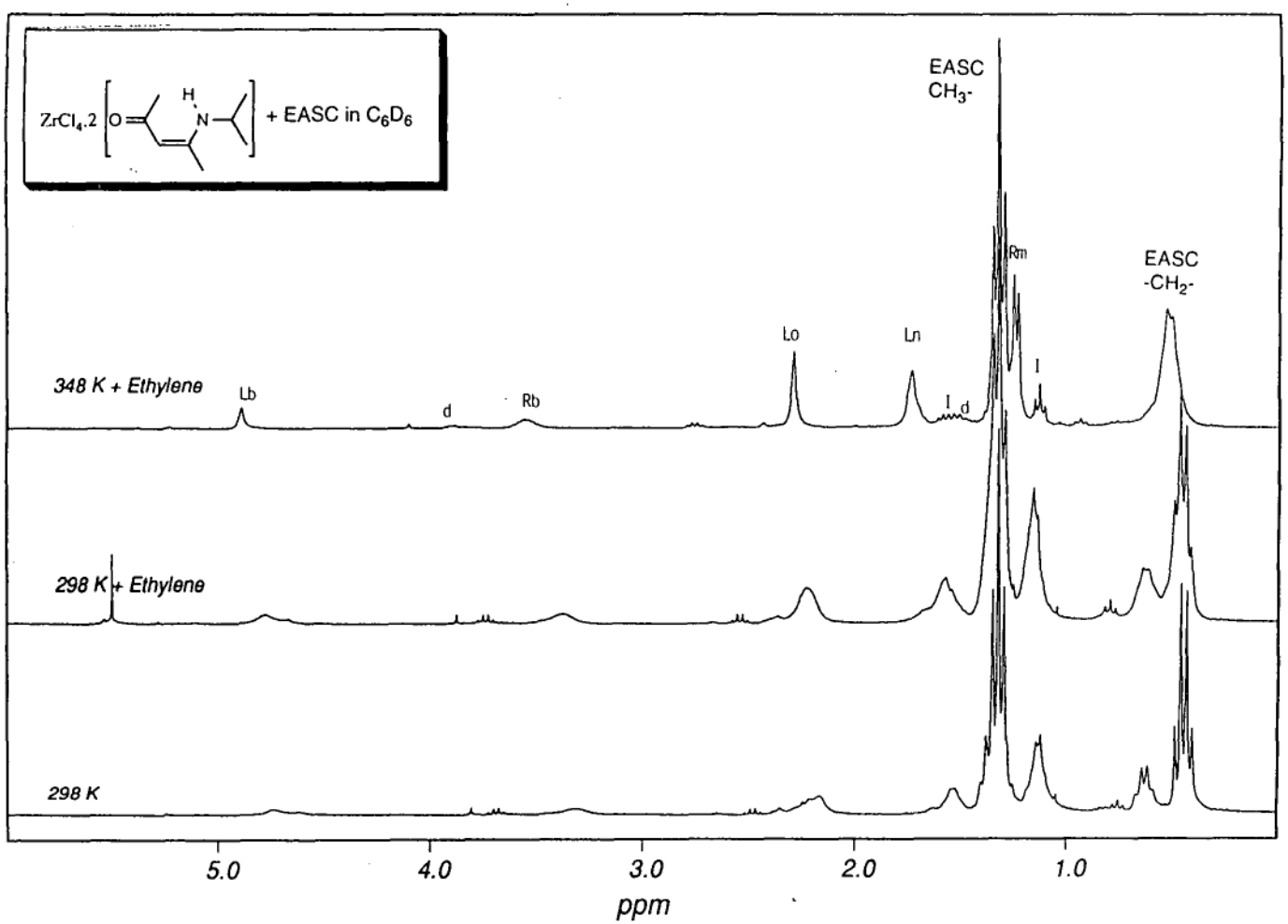

Where: I=insertion product, rest as in Figure 5.18, for clarity the NH region has not been shown (δ 10.23ppm, N-H); Bottom spectrum is before ethylene was added.

A proposed intermediate structure is shown in Figure 5.18. The proton (H') cannot be located from spectral data but due to similarity of previous spectra has been drawn on the amine. Other ligand exchange processes can be envisaged but no spectral evidence was seen for their presence. Metal centre-cocatalyst interactions leading to active catalyst formation have been omitted for simplicity.

Figure 5.18.

Proposed Structure of $ZrCl_4$:2*i*-Pr-HNacac/EASC Adduct

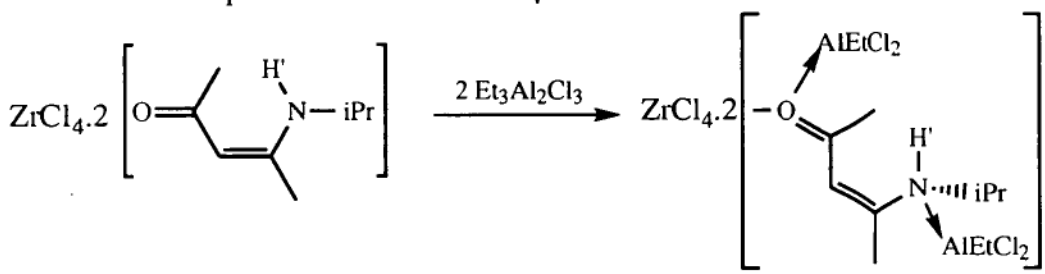

Table 5.8.

Typical ^{1}H NMR Shifts for Zr-R Groups

	CH_2	CH_3	
[1] $[Cp'_2Zr(Et)(THF)]^+$	1.17	1.41	
[2] $[Cp'_2Zr(Et)(NCMe)_n]^+$	0.77	1.21	
[2] $[Cp'_2Zr(Et)(PMe_3)]^+$	0.91	-1.26	β-agostic bond
[2] $Cp'_2Zr(Et)Cl$	0.88	1.29	
[1] $[Cp'_2Zr(n\text{Pr})(THF)]^+$	1.19, 1.63	0.95	
[1] $[Cp'_2Zr(n\text{Bu})(THF)]^+$	1.57,1.26, 1.19	0.89	

[1]Jordan, R.F., La Pointe, R.E., Bradley, P.K., Baenziger, N., *Organometallics* 8, **1989**, 2892-2903; [2] Alelyunas, Y.W., Guo, Z., LaPointe, R.E., Jordan, R.F., *Organometallics* 12, **1993**, 544-553.

The appearance of two sets of ethyl resonances (labelled d δ 0.76, 1.52 and 2.50, 3.70 ppm) need to be explained. The resonances at δ 1.52 and 3.70 ppm appear on the free EASC spectra and are assumed to be due to traces of cocatalyst decomposition product. Both sets of peaks are present with other β-aminoketones in the absence of $ZrCl_4$ and are therefore not associated with metal alkylation reactions. Such Et-Zr resonances appear at ≈1.4 and <1.2 ppm for the methyl and methylene resonances respectively (Table 5.8). Possible β-aminoketone alkylation at the carbonyl carbon induced by the presence of $ZrCl_4$ have been excluded by

experiments discussed in the next section. It is therefore believed that both sets of peaks are due to cocatalyst decomposition products.

5.5.4. EASC/$ZrCl_4$:2*i*-Pr-HNacac/Ethylene System

Bubbling ethylene through the EASC/$ZrCl_4$:2*i*-Pr-HNacac system solution described above and heating to 75°C results in the loss of the ethylene resonance at ≈5.4 ppm and the appearance of new sets of peaks at δ 1.13 and 1.55 ppm (Figure 5.19). Other peaks may be obscured at ≈0.6 ppm. This is the first direct evidence for the insertion of ethylene at low pressure (1atm ethylene). Due to the presence of ligand-*i*-Pr resonances at ≈1.1 at 25°C it remains uncertain as to whether insertion occurs at lower temperatures (i.e. RT). If insertion does occur at the lower temperatures it is slow.

Perhaps surprising is the fact that even under conditions where ethylene insertion occurs and therefore in the presence of a Zr-R bond, the β-aminoketone ligand is not deprotonated.

5.5.5. (*i*-Pr-Nacac)$_2$$ZrCl_2$/EASC System

The difference in activity between adducts and bis-ligand complexes for these oligomerisation catalysts can be ascribed to the formation of Ligand:EASC adducts rather than direct reaction of the cocatalyst with the ligand leading to ligand deprotonation. This prevents the possible formation from the adduct systems of a bis-ligand complex/EASC system. To further assess this proposal the (*i*-Pr-Nacac)$_2$$ZrCl_2$/EASC system was also examined.

VT-NMR spectra obtained from the *in situ* monitoring of reactions between (*i*-Pr-Nacac)$_2$$ZrCl_2$ and EASC show significant differences to the previous adduct system (Figure 5.20). Three distinct sets of EASC resonances are observed which do not coalesce at 75°C as in the previous system. Ligand resonances are relatively sharp and are in general shifted significantly downfield (L), as would be expected for strong electron withdrawal from the delocalised system (Table 5.8). As the temperature is increased a distinct second set of ligand resonances grow which again are significantly different from those previously seen (L'). The intensity of the new EASC resonances decreases as these new ligand resonances increase. A trace triplet is observed at δ 1.11 ppm.

Figure 5.20.

Reaction of EASC with (*i*-Pr-Nacac)$_2$ZrCl$_2$ in C_6D_6

monitored by Variable Temperature ^{1}H-NMR

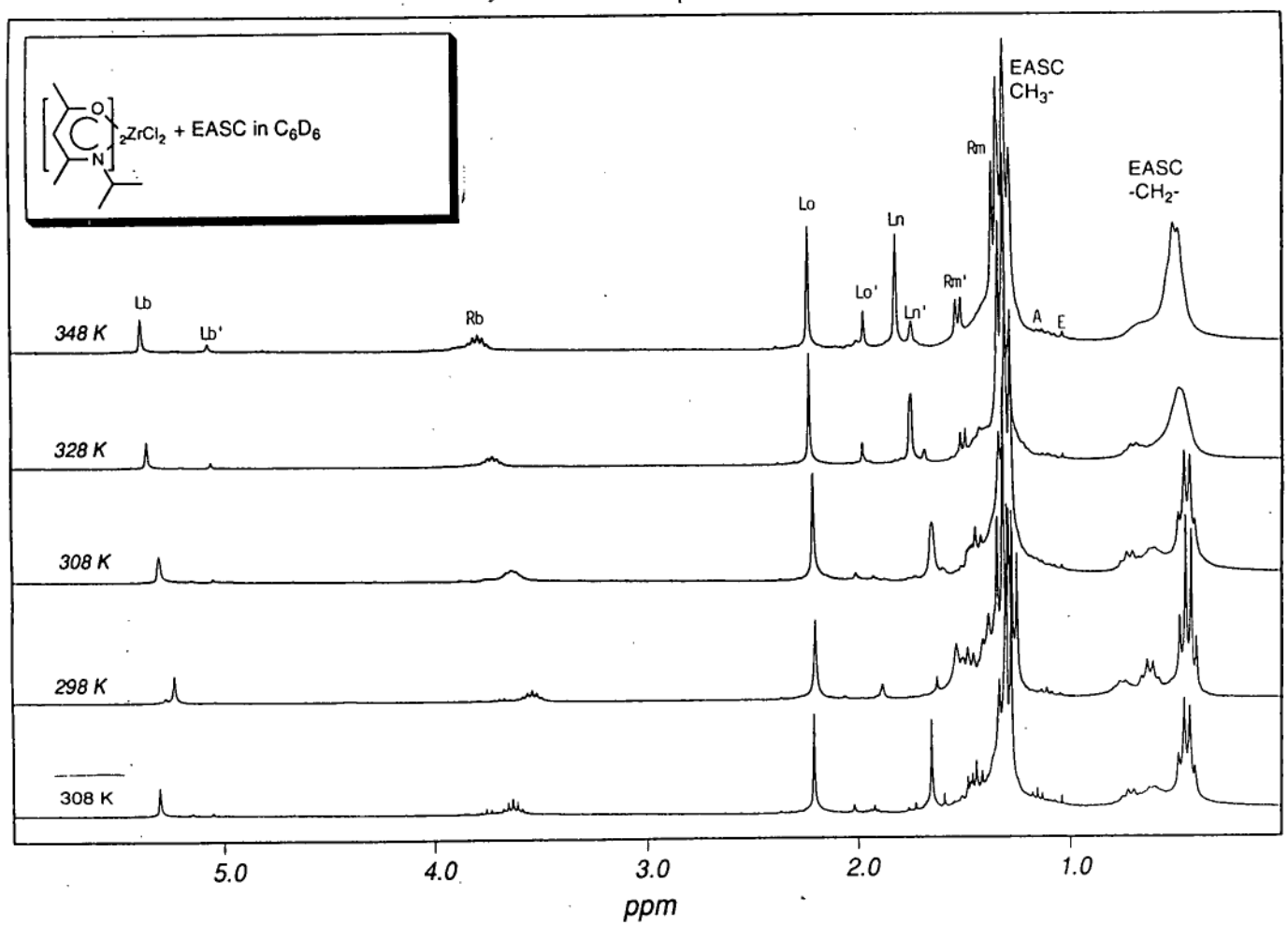

Temperature cycled from 298K to 348K before returning to 308K (bottom Spectrum);Where: Ligand backbone: Lo & Lo=carbonyl methyls; Ln & Ln'=amino carbon methyls, Lb & Lb'=methine; N-*iso*-propyl substituent: Rb=*iso*-propyl methine, Rm & Rm'=*iso*-propyl methyls; E=ethane, A=metal centre alkylation.

Figure 5.23.

Reaction of EASC with (*i*-Pr-Nacac)$_2$ZrCl$_2$ in the presence of Ethylene in C_6D_6 monitored by Variable Temperature ^{1}H-NMR

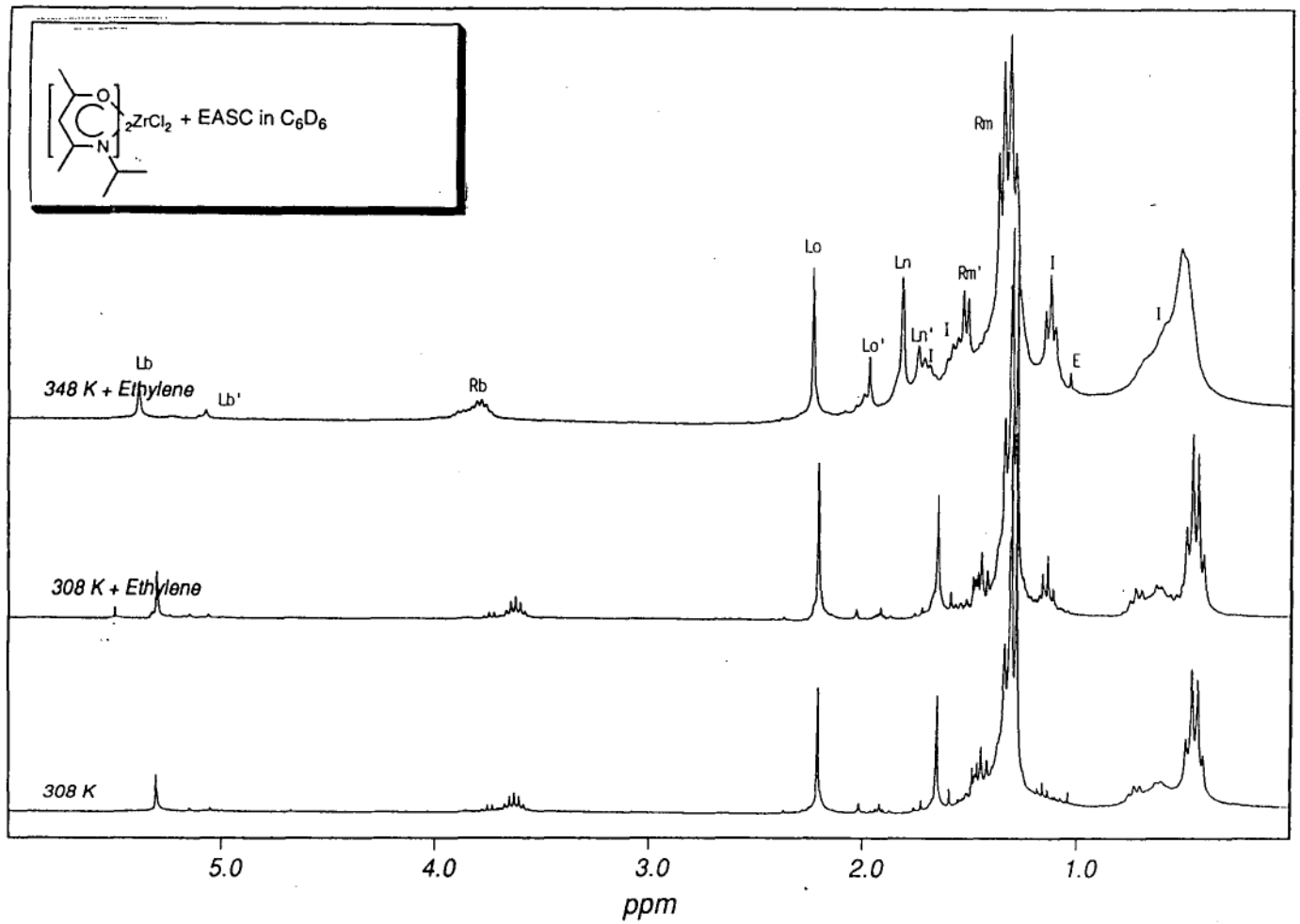

Where : I=ethylene insertion products, E=Ethane, rest as in Figure 5.20; Bottom spectrum is before ethylene was added.

The complex under these high temperature conditions is relatively stable with no significant decomposition noted on cooling the system back to 35°C.

In general the β-aminoketone resonances are shifted downfield for the complex, as has been shown in the absence of EASC (Chapter 3.5.10). The overall behaviour of the system is as previously described for the adduct, with resonances for inequivalent aluminium ethyl environments coalescing at higher temperatures as cocatalyst ethyl exchange becomes rapid on the NMR time scale. Three new features need to be explained, these are; the relative sharpness of the downfield methyl peak (δ 2.20 ppm, COMe), the appearance of a new set of ligand resonances (L') at higher temperatures coupled to the appearance of a new set of EASC resonances which decrease in intensity at higher temperatures and the presence of a triplet at δ 1.11 ppm.

Three possible causes for these observations were considered: ligand exchange reactions between zirconium and aluminium, nitrogen-zirconium interactions causing EASC dissociation or EASC-oxygen adduct formation. The first two can quickly be disregarded as they can not be explained by the observed variations.

i. If the β-aminoketone ligands exchange from zirconium to aluminium at higher temperature the intensity of the set of new EASC-ethyl resonances would be expected to increase as more of the ligand exchanges. This is not observed. If the β-aminoketone ligands were originally transferred to aluminium and exchange back to zirconium at higher temperature the primary ligand resonances (Lb, Lo, Ln & Rm) would be expected to reflect the two different EASC-ethyl environments at low temperature, as is observed for the free ligand and adduct systems with EASC (Figure 5.15 & 5.19). This is also not observed. The sharpness of the carbonyl methyl peak (Lo) indicates that oxygen-EASC interactions are not dominant and this has been taken to indicate a strong zirconium-oxygen interaction. This also gives direct evidence for the coordination of the ligand to zirconium during the oligomerisation process.

ii. It is not possible from the NMR spectra to determine if significant zirconium-nitrogen interactions are present in this system. Strong interactions between nitrogen and the metal centre would be likely to result in EASC dissociation from nitrogen resulting in a greater concentration of free cocatalyst. No new EASC resonance would be expected. Alternatively, reduced nitrogen donor ability due to EASC

adduct formation leading to increased nitrogen lability and therefore free and coordinated nitrogen environments would lead to two sets of *iso*-propyl resonances which would coalescence at higher temperatures. The large upfield shift (from δ 2.25 to 1.98 ppm) of the carbonyl methyl cannot be explained by such an interaction.

iii. The formation of the second set of ligand peaks is associated with the disappearance of the second minor EASC resonance and leads to a new ligand environment. The sharpness of these peaks indicates a well defined process in which exchange is slow on the NMR time scale. The growth of these peaks at higher temperatures also indicates the possibility of some equilibrium process. It is proposed that, due to strengthened zirconium-oxygen interactions, a weak EASC-oxygen adduct forms (Figure 5.21, zirconium interactions with the cocatalyst have been omitted for clarity). The high temperature process is then the release of the coordinated EASC from the oxygen (Figure 5.22). On dissociation an electronic redistribution occurs altering dramatically the ligand environment with increased electron density around the carbonyl carbon leading to the upfield shift. The downfield shift of the *iso*-propyl group may be due to a stronger or multiple interactions of the nitrogen with EASC after oxygen-EASC dissociation.

Figure 5.21.

Formation of (*i*-Pr-Nacac)$_2$ZrCl$_2$/EASC Adducts

(possible cocatalyst interactions with the metal centre have been omitted for clarity)

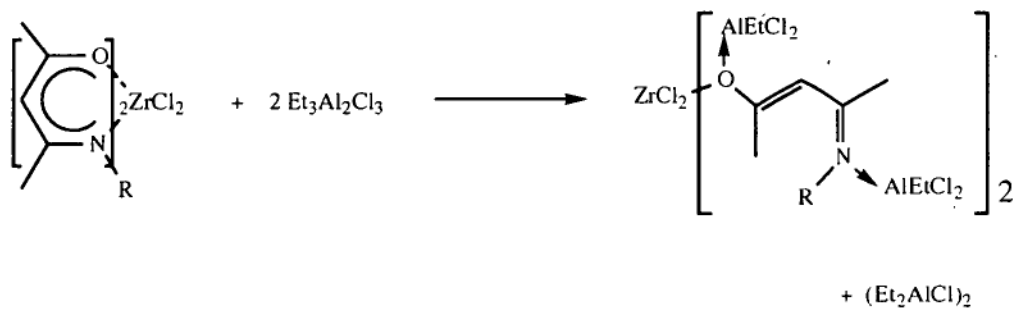

Figure 5.22.

High Temperature Dissociation of the (*i*-Pr-Nacac)$_2$ZrCl$_2$/EASC Adduct

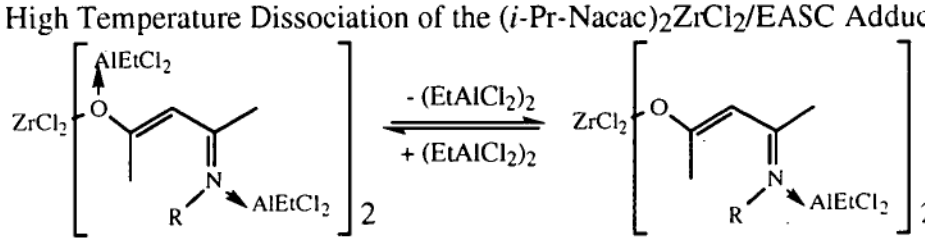

It is possible that the appearance of trace peaks, triplet at 1.15 ppm, on mixing (*i*-Pr-Nacac)$_2$ZrCl$_2$ with EASC may be associated with metal alkylation. In this case the quartet would most likely be obscured by the EASC methylene resonances (see Table 5.7 for typical Zr-Et shifts).

5.5.6. (*i*-Pr-Nacac)$_2$ZrCl$_2$/EASC/Ethylene System

On bubbling ethylene through this solution at 35°C the peak at 1.11 ppm is immediately enhanced with the appearance of new peaks centred at 0.55 and 1.59 ppm. Addition of more ethylene and raising the temperature to 75°C shows the loss of the ethylene resonance and the enhancement of the new peaks at 1.14, 1.59, 1.71, 2.02 and 0.58 ppm (Figure 5.23). These peaks indicate ethylene insertion. Typical terminal olefins peaks, 4.5-6.0 ppm, were not seen. This may be due to high insertion rates compared to low β-hydride elimination rates as well as reflecting the small amount of ethylene added. The peak positions for the insertion product are similar to those for the *n*-propyl group in [Cp'$_2$Zr(*n*Pr)(THF)]$^+$ and the *n*-butyl group in [Cp'$_2$Zr(nBu)(THF)]$^+$ (Table 5.1.) with differences due to the higher Lewis acidity for complexes in this study or different solvents, toluene-d_8 vs. THF-d_8.

5.5.7. Ph-HNacac/EASC System

It is seen for the N-*iso*-propyl substituted β-aminoketone that the large catalytic activity difference between the bis-ligand adduct and bis-ligand complex results from the absence of a reaction between the protonated ligand and the cocatalyst which would lead to ligand deprotonation. The use of N-phenyl substituted ligands in *in situ* tests however led to high activity catalysts, whether the bis-ligand adduct or bis-ligand complex is used, although small differences in activity and product distribution were noted (Chapter 4.3.5). The N-phenyl substituted system was examined in order to investigate reasons for the reactivity differences.

In situ mixing of Ph-HNacac with EASC monitored by VT ^{1}H-NMR indicates immediate reaction of the N-phenyl substituted β-aminoketone with EASC; evolution of ethane, sharp singlet at 1.02 ppm (Figure 5.24). Warming the solution leaves two sets of ligand resonances (L and L') and one broad EASC resonance. The two carbonyl methyls (Lo δ 2.17 & 1.88 ppm) are significantly different with the downfield peak being broad (reflecting EASC variation) while the upfield peak is sharp. The large variation in the position of the C(O)Me resonance between the two

sets of peaks indicates a vastly different environment around the carbonyl carbon. An oxygen-EASC dissociation process, similar to that discussed previously for the (*i*-Pr-Nacac)$_2$ZrCl$_2$/EASC system, is proposed (Figure 5.25).

Figure 5.25.
Proposed Complex formed on Reacting EASC with Ph-HNacac

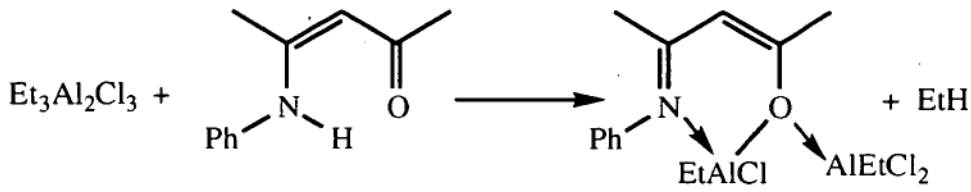

Figure 5.26.
Proposed Dissociation Reaction for the Ph-Nacac(AlEtCl):AlEtCl$_2$ Adduct

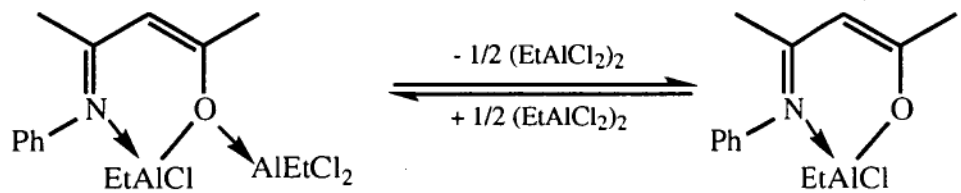

L'(associated) L(dissociated)

The appearance of a set of ethyl resonances at ≈1.25 and 3.70 ppm, mentioned briefly for ZrCl$_4$:2*i*-Pr-HNacac in the previous section, remains unexplained. Ligand alkylation has been excluded by reacting the ligand with EASC at 100°C for 2 hours, hydrolysis and work up. No indication of an alkylated product was found. These peaks are believed to be due to unidentified traces of EASC decomposition products.

5.5.8. ZrCl$_4$:2Ph-HNacac/EASC System

The deprotonation of Ph-HNacac by EASC gives the possibility of an identical catalytic system being derived from the bis-ligand adduct and bis-ligand complex in the presence of EASC. However, depending on the reaction pathway, a number of ligand transfer reactions may be required before the same species is generated in solution leading to different catalytic activities or product distributions. .

Figure 5.24.

Reaction of EASC with Ph-HNacac in Toluene-d_8

monitored by Variable Temperature ^{1}H-NMR

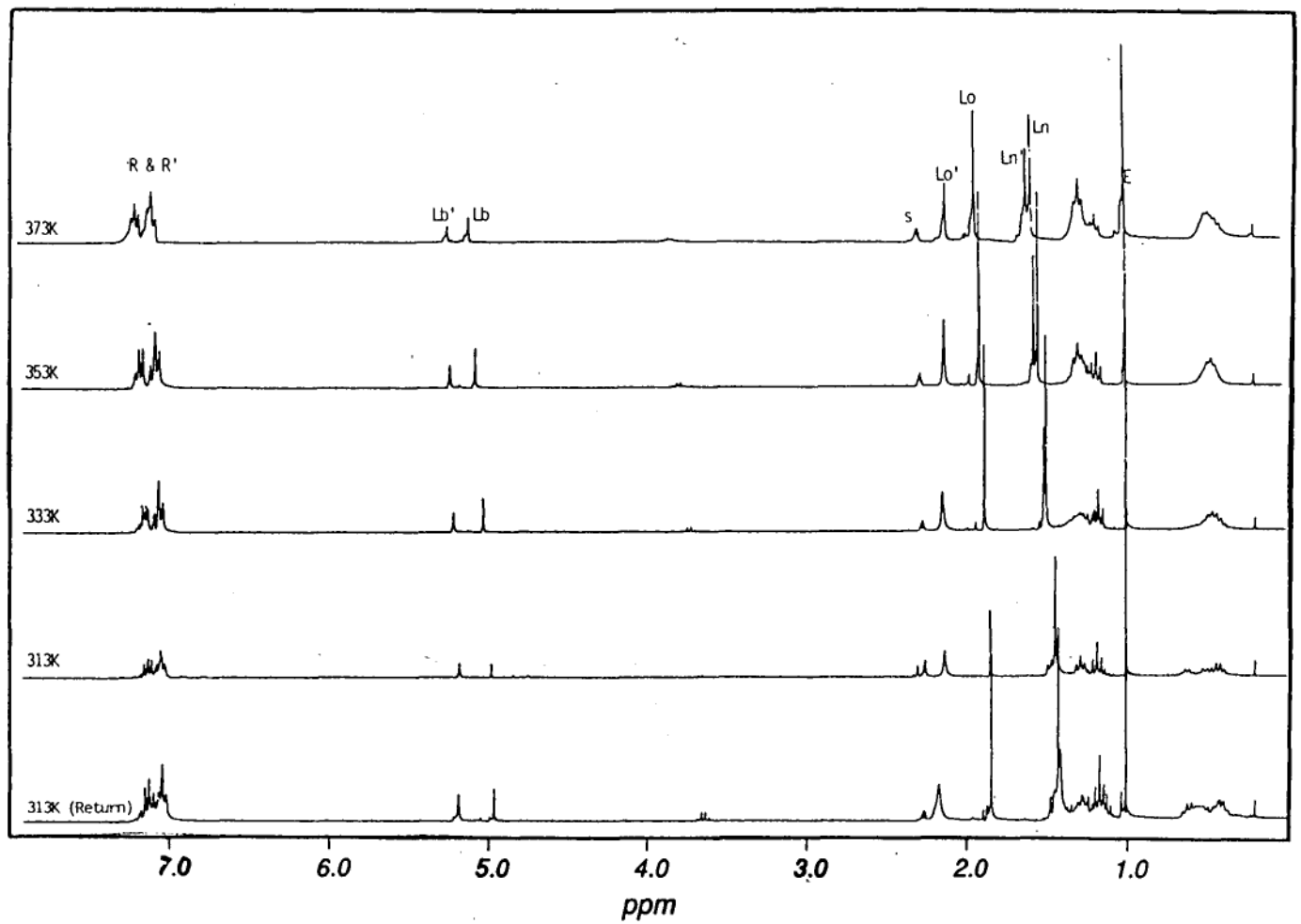

Temperature cycled from 313K to 373K before returning to 313K (bottom Spectrum);Where: Ligand backbone: Lo & Lo'=carbonyl methyls; Ln & Ln'=amino carbon methyls, Lb & Lb'=methine; N-phenyl substituent: R & R'=phenyl protons; E=ethane, s=toluene.

Table 5.9.
Selected ^{1}H-NMR Data for Phenyl-β-Aminoketone Containing Complexes or Adducts in Toluene-d_8 at 40°C

System	β-aminoketone Ligand ^{1}H Shifts						EASC Shifts	
	Me C(O)	H	Me C(N)	*o* Ph	*m* Ph	*p* Ph	EASC CH_2	EASC CH_3
EASC (free)							0.40	1.28
(in C_6D_6 at 25°C)							0.50	1.23
Ph-HNacac (free)	2.21	5.17	1.79	6.93	7.16	7.05	-	-
Ph-HNacac (L')	2.17	5.25	1.47	6.90-	6.90-	6.90-	0.44	1.28
+ EASC (L)	1.88	5.05		7.25	7.25	7.25	0.53	1.30
							0.66	1.50?
$ZrCl_4$:2Ph-HNacac	2.31	5.29	1.55-	6.90-	6.90-	6.90-	0.44	1.31
+ EASC	2.20	4.98	1.70	7.30	7.30	7.30	0.65	1.52
$(Ph\text{-}Nacac)_2ZrCl_2$	2.07	5.18	1.50	7.09-	7.09-	7.09-	0.47	1.35
+ EASC				7.30	7.30	7.30	0.84	1.24

The *in situ* reactions between $ZrCl_4$.2Ph-HNacac or $(Ph\text{-}HNacac)_2ZrCl_2$ and EASC have been monitored by VT ^{1}H-NMR up to 100°C (Appendix III, B.4.4-B.4.8). On bubbling ethylene through these solutions little or no ethylene insertion was observed. As these systems had a high activity in *in situ* tests, this has been taken as a sign of catalyst decomposition. Additionally, on warming a number of new resonances appeared which remain when the solution was cooled (e.g. a methine peak at δ 5.5 ppm and two aromatic peaks at δ 7.2-7.4 ppm), these were also regarded as indicators of decomposition as was the loss of trace peaks at 1.11 ppm thought to be due to metal alkylation by the cocatalyst . The N-Phenyl substituted systems are therefore significantly less stable than the N-*iso*-propyl substituted system. Selected NMR data collected at 40°C (before decomposition) are presented in Table 5.9.

5.5.10. $ZrCl_4$:2MeOPh-HNacac/EASC Ethylene System

Due to the deactivation of the phenyl substituted system at elevated temperatures leading to low or no activity on addition of ethylene the test was repeated using the methoxyphenyl substituted β-aminoketone without excessive heating. The bis-ligand adduct reacts completely with the added cocatalyst by 40°C; as was indicated

by the loss of the amino hydrogen resonance at 11.6 ppm and the formation of ethane, sharp singlet at 1.02 ppm. Under these conditions there is no indication of significant catalyst decomposition; as would be indicated by formation of a second ligand environment with a methine proton resonance at around 5.5 ppm or loss of the triplet peaks at 1.07 ppm. Two distinct ligand environments form (Appendix III, B.4.9).

The triplet at δ 1.11 ppm (50°C, Figure 5.31) is thought to indicate partial metal centre alkylation by the cocatalyst, as discussed previously. On addition of ethylene this peak along with the other new peaks at 1.50, 1.63 and 0.50 ppm increase in intensity (Figure 5.32). At 50°C the insertion reaction remains slow with the ethylene proton resonance observed in the ^{1}H-NMR spectrum at 5.45 ppm. On increasing the reaction and measurement temperature to 85°C the insertion rate increases. As more ethylene is repeatedly bubbled through the NMR tube the new peaks grow in intensity and the initially formed ethane is flushed from the solution. These observations and peak positions are the same as those discussed for the *iso*-propyl β-aminoketone bis-ligand complex system and compare favourably with those values reported in Table 5.1 for other zirconium alkyl systems.

In this experiment the slow appearance of peaks at 5 ppm (three multiplets) and 6 ppm (a broad multiplet) indicate the formation of linear α-olefins. Under these conditions β-hydride elimination occurs and therefore the catalyst species formed under these mild conditions is also an oligomerisation catalyst (Figure 5.31. and Appendix B.4.6, see Figure 4.4 for comparison). The insertion rate is significantly higher than the elimination rate.

As the catalyst concentration in this and other NMR tests was high, the ethylene concentration low and while these systems have been examined on a larger scale no attempt has been made to quantify catalytic activities.

5.5.11. (MeOPh-HNacac)$_2$ZrCl$_2$/EASC Ethylene System

For comparison the methoxyphenyl substituted bis-ligand complex was tested however, to avoid decomposition, no initial heating was attempted and after obtaining a ^{1}H NMR spectrum at 25°C ethylene was immediately added leading to a similar set of insertion spectra (Appendix III, B.4.11) as presented for the bis-ligand

Figure 5.31

Reaction of EASC with $ZrCl_4$:2MeOPh-HNacac in the presence of Ethylene in Toluene-d_8 monitored by Variable Temperature ^{1}H-NMR

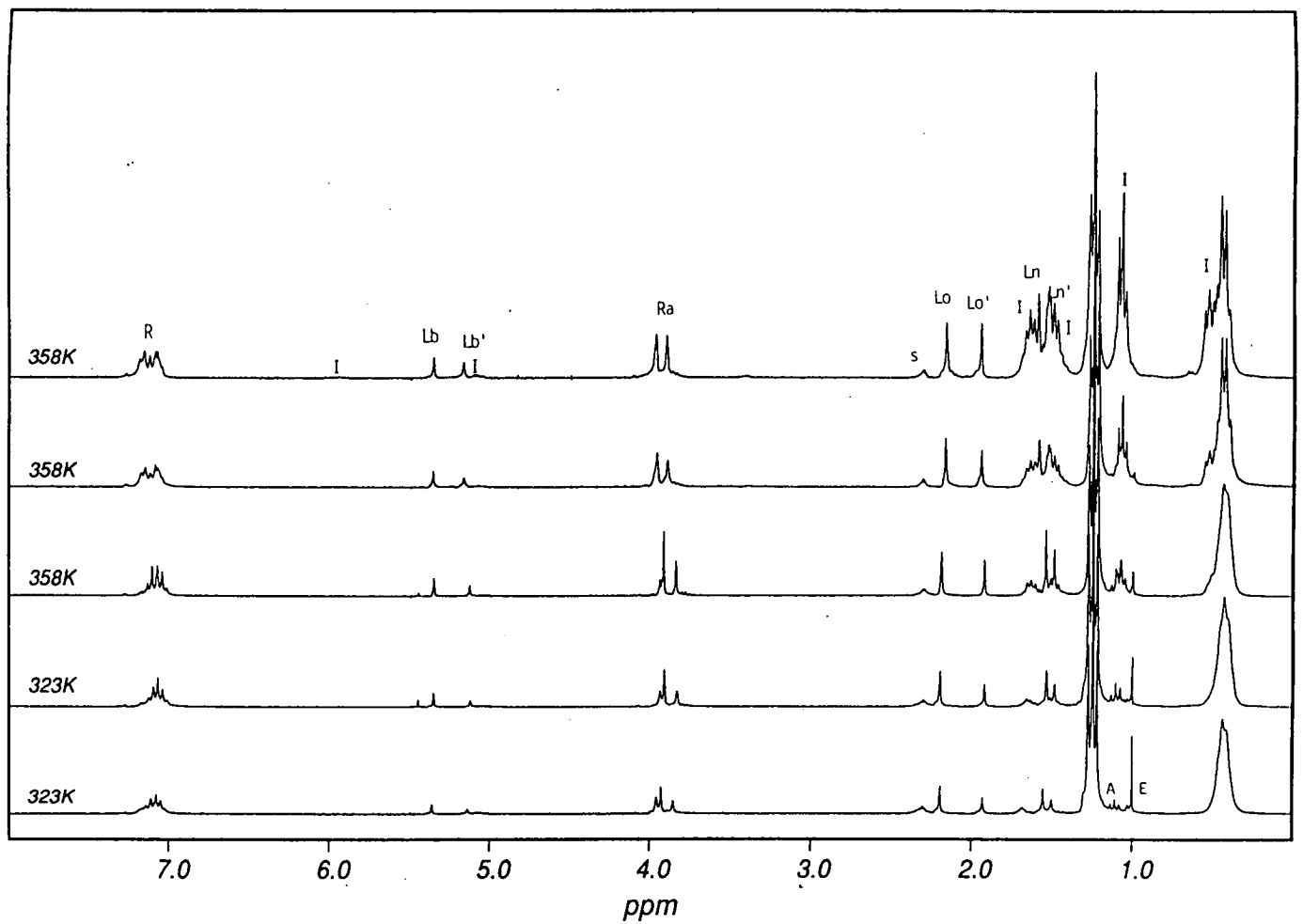

Where: Ligand backbone: Lo & Lo'=carbonyl methyls; Ln=amino carbon methyl, Lb & Lb'=methine; N-phenyl substituent: R=phenyl protons, Ra=methoxy methyl; E=ethane, A=metal alkylation, s=solvent (toluene); Bottom spectrum collected before the addition of ethylene.

adduct. A reaction temperature of 40°C was used. As with the bis-ligand adduct a triplet at 1.07 ppm forms after mixing the complex with the cocatalyst. The peak increases in intensity on addition of ethylene continuing to do so, along with the associated insertion peaks, as more ethylene is repeatedly bubbled through the catalyst solution. Although the reaction was not allowed to continue for very long small peaks are observed forming at 5 and 6 ppm again indicating that β-hydride elimination is occurring even under these mild conditions.

As with the *in situ* catalyst formed from the bis-ligand adduct two distinct ligand environments are noted. As ethylene insertion continues one becomes dominant. Neither of these two ligand environments matches those formed in the previous adduct system. It is also noted that the aromatic region is significantly different for the two systems with a singlet in the bis-ligand complex system while a set of broad doublets is seen in the bis-ligand adduct system. This can be explained by continued interaction of the nitrogen end group with the metal centre. Further work is required to confirm this.

Table 5.10.
Typical ^{13}C-NMR Shifts for Zr-R Groups

	CH_2	CH_3	
(MeOPh-HNacac)$_2$ZrCl$_2$/EASC	58.69	17.98(?)	
(MeOPh-HNacac)$_2$ZrCl$_2$/EASC	64.86, 29.18, 27.60, 14.83	12.32	
[1] [Cp'$_2$Zr(Et)(THF)]$^+$	60.61	17.52	
[2] [Cp'$_2$Zr(Et)(NCMe)$_n$]$^+$	40.5	17.1	
[2] [Cp'$_2$Zr(Et)(PMe$_3$)]$^+$	28.6	-6.9	β-agostic bond
[2] Cp'$_2$Zr(Et)Cl	45.5	17.9	
[1] [Cp'$_2$Zr(*n*Pr)(THF)]$^+$	72.76, 27.37	20.76	
[1] [Cp'$_2$Zr(*n*Bu)(THF)]$^+$	69.62, 36.20, 29.43	13.66	

[1] Jordan, R.F., La Pointe, R.E., Bradley, P.K., Baenziger, N., *Organometallics* 8, **1989**, 2892-2903; [2] Alelyunas, Y.W., Guo, Z., LaPointe, R.E., Jordan, R.F., *Organometallics* 12, **1993**, 544-553.

The changes observed in the proton spectra are reflected in the ^{13}C-NMR spectra of this system (Appendix III, B.4.13). Before ethylene addition trace peaks thought to be associate with alkylation of the metal by the cocatalyst are found at δ 17.9(?) and

58.69 ppm (Table 5.10). These are similar to those found for other alkyl zirconium complexes. On addition of ethylene new peaks are observed at 12.34, 14.83, 29.18 and 64.68 ppm.

It is observed that ligand cocatalysts interactions are complex. It is recognised that the actual interactions may be comprised of complicated equilibria including complicated cocatalyst metal centre interaction but no spectral evidence has been presented to confirm or eliminate these interactions. Based on the observations a number of species have proposed in solution. It has been shown that catalytic species formed in solution in the presence of β-aminoketone adducts or complexes of zirconium insert ethylene under very mild conditions. In one case the formation of oligomers is observed indicating that even under these mild conditions an oligomerisation catalyst has been formed.

1 King, R.B., Fronzaglia, A., *J. Am. Chem. Soc.* 88, **1966**, 709.

2 a. Mann, B.E., Keasey, A., Sonoda, A., Maitlis, P.M., *J. Chem. Soc., Dalton* **1979**, 338-345.
b. Becker, Y., Stille, J.K., *J. Am. Chem. Soc.* 100, **1978**, 845-850.
c. Sonoda, A., Mann, B.E., Maitlis, P.M., *J. Chem. Soc., Chem. Comm.* **1975**, 108-109.
d. Stühler, H-O., *Angew. Chem., Int. Ed. Engl.* 19, **1980**, 468-469.
e. Stille, J.K., Fries, J.K., *J. Am. Chem. Soc.* 96, **1974**, 1514-1518.
f. Muetterties, E.L., Hirsekorn, F.J., *J. Am. Chem. Soc.* 96, **1974**, 7920-7926.

3 Cotton, F.A., Marks, T.J., *J. Am. Chem. Soc.* 91, **1969**, 1339-1346.

4 Mintz, E.A., Moloy, K.G., Marks, T.J., Day, V.W., *J. Am. Chem. Soc.* 104, **1982**, 4692-4695.

5 a. Davis, G.R., Jarvis, J.A.J., Kilbourn, B.T., Pioli, A.J.P., *J. Chem. Soc., Chem. Comm.* **1971**, 677.
b. Bassi, I.W., Allegra, G., Scordamaglia, R., Chioccola, G., *J. Am. Chem. Soc.* 93, **1971**, 3787-3788.
c. Davis, G.R., Jarvis, J.A.J., Kilbourn, B.T., *J. Chem. Soc., Chem. Comm.* **1971**, 1511-1512.
d. Edwards, P.G., Anderson, R.A., Zalkin, A., *Organometallics* 3, **1984**, 293-298.

6 Cardin, D.J., Lappert, M.F., Raston, C.L., *Chemistry of Organo-Zirconium and -Hafnium Compounds*, Ellis Horwood Limited,Chichester, **1986**, 373-388.

7 a. Giolami, G.S., Wilkinson, G., Thornton-Pett, M., Hursthouse, M.B., *J. Chem. Soc., Dalton Trans.*, **1984**, 2789-2794.
b. Latesky, S.L., McMullen, A.K., Nicclai, G.P., Rothwell, I.P., *Organometallics* 4, **1985**, 902-908.

8 Bochmann, M., Lancaster, S.J., *Organometallics* 12, **1993**, 633-640.

9 Kochi, J.K., *Organometallic Mechanisms and Catalysis* Academic Press, **1978**, page 409.

10 Jordan, R.F., La Pointe, R.E., Bradley, P.K., Baenziger, N., *Organometallics* 8, **1989**, 2892-2903.

11 for example see,

a. Pasynkiewicz, S., Dowbar, K., *J. Organometallic Chem.* 43, **1972**, 75-80.
b. van Vliet, M.R.P., Buysingh, P., van Koten, G., Vrieze, K., *Organometallics* 4, **1985**, 1701-1707.
c. Jeffery, E.A., Meisters, A., Mole, T., *J. Organometallic Chem.* 74, **1974**, 373-384.
d. Sen, B., White, G.L., *J. inorg. nucl. Chem.* 35, **1973**, 497-504.
e. Sen, B., White, G.L., Wander, J.D., *J. Chem. Soc., Dalton* **1972**, 447-449.

12 Cotton, F.A., Wilkinson, G., *Advanced Inorganic Chemisty* 4 th Ed., John Wiley & Sons, Inc., 1980; pg 344.

13 Jennings, J.R., Wade, K., Wyatt, B.K., *J. Chem. Soc. (A)* **1968**, 2535-2538.

14 van Viliet, M./R.P., van Koten, G., de Keijser, M.S., Vrieze, K., *Organometallics* 6, **1987**, 1652-1664.

15 Dzugan, S.J., Goedken, V.L., *Inorg. Chem.* 25, **1986**, 2858-2864.

Chapter 6

Conclusions

It is possible to combine the information obtained from catalytic testing, synthesis and *in situ* VT-NMR experiments to propose active species for the oligomerisation process in line with the model developed in Chapter 2. These proposed intermediates should allow the design of better more efficient oligomerisation catalysts.

6.1.0 Summary of Results

In order to facilitate the discussions on proposed intermediates, the results from this study are summarised below.

6.1.1. Model Development

The model developed in Chapter 2 proposed that promotion of conditions which favour β-hydride elimination would lead to better oligomerisation catalysts, these were,

i. available low lying metal orbital
ii. sterically unsaturated metal centre-to allow formation of the appropriate transition state
iii. Lewis acidic metal centre

Oligomerisation can also be influenced by process variables, i.e. temperature, ethylene pressure and catalyst concentration, but these are not discussed here.

Conditions i. & ii. are necessary for formation of the required intermediate where β-hydride agostic bonding precedes hydride transfer. The higher Lewis acidity is thought to promote β-hydride bond formation.

6.1.2. Synthesis

β-Aminoketones can be effectively used to form stable coordination and organometallic complexes of zirconium. For these complexes evidence has been presented describing new and unusual ligand bonding with dynamic NMR behaviour. The bidentate β-aminoketones are in most cases chelated except when electron withdrawing groups are present on the ligand backbone, e.g. two ligand environments for the (*i*-Pr-Ntfac)$_2$ZrBz$_2$ complex are observed. For the benzyl-bis-ligand complexes evidence has been presented indicating inequivalent environments for the benzyl methylene protons at or below room temperature. These variations have been explained through steric rather than electronic influences.

Large variations in the metal centre Lewis acidity are not seen with the complexes formed in this study. Results for the trifluoro-substituted β-aminoketone however indicate that it is possible to change the Lewis acidity by simple ligand substitutions. It is proposed that in these complexes the ligand methine group can be used as a measure of Lewis acidity. In benzyl complexes, where one end group of the β-aminoketone may dissociate, the benzyl group and its degree of η^2-bonding can be used as an indicator for metal centre Lewis acidity.

6.1.3. Catalysis

A number of new ethylene oligomerisation systems have been developed leading to better fundamental knowledge of the oligomerisation process. β-Aminoketones, the primary ligands in this study, have been shown to be particularly effective in promoting the oligomerisation process.

A number of observations have been made during catalytic testing, on both large scale and in NMR scale tests, of free β-aminoketones, bis-β-aminoketone adducts, bis-β-aminoketone complexes, benzyl bis-β-aminoketone complexes and their cationic analogues. These are;

1. β-Aminoketones effectively promote oligomerisation reactions under mild conditions.
2. N-alkyl bis-β-aminoketone adducts result in catalysts which produce consistently lower average oligomer weights at moderate activity.
3. N-alkyl β-aminoketones are in general not deprotonated in the presence of the cocatalyst while N-phenyl β-aminoketones are. These N-alkyl-amino protons do not react even in the presence of active zirconium-alkyl bonds, that is during oligomerisation.
4. The use of bis-β-aminoketone-zirconium complexes results in the formation of catalytic systems which have higher activities but also give rise to products with a higher average molecular weight.
5. Cationic species in the absence of a cocatalyst polymerise ethylene.
6. Catalytic activities can be readily modified through variations in the ligand backbone or amine substituents. Electron withdrawing groups on the amine/imine increase reactivity.
7. β-Aminoketones containing tertiary amines result in catalytic systems of lower activity.

8. The β-aminoketones appear to remain O-bonded to zirconium during oligomerisation.

The systems examined in this thesis are extremely complex and more studies are required to understand the full range of behaviour of β-aminoketone containing adducts and complexes in the presence of a cocatalyst. Three points that will have a significant impact on a full understanding of these systems but which have not been fully explored in this study are,

1. Degree of zirconium-nitrogen interactions.
2. Effective Lewis acidity of the metal centre.
3. Cocatalyst-ligand interactions.

No significant zirconium-nitrogen interactions are present in the bis-β-aminoketone adduct systems tested. This can be stated as the amine is not deprotonated even in the presence of an active oligomerisation centre, i.e. in the presence of a zirconium-alkyl bond. The situation for β-aminoketones in systems derived from bis-ligand complexes is less certain. Spectroscopic evidence appears to indicate significant interactions but this remains to be confirmed.

Spectroscopic data collected during synthesis indicated that metal centre Lewis acidity can be influenced and modified by ligand substituent variations. In the presence of a cocatalyst the effective Lewis acidity remains uncertain with the best indicator being product distribution, i.e. high Lewis acidity leads to low average oligomer weight. This is thought to be due to variable ligand-cocatalyst interactions which may average the effective donor ability of the β-aminoketone.

In the presence of a cocatalyst a complex series of interactions have been shown to take place. Adduct formation, deprotonation or complicated equilibria may be set up when the ligand mixes with the cocatalyst. These reactions are modified in the presence of $ZrCl_4$ or when bis-ligand complexes are used. Deprotonation of the β-aminoketone ligand depends on the basicity of the ligand amine.

Based on spectroscopic evidence major β-aminoketone-cocatalyst interactions have been proposed, however a detailed description cannot be given. Based on the evidence presented, some ligand exchange reactions can be eliminated but numerous exchange processes or interactions, such as the number and type of nitrogen or

oxygen-cocatalyst interactions, cannot be defined or excluded. Such interactions may be more fully defined in further studies to allow the effect of these interactions on catalyst activity, metal centre Lewis acidity and other metal ligand interactions to be accurately described.

Results have indicated O-bonded β-aminoketone adducts or complexes are formed and may be present in the presence of the cocatalyst, EASC. The ligands remain bound to zirconium via the oxygen during oligomerisation. The appearance of a triplet at δ 1.11ppm has been taken to indicate zirconium alkylation by the cocatalyst. Insertion occurs at this point in the presence of ethylene. Zirconium is the most likely site for the insertion reactions.

6.2.0 Reactive Intermediates in β-Aminoketone Containing Oligomerisation Systems

In light of these observations the following active intermediates for zirconium based oligomerisation systems studied in this work are proposed (Figure 6.1-3).

6.2.1. Bis-β-Aminoketone Adduct Systems.

The proposed intermediate derived from a bis-ligand zirconium adduct is shown in Figure 6.1a, i.e where the ligand is not deprotonated. The metal centre is relatively crowded but the presence of strongly electron with-drawing groups would make the metal centre very Lewis acidic. The steric crowding would not allow easy monomer access or formation of the required intermediates. However the high Lewis acidity, due to the presence of two chloride ions, would promote elimination reactions. It is interesting to observe that for these systems the ligand was not deprotonated even though an active oligomerisation system was formed, that is in the presence of metal-alkyl bonds. This suggests a very strong steric interaction preventing the amine from interacting with the metal centre. With regard to the crowded nature of the metal centre and of the amine environments it is probably not surprising that they do not interact.

The use of this catalyst system results in the shortest average oligomer length.

Figure 6.1a.

Proposed Active Species in the $ZrCl_4$:2R-HNacac/EASC Systems

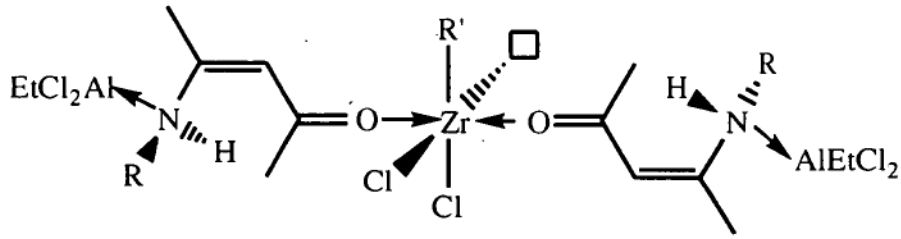

Possible EASC-oxygen or metal centre interactions have been omitted for clarity.

Figure 6.1b.

Proposed Intermediates derived from the $ZrCl_4$:2R-HNacac/EASC System upon Ligand Deprotonation

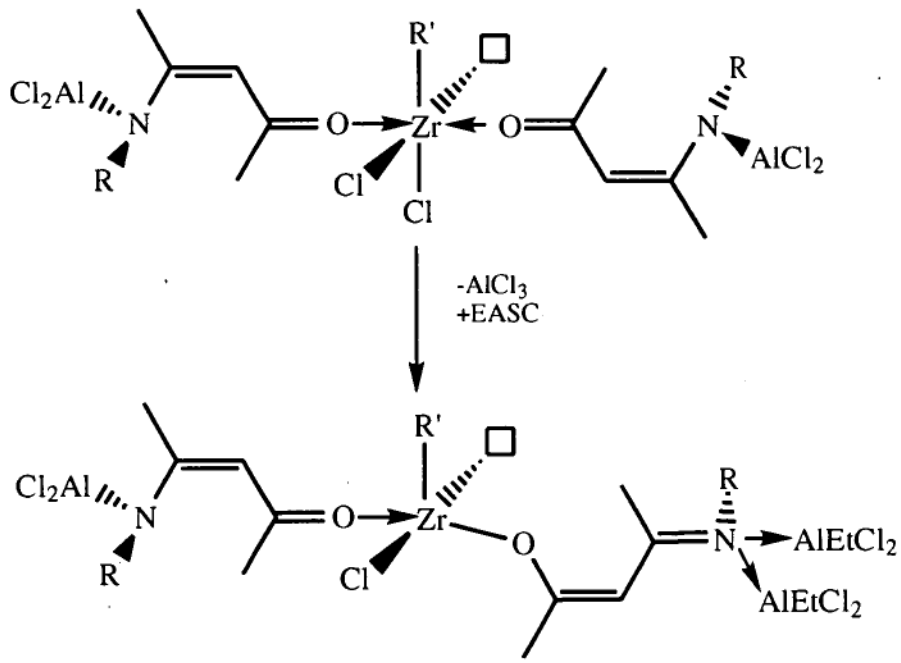

Possible EASC-oxygen or metal centre interactions have been omitted for clarity.

On β-aminoketone ligand deprotonation a number of reactions are possible. It has been observed that oligomerisation systems with high activities, which are derived from bis-N-phenyl β-aminoketone adducts, do not have the same activities and product distributions as catalyst systems derived from the analogous bis-N-phenyl β-aminoketone complexes while *in situ* observations indicated significantly different ligand shifts for the two systems. It is therefore proposed that an intermediate series of complexes may be formed.

A feasible set of steps leading to possible active species, which are consistent with reported observations, are described and shown in Figure 6.1b. Amine deprotonation results in aluminium-nitrogen bond formation and the release of ethane. It can be seen that significant ligand exchange reactions would then be required to form the same proposed active species which is derived from the bis-ligand complex (Figure 6.2), i.e. chloride abstraction, electron redistribution and further nitrogen-EASC adduct formation (Figure 6.1b where a first possible stage is shown after halide abstraction and ligand redistribution). As differences are observed in the catalytic activities and product distributions for these systems ligand exchange reactions must be slow, if they occur at all.

6.2.2. Bis-β-Aminoketone Complex Systems.

A proposed intermediate, which is less sterically crowded than previous intermediates, derived from the bis-ligand complex and consistent with *in situ* NMR studies is shown in Figure 6.2. Monomer access would be relatively easy leading to the required intermediates. However, the removal of two very electron withdrawing chloride ligands may tend to decrease the metal centre Lewis acidity. Catalytic testing supports such a view with significantly higher activities for intermediates derived from bis-ligand complexes and higher average oligomer weights. *In situ* tests have indicated that ethylene oligomerisation for these systems occurs under very mild conditions, with insertion at room temperature and 1atm of ethylene.

From Figure 6.2 it may be noted that no nitrogen-zirconium interaction is shown. It cannot be determined definitively from spectroscopic data if significant zirconium-nitrogen interactions are present or not in these species. However data collected during the *in situ* catalytic tests of the phenyl and methoxyphenyl substituted β-aminoketones indicate that such interactions may be present. These interactions would reduce the metal centre Lewis acidity further leading to higher average oligomer weights.

The fact that catalytic activity variations are observed on altering the ligand substituents indicates that electronic changes are felt at the metal centre either by altering zirconium-nitrogen interactions or inductively through the delocalised system.

Figure 6.2.
Proposed Active Species in the (R-Nacac)$_2$ZrCl$_2$/EASC System

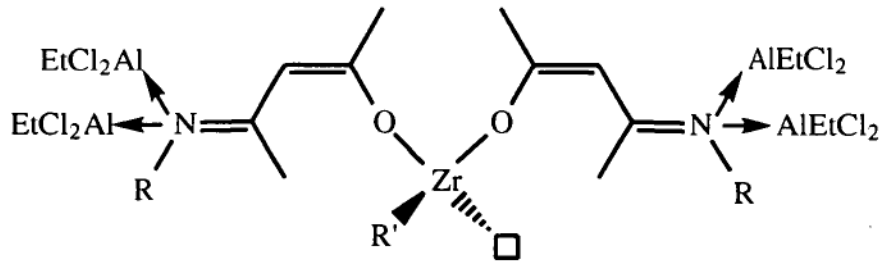

Possible EASC-oxygen or metal centre interactions have been omitted for clarity.

6.2.3. Cationic Bis-β-Aminoketone Complexes .

Of particular importance is the observation that, in the absence of a cocatalyst, cationic bis-ligand alkyl species polymerise ethylene (a possible active species is shown in Figure 6.3). In the absence of the cocatalyst and therefore in the absence of the extensive ligand-cocatalyst or metal centre-cocatalyst interactions it is proposed that metal centre Lewis acidity would be significantly reduced through more extensive chelate ligand-metal centre interactions. This adds support to the proposal that a highly Lewis acidic metal centre is required for oligomerisation.

Figure 6.3.
Proposed Active Species in the Cationic
[(*i*-Pr-Nacac)$_2$ZrBz]$^+$ System

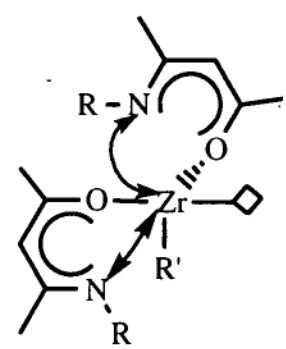

Time did not allow a thorough examination of the change in the catalytic behaviour of the cationic species when a cocatalyst was added to the system. The cause of the shortening of the product chain length would constitute a major investigation in its own right and consequently was not undertaken here. Such a study is now one aspect of a new PhD program currently underway in this department.

6.3.0. Overview and Directions

The results presented are in agreement with the model proposed in Chapter 2 and therefore it is possible to propose a number of ligand substituent variations which should modify the oligomers produced in a specific way. The major synthetic problem appears to be the generation of highly active catalysts which produce low molecular weight oligomers. Intermediates of the type shown in Figure 6.2 are required. Efficient electron withdrawing groups are necessary to generate a high Lewis acidity at the metal centre to give short chain products. The direction of synthesis will therefore depend on the influence of the delocalised system and the presence or strength of metal centre-nitrogen interactions.

Charge delocalisation over the chelate ring is thought to reduce the impact of any ligand substituent changes or ligand-cocatalyst interactions by introducing an averaging effect. This may average the effect of changes to the ligand at the metal centre but may also provide an effective route by which remote electronic perturbations may be transferred to the metal centre. For example, substitution of strongly electron withdrawing groups on the ligand backbone may lead to weaker nitrogen-cocatalyst interactions without significant changes to the metal centre Lewis acidity. This could increase activity by reducing nitrogen-metal centre interactions and/or steric crowding due to fewer nitrogen-cocatalyst interactions. As the metal centre Lewis acidity would be relatively unchanged the product distribution would not be significantly altered.

Where nitrogen-metal centre interactions are significant and lower oligomers are required, reducing the donor ability of the nitrogen is thought to be necessary in order to improve oligomerisation This may be achieved either by substitution of electron withdrawing groups or by the substitution of large bulky groups to sterically hinder such interactions. Similarly, synthesis may be directed to reduce such influences by substitution of a softer, weaker donor atom. Studies are continuing within this research group into such species[1]. Non-delocalised systems in which the donor properties of the two coordinating groups of the hemilabile ligand are more easily varied, may also provide useful data.

Fundamental studies into the formation of cocatalyst free, cationic oligomerisation catalysts present a difficult synthetic problem with highly unstable complexes. It is

expected that such species would need a metal centre of high Lewis acidity and hemilabile bidentate ligands. That is, for the formation of cationic oligomerisation complexes it is believed that a very soft donor atom and strongly electron withdrawing ligand backbone substituents would be required.

Industrially useful catalysts, where the use of a cocatalyst is not a problem, are often more easily prepared. Cocatalyst-ligand substituent interactions may be used to modify the effect of electron donating groups on the ligand. By interaction with a cocatalyst substituent groups which are normally electron donating, e.g. MeO-, can be made, on complexation with the added cocatalyst, to act as electron withdrawing groups. This effect, which has been noted previously, is observed in this work and may be a powerful tool for catalyst modification thus allowing complex stabilisation through electron donating groups which, in the presence of a cocatalyst, improve catalyst activity.

Interestingly this work has clearly demonstrated that many of the features and catalytic controls currently being developed in zirconium metallocene (and related systems) based catalysts may be achieved more simply from zirconium coordination complexes and their organometallic derivatives. During the period in which this thesis was being written, Jordan[2] published a paper discussing similar studies on a coordination complex of zirconium containing a macrocyclic N_4-tetradentate ligand. Jordan's work also highlights many of the synthetic features discussed in this thesis. However, no catalytic studies were reported by Jordan.

1 Theses ideas have been confirmed in a recent catalyst optimisation program for a forthcoming patent application where ligand backbone substitution with electron withdrawing groups lead to higher activities with no significant change in product distribution. Other studies have shown that increasing metal centre Lewis acidity decreases average oligomer weights without significant increases in activity.

2 Uhrhammer, R.; Black, D.J.; Gardner, T.G.; Olsen, J.D.; Jordan, R.F., *J. Am. Chem. Soc.* 115, **1993**, 8493-8494.

Chapter 7

Experimental

7.1.0. General Procedures

All reactions except where indicated were carried out using inert gas techniques. The nitrogen was dried and deoxygenated by successive passage through a column of 4A molecular sieves, a reduced BASF Cu Catalyst, R3-11, at 135°C followed by a second column of 4A molecular sieves. For more sensitive work is found necessary to pass the purified nitrogen through a further trap consisting of a silicon oil bubbler containing ≈5% TEA.

Solvents were dried by normal methods as described by Perrin, Armarego, and Perrin[1], and distilled under nitrogen directly before use. A more detailed description for the purification of general chemicals is given below.

Di-benzyl bis-ligand complexes were synthesised and handled with the exclusion of light.

7.2.0 Apparatus

GC Institut für Technische Chemie der RWTH Aachen

Siemens Sichromat 1
c.a. 30m SE 54-CS
Temp. Program 50-280°C; 10 min. iso 10°C/min.
Vaporisation Temp. 300°C.
Sample 0.3uL
Carrier Gas 1.5 Bar Nitrogen
FID HP 3359 LAS System

GC University of Tasmania

HP 5890 A
c.a. 50m BP-1
Temp. Program 50-260°C; iso 10°C/min.
Vaporisation Temp. 300°C.
Sample 0.5uL
Carrier Gas 150KPa. Nitrogen
FID

GC-MS Institut für Technische Chemie der RWTH Aachen
Siemens Sichromat 1 with open coupling to MS
Conditions as above
MS: Varian Mat 112S
Temperature (1Q); 200°C
Pressure (1Q); 2x10-6 Tor
Ionisation Current; 0.7 mA

NMR Institut für Technische Chemie der RWTH Aachen
^{1}H Varian EM390, 90 MHz. Standard TMS
^{1}H Bruker CXP 200, 200MHz, Standard TMS or Solvent
^{13}C Bruker CXP 200, 50.3MHz, Standard TMS or Solvent
NMR University of Tasmania
^{1}H Bruker AM300, 300MHz, Standard TMS or Solvent
^{13}C Bruker AM300, 75.5MHz, Standard TMS or Solvent

Elemental Analysis
Carlo Erba 1106, CHN Analyser
Carlo Erba 1108, CHNS-O-EA Analyser

IR Spectroscopy
Perkin Elmer 782, 5 minute scan.

7.3.0. Purification of Solvents and General Chemicals

Acetone[2]	Pre-dried with 3A molecular sieves then refluxed and distilled under nitrogen from B_2O_3.
Acetonitrile	Refluxed and distilled from CaH_2 under nitrogen before use.
Chloroform	Washed with water and pre-dried over $CaCl_2$. Refluxed and distilled under nitrogen from P_4O_{10} before use.
Dichloromethane	Refluxed and distilled under nitrogen from CaH_2 before use.
Diethyl ether	Distilled then pre-dried with $CaCl_2$ and then CaH_2 before refluxing and distilling under nitrogen from sodium/benzophenone before use.
Dimethoxyethane	Pre-dried with $CaCl_2$ and then refluxed and distilled under nitrogen from sodium/benzophenone before use.

Ethanol	Pre-dried over KOH. Distilled from magnesium ethoxide under nitrogen.
Hexane/Pentane	Refluxed and distilled under nitrogen from sodium or a sodium/potassium amalgam with benzophenone present before use.
t-Butanol	Pre-dried with $CaSO_4$, distilled and then refluxed and distilled under nitrogen from sodium before use.
THF	Pre-dried by mixing with CaH_2 then refluxed and distilled under nitrogen from sodium/benzophenone before use.
Toluene	Washed with conc. H_2SO_4 at 0°C until the acid was colourless then with water, 5% Na_2CO_3 and finally water. Toluene was pre-dried over $CaCl_2$ and then refluxed and distilled under nitrogen from sodium before use.
β-Diketones	Fractionally distilled or recrystallised from a suitable solvent before use.
Amines	Fractionally distilled or recrystallised from hexane before use.
Iodomethane	Fractionally distilled and degassed before use.
Benzylchloride	Refluxed and distilled under nitrogen from CaH_2 before use.
Chlorobenzene	Refluxed and distilled under nitrogen from P_4O_{10} before use.
Bromobenzene	Washed with conc. H_2SO_4 (until acid was colourless), 5% Na_2CO_3 and water. Pre-dried over $CaCl_2$ then refluxed and distilled under nitrogen from sodium.
t-Butylchloride	Pre-dried with $CaCl_2$ then fractionally distilled before use.
n-Butylchloride	Washed with conc. H_2SO_4 (until acid was colourless), water, 5% Na_2CO_3 and water before pre-drying over $CaCl_2$. Fractionally distilled before use.
Thiophene	Refluxed and distilled under nitrogen from sodium. Stored under nitrogen in a Schlenk tube for use.
Ethylene	Passed through 4A molecular sieves.
Molecular Sieves	Pre-dried in an oven overnight at 120°C followed by drying under vacuum at 300°C.
Celite	Washed for 24 hours in a soxhlet with refluxing chloroform and pre-dried in an oven at 120°C for 24 hours before drying

under vacuum at 350°C for 24 hours. Celite stored under nitrogen after drying.

Other reagents were used as received or used after drying under vacuum if inert gas techniques were required unless otherwise stated

7.4.0. Organometallic Reagents

MeLi

Halide free methyllithium was made by the method of House *et al* [3] but the yields were low, 20-30%, or from MeI in more normal yields[4], 60-70%.

MeLi, and other alkyl/aryl lithium solutions, could be titrated against DPAA or 1,3-diphenyl-2-propanone tosylhydrazone[5], other alternatives are available.

BzMgCl, Bz_2Mg

Benzylmagnesium chloride was synthesised using standard methods as required[6]. Reactions were assumed to be 95% complete and used without standardisation.

Dibenzylmagnesium could be made directly from benzylmagnesium chloride solutions by the addition of 1,4-dioxane.

t-BuLi

Solutions of *tert*-Butyllithium were synthesised by standard methods under argon with high sodium lithium dispersion[7]. Yields were generally 50-70% and solutions were titrated before use with DPAA as in indicator.

n-BuLi

Solutions of *n*-butyllithium were synthesised by standard methods from *n*-butyl chloride[8]. Solutions were stored at 0°C and titrated before use. Yields were in the range of 55-75%.

NaCp

Cyclopentadienylsodium solutions for the preparation of $CpZrCl_3$.DME were prepared by standard methods[9] from cracked dicyclopentadiene and sodium sand. The solutions were used directly with an assumed yield of 95%.

PhLi

Phenyllithium was prepared either by a variation of Schlosser's method from PhBr[10] or directly by reaction of PhBr with lithium[11], the produced PhLi was purified by recrystallisation from diethyl ether. Yields were between 50-70%.

PhMgCl

Phenylmagnesium chloride was synthesised from PhCl by reaction with activated magnesium formed by reaction of $MgCl_2$ with potassium[12]. Yields were generally low at 40-50%.

BzK

Benzylpotassium was synthesised from toluene in the presence of *n*-BuLi and KO-*t*-Bu as described by Schlosser[13]. The extremely moisture sensitive red solid was produced in yields of 70-90%.

7.5.0. Synthesis of Monothio-β-diketones

Monothio-β-diketones could be synthesised in two ways depending on the requirement for sulfur placement. Reaction of a β-diketone in acidic ethanol with H_2S did not allow control of sulfur placement[14] but allows a wide range of Sacac's to be synthesised. The workup was altered, as described by Chaston *et al*[15] to give the lead salt rather than the free ligand leading to improved yields.

Synthesis of HSacac

Acetylacetone (36 g, 0.36 moles) and 150 ml of acetonitrile were placed in a double walled 500 ml Schlenk flask and cooled to -45°C under nitrogen. A stream of H_2S was passed through the solution for 1 hour followed by a stream of HCl for 1 hour followed by a slow flow of H_2S for 2 hours. Nitrogen was slowly bubbled through the cooled solution overnight after which the solution was placed under vacuum for 2 hours to collect excess HCl or H_2S. The reaction mixture was poured into a slurry of 200 ml ice and 400 ml ether/pet. ether (1:4). The organic layer was removed and the aqueous layer washed with 2x200 ml of ether/pet. ether mix. The combined organic fractions were washed twice with 200 ml of distilled water and reduced in volume to about 100 ml before being added to a solution of 40 g of $Pb(acetate)_2$ in 300 ml of

ethanol. The crude product was collected by filtration washed with ethanol then hot water. The impure product can be recrystallised from DCM with hexane.

Yield of $Pb(Sacac)_2$ from Hacac 78.8 g, 71%

MW :437.54

Appearance :yellow powder

^{1}H-NMR ($CDCl_3$, 300 MHz):

δ 2.433(s, 3H, Me(CO)), 2.197(s, 3H, Me(CS)), 6.355(s, 1H, CH)

The free ligand can be obtained by suspending the lead salt in anhydrous ether and bubbling H_2S through the solution for 3-5 minutes. The precipitated PbS is filtered off and the free ligand is recovered on removing the solvent.

Yield of HSacac from $Pb(Sacac)_2$ 100%

MW :116.18

Appearance :yellow oil.

^{1}H-NMR ($CDCl_3$, 300 MHz):

δ 2.259(s, 3H, Me(CO)), 2.076(s, 3H, Me(CO)), 6.241(s, 1H, CH), 10.628(bs, 1H, SH).

lit. (CCl_4): δ 2.37(d, 3H, Me(CS)), 2.09(s, 3H, Me(CO)), 6.2(q, 1H, CH), 13.59(bs, 1H, SH).

The position of the sulfur in relation to the R groups on the Sacac backbone can be controlled if the monothio-β-diketones are prepared via a Claisen condensation[16]. The use of a strong base, *t*-Butyllithium in place of sodium amide, allows a greater range of Sacac's to be synthesised[17].

HPhSacac

In a 250 ml Schlenk flask, acetone (3.63 g, 62.5 mmol) was mixed with 40 ml of anhydrous ether at -10°C. To this solution was slowly added *t*-Butyllithium (50 ml, 1 M in pentane) over 30 minutes and the solution was allowed to mix for a further 30 minutes. A solution of O-ethyl thiobenzoate (4.16 g, 25 mmol) in 50 ml of anhydrous ether was then slowly added over 30 minutes and the solution was allowed to stir for a further 20 minutes. No longer working under nitrogen, excess *t*-butyllithium was destroyed by the slow addition of 5 ml of water followed by a further 200 ml of water. The organic layer was removed and the aqueous layer

extracted with 200 ml of a 1:1 pentane : ether mix. the aqueous layer was acidified with 4 M HCl and again extracted 3 times with 200 ml of the ether : pentane mix. The combined organics were washed until neutral and the majority of the solvent removed under vacuum. A lead salt was made as above.

Yield of $Pb(PhSacac)_2$ 2.10 g, 15%
MW :561.68
Appearance :yellow powder
^{1}H-NMR ($CDCl_3$, 300 MHz):
δ 2.728(s, 3H, Me(CO)), 6.659(s, 1H, CH), 7.524(d, 2H, *o*-Ph), 7.326(t, 2H, *m*-Ph), 7.301(t, 1H, *p*-Ph)

As free ligand H-PhSacac
MW :178.25
Appearance :yellow/red crystalline solid
^{1}H-NMR ($CDCl_3$, 300 MHz):
δ 2.623 & 2.678(s, 3H, Me), 6.673 & 6.694(s, 1H, CH), 13.748 & 12.225(s, 1H, SH), 7.699(d, 2H, *o*-Ph), 7.432(t, 2H, *m*-Ph), 7.430(t, 1H, *p*-Ph)

The other ligands used in this work, H-SacPhac and H-PhSacPhac, may be prepared by a similar Claisen condensation in varying yields (20-70%)[18].

In order to generate the above Sacac ligands, the required thioesters needed to be synthesised. After a number of attempts with P_4S_{10} and Lawesson's Reagent, which led to separation difficulties, the required thioesters were synthesised by the hydrosulfination of the alkyl/aryl imidate hydrochloride[19]. The choice of base was important to aid separation. Initial distillation was completed at low temperature, ≤50°C, to avoid decomposition, side reactions and further sulfination. The major contaminants, when care is not taken during distillation, are the disulphide and dithioester from further reaction.

O-Ethyl thioacetate, MeCS-OEt
Step 1.: Synthesis of Me(CNH.HCl)-OEt
In a 250 ml flask MeCN (15.72 g, 0.38mole) and absolute EtOH (17.6 g, 0.38 mole) were mixed in 100 ml of anhydrous ether at 0°C with the exclusion of moisture. Dry HCl was slowly bubbled through the vigorously stirred solution for 4 hours and the

reaction vessel allowed to come to RT overnight. The solvent and unreacted starting materials were removed under vacuum to leave a white powder. The product was identified by ^{1}H-NMR. The powder was used without further purification.

MW :123.58
Appearance :white powder
^{1}H-NMR ($CDCl_3$, 300 MHz):
δ 2.429(s, 3H, Me(CN)), 1.431(t, 3H $J_{H,H}$6.99Hz, -CH_2-$\underline{CH_3}$), 4.578(q, $J_{H,H}$6.99Hz, -$\underline{CH_2}$-CH_3), 11.366(bs, 1H, NH) & 12.283(bs, 1H, NH)

Step 2: Synthesis of MeCS-OEt
The imidate hydrochloride was dissolved/suspended in 100 ml of anhydrous chloroform at -10°C and 40 ml of quinoline added. A strong stream of H_2S was bubbled through the vigorously stirred solution for 2 hours followed by a stream of nitrogen for 1 hour. Reaction proceeds with the precipitation of NH_4Cl. The solution was degassed at low temperature and the solvent removed at 0°C under vacuum. The remaining volatiles were removed under vacuum at 40°C and the product fractionally distilled under nitrogen at normal pressure. The product, a pale yellow liquid, fumes on contact with air and was stored under nitrogen.

Yield :28.5 g, 72%
MW :104.17
Appearance :pale yellow liquid, Bp 104-110°C (Lit.[20] 105°C)
^{1}H-NMR ($CDCl_3$, 300 MHz):
δ 2.571(s, 3H, Me(CN)), 1.392(t, 3H $J_{H,H}$7.11Hz, -CH_2-$\underline{CH_3}$), 4.482(q, 2H $J_{H,H}$7.11Hz, -$\underline{CH_2}$-CH_3)

<u>O-Ethyl thiobenzoate, PhCS-OEt</u>
Ph(CNH.HCl)-OEt
MW 173.64
Appearance white powder (not isolated and characterised)
Pyridine used as the base for the hydrosulfination.

PhCS-OEt Yield 34.1% (from benzonitrile)

MW 166.24

Appearance pale yellow liquid, Bp 234-236°C (Lit.[20] 24°C)

^{1}H-NMR ($CDCl_3$, 300 MHz):

δ 1.51(t, 3H $J_{H,H}$7.11Hz, -CH_2-$\underline{CH_3}$), 4.12(q, 2H $J_{H,H}$7.11Hz, -$\underline{CH_2}$-CH_3), 8.18(d, 2H $J_{H,H}$8.00Hz, *o*-Ph), 7.38(t, 2H $J_{H,H}$7.38Hz, *m*-Ph), 7.50(t, 1H $J_{H,H}$7.71Hz, *p*-Ph)

7.6.0. Dithio-β-Diketone Precursors

Dithiolium salts have been used as precursors for the formation of dithio-β-diketones and can be used in the formation of β-aminothioketones. Iodide salts are readily synthesised by the reaction of β-diketones in acidic ethanol with H_2S in the presence of iodine[21], for example,

7.6.1. 3,5-Dimethyl-1,2-dithiolium Iodide (DT^+I^-)

In a 500 ml flask fitted with a gas inlet and an outlet bubbler, iodine (25 g, 0.1 mole) and acetylacetone (10 g, 0.10 mole) were dissolved in 150 ml of anhydrous ethanol. With rapid agitation a stream of H_2S was passed through the solution for 3 hours. A yellow solid formed. Nitrogen was then slowly bubbled through the solution overnight. The solid was recovered by filtration and washed twice with 50 ml of ether. The dithiolium salt was recrystallised from methanol with ether.

DT^+I^- Yield 16% (from acetylacetone)

MW 258.14

Appearance yellow crystalline solid

^{1}H NMR (CD_3O, D300 MHz):

δ 1.817(s, 6H, Me), 5.275(s,1H, CH)

7.7.0. β-Aminoketones

Synthesis for β-aminoketone involves the direct reaction of a β-diketone with a primary amine in a straight forward condensation reaction. The factors to be considered in the synthesis are the boiling point of the amine and the acidity of the β-diketone. For low boiling amines reaction is promoted in the presence of a drying agent[22], e.g. $CaSO_4$ or molecular sieves, for higher boiling amines refluxing toluene

(or similar) with a water trap can be used[23] while for very acidic β-diketones transformation into a silyl ether may first be required to introduce a better leaving group before reaction with the amine[24]. Reaction rates can be increased by microwave irradiation or by addition of an acid catalyst[25]. Most of these ligands have not been previously reported and for others NMR data had not been reported.

7.7.1. Method A

4-(iso-propylamino)-3-penten-2-one (*i*-Pr-HNacac)

In a 250 ml flask fitted with a reflux condenser and $CaCl_2$ drying tube was placed 40 g of $CaCl_2$ and acetylacetone (39.4 g, 0.394 mole) in 100 ml of toluene. The mixture was rapidly stirred while *i*-Pr-NH_2 (35.6 g, 0.60 mole) was added. The exothermic reaction caused the solution to reflux which was continued under heating for 6 hours. The $CaSO_4$ was filtered off and washed twice with 50 ml of toluene and the product recovered by fractional distillation from toluene.

i-Pr-HNacac Yield 88.5%
MW 141.21
Appearance clear liquid
^{1}H-NMR ($CDCl_3$, 300 MHz):
δ 1.96(s, 3H, Me) & 1.92(s, 3H, Me), 4.88(s, 1H, CH), 10.80(bs, 1H, NH), 3.68(m, 1H, N-C<u>H</u>$(CH_3)_2$), 1.20(d, 6H $J_{H,H}$ 6.48Hz, N-CH(C<u>H</u>$_3)_2$).

7.7.2. Method B

1,3-diphenyl-2-(phenylamino)-acrolein (Ph-HPhNacPhac)

Aniline (3.14 g, 33.4 mmol) and dibenzoylmethane (5.0 g, 22.3 mmol) were dissolved in 50 ml of xylene and placed into a 100 ml flask fitted with a reflux condenser and water trap (Dean Stark apparatus). The xylene was refluxed for 1 hour with no reaction observed. H_2SO_4 (2 drops, conc.) was added and the xylene again refluxed. After 4 hours approximately 80% of the theoretical yield of water was collected and the refluxing was stopped. The solvent was removed under vacuum and the product recrystallised from hexane.

Ph-HPhNacPhac Yield 60.2%
MW 299.37
Appearance Yellow crystalline solid.

^{1}H-NMR ($CDCl_3$, 300 MHz):

δ 6.095(s, 1H, CH), 12.91(bs, 1H, NH); N-Ph δ 6.767(d, 2H $J_{H,H}$8.82Hz, *o*-Ph), 7.126(t, 2H $J_{H,H}$6.78Hz, *m*-), 6.990(t, 1H, p-); C(O)-Ph δ 7.33-7.48(m, 8H, *o*- & *m*-), 7.971(d, 2H $J_{H,H}$8.18Hz, *o*-)

^{13}C{^{1}H}-NMR ($CDCl_3$, 75.5 MHz):

δ 190.2(CO), 162.2(CN), 97.9(CH), 136.4, 140.1 & 140.5(*i*-Ph), 123.9, 124.7, 128.0, 129.1, 129.3, 130.6, 132.2(other *o*-,*m*- &*p*-Ph's & one peak obscured).

7.7.3. Method C

4-(iso-propylamino)-1,1,1-trifluoropent-3-en-2-one (*i*-Pr-HNtfac)

This ligand was synthesised by the method of Shin et al.[26] substituting Me_3SiCl for $Me_2PhSiCl$.

Part A; synthesis of Natfac.

To a 250 ml Schlenk flask containing a suspension of NaH (3.00 g, 80% disp. in mineral oil, 50% excess) in 40 ml of THF at 0°C was slowly added a solution of Htfac(11.43 g, 74.18 mmol) in 30 ml of THF. A vigorous reaction occurred. The solution, containing unreacted NaH in suspension, was stirred at RT for 1 hour and then filtered through celite. The sodium salt was not isolated.

Part b; synthesis of Me_3Si-tfac.

To a 250 ml Schlenk flask containing the THF solution of Natfac formed in the previous step, equipped with a double surface reflux condenser, was slowly added Me_3SiCl (10.00 g, 92.73 mmol, a 25% excess) in 40 ml of ether. A precipitate formed on addition of the Me_3SiCl. The slurry was refluxed for 1 hour, after which the solvent and product were removed by flash distillation leaving a fine white powder. The colourless product was recovered by fractional distillation. The ^{1}H-NMR indicating a mixture of isomers.

Me_3Si-tfac	Yield 78.4%
MW	226.27
Appearance	clear liquid, Bp 66-72°C at 20mm Hg.

^{1}H-NMR ($CDCl_3$, 300 MHz):

δ 2.3336(s, 3H, Me), 2.2091(s, 4.5H, Me), 5.9318(s, 1H, CH) & 5.6906(s, 1.5H, CH), 0.2828(s, 9H, $Si(CH_3)_3$) & 0.2511(s, 13.5H, $Si(CH_3)_3$).

$^{13}C\{^1H\}$-NMR ($CDCl_3$, 75.5 MHz):

δ 196.30 & 179.91(CO-Me), 179.60(m) & 148.45(m, C(O)-CF_3), 100.31 & 110.26(CH), 23.46 & 32.05(Me), 0.60 & 0.79($Si(CH_3)_3$), 120.31(q $J_{F,C}$ 277.8Hz, CF_3) & 117.37(q $J_{F,C}$ 291.4, CF_3).

Part C; synthesis of *i*-Pr-HNtfac

To a 100 ml Schlenk flask containing Me_3Si-tfac (4.14 g, 18.30 mmol) dissolved in 20 ml of hexane at 0°C was added *i*-Pr-NH_2 (1.10 g, 18.6 mmol). The solution was stirred for 20 minutes at room temperature. The solvent, unreacted amine and the by-product were removed under vacuum to leave a pure product.

i-Pr-HNtfac Yield 95.4%

MW 226.27

Appearance clear liquid, Bp not recorded.

^1H-NMR ($CDCl_3$, 300 MHz):

δ 2.055(s, 3H, Me), 5.214(s, 1H, CH), 11.1(bs, 1H, NH), 3.798(m, 1H, N-$CH(CH_3)_2$), 1.236(d, 6H $J_{H,H}$ 6.48Hz, N-$CH(CH_3)_2$).

$^{13}C\{^1H\}$-NMR ($CDCl_3$, 75.5 MHz):

δ 168.81(CN), 175.39(q, $3J_{F,C}$32.5Hz, CO), 89.56(CH), 19.43(Me), 118.34(q $J_{F,C}$ 287.5Hz, CF_3), 46.41($NCH(CH_3)_2$), 23.72($NCH(CH_3)_2$).

1-benzoyl-2-(hexylamino)-propene (Hex-HNacPhac); method B

Hex-HNacPhac Yield 52.9%

MW 245.36

Appearance pale yellow liquid

^1H-NMR ($CDCl_3$, 90 MHz):

δ 2.01(s, 3H, Me), 5.63(s, 1H, CH), 11.4(bs, 1H, NH); C(O)-Ph δ 7.7-7.9(m, 2H, Ph), 7.3-7.4(m, 3H, Ph); N-Hex δ 0.87(m, 3H, $NCH_2(CH_2)_4CH_3$), 1.2-1.8(m, 8H, $NCH_2(CH_2)_4CH_3$), 3.30(q, 2H $J_{H,H}$6.6Hz, $NCH_2(CH_2)_4CH_3$).

1-benzoyl-2-(hexylamino)-styrene (Hex-HPhNacPhac); method B

Hex-HPhNacPhac Yield 34.1%

MW 307.43

Appearance pale yellow liquid

^{1}H-NMR ($CDCl_3$, 90 MHz):

δ 7.75-7.95(m, 2H, Ph), 7.25-7.55(m, 9H, Ph & CH), 11.5(bs, 1H, NH); Hex δ 0.83(m, 3H, $NCH_2(CH_2)_4\underline{CH_3}$), 1.1-1.8(m, 8H, $NCH_2(\underline{CH_2})_4CH_3$), 3.17(q, 2H $J_{H,H}$6.0Hz, $N\underline{CH_2}(CH_2)_4CH_3$).

4-(Hexylamino)-3-penten-2-one (Hex-HNacac); method B

Hex-HNacac Yield 43.8%

MW 183.29

Appearance pale yellow liquid

^{1}H-NMR ($CDCl_3$, 90 MHz):

δ 1.97(s, 3H, Me) & 1.90(s, 3H, Me), 4.92(s, 1H, CH), 10.85(bs, 1H, NH); Hex δ 0.87(m, 3H, $NCH_2(CH_2)_4\underline{CH_3}$), 1.2-1.7(m, 8H, $NCH_2(\underline{CH_2})_4CH_3$), 3.20(q, 2H $J_{H,H}$6.0Hz, $N\underline{CH_2}(CH_2)_4CH_3$).

4-(Phenylamino)-3-propen-2-one (Ph-HNacac); method B

Ph-HNacac Yield 42.6%

MW 175.23

Appearance white crystalline solid

^{1}H-NMR (CD_2Cl_2, 300 MHz):

δ 2.034(s, 3H, Me) & 1.975(s, 3H),(CH) 5.179(s, 1H), NH 12.05(bs, 1H), Ph 7.3324(m, 2H), 7.172(m, 1H) & 7.099(m, 2H).

^{1}H-NMR (Toluene-d_8, 300 MHz):

δ 2.009(s, 3H, Me) & 1.560(s, 3H, Me), 4.958(s, 1H, CH), 12.95(bs, 1H, NH); N-Ph δ 6.803(d, 2H$J_{H,H}$7.4Hz, *o*-Ph), 6.853(t, 1H $J_{H,H}$7.4Hz, *p*-Ph), 7.097(m, 2H $J_{H,H}$6.4Hz, *m*-Ph).

^{1}H-NMR (CD_3OD, 300 MHz):

δ 2.104(s, 3H, Me) & 2.073(s, 3H, Me), 5.327(s, 1H, CH); N-Ph δ 7.410(m, 2H), 7.29(m, 1H) & 7.21(m, 2H).

$^{13}C\{^1H\}$-NMR (CD_2Cl_2, 75.5 MHz):

δ 196.56(CO), 160.65(CN), 20.35 & 29.62(Me), 98.19(CH); N-Ph δ 139.69(*i*-Ph), 125.25(*o*-Ph), 126.03(*p*-Ph), 129.77(*m*-Ph).

1-Benzoyl-(phenylamino)-propene (Ph-HNacPhac); method B

Ph-HNacPhac Yield 52.0%

MW 237.3

Appearance white crystalline solid

^{1}H-NMR ($CDCl_3$, 90 MHz):

δ 2.13(s, 3H, Me), 5.86(s, 1H, CH), 13.07(bs, 1H, NH); N-Ph & C(O)-Ph δ 7.75-8.00(m, 2H), 7.0-7.5(m, 8H).

4-(Cyclohexylamino)-3-penten-2-one (Cy-HNacac); method B

Cy-HNacac Yield 77.0%

MW 181.21

Appearance pale orange liquid

^{1}H-NMR ($CDCl_3$, 300 MHz):

δ 1.988(s, 3H, Me) & 1.941(s, 3H, Me), 4.912(s, 1H, CH), 11.0(bs, 1H, NH); Cy δ 3.369(m, 1H, Cy-H), 1.2-1.9(m, 10H, Cy-CH_2).

4-(*t*-Butylamino)-3-penten-2-one (*t*-Bu-HNacac); method A

t-Bu-HNacac Yield 65.0%

MW 155.24

Appearance pale orange liquid

^{1}H-NMR ($CDCl_3$, 300 MHz):

δ 2.050(s, 3H, Me) & 1.986(s, 3H, Me), 4.898(s, 1H, CH), 11.37(bs, 1H, NH), 1.402(s, 9H, *t*-Bu-Me).

4-(2,4,6-Trimethylphenylamino)-3-penten-2-one (tmp-HNacac); method B

tmp-HNacac supplied by ICI Australia

MW 155.24

Appearance off white crystalline solid

^{1}H-NMR ($CDCl_3$, 300 MHz):

δ 2.089(s, 3H, Me) & 1.610(s, 3H, Me), 5.170(s, 1H, CH), 11.83(bs, 1H, NH); N-trimethyphenyl δ 2.142(s, 6H, *o*-PhMe), 2.269(s, 3H, *p*-PhMe), 6.885(s, 2H, *m*-PhH).

^{13}C{^{1}H}-NMR ($CDCl_3$, 75.5 MHz):

δ 196.55(CO), 163.79(CN), 21.6 & 29.74(Me), 96.33(CH); N-trimethylphenyl δ 134.56, 136.42 & 137.71(*i*-, *o*- & *p*-Ph), 129.55(*m*-Ph), 18.82 & 19.53(Ph-Me).

4-(*para*-chlorophenylamino)-3 penten-2-one (ClPH-HNacac); method B

ClPh-HNacac Yield 56.2%

MW 209.67

Appearance orange crystalline solid

^{1}H-NMR ($CDCl_3$, 300 MHz):

δ 2.044(s, 3H, Me), 1.924(s, 3H, Me), 5.153(s, 1H, CH), 12.39(bs, 1H, NH); N-PhCl δ 6.976(d, 2H $J_{H,H}$6.69Hz, *o*-Ph), 7.242(d, 2H $J_{H,H}$6.69Hz, *m*-Ph).

^{13}C{^{1}H}-NMR ($CDCl_3$, 75.5 MHz):

δ 197.02(CO), 160.24(CN), 20.36 & 29.82(Me), 96.72(CH); N-PhCl δ 131.52 & 137.95(*i*- & *p*-Ph), 126.39 & 129.78(*o*- & *m*-Ph).

4-(*para*-Methoxyphenylamino)-3-penten-2-one (MeOPH-HNacac); method B

MeOPh-HNacac Yield 26.0%

MW 205.26

Appearance white crystalline solid

^{1}H-NMR ($CDCl_3$, 300 MHz):

δ 2.048(s, 3H, Me), 1.865(s, 3H, Me), 5.119(s, 1H, CH), 12.27(bs, 1H, NH); N-PhOMe δ 6.826(d, 2H $J_{H,H}$8.93Hz, *m*-Ph), 6.998(d, 2H $J_{H,H}$8.93Hz, *o*-Ph), 3.759(s, 3H, OMe).

^{1}H-NMR (CD_2Cl_2, 300 MHz):

δ 2.021(s, 3H, Me), 1.877(s, 3H, Me), 5.141(s, 1H, CH), 12.34(bs, 1H, NH); N-PhOMe δ 6.853(d, 2H $J_{H,H}$6.74Hz, *m*-Ph), 7.021(d, 2H $J_{H,H}$6.74Hz, *o*-Ph), 3.757(s, 3H, OMe).

^{13}C{^{1}H}-NMR ($CDCl_3$, 75.5 MHz):

δ 196.38(CO), 161.78 & 158.30(CN & *p*-Ph), 20.20 & 29.66(Me's), 97.41(CH); N-PhOMe δ 132.09(*i*-Ph), 114.82(*m*-Ph), 127.24(*o*-Ph), 56.02(Ph-OMe).

^{13}C{^{1}H}-NMR ($CDCl_3$, 75.5 MHz):

δ 196.11(CO), 161.60 & 158.42(CN & *p*-Ph), 20.07 & 29.48(Me's), 97.31(CH); N-PhOMe δ 132.34(*i*-Ph), 114.88(*m*-Ph), 127.20(*o*-Ph), 56.02(Ph-OMe).

4-(Diphenylamino)-3-penten-2-one (Ph_2-HNacac); method B

Ph_2-HNacac Yield 62.0%

MW 251.33

Appearance yellow crystalline solid

^{1}H-NMR ($CDCl_3$, 300 MHz):

δ 2.402(s, 3H, Me) & 1.988(s, 3H, Me), 5.389(s, 1H, CH); N-Ph_2 δ 7.148(d, 2H $J_{H,H}$7.27Hz, *o*-Ph), 7.355(d, 2H $J_{H,H}$7.86Hz, *m*-Ph), 7.248(d, 2H, *p*-Ph).

4-(Diethylamino)-3-penten-2-one (Et_2-HNacac); method A

Et_2-HNacac	Yield 44.0%
MW	155.24
Appearance	yellow crystalline solid

^{1}H-NMR ($CDCl_3$, 300 MHz):

δ 2.444(s, 3H, Me) & 1.982(s, 3H, Me), 5.007(s, 1H, CH), 1.087(t, 3H $J_{H,H}$7.11Hz, -CH_2-$\underline{CH_3}$), 3.217(q, 2H $J_{H,H}$7.11Hz,-$\underline{CH_2}$-CH_3).

^{13}C{^{1}H}-NMR ($CDCl_3$, 75.5 MHz):

δ 194.81(CO), 160.80(CN), 15.87 & 32.33(Me's), 94.56(CH), 13.23(-CH_2-$\underline{CH_3}$), 44.55(-$\underline{CH_2}$-CH_3).

Ethyl-bis(4-amino-3-penten-2-one) (Et(-HNacac)$_2$); method A

Et(-HNacac)$_2$	Yield 67%
MW	224.30
Appearance	white crystalline solid

^{1}H-NMR ($CDCl_3$, 300 MHz):

δ 2.004(s, 3H, Me) & 1.912(s, 3H, Me), 5.001(s, 1H, CH), 10.92(s, 1H, NH), 3.426(d, 2H $^2J_{H,H}$6.34Hz, -$\underline{CH_2}$-$\underline{CH_2}$).

7.8.0. Synthesis of β-Aminothioketones

A number of methods were examined to find an effective general thiolation technique for synthesising β-aminoketones, e.g. reaction with B_2S_3, P_4S_{10} or direct formation from dithiolium salts[27]. Two methods were found to be generally suitable; thiolation using Lawesson's Reagent in DME[28] or reaction of hydrosulphide ion with O-alkylated β-aminoketone salts[29].

7.8.1. Method 1

4-(*iso*-Propylamino)-3-penten-2-thione (*i*-Pr-HNacSac)

In a 500 ml flask fitted with a $CaCl_2$ drying tube *i*-Pr-HNacac (6.90 g, 50.0 mmol) was dissolved in 150 ml of anhydrous DME at 20°C. Lawesson's Reagent (11 g, 25

mmol) was slowly added and the solution went yellow as the reagent dissolved. The mix was stirred for 20 minutes and then poured into 300 ml of distilled water, stirred and extracted three times with 50 ml of chloroform. The combined extracts were dried over Na_2SO_4 and the solvent removed under vacuum. The residue was taken up in 10 ml of chloroform and passed through a 50:50 silica : alumina column, 5x25 cm, using chloroform as the eluent. The solvent was removed from the collected fraction and the product recrystallised from hexane.

It was also possible to work up the solution by adding 100 ml of toluene. The volume of the reaction mixture was reduced to ca. 150 ml by which time a dark residue had separated. The solution was removed by decantation and the volume reduced to ca. 10 ml and 50 ml of hexane slowly added. The solution was filtered and the product precipitated by cooling to ≈-20°C. The product was recrystallised from hexane.

7.8.2. Method 2

In a Schlenk flask *i*-Pr-HNacac (7.48 g, 53.0 mmol) was dissolved in 100 ml of anhydrous DCM. A solution of Et_3OBF_4 (10 g, 53.0 mmol) in 50 ml of DCM was slowly added and the mixture allowed to stir for 20minutes. NaHS (2.97 g, 53 mmol) in 25 ml of absolute ethanol was then slowly added. The solution went dark yellow and a precipitate formed. After 15 minutes the solution was filtered to remove the $NaBF_4$ and the solvent removed under vacuum to leave a crude product which was recrystallised from hexane leaving a bright yellow powder.

i-Pr-HNacSac	Yield 69.9%
MW	157.27
Appearance	yellow crystalline solid

^{1}H-NMR ($CDCl_3$, 200 MHz):

δ 2.490(s, 3H, Me) & 2.083(s, 3H, Me), 6.040(s, 1H, CH), 12.09(s, 1H, NH), 3.873(d of sept, 1H $^3J_{H,H}$6.46Hz, $^2J_{H,H}$8.30Hz, N-C<u>H</u>$(CH_3)_2$), 1.337(d, 6H $^3J_{H,H}$6.46Hz, N-CH(C<u>H</u>$_3)_2$).

^{13}C{^{1}H}-NMR ($CDCl_3$, 75.5 MHz):

δ 203.06(CS), 165.17(CN), 20.77 & 39.13(Me's), 113.59(CH), 23.96(N-CH(C<u>H</u>$_3)_2$), 46.95(N-C<u>H</u>$(CH_3)_2$).

4-(Hexylamino)-3-penten-2-thione (Hex-HNacSac); method 1

Hex-HNacac Yield 14.2%

MW 199.35

Appearance yellow crystalline solid

^{1}H-NMR ($CDCl_3$, 200 MHz):

δ 2.503(s, 3H, Me) & 2.0517(s, 3H Me), 6.084(s, 1H, CH), 12.25(s, 1H, NH); N-Hex δ 3.365(q, 2H $J_{H,H}$6.51Hz, $NCH_2(CH_2)_4CH_3$), 1.686(m, 2H, $NCH_2(CH_2)_4CH_3$) & 1.43-1.20(m, 4H, $NCH_2(CH_2)_4CH_3$), Hex-Me 0.873(t, 3H $J_{H,H}$6.54Hz, $NCH_2(CH_2)_4CH_3$).

4-(Phenylamino)-3-penten-2-thione (Ph-HNacSac); method 1

Ph-HNacac Yield 19.7%

MW 191.29

Appearance yellow crystalline solid

^{1}H-NMR ($CDCl_3$, 200 MHz):

δ 2.602(s, 3H, Me) & 2.104(s, 3H, Me), 6.278(s, 1H, CH), 14.9(s, 1H, NH); N-Ph δ 7.15-7.45(m, 5H).

Lit.[29] : δ 6.28(SH), 15.00(NH).

7.9.0. Schiff's Bases

These ligands were synthesised from salicylaldehyde and the appropriate amine using the method for β-aminoketones described above, reactivity is much higher.

Phenyl-salicylaldimine (Ph-NPhOH); method A

Ph-NPhOH Yield 47.4%

MW 197.24

Appearance yellow crystalline solid

^{1}H-NMR ($CDCl_3$, 300 MHz):

δ 8.600(s, 1H, CH), 13.26(s, 1H, OH); Ph's δ 6.90-7.04(d & t, 2H), 7.24-7.44(m, 7H).

Iso-propyl-salicylaldimine (*i*-Pr-NPhOH); method A

i-Pr-NPhOH Yield 52.0%

MW 163.22

Appearance yellow liquid

^{1}H-NMR ($CDCl_3$, 300 MHz):

δ 8.333(s, 1H, CH), 13.68(s, 1H, OH); N-Ph δ 7.272-7.200(m, 2H), 6.953-6.644(m, 2H); N-*i*-Pr δ 3.529(sept, 1H $J_{H,H}$6.4Hz, $\underline{CH}(CH_3)_2$), 1.273(sept, 6H $J_{H,H}$6.4Hz, $CH(\underline{CH_3})_2$).

7.10.0 Potassium β-Aminoketonates

Prior to this study, β-aminoketone salts had only been generated in situ[22]. Initially a similar synthetic method was used to generate the required potassium salts, however, pure products, due to incomplete reaction, were not always generated. The following is a general synthesis for the required potassium β-aminoketonates.

Potassium 4-(*para*-Methoxyphenylamino)-3-penten-2-onate (MeOPH-KNacac)

In 250 ml Schlenk flask KO-*t*-Bu (1.6 g, 14.25 mmol) was suspended in a mix of 20 ml toluene and 50 ml of THF. A solution of MeOPH-HNacac (3.22 g, 15.68 mmol (10% excess)) in 20 ml of THF was added and the flask heated with stirring to 60°C for 4 hours. The solution went yellow orange as the KO-*t*-Bu dissolved. After 4 hours the solution was cooled to RT and the THF was removed under vacuum (a voluminous precipitate formed). Enough toluene (20-30 ml) was added to slurry the precipitate and the product collected by filtration. Excess free ligand and impurities were removed by washing with toluene (2x20 ml) then with hexane (2x20 ml). The product was dried under vacuum and did not need recrystallising. Yield 2.96 g.

MeOPh-KNacac Yield 86.0%

MW 243.35

Appearance pale yellow powdery solid

^{1}H-NMR (CD_3OD, 300 MHz):

δ 2.227(s, 3H, Me) & 2.14(m, 2H, CH_2), 5.301(s, 2H, CH); N-PhOMe δ 7.1269(d, 2H $J_{H,H}$8.26Hz, *m*-Ph), 7.262(d, 2H $J_{H,H}$8.26Hz, *o*-Ph), 3.982(s, 3H, OMe).

Potassium 4-(phenylamino)-3-penten-2-onate (Ph-KNacac)

Ph-KNacac Yield 92.0%

MW 213.32

Appearance pale yellow powdery solid

^{1}H-NMR (CD_3OD, 300 MHz):

δ 2.101(s, 3H, Me), 2.085(m, 2H, CH_2), 4.974(s, 2H, CH); N-Ph δ 7.414(t, 2H $J_{H,H}$8.13Hz, *m*-Ph), 7.7.284(m, 1H, *p*-Ph), 7.365(m, 2H $J_{H,H}$8.37Hz, *o*-Ph).

An identical spectrum is obtained when NaOMe is added to Ph-HNacac in CD_3OD in a 1:1 ratio. When D_2O is added the spectrum of the free ligand is seen.

Potassium 4-(*para*-chlorophenylamino)-3-penten-2-onate (ClPh-KNacac)

ClPh-KNacac Yield 92.7%

MW 247.726

Appearance pale yellow powdery solid

^{1}H-NMR (CD_3OD, 300 MHz):

δ 2.099(s, 3H, Me), 2.089, 2.083, 2.076, 2.068(m, 2H, CH_2), 5.054(s, 2H, CH); N-PhCl δ 7.421(d, 2H $J_{H,H}$6.62Hz), 7.204(d, 2H $J_{H,H}$6.62Hz).

Potassium 4-(*iso*-Propylamino)-3-penten-2-thione (*i*-Pr-KNacSac)

i-Pr-KNacac Yield 85.2%

MW 195.36

Appearance yellow/brown powdery solid

^{1}H-NMR (CD_3OD, 300 MHz):

δ 2.459(s, 3H, Me), 2.442(m, 2H, CH_2), 6.148(s, 2H, CH); N-*i*-Pr δ 4.077(sept., 1H $J_{H,H}$6.44Hz, $\underline{CH}(CH_3)_2$), 1.372(d, 2H $J_{H,H}$6.44Hz, $CH(\underline{CH_3})_2$).

On adding D_2O the normal spectrum of the free ligand is seen.

Other salts have been synthesised and used without further characterisation.

7.11.0 Zirconium Adducts

$ZrCl_4$.2THF

This complex was synthesised as described by Manzer[30].

In a 100 ml Schlenk flask fitted with a reflux condenser $ZrCl_2$ (4.28 g, 18.4 mmol) was suspended in 40 ml of DCM. The flask was cooled to 0°C and THF (2.65 g, 36.7 mmol) slowly added. After the first 2 ml of THF were added the bath was removed and the solution allowed to come to reflux. The solution was mixed for a further 30 minutes, filtered to give a clear solution and 20 ml of hexane added to

precipitate a white powder. The solution was cooled to -20°C for 2 hours then filtered. The solids were washed twice with 10 ml of hexane and dried under vacuum. Yield 5.64 g.

$ZrCl_4.2THF$ Yield 81.3%

MW 377.25

Appearance white crystalline solid

^{1}H-NMR ($CDCl_3$, 300 MHz):

δ 4.597(bs, 4H, $O\underline{CH_2}CH_2$), 2.145(bs, 4H, $OCH_2\underline{CH_2}$).

$\underline{ZrCl_4.2i\text{-Pr-HNacac}}$

A similar method to that employed for the preparation of the THF adduct was used. In a 250 ml Schlenk flask $ZrCl_4$.(11.83 g, 50.8 mmol) was suspended in 150 ml of DCM at 0°C. To this was added a solution of *i*-Pr-HNacac (16 g, 115 mmol (10% excess)) in 20 ml of DCM. The solution initially went clear before a white solid precipitated. The slurry was stirred for 60 minutes at RT and the solids collected by filtration, washed twice with 20 ml of DCM and dried under vacuum. The product could be purified by continuous extraction with refluxing DCM. Crystals suitable for X-Ray structure analysis were obtained by slow cooling of a saturated DCM solution.

The synthesis can be performed in the presence of an excess ligand, 200%, or in the presence of Et_3N with no change in the final product.

$ZrCl_4.2i$-Pr-HNacac Yield 74.8%

MW 513.44

Appearance white crystalline solid

^{1}H-NMR ($CDCl_3$, 300 MHz):

δ 2.44(s, 3H, Me), 2.10(s, 3H, Me), 5.07(s, 1H, CH), 10.50(s, 1H, NH); N-*i*-Pr δ 3.90(d of sept, 1H $^3J_{H,H}$6.54Hz, $\underline{CH}(CH_3)_2$), 1.43(d, 6H $^3J_{H,H}$6.54Hz, $CH(\underline{CH_3})_2$).

Analysis calculated for $C_{16}H_{30}N_2O_2Cl_4Zr$: C, 37.28; H, 5.87; N, 5.43.

Found: C, 37.21; H, 5.90; N, 5.46.

$\underline{ZrCl_4.2Ph\text{-HNacac}}$

$ZrCl_4.2Ph$-HNacac Yield 76.2%

MW 583.49

Appearance pale yellow crystalline solid

^{1}H-NMR ($CDCl_3$, 300 MHz):

Me 2.537(s, 3H) & 2.136(s, 3H), CH 5.397(s, 1H), NH 12.1(s, 1H), Ph-H7.3-7.4(bm, 5H).

Analysis calculated for $C_{22}H_{26}N_2O_2Cl_4Zr$: C, 45.29; H, 4.49; N, 4.80.

Found: C, 44.98; H, 4.61; N, 4.79.

$ZrCl_4.2Ph_2$-Nacac

$ZrCl_4.2Ph_2$-Nacac Yield 60.6%

MW 735.69

Appearance yellow crystalline solid

^{1}H-NMR ($CDCl_3$, 300 MHz):

δ 2.983(s, 3H, Me), 2.464(s, 3H, Me), 5.335(s, 1H, CH); N-Ph δ 7.1-7.5(bm, 10H).

Analysis calculated for $C_{34}H_{34}N_2O_2Cl_4Zr$: C, 55.51; H, 4.66; N, 3.81.

Found: C, 55.42; H, 4.91; N, 3.84.

$ZrCl_4.2Et_2$-Nacac

$ZrCl_4.2Et_2$-Nacac Yield 82.3%

MW 735.69

Appearance yellow crystalline solid, recrystallised from DCM

^{1}H-NMR ($CDCl_3$, 300 MHz):

δ 2.983(s, 3H, Me), 2.539(s, 3H, Me), 5.309(s, 1H, CH); N-Et_2 δ 1.28(b d of t, 6H, -CH_2-$\underline{CH_3}$), 3.53(b d of q, 4H, -$\underline{CH_2}$-CH_3).

Analysis calculated for $C_{18}H_{34}N_2O_2Cl_4Zr$: C, 39.78; H, 6.31; N, 5.15.

Found: C, 39.55; H, 6.09; N, 5.04.

7.12.0. Bis-Ligand Complexes of Picolinates & Schiff's Bases

Bis-ligand complexes of picolinic acid and Schiff's bases were prepared but satisfactory microanalysis could not be obtained due to poor solubilities and hence inability to recrystallise or extract the complexes. Standard methods are available for their preparation[31].

(Picolinate)$_2$ZrCl$_2$

In a 100 ml Schlenk flask $ZrCl_4$.2THF (1.25 g, 3.31 mmol) was suspended in 20 ml of THF at -20°C. To this was added a solution of picolinic acid (0.82 g, 6.62 mmol) and Et_3N (0.67 g, 6.62 mmol) in 20 ml of THF. A voluminous white precipitate formed. The slurry was allowed to come to RT and stirred for 2 hours and filtered. The filtered solids were extracted twice with 20 ml DCM to remove Et_3NHCl (identified by ^{1}H-NMR). The remaining white solid, presumably (Picolinate)$_2$ZrCl$_2$, was insoluble in all solvents tried, DCM, chloroform, acetone and acetonitrile.

Under similar conditions to those outlined above $ZrCl_2$.2THF was reacted with sodium picolinate (formed by reaction of picolinic acid with sodium hydride) but a pure product could not be isolated.

(*i*-Pr-NPhO)$_2$ZrCl$_2$

To a 100 ml Schlenk flask containing $ZrCl_4$ (0.57 g, 2.45 mmol) suspended in 10 ml of toluene at -20°C was added a slurry of *i*-Pr-NPhONa (0.906 g, 4.89 mmol). The slurry was placed in an ice bath and allowed to stir overnight and slowly come to RT. The solution was a pale yellow. The solids were recovered by filtration and dried under vacuum. The solids were not soluble in the solvents (that did not react with the product) tested and the product could not therefore be separated from the NaCl produced. ^{1}H-NMR in $CDCl_3$ showed no significant peaks, indicating a very low solubility.

(Ph-NPhO)$_2$ZrCl$_2$

In a 100 ml Schlenk flask (0.48 g, 1.27 mmol) was suspended in 5 ml of THF at RT. To this was added a solution of Ph-NPhOH (0.50 g, 2.54 mmol) and Et_3N (0.29 g, 2.87 mmol) in 5 ml of THF. The solution went a dark orange and a precipitate formed. The solution was mixed for 2 hours, filtered, to remove the Et_3NHCl (identified by ^{1}H-NMR), and the solvent removed under vacuum. The product was recrystallised twice from THF/hexane. Satisfactory elemental analysis was not obtained and ^{1}H-NMR indicated a number of ligand environments.

Analysis calculated for $C_{26}H_{20}N_2O_2Cl_2Zr$: C, 56.31; H, 5.05; N, 3.63.
Found: C, 60.98; H, 5.34; N, 4.20.

7.13.0. Bis-Ligand Complexes, β-Diketones, β-Monothiodiketones

$Zr(acac)_2Cl_2$

Synthetic methods are well defined in the literature[31] and $(acac)_2ZrCl_2$ was prepared by a ligand redistribution reaction between $Zr(acac)_4$ and $ZrCl_4$.

To a suspension of $ZrCl_4$ (5.79 g, 24.8 mmol) in 40 ml DCM was slowly added a solution of $Zr(acac)_4$ (12.12 g, 24.8 mmol) in 20 ml of DCM. The solution was stirred for 2 hours at RT, filtered and the product precipitated by adding 30 ml of hexane. The product was collected by filtration washed twice with 20 ml of hexane and dried under vacuum. Yield 10.18 g.

$(acac)_2ZrCl_2$	Yield 57%
MW	360.34
Appearance	white crystalline solid

^{1}H-NMR ($CDCl_3$, 300 MHz):

δ 2.104(s, 6H, Me), 5.793(s, 1H, CH).

Analysis calculated for $C_{10}H_{14}O_4Cl_2Zr$: C, 33.33; H, 3.92.

Found: C, 33.16; H, 3.92.

$Zr(Sacac)_4$

To a suspension of $ZrCl_4$ (1.29 g, 5.54 mmol) in 20 ml DCM at RT was slowly added a solution of $Pb(Sacac)_2$ (4.84 g, 11.07 mmol) in 40 ml of DCM. The solution was stirred for half an hour at RT, filtered and the volume reduced until a solid started to precipitate. The precipitation was completed by adding 20 ml of hexane. The product was collected by filtration washed twice with 20 ml of hexane and dried under vacuum. Yield 2.15g.

$Zr(Sacac)_4$	Yield 70.3%
MW	551.70
Appearance	Yellow powder

^{1}H-NMR ($CDCl_3$, 300 MHz):

δ 2.243(s, 3H, COMe), 2.492(s, 3H, CSMe), 6.634(s, 1H, CH).

Lit.[32], 2.07(s, 3H), 2.39(s, 3H), 6.38(s, 1H).

$Zr(Sacac)_2Cl_2$

To a suspension of $ZrCl_4$ (0.25 g, 1.08 mmol) in 10 ml DCM at 0°C was slowly added a solution of $Pb(Sacac)_2$ (0.47 g, 1.08 mmol) in 10 ml of DCM. A precipitate formed immediately ($PbCl_2$). The solution was stirred for one hour at RT, filtered and the volume reduced until a solid started to precipitate. The remaining product precipitated on adding 20 ml of hexane. The product was collected by filtration washed twice with 10 ml of hexane and dried under vacuum. Yield 0.32g.

The same complex can also be made by a ligand redistribution reaction between $ZrCl_4$ and $Zr(Sacac)_4$ in DCM

$Zr(Sacac)_2Cl_2$ Yield 76.4%
MW 392.47
Appearance Yellow powder
^{1}H-NMR ($CDCl_3$, 300 MHz):
δ 2.280(s, 3H, COMe), 2.589(s, 3H, CSMe), 6.767(s, 1H, CH).

$Zr(Sacac)_2Cl_2.2THF$

The THF adduct of the bis-Sacac complex formed when THF was used as the solvent.

$Zr(Sacac)_2Cl_2.2THF$ Yield 68.5%
MW 536.68
Appearance Yellow powder
^{1}H-NMR ($CDCl_3$, 300 MHz):
δ 2.161(s, 3H, COMe), 2.360(s, 3H, CSMe), 6.317(s, 1H, CH); THF δ 3.749(m, 4H, $O\underline{CH_2}CH_2$), 1.853(m, 4H, $OCH_2\underline{CH_2}$).

7.14.0. Bis-Ligand Complexes, β-Aminoketones

This is the first time that bis-β-aminoketone complexes of zirconium have been synthesised. The method given below is general and works in most cases. Recently two new method have been developed. The first involves reacting $ZrCl_4$ with a sodium β-aminoketonate which is formed by reaction of the β-aminoketone with

NaH and used without isolation. The second involves reaction of *n*-BuLi with a zirconium tetrachloride bis-ligand adduct.

7.14.1. Method 1

$(i\text{-Pr-Nacac})_2ZrCl_2$

In a 100 ml Schlenk flask $ZrCl_4$ (1.26 g, 5.39 mmol) was suspended at -20°C in 20 ml of DCM. To this was slowly added a cold solution, -20°C, of *i*-Pr-KNacac (1.76 g, 10.8 mmol) in DCM. The solution, which went pale yellow with some suspended solids, was stirred for 1 hour and filtered keeping the solution below 0°C. Hexane, 30 ml, was added to the filtrate and the volume reduced under vacuum to ≈40 ml. The flask was placed in a freezer overnight yielding a crop of pale yellow crystals. Yield 1.56 g. (Can be recrystallised from THF with hexane)

$(i\text{-Pr-Nacac})_2ZrCl_2$ Yield 65.6%

MW 442.54

Appearance pale yellow crystalline solid

^{1}H-NMR ($CDCl_3$, 300 MHz):

δ 2.159(s, 3H, Me), 1.918(s, 3H, Me), 5.382(s, 1H, CH); N-*i*-Pr δ 4.539(sept, 1H $J_{H,H}$6.78Hz, $\underline{CH}(CH_3)_2$), 1.450(d, 6H $J_{H,H}$6.78Hz, $CH(\underline{CH_3})_2$).

^{1}H-NMR (CD_2Cl_2, 300 MHz, 0°C):

δ 2.154(s, 3H, Me), 1.909(s, 3H, Me), 5.398(s, 1H, CH); N-*i*-Pr δ 4.497(sept, 1H $J_{H,H}$6.82Hz, $\underline{CH}(CH_3)_2$), 1.392(d, 6H $J_{H,H}$6.82Hz, $CH(\underline{CH_3})_2$).

$^{13}C\{^1H\}$-NMR 75.5 MHz, CD_2Cl_2, 0°C:

δ 173.9 or 172.6(CO), 173.9 or 172.6(CN), 25.0 & 24.1(Me's), 109.0(CH); N-*i*-Pr δ 52.6($\underline{CH}(CH_3)_2$), 22.2($CH(\underline{CH_3})_2$).

Analysis calculated for $C_{16}H_{28}N_2O_2Cl_2Zr$: C, 43.43; H, 6.38; N, 6.33.

Found: C, 43.61; H, 6.44; N, 6.28.

$(\underline{Ph\text{-Nacac}})_2ZrCl_2$

The $(Ph\text{-Nacac})_2ZrCl_2$ complex precipitates from DCM on adding hexane. Recrystallised from THF with hexane at 0°C.

$(Ph\text{-Nacac})_2ZrCl_2$ Yield 65.6%

MW 510.57

Appearance pale yellow crystalline solid

^{1}H-NMR ($CDCl_3$, 200 MHz, 20°C):

δ 1.701(s, 3H, Me), 1.327(s, 3H, Me), 5.247(s, 1H CH); N-Ph δ 6.5-7.4(bm, 5H, *o*-, *m*- & *p*-Ph), see Synthesis Chapter for interpretation.

^{1}H-NMR (CD_2Cl_2, 200 MHz, -20°C):

δ 1.681(s, 3H, Me), 1.248(s, 3H, Me), 5.309(s, 1H CH); N-Ph δ 6.662(d, 1H $J_{H,H}$7.6Hz, *o*-Ph), 7.201(d, 1H $J_{H,H}$7.6Hz, *o*-Ph), 7.295(t, 1H $J_{H,H}$7.0Hz, *m*Ph), 7.373(d, 1H$J_{H,H}$7.0Hz, *m*-Ph), 7.189(t, 1H $J_{H,H}$6.33, *p*Ph overlapping with *o*-Ph), see Synthesis Chapter for interpretation.

^{13}C{^{1}H}-NMR (CD_2Cl_2, 75.5 MHz, -20°C):

δ 174.6 or 174.0(CO), 174.6 or 174.0(CN), 25.1 & 22.9(Me's), 107.1(CH); N-Ph δ 148.3(*i*-Ph), 126.1 & 123.3(*o*-Ph), 129.3 & 129.1(*m*-Ph),125.2 (*p*-Ph).

Analysis calculated for $C_{22}H_{24}N_2O_2Cl_2Zr$: C, 51.75; H, 4.74; N, 5.49.

Found: C, 51.56; H, 4.72; N, 5.30.

(MeOPh-Nacac)$_2$ZrCl$_2$

The (MeOPh-Nacac)$_2$ZrCl$_2$ complex precipitates from DCM on adding hexane. Recrystallised from THF/DCM with hexane at 0°C.

(MeOPh-Nacac)$_2$ZrCl$_2$ Yield 57.2%

MW 510.57

Appearance pale yellow crystalline solid

^{1}H-NMR (CD_2Cl_2, 200 MHz, -20°C):

δ 1.687(s, 3H, Me) & 1.359(s, 3H, Me), 5.305(s, 1H, CH); N-PhOMe δ 3.755(s, 3H, PhOMe), 6.566(d, 1H $J_{H,H}$8.5Hz, *o*-Ph) & 7.098(d, 1H $J_{H,H}$8.5Hz, *o*-Ph), 6.796(d, 1H $J_{H,H}$8.5Hz, *m*Ph) & 6.876(d, 1H $J_{H,H}$8.5Hz, *m*-Ph), see Synthesis Chapter for interpretation.

^{13}C{^{1}H}-NMR (CD_2Cl_2, 75.5 MHz, -20°C):

δ 174.7(CO), 74.7(CN), 25.0 & 23.2(Me's), 107.2(CH); N-PhOMe δ 55.8(PhOMe), 140.9(*i*-Ph), 126.4 & 124.5(*o*-Ph), 114.7& 113.5(*m*-Ph), 157.6(*p*-Ph).

^{1}H-NMR ($CDCl_3$, 200 MHz, 20°C):

δ 1.721(s, 3H, Me), 1.433(s, 3H, Me), 5.271(s, 1H, CH); N-PhOMe δ 3.811(s, 3H, PhOMe), 6.5-7.3(bm, 4H, PhOMe), see Synthesis Chapter for interpretation.

Analysis calculated for $C_{24}H_{28}N_2O_4Cl_2Zr$: C, 50.52; H, 4.95; N, 4.91.

Found: C, 50.56; H, 5.07; N, 4.87.

(ClPh-Nacac)$_2$ZrCl$_2$

The (Ph-Nacac)$_2$ZrCl$_2$ complex precipitates from DCM on adding hexane. Recrystallised from DCM with hexane at 0°C .

(ClPh-Nacac)$_2$ZrCl$_2$.CD$_2$Cl$_2$ Yield 56.14%

MW 664.39

Appearance pale yellow crystalline solid

^{1}H-NMR (CD$_2$Cl$_2$, 200 MHz, -20°C):

δ 1.690(s, 3H, Me), 1.327(s, 3H, Me), 5.341(s, 1H, CH); N-PhCl δ 6.566(dd, 1H $J_{H,H}$8.4Hz, *o*-Ph) & 7.260(dd, 1H $J_{H,H}$8.4Hz, *o*-Ph), 7.157(dd, 1H $J_{H,H}$8.4Hz, *m*Ph) & 7.348(dd, 1H $J_{H,H}$8.4Hz, *m*-Ph), see Synthesis Chapter for interpretation, δ 5.300(s, 2H, solvent).

^{13}C{^{1}H}-NMR (CD$_2$Cl$_2$, 75.5 MHz, -20°C):

δ 175.2 or 174.6(CO), 175.2 or 174.6(CN), 25.3 & 23.1(Me's), 107.2(CH); N-PhCl δ 147.0(*i*-Ph), 127.3 & 125.0(*o*-Ph), 129.4(*m*-Ph), 131.6(*p*-Ph).

Analysis calculated for $C_{23}H_{24}N_2O_2Cl_6Zr$: C, 41.58; H, 3.64; N, 4.22.

Found: C, 40.99; H, 3.68; N, 4.11.

(*i*-Pr-NacSac)$_2$ZrCl$_2$

The (*i*-Pr-Nacac)$_2$ZrCl$_2$ complex precipitates from DCM on adding hexane.

(*i*-Pr-NacSac)$_2$ZrCl$_2$ Yield: not calculated (impure)

MW 474.66

Appearance brown crystalline solid

^{1}H-NMR (CDCl$_3$, 300 MHz):

δ 2.517(s, 3H, Me), 2.117(s, 3H, Me), 6.066(s, 1H, CH); N-*i*-Pr δ 3.91(bm, 1H, C<u>H</u>(CH$_3$)$_2$), 1.36(d, 6H $J_{H,H}$6.48Hz, CH(C<u>H</u>$_3$)$_2$).

7.14.2. Method 2

(Ph-Nacac)$_2$ZrCl$_2$

To a 100 ml Schlenk flask containing NaH(1g 80% in mineral oil, 15% excess) suspended in 20 ml of THF at 0°C was slowly added a solution of Ph-HNacac(5.00 g, 28.5 mmol) in 20 ml of THF. A vigorous reaction occurs. The suspension was stirred at RT for 1 hour and then filtered through celite. The solution volume was

reduced by about 10 ml under vacuum to ensure all hydrogen was removed. This THF solution of Ph-NaNacac was slowly added to a suspension of $ZrCl_4$ (3.30 g, 14.16 mmol) in 30 ml of toluene at 0°C (the initial addition must be very slow). The $ZrCl_4$ dissolved during the addition and the solution went a cloudy pale yellow. The solution was stirred for 1hour at RT, filtered through celite to remove the NaCl and the volume reduced to about half. The product precipitated on adding 40 ml of hexane. The product was recrystallised from DCM with hexane. Yield 4.76 g, 65.5 %

7.14.3. Method 3

Synthesis of (i-Pr-Nacac)$_2$$ZrCl_2$

In a 250 ml Schlenk flask fitted with a dropping funnel $ZrCl_4$.2i-Pr-HNacac (1.21 g, 2.33 mmol) was suspended in THF at -70°C. To this was slowly added via the dropping funnel t-BuLi (6.98 ml, 0.671 M, 4.668 mmol) in pentane leaving a pale yellow solution with some suspended solids. The solution was stirred and allowed to warm to RT. The solution was filtered. The volume reduced to 30 ml and 40 ml of pentane added to precipitate a pale yellow solid. The solid was identified as (i-Pr-Nacac)$_2$$ZrCl_2$.

7.15.0. Alkyl-Zirconium Complexes

$CpZrCl_3$.DME

This monocylopentadienylzirconium species was synthesised by literature methods[33].

In a 100 ml Schlenk flask fitted with a dropping funnel $ZrCl_4$ (6.40 g, 27.5 mmol) was suspended in 60 ml of DCM at 0°C. Dimethylsulphide (3.41 g, 54.9 mmol) was slowly added to give a clear solution. This was followed by drop wise addition of Me_3SiCp[34] to leave a light red solution with precipitated solids. The solution was stirred at RT for 2 hours and DME (14 ml) added. The volume was reduced to ca. 15 ml and the solids collected by filtration and washed with 20 ml of cold DME. The off white solid was recrystallised from DCM with DME at 0°C. Yield 2.49 g.

$CpZrCl_3$.DME	Yield: 26.0%
MW	352.79

Appearance white crystalline solid

^{1}H-NMR ($CDCl_3$, 90 MHz):

δ 6.66(s, 5H, C_5H_5), 4.10(s, 4H, DME-CH_2), 3.88(s, 6H, DME-Me).

Lit.: δ 6.66(s, 5H), 4.10(s, 4H), 3.88(s, 6H).

$ZrBz_4$

Tetrabenzyl zirconium could be synthesised in good yield by standard literature methods[35] from $ZrCl_4$ and BzMgCl or by a modified reaction from $ZrCl_4$ and BzK[36].

In a 500 ml, double walled Schlenk vessel fitted with a strong magnetic stirrer a solution of BzMgCl (made from 8.00 g Mg, 0.33 g-atom assuming 95% reaction) in 250 ml of ether was cooled to -15°C. A slurry $ZrCl_4$ (15.0 g, 64.0 mmol) in 50 ml of ether was slowly added over 1 hour. The reaction vessel was covered to exclude light. The solution, which went deep orange and contained suspended solids, was stirred overnight at -15°C. The ether was removed under vacuum and the solids extracted four times with 50 ml of toluene. The volume of the combined toluene extracts was reduced to 50 ml and 40 ml of pentane added to precipitate an orange powder. The solution was cooled to -20°C and filtered. The impure product was recrystallised from toluene with pentane and washed twice with 10 ml of cold pentane to give a yellow powder. Yield 19.57 g. (It is possible to extract impure material with refluxing pentane to give a yellow powder.)

$ZrBz_4$ Yield: 67.0%

MW 455.75

Appearance yellow crystalline solid

^{1}H-NMR (CD_2Cl_2, 300 MHz):

δ 1.347(s, 1H, CH_2), 6.334(d, 2H $J_{H,H}$8.34Hz, *o*-Ph), 7.120(t, 1H, *p*-Ph), 7.209(t, 2H $J_{H,H}$7.61Hz, *m*-Ph).

^{1}H-NMR (C_6D_6, 300 MHz):

CH_2 1.741(s, 1H) *o*-Ph 6.580(d, 2H $J_{H,H}$8.08Hz), *p*-Ph 7.169(t, 1H $J_{H,H}$7.21Hz) & *m*-Ph .7.261(t, 2H $J_{H,H}$4.68Hz).

[Lit. $C_6D_6CD_3$: 1.44(s, 2H, CH_2),6.36(d, 2H, *o*-Ph), 7.0(m, 3H, m- & *p*-Ph)]

^{13}C{^{1}H}-NMR (C_6D_6, 75.5 MHz):

δ 73.03(CH_2), 125.14(*o*-Ph), 129.35(*p*-Ph), 131.59(*m*-Ph), 140.06(*i*-Ph).

A number of attempts were made to form alkylated (Ph-, Me- or Bz-) zirconium complexes with β-diketones following modified literature methods. It was reported that tetraphenyl zirconium[31] was formed in situ at -50°C and subsequently reacted with an active molecule. In this study acetylacetone was used. None of these attempts lead to isolation of required mono- or bis-alkylated species.

$(acac)_2ZrBz_2$

In a variation of Collier et al's synthesis[37], that is substituting $ZrBz_4$ for $Zr(CH_2Si(CH_3)_3)_4$, an attempt was made to prepare dibenzyl zirconium complexes containing acetylacetone ligands. For example,

In a 100 ml Schlenk flask held at -70°C $ZrBz_4$ (0.13 g, 0.285 mmol) was dissolved in 10 ml of toluene with exclusion of light. To this solution was slowly added Hacac (0.057 g, 0.570 mmol) in 10 ml of toluene. The colour remained golden yellow. The temperature was increased to -20°C, the solution was filtered and the solvent removed under vacuum leaving a brown yellow solid. Attempts to recrystallise the solids from 5 ml of toluene with pentane at -10°C were not successful with the solution slowly losing it's colour. ^{1}H-NMR spectrum showed only broad, indistinct bands.

Reactions in which $ZrBz_4$ was mixed with $Zr(acac)_4$ or $Zr(hfac)_4$ at low temperature led to similar results with solutions loosing their colour at ≈-20-30°C. Solids isolated at -40°C decomposed during storage. VT ^{1}H-NMR experiments discussed in Chapter 5 indicated that decomposition occurs at around these temperatures for these complexes. The major decomposition product appears to be benzyl-acac coupling product but the exact nature of this species was not identified, GC-MS data is given in Appendix 1.

7.16.0. VT-NMR Experiments

In situ Formation of Alkyl-Bis-β-Aminoketone Complexes of Zirconium

Formation of bis-β-aminoketone alkyl complexes of zirconium could be monitored by NMR in VT experiments. The following is the general procedure used for such tests.

Approximately 0.050 mmol (0.025 g) of $ZrBz_4$ was transferred to an NMR tube fitted with a screw cap and septum and dissolved in 0.25 ml of CD_2Cl_2. The NMR tube was cooled to -80°C and a solution containing the required amount of ligand, R-HNacac ≈0.050 mmol, in 0.25 ml of CD_2Cl_2 slowly added. The solution was mixed by gently injecting nitrogen to the base of the NMR tube. The final concentration for the complex was therefore approximately 0.1 M. The NMR was pre-cooled to -60°C and the NMR tube transferred quickly. The temperature was increased from -60°C to 40°C in 20°C steps and the NMR allowed to equilibrate for 20-30 minutes at each temperature before beginning the process of spectrum acquisition. Where reaction appeared to be complete at -60°C and the complex had not decomposed at 40°C a second spectrum was collected at -60°C to see if the original spectrum could be observed.

NMR Monitoring of the *in situ* Generation of Catalytic Species

It has been possible to monitor reactions between zirconium complexes or adducts and EASC in VT-1H-NMR studies leading to observation of ethylene insertion under mild conditions. The results of these VT-NMR experiments are presented in Chapter 5 where they are discussed in full. The general procedure followed for these experiments is detailed here. All operations were conducted under the strict exclusion of air or moisture by using standard Schlenk techniques.

Into an NMR tube fitted with a screw cap and septa was placed approximately 0.050 mmol of the required ligand, adduct or complex, e.g. Ph-HNacac, $ZrCl_4$.2Ph-HNacac and (Ph-Nacac)$_2ZrCl_2$. Toluene-d_8 (or benzene-d_6) was added to give a concentration of ≈0.20 M. To this, before the beginning of each VT-NMR experiment, was added the required amount of a 1.0 M EASC solution in toluene-d_8 to give a Zr:Al ratio of 1:10. The concentration of the complex or adduct for each test in the NMR tube was therefore ≈0.10 M or ≈0.20 M when only the ligand was tested.

Spectra of the solution were collected between 30 and 100°C. After which, for systems containing zirconium, ethylene was bubbled through the solution for 5 minutes at room temperature and further spectra obtained. In this way reactions between the cocatalyst and free β-aminoketones, complexes and adducts of zirconium could be monitored, including ethylene insertion after catalyst activation. Results are presented in chapter 5.

7.17.0. Synthesis of Alkyl-Bis-β-Aminoketone Complexes of Zirconium

The following complexes have been synthesised for the first time. The selection of target molecules was based on observations from VT ^{1}H-NMR experiments. Benzylzirconium complexes are in general light sensitive and all the following steps have been carried out with the exclusion of light. Complexes formed in this section have unusual and interesting ligand bonding modes which have been discussed in Chapter 5 of this thesis. Data presented here was obtained at RT (or where necessary, due to peak resolution, at the stated temperatures).

(i-Pr-Nacac)$_2$ZrBz$_2$

In a 100 ml Schlenk flask $ZrBz_4$ (2.27 g, 4.98 mmol) was dissolved in 10 ml of toluene and cooled to -60°C. To this a solution of i-Pr-HNacac (1.40 g, 9.96 mmol) in 5 ml of toluene was slowly added. The solution colour changed from yellow to burgundy. The temperature was increased to -20°C and the solvent volume reduced by half, 20 ml of hexane was added and the flask stored overnight in a freezer yielding a crop of burgundy crystals. Yield 2.11 g. The product can be recrystallised from toluene with hexane if required.

(i-Pr-Nacac)$_2$ZrBz$_2$ Yield: 76.6%

MW 553.90

Appearance burgundy crystalline solid

^{1}H-NMR (CD_2Cl_2, 300 MHz, 20°C):

Ligand: δ 2.005(s, 3H, Me), 1.906(s, 3H, Me), 5.212(s, 1H, CH); N-i-Pr δ 3.760(bm, 1H, C<u>H</u>(CH$_3$)$_2$), 1.088(bd, 6H $J_{H,H}$ 6.84Hz, CH(C<u>H</u>$_3$)$_2$).

Benzyl : δ 1.895(s, 2H, CH_2), 6.654(d, 2H $J_{H,H}$ 7.29Hz, o-Ph), 6.938(t, 2H $J_{H,H}$ 7.05Hz, m-Ph), 6.622(t, 1H $J_{H,H}$ 7.29Hz, p-Ph).

^{1}H-NMR (C_6D_6, 300 MHz, 25°C):

Ligand: δ 1.913(s, 3H, Me), 1.676(s, 3H, Me), 5.072(s, 1H, CH); N-i-Pr δ 3.90(bm, 1H, C<u>H</u>(CH$_3$)$_2$), 1.086(bd, 6H, CH(C<u>H</u>$_3$)$_2$).

Benzyl : δ 2.421(bs, 2H, CH_2), 7.05(bd, 2H, o-Ph), 7.203(t, 2H, m-Ph), 6.880(bt, 1H, p-Ph).

^{13}C{^{1}H}-NMR (CD_2Cl_2, 75.5 MHz, 20°C):

Ligand: δ 171.5 & 171.2(CO & CN), 25.3 &24.7(Me's), 106.3(CH), 51.2(C<u>H</u>(CH$_3$)$_2$), 22.6(s, CH(C<u>H</u>$_3$)$_2$).

Benzyl: δ 66.6(b, CH_2), 148.7(*i*-Ph), 128.0 & 127.7(o- & *m*-Ph), 120.2(*p*-Ph).

$^{13}C\{^1H\}$-NMR (C_6D_6, 75.5 MHz):

Ligand: δ 171.73 & 170.95(CO & CN), 25.27 &25.00(Me's), 106.90(CH), 51.75(CH$(CH_3)_2$), 23.09(CH(CH_3)$_2$).

Benzyl: δ 67.72(CH_2), 121.26(*p*Ph), 130.00 & 149.23(*i* & *m*- or *o*-Ph, one peak obscured by solvent).

Analysis calculated for $C_{30}H_{42}N_2O_2Zr$: C, 65.05; H, 7.64; N, 5.06.

Found: C, 63.67; H, 7.75; N, 5.36 (the complex is air and moisture sensitive leading to the poor analysis).

(*t*-Bu-Nacac)$_2$ZrBz$_2$

A very unstable complex could be obtained as an orange powder at -20°C but it decomposed on storage in a freezer. Spectra showing the in situ generation of this complex are in Appendix I.

(Cy-Nacac)$_2$ZrBz$_2$

(Cy-Nacac)$_2$ZrBz$_2$ Yield: 66.0%

MW 634.03

Appearance orange solid

^1H-NMR (CD_2Cl_2, 300 MHz), 20°C:

Ligand: δ 2.021(s, 3H, Me), 1.908(s, 3H, Me), 5.214(s, 1H, CH), 3.194(bs, 1H, Cy-CH), 1.06-1.78(m, 10H, Cy-CH2's).

Benzyl: δ 1.9221(s, 2H, CH_2), 6.641(d, 2H $J_{H,H}$ 7.26Hz, *o*-Ph), 6.900(t, 2H $J_{H,H}$ 7.71Hz, *m*-Ph), 6.708(t, 1H $J_{H,H}$ 7.35Hz, *p*-Ph).

$^{13}C\{^1H\}$-NMR (CD_2Cl_2, 75.5 MHz, 20°C):

Ligand: δ 171.6(C-O & C-N, coincident), 25.6 & 24.9(Me's), 106.8(CH), 61.5(Cy-CH), 32.4, 27.4 & 26.6(Cy-CH_2's).

Benzyl: δ 69.8(CH_2), 149.9(*i*-Ph), 128.1(*o*-Ph), 127.6(*m*-Ph), 120.2(*p*-Ph).

(*i*-Pr-Ntfac)$_2$ZrBz$_2$

(*i*-Pr-Ntfac)$_2$ZrBz$_2$ Yield: 39.7%

MW 661.84

Appearance orange crystalline solid

^1H-NMR (CD_2Cl_2, 300 MHz, 40°C all peaks broad):

Ligand: δ 174.2(CO), 171.7(CN), 25.1 & 24.6(Me's), 105.2(CH), 149.3(*i*-Ph), 125.4(*o*-Ph), 128.8(*m*-Ph), 125.0(*p*-Ph).
Benzyl: δ 65.8 ($J_{C,H}$ 124.0Hz, CH_2), 147.3(*i*-Ph), 128.5(*o*-Ph), 127.9(*m*-Ph), 120.8(*p*-Ph).

7.18.0. Cationic Complexes of Zirconium

Cationic complexes of zirconium have been synthesised by the partial protolysis of synthesised alkylated complexes with tertiary ammonium salt of tetraphenylborate[38]. The required tertiary ammonium salts are made by standard methods[39].

Dimethylanilinium Tetraphenylborate, $[PhNMe_2H][BPh_4]$

In a 1 L beaker $PhNMe_2$ (1.1 ml, 8.8 mmol, 10% excess) was dissolved in 200 ml of distilled water and the pH adjusted to 2 with dilute HCl. A solution of $NaBPh_4$ (2.5 g, 7.305 mmol) in 500 ml of distilled water was added and a voluminous white precipitate formed. The suspension was stirred for 1 hour and the solids collected by filtration and dried under vacuum for 24 hours. The product was stored with the exclusion of light. Yield 3.2 g.

$[PhNMe_2H][BPh_4]$ Yield: 99.0%
MW 441.42
Appearance white powder
^{1}H-NMR (CD_2Cl_2, 300 MHz):
$[PhNMe_2H]^+$: δ 2.608(s, 3H, Me), 5.941(bs, 1H, NH), 7.620(d, 2H, *o*-Ph), 7.339(bt, 2H, *m*-Ph), 7.608(t, 1H, *p*-Ph).
$[BPh_4]^-$: 7.460(bs, 8H, *o*-Ph), 7.047(t, 8H, *m*-Ph), 6.873(t, 4H, *p*-Ph).
Analysis calculated for $C_{32}H_{32}NB$: C, 87.02; H, 7.31; N, 3.17.
Found: C, 87.03; H, 7.50; N, 3.36.

Tri-*n*-butylammonium Tetraphenylborate, $[n\text{-}Bu_3NH][BPh_4]$

$[n\text{-}Bu_3NH][BPh_4]$ Yield: 99.0%
MW 505.59
Appearance white powder
^{1}H-NMR (CD_2Cl_2, 300 MHz):

$[n\text{-}Bu_3NH]^+$: δ 0.882(s, 9H, $NCH_2CH_2CH_2\underline{CH_3}$), 1.026(m, 6H, $NCH_2CH_2\underline{CH_2}CH_3$), 1.142(m, 6H, $NCH_2\underline{CH_2}CH_2CH_3$), 2.034(m, 6H, $N\underline{CH_2}CH_2CH_2CH_3$), 4.07(bs, 1H, NH).

$[BPh_4]^-$: δ 7.484(bs, 8H, *o*-Ph), 7.081(t, 8H, *m*-Ph), 6.947(t, 4H, *p*-Ph).

$[ZrBz_3][(\eta^6\text{-Ph-})BPh_3]$

In a 100 ml Schlenk flask $ZrBz_4$ (1.16 g, 2.54 mmol) was dissolved in 10 ml of toluene at RT. To this was added $[PhNMe_2H][BPh_4]$ (0.80 g, 1.82 mmol). An orange precipitate formed and the slurry was allowed to stir for 60 minutes. The product was collected by filtration and the excess $ZrBz_4$ and other soluble reaction products washed away with toluene (2x10 ml) and then with hexane (2x10 ml). The product was dried under vacuum.

$[ZrBz_3][(\eta^6\text{-Ph-})BPh_3]$ Yield: 99.0%

MW 683.85

Appearance orange powder

^{1}H-NMR (CD_2Cl_2, 300 MHz), -20°C:

$[ZrBz_3]^+$: δ1.54(s, 6H, CH_2), 6.28(m, 6H, *o*-Ph), 7.16(*m*-Ph, over-lapping with BPh3), 7.06(m, 3H, *p*-Ph).

$(\eta^6$-Ph-)B-: δ 8.21(d, 2H $^3J_{H,H}$6.8Hz, *o*-Ph), 6.58(t, 2H $^3J_{H,H}$7.3Hz, *m*-Ph), 6.19(t, 1H $^3J_{H,H}$6.8Hz, *p*-Ph).

-BPh_3: δ 7.16(overlapping with 6 Benzyl H's, 21H)

Lit., (CD_2Cl_2, -40°C):

$[ZrBz_3]^+$: δ 1.56(s, 6H, CH_2), 6.29(m, 6H, *o*-Ph), 7.22(*m*-Ph, over-lapping with BPh3), 7.10(m, 3H, *p*-Ph).

$(\eta^6$-Ph-)B-: δ 8.25(d, 2H $^3J_{H,H}$7.3Hz, *o*-Ph), 6.59(t, 2H $^3J_{H,H}$7.3Hz, *m*-Ph), 6.22(t, 1H $^3J_{H,H}$7.3Hz, *p*-Ph).

-BPh_3 : δ 7.22(overlapping with 6 Benzyl H's, 21H)

$^{13}C\{^1H\}$-NMR (CD_2Cl_2, 75.5 MHz, -20°C):

$[ZrBz_3]^+$: δ 74.4(CH_2), 136.9(*i*-Ph), 130.6(*o*-Ph), 130.2(*m*-Ph), 124.4(*p*-Ph).

$(\eta^6$-Ph-)B : δ 180(*i*-Ph), 127.4(*o*-Ph), 136.2?(*m*-Ph, overlapping with -o-BPh_3), 138.8(*p*-Ph)

-BPh_3 : δ 159(*i*-Ph), 136.2(*o*-Ph), 127.1(*m*-Ph), 126.9(*p*-Ph)

Lit., (CD_2Cl_2, -40°C):

$[ZrBz_3]^+$: δ 73.69(JC,H 134Hz, CH_2), 137.5(*i*-Ph), 130.1(*o*-Ph), 129.8(*m*-Ph), 123.89(*p*-Ph).

(η^6-Ph-)B : δ 178.5(*i*-Ph), 127.27(*o*-Ph), 136.3(*m*-Ph), 138.8(*p*-Ph).

-BPh_3 : δ 157.8(*i*-Ph), 135.8(*o*-Ph), 126.65(*m*-Ph), 126.39(*p*-Ph).

[(*i*-Pr-Nacac)$_2$ZrBz][BPh_4]

This complex was also prepared in this study by the reaction of the free ligand with [$ZrBz_3$][(η^6-Ph-)BPh_3] in DCM at -20°C.

The product separates as an oil on adding hexane and has not yet been obtained as an analytically pure material.

MW 782.00

Appearance orange powder

^{1}H-NMR (CD_2Cl_2, 300 MHz, -20°C):

Ligand : δ 2.146(s, 6H, Me), 2.102(s, 6H, Me), 5.623(s, 2H, CH), 3.962(bsept, 2H $J_{H,H}$6.4Hz, N-C<u>H</u>(CH_3)$_2$), 1.347(bd, 6H $J_{H,H}$6.4Hz, N-CH(C<u>H</u>$_3$)$_2$), 1.118(bd, 6H $J_{H,H}$6.4Hz, N-CH(C<u>H</u>$_3$)$_2$).

[ZrBz] : δ 2.102(s, 2H overlapping with ligand Me, CH_2), (*o*, *m*- *p*-Ph, overlapping with BPh_4, 5H).

[BPh_4]: δ 6.974(bs, 8H, *o*-Ph), 6.734(t, 8H, *m*-Ph), 6.558(t, 4H, *p*-Ph).

^{13}C{^{1}H}-NMR (CD_2Cl_2, 75.5 MHz, -20°C):

Ligand: δ 176.1 & 173.0(CO & CN), 24.8 & 23.8(Me's), 109.1(CH), 53.3(bs, N<u>C</u>H(CH_3)$_2$), 22.4(s, NCH(C<u>H</u>$_3$)$_2$) & 21.4(s, NCH(C<u>H</u>$_3$)$_2$).

[ZrBz] : δ 75.2 (b, CH_2), 134.2(*i*-Ph), 131.2 & 130.5(*o*- & *m*-Ph), 126.8(*p*-Ph).

[BPh_4]: δ 164.3(*i*-Ph), 126.2(*o*-Ph), 136.2(*m*-Ph), 122.3(*p*-Ph).

Attempted preparation of [(Ph-Nacac)$_2$ZrBz][BPh_4]

Reaction of (Ph-Nacac)$_2$$ZrBz_2$ with [$PhNMe_2H$][BPh_4] in toluene or [$ZrBz_3$][(η^6-Ph-)BPh_3] with Ph-HNacac in DCM at -20°C resulted in the same redistribution products, a mixture of [$ZrBz_3$][(η^6-Ph-)BPh_3] and [(Ph-Nacac)$_3$Zr][BPh_4]. Spectral data for the [(Ph-Nacac)$_3$Zr][BPh_4] complex is reported here.

MW 850.03

Ligand: δ 2.173(s, 3H, Me), 5.754(s, 1H, CH), 4.1(bm, 1H, N-CH$(CH_3)_2$), 1.249(bs, 6H, N-CH$(CH_3)_2$).

Benzyl: δ 1.948(s, 2H, CH_2), 6.636(s, 2H, *o*-Ph), 7.005(t, 2H, *m*-Ph), 6.766(t, 1H, *p*-Ph).

^{1}H-NMR (CD_2Cl_2, 300 MHz, -20°C):

Ligand: δ 2.156(s, Me) & 2.120(bs, Me), 5.737 & 5.632(s, CH), 4.24(b, N-CH$(CH_3)_2$) & 3.717(bm, N-CH$(CH_3)_2$), 1.291(d, $J_{H,H}$6.8Hz, N-CH(CH$_3)_2$) & 1.113(dd, $J_{H,H}$ 7.0Hz, N-CH(CH$_3)_2$).

Benzyl: δ 1.990(d, $J_{H,H}$9.69, CH_2) & 1.841(d, $J_{H,H}$9.69, CH_2) & 1.647(bs, CH_2) & 1.543(bs, CH_2), 6.478(d, J 7.59Hz, *o*-Ph) & 6.652(d $J_{H,H}$7.59Hz, *o*-Ph), 7.036(t, $J_{H,H}$7.57Hz, *m*-Ph) & 6.952(t, $J_{H,H}$7.57Hz, *m*-Ph), 6.850(t, $J_{H,H}$7.20Hz, *p*-Ph) & 6.689(t, $J_{H,H}$7.20Hz, *p*-Ph).

^{13}C{^{1}H}-NMR (CD_2Cl_2, 75.5 MHz, 40°C all peaks broad):

Ligand: δ 26.6(Me), (C-O & C-N not found), 105.7(CH), 53.0(N-CH$(CH_3)_2$), 22.7(N-CH(CH$_3)_2$).

Benzyl: δ 67.3(b, CH_2), (*i*-Ph, weak not found), 129.0(*o*-Ph &*m*-Ph), 122.6(*p*-Ph).

^{13}C{^{1}H}-NMR (CD_2Cl_2, 75.5 MHz, -20°C):

Ligand: δ 153.5 & 152(bm, CO), 172.4 & 171?(b, C-N), 26.5 & 26.3(Me's), 120.6 & 120.2 (q, $J_{C,F}$283Hz, CF_3), 105.8 & 104.7(CH), 52.8 & 52.2(N-CH$(CH_3)_2$), 22.3 & 21.7(N-CH(CH$_3)_2$).

Benzyl: δ 65.9 & 65.2(s, $J_{C,H}$128Hz, CH_2), 145.3 & 144.0(*i*-Ph), 129.7 & 128.9(*o*-Ph), 128.5 & ?(*m*-Ph), 122.4 & 122.0(*p*-Ph).

(Ph-Nacac)$_2$ZrBz$_2$

(Ph-Nacac)$_2$ZrBz$_2$ Yield: 95.4

MW 621.93

Appearance orange solid

^{1}H-NMR (CD_2Cl_2, 300 MHz, 20°C):

Ligand: δ 1.637(s, 3H, Me) & 1.628(s, 3H, Me), 5.119(s, 1H, CH), 6.687(d, 2H $J_{H,H}$ 7.20Hz, *o*-Ph), 7.02(t, 2H $J_{H,H}$ 7.65Hz, *m*-Ph), 7.107(t, 1H $J_{H,H}$ 7.4Hz, *p*-Ph).

Benzyl: δ 2.365(s, 2H, CH_2), 6.523(d, 2H $J_{H,H}$ 7.43Hz, *o*-Ph), 7.203(t, 2H $J_{H,H}$ 7.41Hz, *m*-Ph), 6.755(t, 1H $J_{H,H}$ 7.40Hz, *p*-Ph).

^{13}C{^{1}H}-NMR (CD_2Cl_2, 75.5 MHz, 20°C):

Appearance orange powder (mix of $[(Ph\text{-}Nacac)_3Zr][BPh_4]$ & $[ZrBz_3][(\eta^6\text{-}Ph\text{-})BPh_3]$)

^{1}H-NMR (CD_2Cl_2, 300 MHz), -20°C:

Ligand: δ 1.706(s, 9H, Me), 1.627(s, 9H, Me), 5.447(s, 3H, CH), 6.510(d, 6H, *o*-Ph), 7.038(t, 6H, *m*-Ph), 7.19(m, 3H, *p*-Ph).

$[BPh_4]^-$: δ 7.322(bs, 8H, *o*-Ph), 7.038(t, 8H $J_{H,H}$7.2Hz, *m*-Ph), 6.888(t, 4H $J_{H,H}$7.2Hz, *p*-Ph).

$^{13}C\{^1H\}$-NMR (CD_2Cl_2, 75.5 MHz, -20°C):

Ligand: δ 177.9(CO), 176.0(CN), 24.6 & 24.1(Me's), 106.6(CH), 144.7(*i*-Ph), 125.2(*o*-Ph), 130.2(*m*-Ph), 127.7(*p*-Ph).

$[BPh_4]^-$: δ 164.3(q, $J_{C,B}$49.3Hz, *i*-Ph), 126.2(*o*-Ph), 136.2(*m*-Ph), 122.3(*p*-Ph).

Attempted preparation of $[(i\text{-}Pr\text{-}Ntfac)_2ZrBz][BPh_4]$

Spectral data for the $[(i\text{-}Pr\text{-}Nacac)_3Zr][BPh_4]$ complex is reported here.

MW

Appearance orange powder (mix of $[(i\text{-}Pr\text{-}Ntfac)_3Zr][BPh_4]$ & $[ZrBz_3][(\eta^6\text{-}Ph\text{-})BPh_3]$)

^{1}H-NMR (CD_2Cl_2, 300 MHz, -20°C):

Ligand: δ multiple broad peaks 1.0-1.35(m, 18H, $NCH(\underline{CH_3})_2$), 2.1-2.4(m, 9H, Me), 3.5-3.7(bm, 3H, $N\underline{CH}(CH_3)_2$), 5.95-6.1(m, 3H, CH), other peaks overlapping with BPh resonances.

$[BPh_4]^-$: δ 7.322(bs, 8H, *o*-Ph), 7.038(t, 8H $J_{H,H}$7.2Hz, *m*-Ph), 6.888(t, 4H $J_{H,H}$7.2Hz, *p*-Ph).

$^{13}C\{^1H\}$-NMR (CD_2Cl_2, 75.5 MHz, -20°C):

Ligand: δ ligand resonances generally broad and indistinct 21.6(bm, $NCH(\underline{CH_3})_2$), 23.4(b, Me), 52.7($N\underline{CH}(CH_3)_2$), 97.8(CH), not identified CF_3, CO & CN.

$[BPh_4]^-$: δ 164.3(q, $J_{C,B}$49.3Hz, *i*-Ph), 126.2(*o*-Ph), 136.2(*m*-Ph), 122.3(*p*-Ph).

7.19.0. Reduced Zirconium Species

Reduced zirconium species were synthesised and used in situ and no analytical data is presented. The species, $Zr(bipy)_3$, $[ZrCl_3(PBu_3)_2]_2$, and $[ZrCl_3(dppe)]_2$, were generated following literature methods[40] by Na/amalgam reduction of $ZrCl_4$ in the presence of the appropriate ligand.

7.20.0. Catalysis

Catalytic test work was carried out following the method described by Shiraki[41], and all reactions and transfers were completed using inert gas techniques.

In situ catalytic testing of Free Ligands

In a 100 ml Schlenk flask $ZrCl_4$ (0.1227 g, 0.5265 mmol) was suspended in 20 ml of toluene and stirred for 20 minutes. EASC (0.652 g, 2.632 mmol) was added and the suspension stirred at 60°C for 20 minutes. The suspension was cooled to 25°C and *i*-Pr-HNacac (0.1487 g, 1.053 mmol) was added. A clear, pale yellow solution formed which was stirred for 20 minutes. An aliquot of the above solution (0.76 ml, 0.02 mmoles of zirconium) was transferred to an autoclave containing 19 ml of toluene at 50°C. The autoclave was transferred to a silicon oil bath preheated to 100°C and pressurised with ethylene to 35 bar. The pressure was manually held at 30-35 bar for 1 hour. After 1 hour the autoclave was placed into an ice bath for 5 minutes, slowly depressurised and 1 ml of 1 M NaOH solution and 0.50 ml of nonane (internal standard for GC analysis) added. The deactivated catalyst solution was filtered through a pre-weighed No 4 filter paper, the solids rinsed twice with 2 ml of toluene, and the filtrates dried over Na_2SO_4 The filter paper was air dried and then weighed to give a waxes recovery.

The dried filtrates were analysed by GC methods and the oligomer distribution calculated relative to the area of the standard nonane peak. A sensitivity of 1:1 was used between nonane and the produced linear α-olefins. The peaks were separated, where possible, between olefins and alkylated toluene as determined by GC-MS analysis. The weight of oligomer produced in the C_{10}-C_{30} range was analysed, a Schultz-Flory plot drawn, a line of best fit calculated by linear regression analysis and a theoretical product distribution calculated up to C_{40} (an arbitrary cut off point). A weight distribution of oligomers recovered, including the weight of recovered waxes, was calculated.

Typical GC-MS data for the produced oligomers, alkylated toluene and other products are shown in Appendix I.

Where thiophene was used a clear solution did not form. An aliquot of the slurry was transferred to the autoclave.

Catalytic Testing of Bis-ligand Adducts or Complexes

In a 100 ml Schlenk flask approximately 0.5 mmoles of $ZrCl_4.2i$-Pr-HNacac was suspended in 20 ml of toluene and stirred for 10 minutes. EASC was added to give an aluminium:zirconium ratio of 10 :1 and the solution stirred at 60°C for 20 minutes. A clear, pale yellow solution formed. The suspension was cooled to 25°C and an appropriate aliquot was taken to give 0.020 mmoles of zirconium in the autoclave. Catalysis and product workup is as described above for the *in situ* catalytic testing of free ligands..

When bis-β-aminoketone complexes were used the solution was kept at 20°C after adding EASC to avoid catalyst decomposition.

Catalytic Testing of Cationic Zirconium Complexes

In a 100 ml Schlenk flask approximately 0.5 mmoles of $[(i\text{-Pr-Nacac})_2ZrBz][BPh_4]$ was suspended in 20 ml of toluene at 0°C and stirred for 10 minutes. An appropriate aliquot of the suspension was taken to give 0.020 mmoles of zirconium in the autoclave. Catalysis was conducted at 60°C. Otherwise catalysis and product workup is as described above for the *in situ* catalytic testing of free ligands..

The autoclave used in most tests has an internal volume of 75 ml and is made from stainless steel, material 1.4571, working pressure and temperature 100 Bar and 300°C. A glass liner for the autoclave was used in all reactions and the contents were mixed using a magnetic stirrer. When larger autoclaves were used a larger aliquot was taken, i.e. 0.04 mmoles of zirconium in a 350 ml autoclave containing 60 ml of solvent..

1 Perrin, D.D.; Armarego, W.L.F.; Perrin, D.R., *Purification of Laboratory Chemicals 2nd. Ed.*, Pergamon Press, Sydney **1980**.

2 Burfield, D.R.; Smithers, R.H., *J. Org. Chem.* 43, **1978**,3966-3968.

3 Lusch, M.J.; Phillips, W.V.; Sieloff, R.F.; Nomura, G.S.; House, H.O., *Org. Synth.* 62, **1984**, 101.

4 Gilman, H.; Zöllner, E.A.; Selby, W.M., *J. Am. Chem. Soc.* 55, **1933**, 1252.

5 a. Lipton, M.F.; Sorensen, C.M.; Sadler, A.C., *J. Organometallic Chem.* 186, **1980**, 155-158.
b. Friedman, L.; Litle, R.L.; Reichle, W.R., *Organic Synthesis* 40, **1960**, 93-95.
c. Winkle, M.R.; Lansinger, J.M.; Ronald, R.C., *J. Chem. Soc., Chem. Comm.* **1980**, 87-88.

6 Bernardon, C.; Derberly, A., *J. Chem. Soc., Perkin I* **1980**, 2631-2636.

7 a. Kamienski, C.W.; Esmay, D.L., *J. Org. Chem.* 25, **1960**, 1807-1808.
b. Novis Smith, W., *J. Organometallic Chem.* 82, **1984**, 1-6.

8 Amonoo-Neizer, E.H.; Shaw, R.A.; Skoulin, D.O.; Smith, B.C., *Inorganic Synthesis VIII*, **1966**, 20-21.

9 King, R.B.; Stone, F.G.A., *Inorganic Synthesis* VII, **1963**, 99-115.

10 a. Trepka, W.J.; Sonnenfeld, R.J., *J. Organometallic Chem.* 16, **1969**, 317-320.
b. Schlosser, M.; Ladenberger, V., *J. Organometallic Chem.* 8, **1967**, 193-197.

11 Evans, J.C.W.; Allen, C.F.H., *Organic Synthesis* II, **1966**, 517-518.

12 Rieke, R.D.; Hidnall, P.M., *J. Am. Chem. Soc.* 94, **1972**, 7178-7179.

13 a. Schlosser, M., Hartmann, J., *Angew. Chem.* 85(12), **1973**, 544-545

b. Schlosser, M., *J. Organometallic Chem.* 8, **1967**, 9-16.
c. Schlosser, M.; Strunk, S., *Tetrahedron Letters* 25, **1984**, 741-744.
d. Lehmann, R.; Schlosser, M., *Tetrahedron Letters* 25, **1984**, 745-748.
e. Lochmann, L.; Lim, D., *J. Organometallic Chem.* 28, **1971**, 153-158.

14 a. Duus, F.; Anthonsen, J.W., *Acta Chem. Scand. B* 31, **1977**, 40-46.
b. Duus, F., *J. Org. Chem.* 42, **1977**, 3123-3127.

15 Chaston, S.H.H.; Livingstone, S.E.; Lockyer, T.N.; Pickles, V.A.; Shannon, J.S., *Aust. J. Chem.* 18, **1965**, 673-679.

16 Duus, F., *Synthesis Communications* **1985**, 672-674.

17 a. Uhlemann, E.; Müller, H., *Angew. Chem.* 77, **1965**, 172.
b. Carlsen, L.; Duus, F., *Synthesis* **1977**, 256-258.

18 Ligands prepared in this research group by G. Tindall.

19 a. Mayer, R.; Scheithauer, S., *Methoden der organischeChenie* vierte Auflage;Band E5, Falbe, J. (Ed.); Houben-Weyl, Stuttgart **1985**, 785-799.
b. Henecka, H.; Kurtz, P., *Methoden der organische Chemie* vierte Auflage; Sauerstoffverbindungen III, Falbe, J. (Ed.), Eugen Müller, Tübingen **1952**, 697-699.

20 Buckingham, J., Ed., *Dictionary of Organic Compounds, 5th Ed.* **1982**, Chapman & Hall.

21 Lockyer, T.N.; Martin, R.M., *Prog. Inorg. Chem.* 27, **1980**, 223-324.

22 Everett, G.W. Jr.; Holm, R.H., *J. Am. Chem. Soc.* 87, **1965**, 2117-2127.

23 Martin, D.F.; Janusonis, G.A.; Martin, B.B., *J. Am. Chem. Soc.* 83, **1961**, 73-75.

24 Shin, H.K.; Hampden-Smith, M.J.; Kodas, T.T.; Rheingold, A.L., *J. Chem. Soc., Chem. Comm.* **1992**, 217-219.

25 Rechsteiner, B.; Texier-Boullet,F.; Hamelin, J., *Tetrahedron Letters* 34, **1993**, 5071-5074.

26 Shin, H.K.; Hampden-Smith, M.J.; Kodas, T.T.; Rheingold, A.L., *J. Chem. Soc., Chem. Comm.* **1992**, 217-219.

27 a. Scheeren, J.W.; Ooms, P.H.J.; Nivard,R.J.F., *Synthesis Comm.* **1973**, 149-151.
b. Trebaul, C., *Bull. Soc. Chim. France* 3, **1971**, 1102-1103.
c. Pedersen, B.S.; Scheibye, S.; Nilsson, N.H.; Lawesson, S.-O., *Bull. Soc. Chim. Belg.* 87, **1978**, 223-228.
d. Scheibye, S.; Pedersen, B.S.; Lawesson, S.-O., *Bull. Soc. Chim. Belg.* 87, **1978**, 229-238.
e. Pedersen, B.S.; Scheibye, S.; Clausen. K., Lawesson, S.-O., *Bull. Soc. Chim. Belg.* 87, **1978**, 293-297.
f. Scheibye, S.; Pedersen, B.S.; Lawesson, S.-O., *Bull. Soc. Chim.. Belg.* 87, **1978**, 299-306.
g. Klingsberg, E., *J. Am. Chem. Soc.* 83, **1961**, 2934-2937.
h. Leaver, D.; McKinnon, D.M.; Robertson, W.A.H., *J. Chem. Soc.* **1962**, 5104.
i. Leaver, D.; McKinnon, D.M.; Robertson, W.A.H., *J. Chem. Soc.* **1965**, 32-40.

28 Walter, W.; Proll, T., *Synthesis Comm.* **1979**, 941.

29 Blum, P.R.; Wei, R.M.C.; Cummings, S.C., *Inorg. Chem.* 13(2), **1974**, 450.

30 Manzer, L.E., *Inorg. Synth.* 21, **1982**, 135.

31 Wilkinson, G., *Comprehensive Coordination Chemistry*, Vol.3, Main Group and Early Transition Metals, Pergamon Press **1987**, (32) 363-451.

32 Silver, M.E.; Chun, H.K.; Fay, R.C., *Inorg. Chem.* 21, **1982**, 3765-3771.

33 Lund, E.C.; Livinghouse, T., *Organometallics* 9, **1990**, 2426-2427.

34 a. Cardoso, A.M.; Clark, R.J.H.; Moorhouse, S., *J. Chem. Soc., Dalton* **1980**, 1156-1160.
b. Fritz, H.P.; Kreitler, C.G., *J. Organometallic Chem.* 4, **1965**, 313-319.

35 a. Zucchini, U.; Albizzati, E.; Giannini, U., *J. Organometallic Chem.* 26, **1970**, 1491.
b. Thiele, K.-H.; Köhler, E.; Adler, B., *J. Organometallic Chem.* 50, **1973**, 153-159.

36 Alelyunas, Y.W.; Jordan, R.F.; Echols, S.F.; Borkowsky, S.L.; Bradley, P.K., *Organometallics* 10, **1991**, 1406-1416.

37 Collier, M.R.; Lappert, M.F.; Pearce, R., *J. Chem. Soc., Dalton* **1973**, 445-451.

38 Bochman, M.; Jagger, A.J.; Nicholls, J.C., *Angew. Chem., Int. Ed. Engl.* 29(7),**1990**, 780-782.

39 Crane, F.E. Jr., *Analytical Chem.* 28, **1965**, 1794-1797.

40 $Zr(bipy)_3$
Quirk, J.; Wilkinson, G., *Polyhedron* 1, **1982**, 209-211.
$[ZrCl_3(PBu_3)_2]_2$
a. Wengrovis, J.H.; Schrock, R.R.; Day, C.S., *Inorg. Chem.* 20, **1981**, 1844-1849.
b. Wengrovis, J.H.; Schrock, R.R., *J. Organometallic Chem.* 205, **1981**, 319-327.
$[ZrCl_3(dppe)]_2$
c. Cotton, F.A.; Diebold, M.P.; Kibala, P.A., *Inorg. Chem.* 27, **1988**, 799-804.
d. Cotton, F.A.; Kibala, P.A., *Inorg. Chem.* 29, **1990**, 3192-3196.
e. Fowles, G.W.A.; Willey, G.R., *J. Chem. Soc. A* **1968**, 1435-1438.

41 Shiraki, Y.; Kawano, S.; Takouchi, K., Eur. Pat. Appl. Ep 0 241 596(Cl. C 07 C2/30), 31.10.1990.

Appendix I

CONTENTS

PRODUCT CHARACTERISATION

A.1.0. Oligomer Characterisation

Test 10.1; (*i*-Pr-Nacac)$_2$ZrCl$_2$ + EASC + 35 bar, Ethylene in Toluene at 100°C

A.1.1. GC Trace

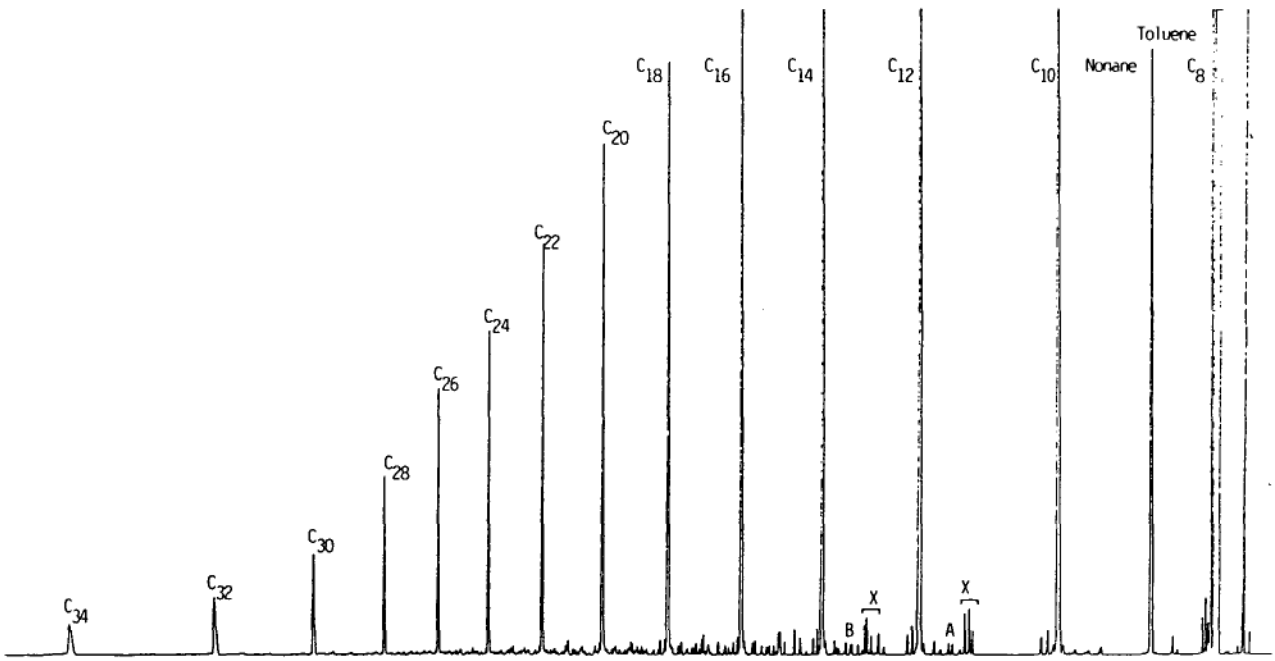

A.1.2. GC-MS Data (linear α-olefins, C_{10-14}, and isomers, A&B)

C_{10} 140(M^+ 10), 97(20), 84(20), 83(22), 70(62), 69(45), 57(58), 56(84), 55(78), 43(84), 42(38), 41(100), 39(42), 29(72), 27(52)

C_{12} 168(M^+ 8), 140(5), 126(5), 111(10), 97(24), 84(26), 83(38), 70(50), 69(50), 57(50), 56(70), 55(86), 43(98), 42(36), 41(100), 39(40), 29(68), 27(44)

A 168(M^+ 4), 126(24), 85(42), 71(66), 57(66), 55(22), 43(100), 41(58), 39(20), 29(40)

C_{14} 196(M^+ 8), 168(5), 154(4), 139(4), 111(18), 97(42), 84(30), 83(52), 71(26), 70(56), 69(58), 57(60), 56(60), 55(96), 43(100), 42(30), 41(100), 39(36), 29(76), 27(40)

B 167(M^+? 2), 125(10), 112(18), 98(20), 97(40), 83(40), 71(22), 70(42), 69(64), 57(100), 56(22), 55(100), 43(58), 41(96), 29(70), 27(20)

A.1.3. ^{1}H-NMR Spectrum, BP>120°C

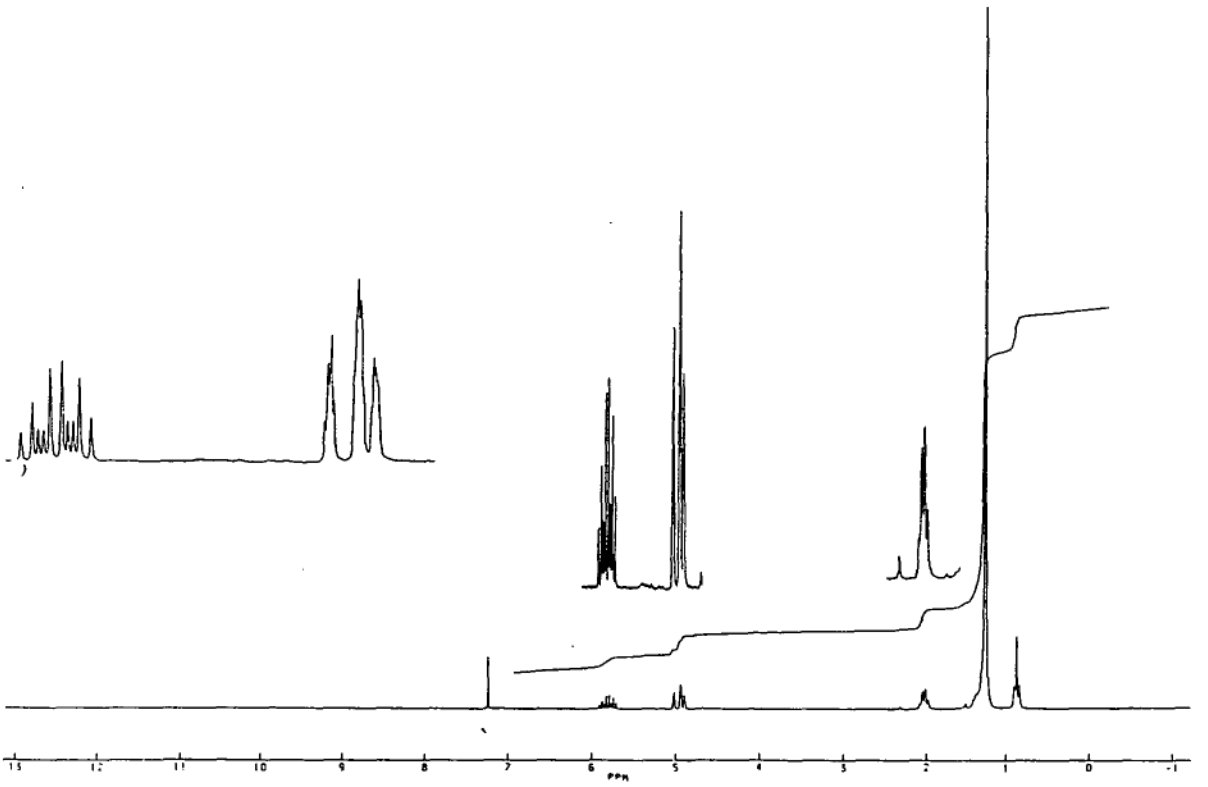

A.2.0. Side Reactions: Alkylated Toluenes

Test 13.8. $ZrCl_4$ + *i*-Pr-HNacac + EASC +35 bar Ethylene in Toluene at 100°C

A.2.1 GC Trace

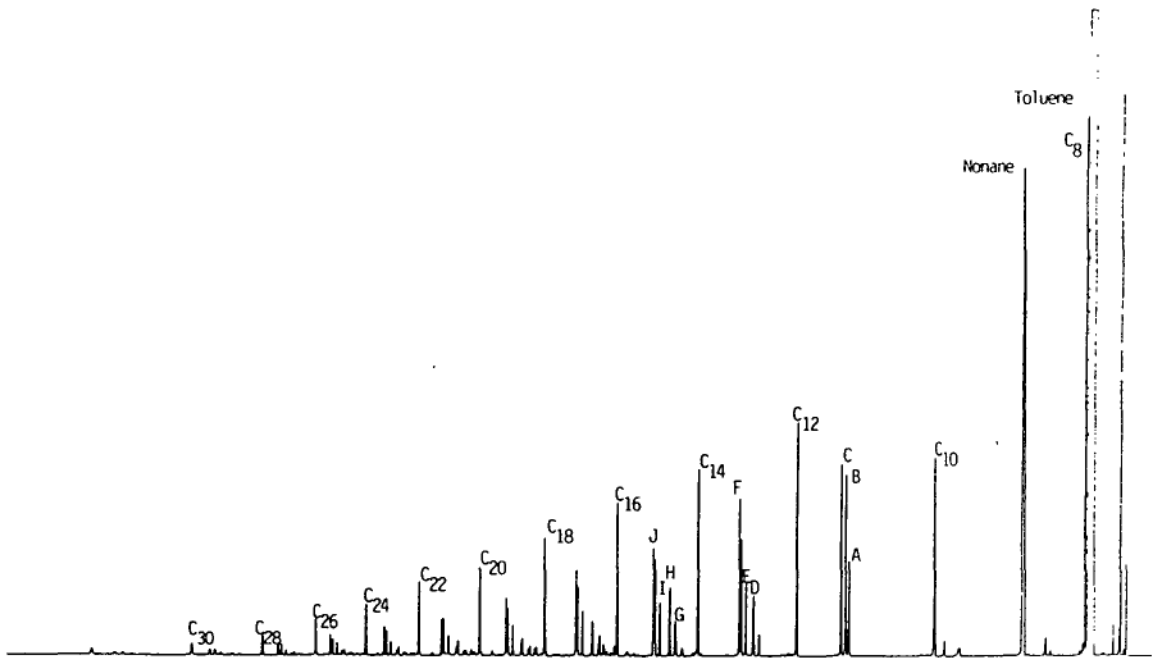

A.2.2. GC-MS Data m/e(I%)

Products A-C: Toluene + 2 Ethylene

A 148(M^+ 15), 119(100), 91(20)

B 148(M^+ 20), 119(100), 91(20)

C 148(M^+ 25), 119(100), 91(20)

Products D-F: Toluene + 3 Ethylenes (or Oligomers)

D 176(M^+ 10), 147(14), 133(22), 105(100)

E 176(M^+ 15), 120(15), 119(100), 105(18)

F 176(M+ 16), 120(8), 119(100), 105(8), 91(9)

Products G-J: Toluene + 4 Ethylenes (or Oligomers)

G 204(M+ 10), 175(50), 161(10), 147(12), 119(12), 105(100)

H 204(M+ 7), 175(5), 161(4), 147(4), 133(15), 105(100)

I 204(M+ 1), 175(5), 133(20), 105(100), 41(24), 29(18)

J 204(M+ 5), 120(18), 119(100), 105(18), 41(18)

A.3.0. Butadiene Oligomerisation / Toluene Alkylation

Test DJ300693D $ZrCl_4$ + 2Hacac + EASC +10ml Butadiene in Toluene at 100°C

A.3.1 GC Trace

(collected after nonane elution)

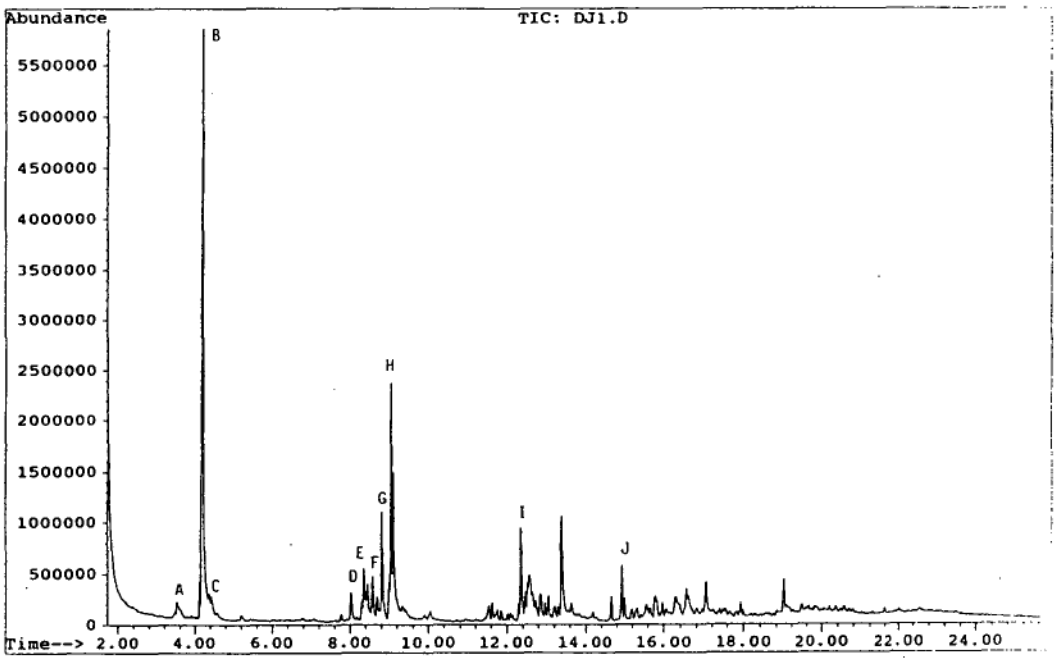

A.3.2. GC-MS Data m/e(I%)

Products A-C: Toluene + Butadiene

A 146(M^+ 25), 131(100), 115(20), 91(40)

B 146(M^+ 60), 131(100), 115(15), 91(30)

C 146(M^+ 60), 131(100), 115(20), 91(40)

Products D-H: Toluene + 2 Butadiene

D 200(M^+ 75), 185(30), 145(100), 129(30), 55(75)

E 200(M^+ 10), 145(100), 130(30), 117(30), 105(70), 91(30)

F 200(M^+ 10), 185(40), 172(20), 157(20), 143(100), 128(30)

G 200(M^+ 100), 145(100), 143(30), 129(30), 115(20), 55(30)

H 200(M^+ 20), 145(100), 130(40), 117(40), 105(60)

Products I-F: Toluene + 3 or more Butadiene

I 254(M^+ 5), 145(100), 105(60), 55(40)

J 308(M^+ 40), 293(20), 279(25), 266(30), 253(100), 237(25), 223(30), 211(60), 197(60), 195(50), 169(55), 55(60)

A.3.3. ^{1}H NMR fraction Boiling 100°C, 14mmHg (peak B)

1-(*o*- & *p*-methylphenyl)-2-butene

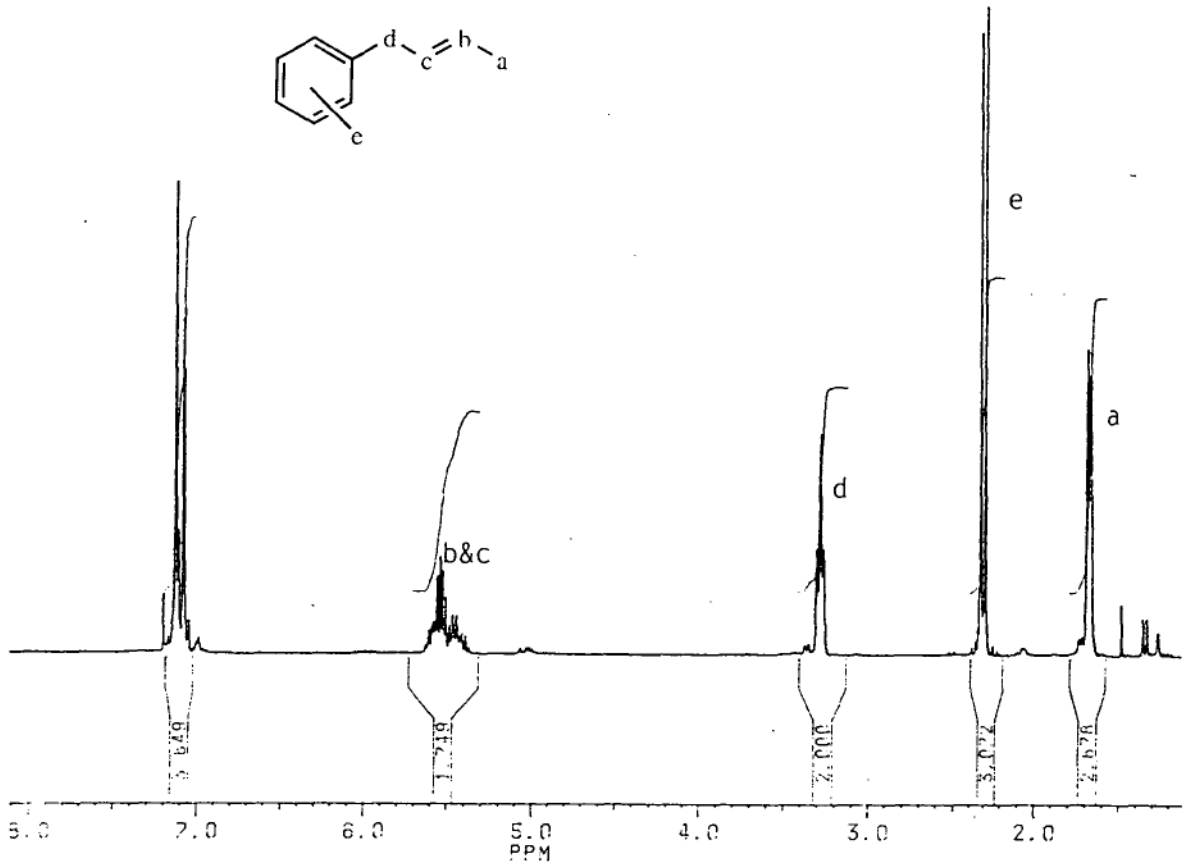

A.4.0. Decomposition Products of $Zr(acac)_2Bz_2$

deactivated with H_2O and extracted into hexane.

A.4.1. GC Trace

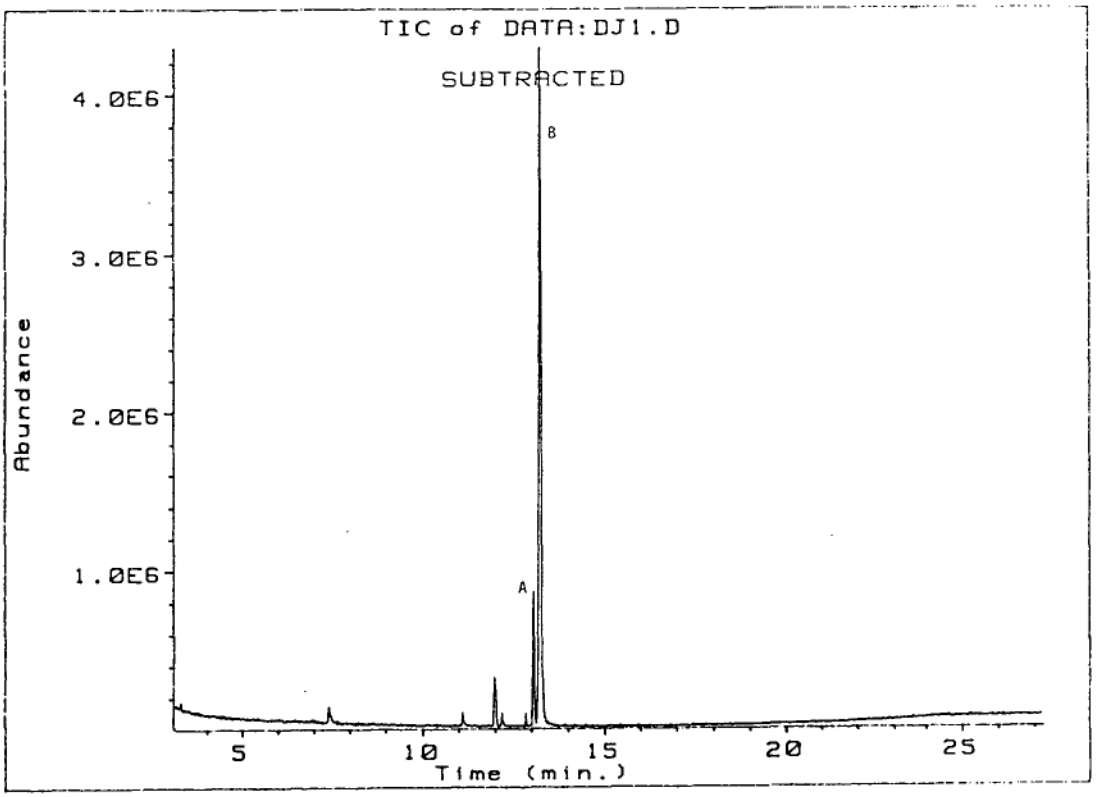

A.4.2. GC-MS Data

Major Peak B 208(M+ 50), 193(10), 175(5), 157(5), 115(15), 91(30), 43(100)

Minor Peak A 248(M+ 5), 204(5), 175(80), 157(75), 142(30), 128(25), 115(25), 91(65), 43(100)

$PhCH_2^-$ FW 91, acac- FW 99, H_2O FW 18, Total 208

m/e 91 $C_7H_7^-$, 43 CH_3CO^-

A.4.3. ^{1}H-NMR of the decomposition products of $Zr(acac)_2Bz_2$

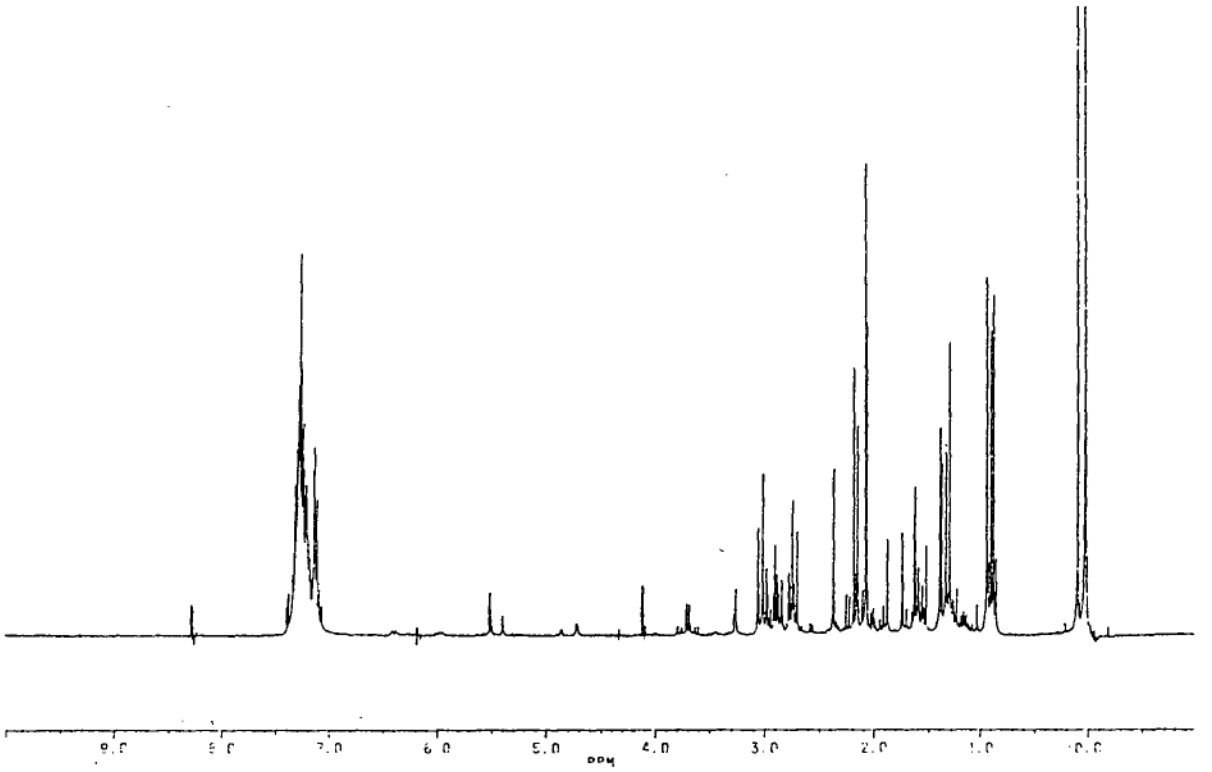

Appendix II

CONTENTS

VARIABLE TEMPERATURE NMR SPECTRA

B.1.0. Bis-Ligands Zirconium Complexes

B.1.1. $(ClPh\text{-}Nacac)_2ZrCl_2$: ^1H-NMR in CD_2Cl_2, 0-10ppm

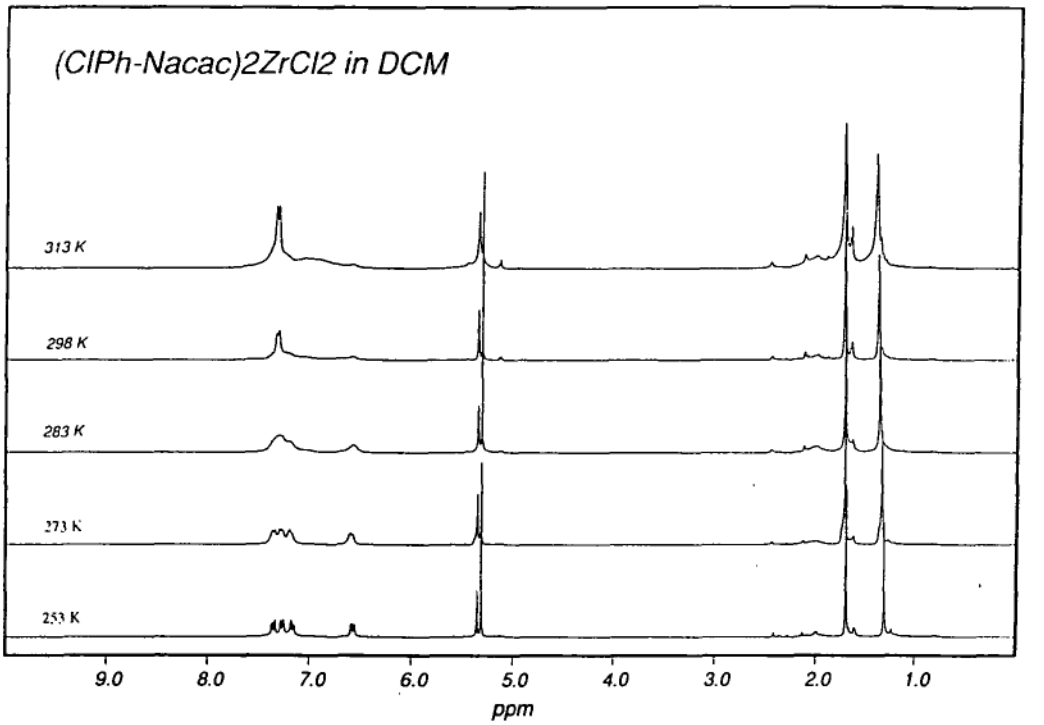

B.1.2. $(ClPh\text{-}Nacac)_2ZrCl_2$: $^{13}C\{^1H\}$-NMR in CD_2Cl_2, 0-200ppm

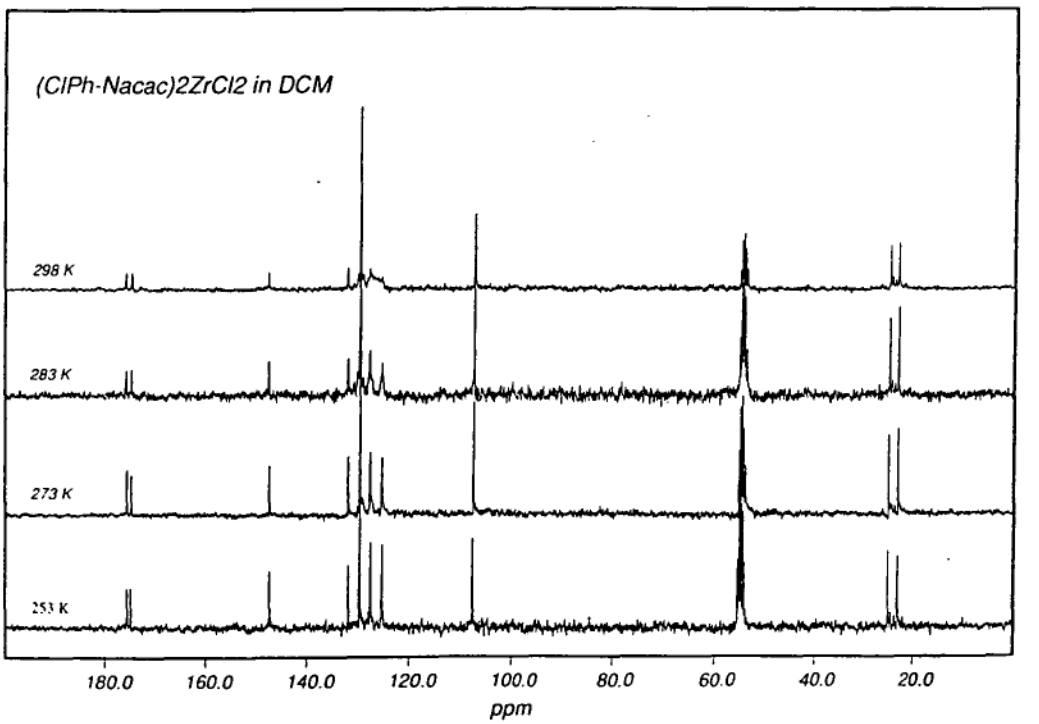

B.1.3. $(ClPh\text{-}Nacac)_2ZrCl_2$: ^1H-NMR in CD_2Cl_2, 6-8ppm

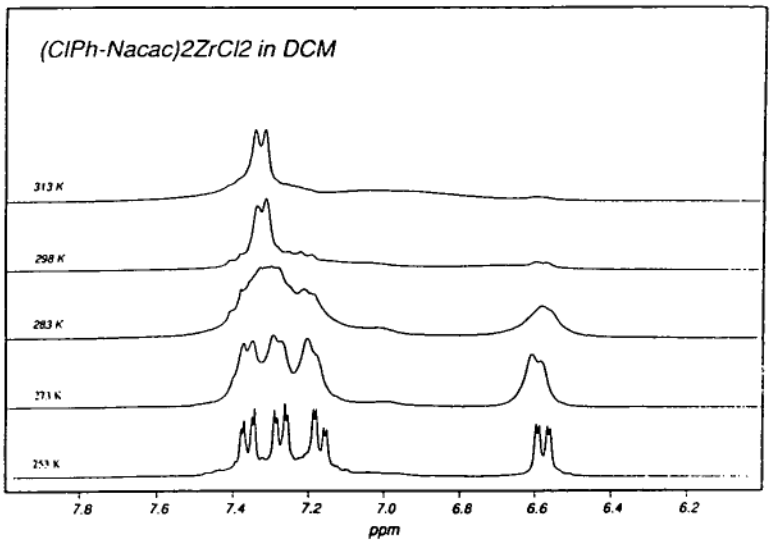

B.1.4. $(ClPh\text{-}Nacac)_2ZrCl_2$: $^{13}C\{^1H\}$-NMR in CD_2Cl_2, 120-150ppm

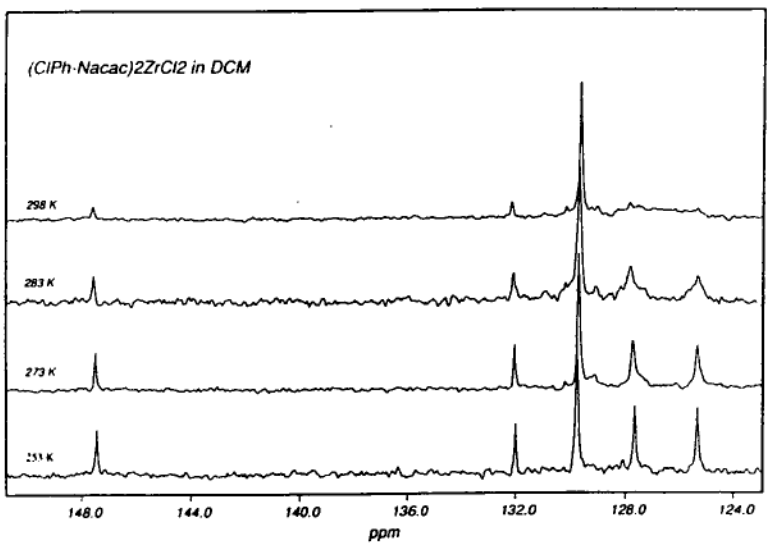

B.1.5. $(ClPh\text{-}Nacac)_2ZrCl_2$: ^{13}C-NMR in CD_2Cl_2, 0-200ppm

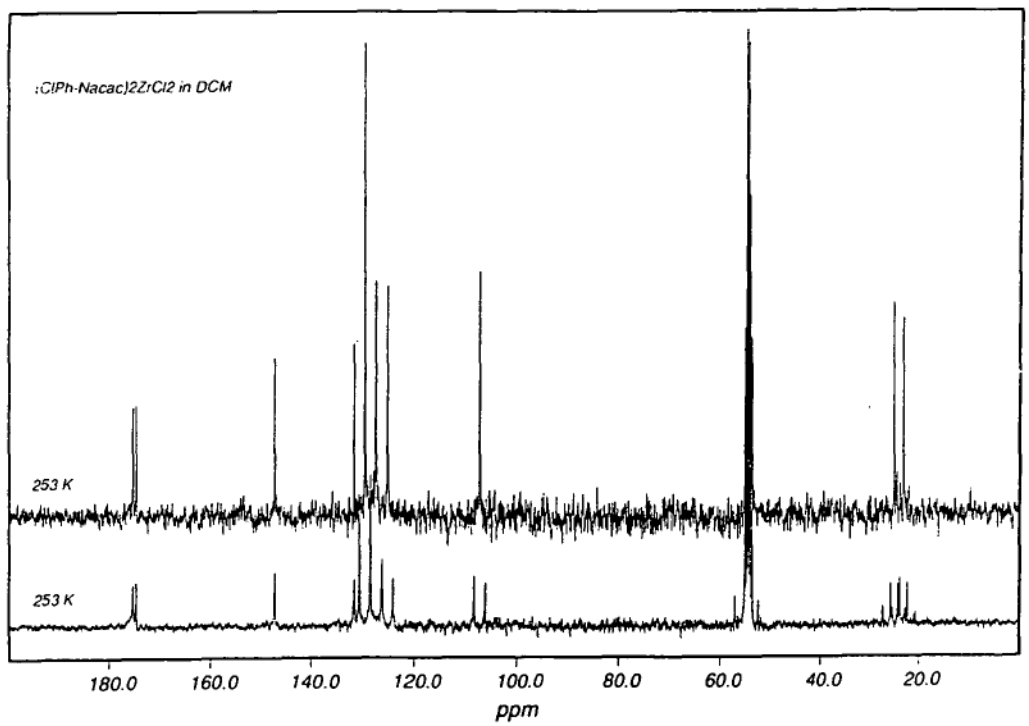

B.1.6. $(MeOPh\text{-}Nacac)_2ZrCl_2$: ^1H-NMR in CD_2Cl_2, 0-10ppm

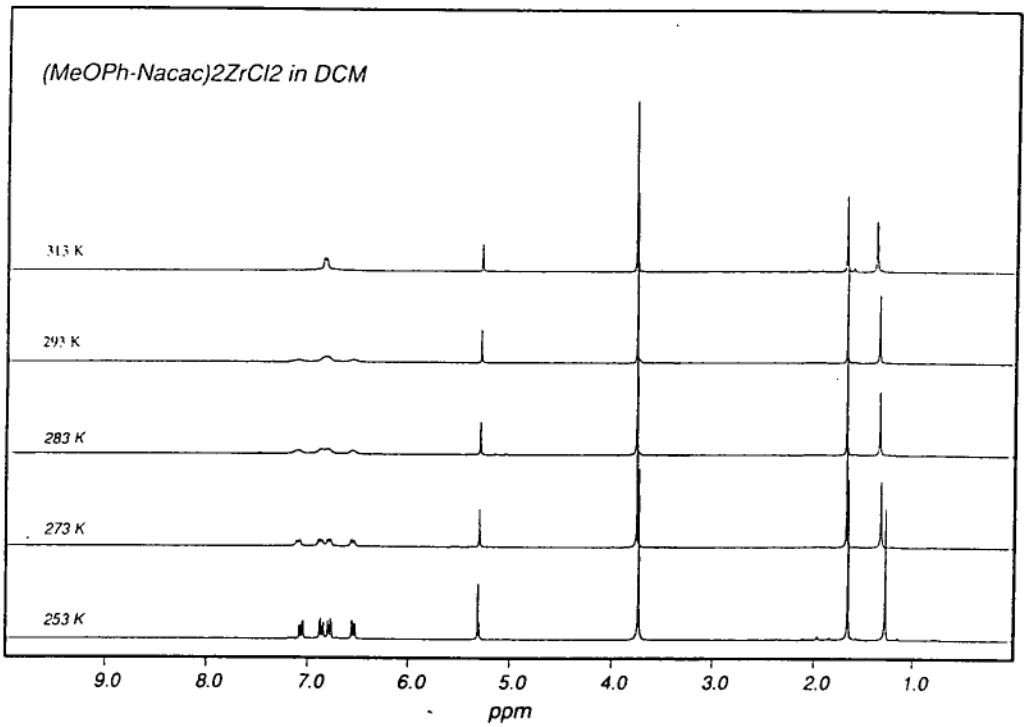

B.1.7. $(MeOPh\text{-}Nacac)_2ZrCl_2$: $^{13}C\{^1H\}$-NMR in CD_2Cl_2, 0-200ppm

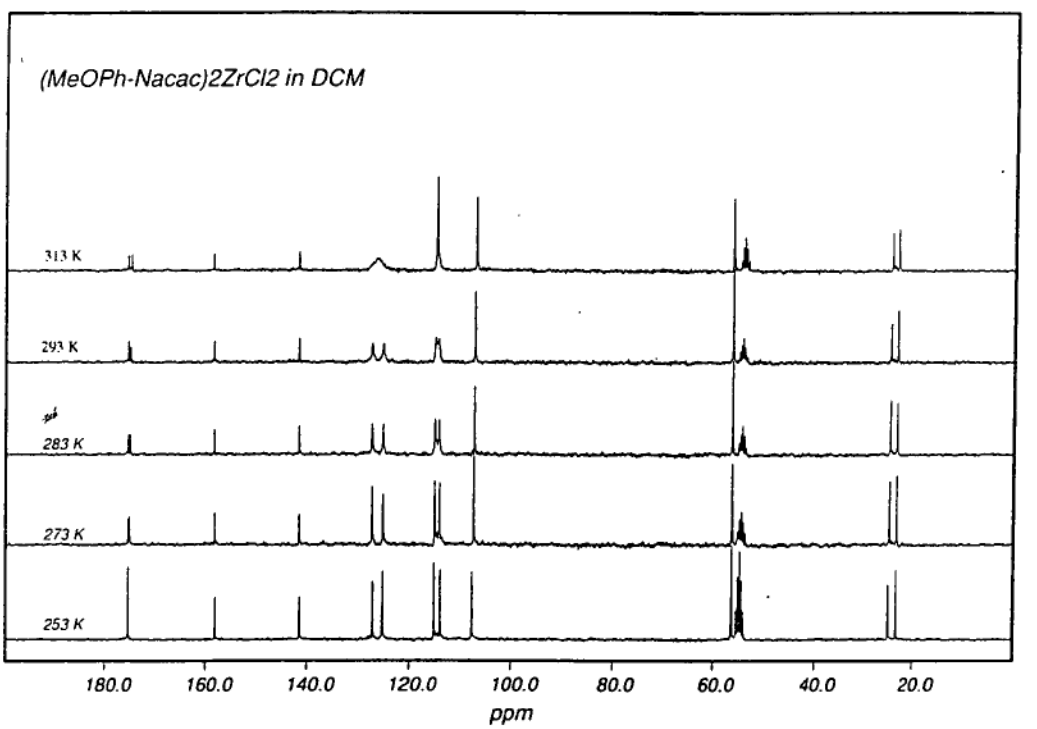

B.1.8. $(Ph\text{-}Nacac)_2ZrCl_2$: ^1H-NMR in CD_2Cl_2, 6-9ppm

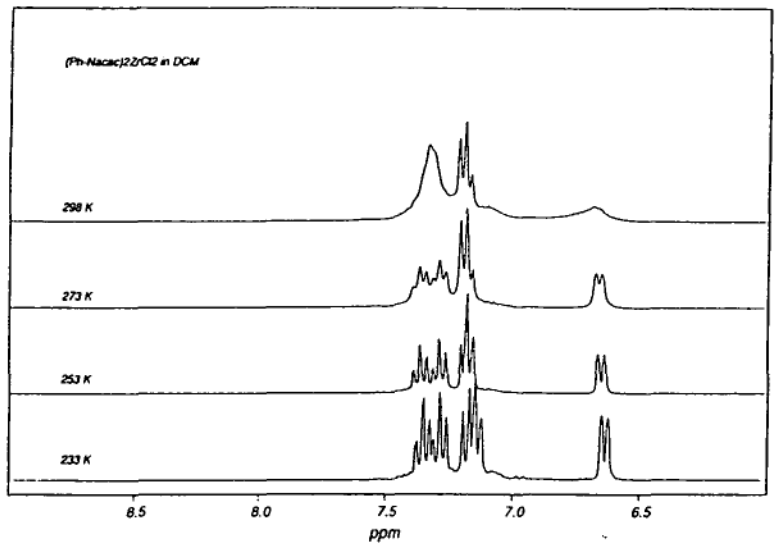

B.1.9. $(Ph\text{-}Nacac)_2ZrCl_2$: $^{13}C\{^1H\}$-NMR in CD_2Cl_2, 120-140ppm

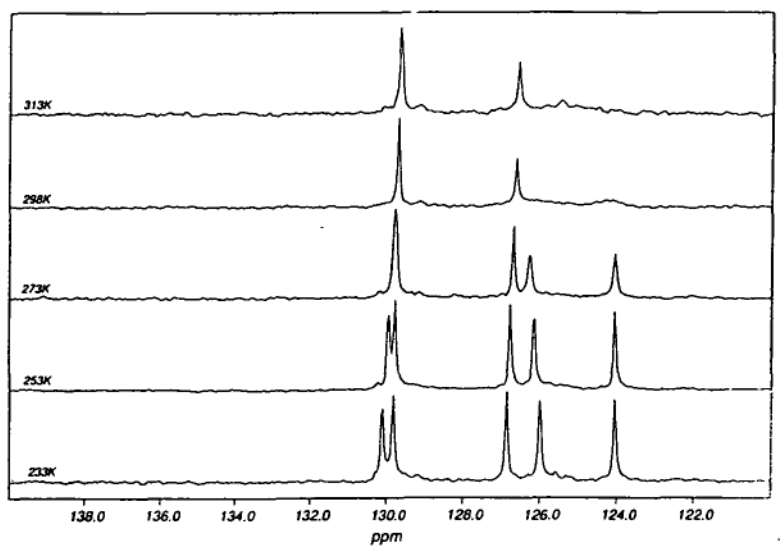

B.1.10. $(Ph\text{-}Nacac)_2ZrCl_2$: ^{13}C-NMR in CD_2Cl_2, 0-200ppm

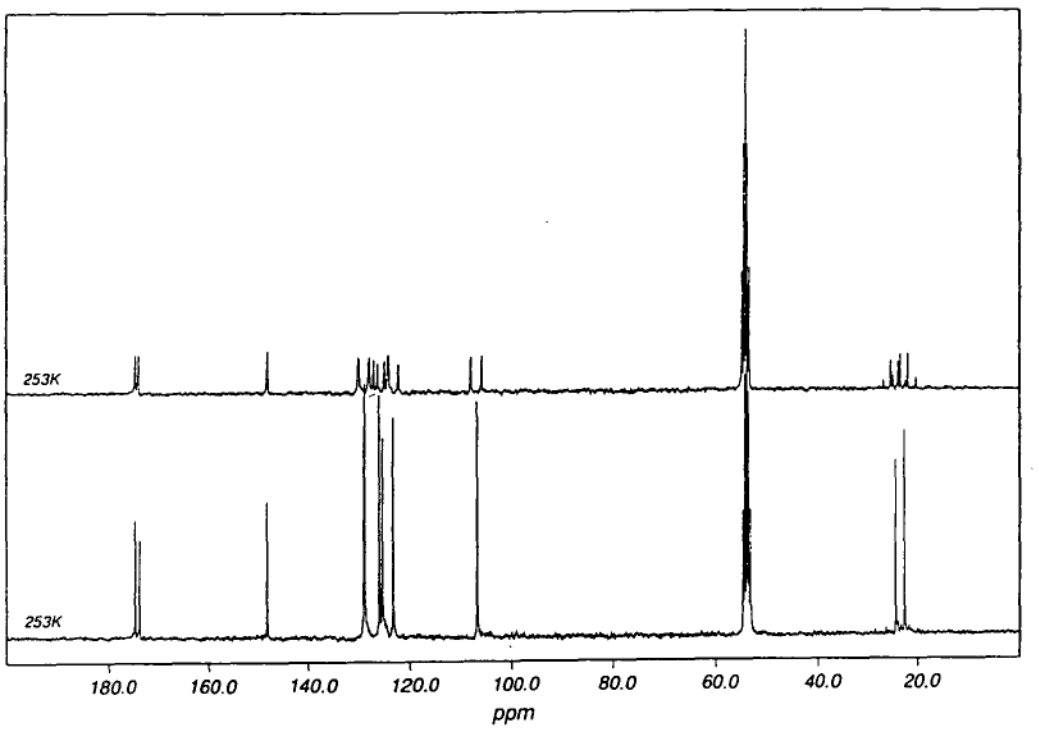

B.1.11. (*i*-Pr-Nacac)$_2$ZrCl$_2$: ^{1}H-NMR in CD_2Cl_2, 0-10ppm

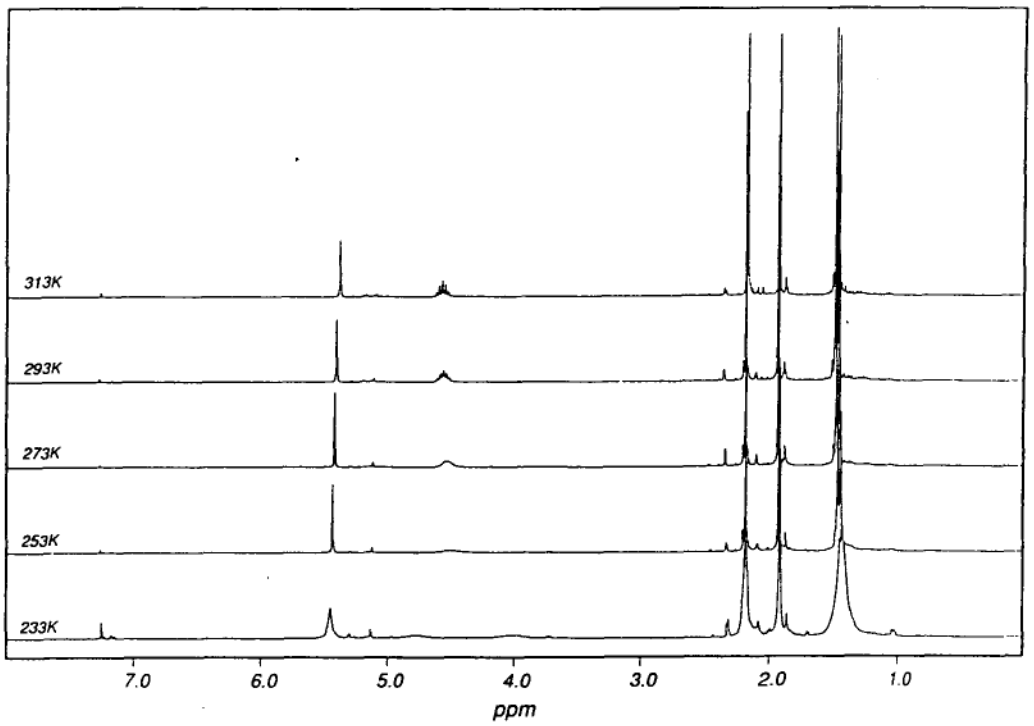

B.1.12. (*i*Pr-Nacac)$_2$ZrCl$_2$: ^{13}C-NMR in CD_2Cl_2, 0-200ppm

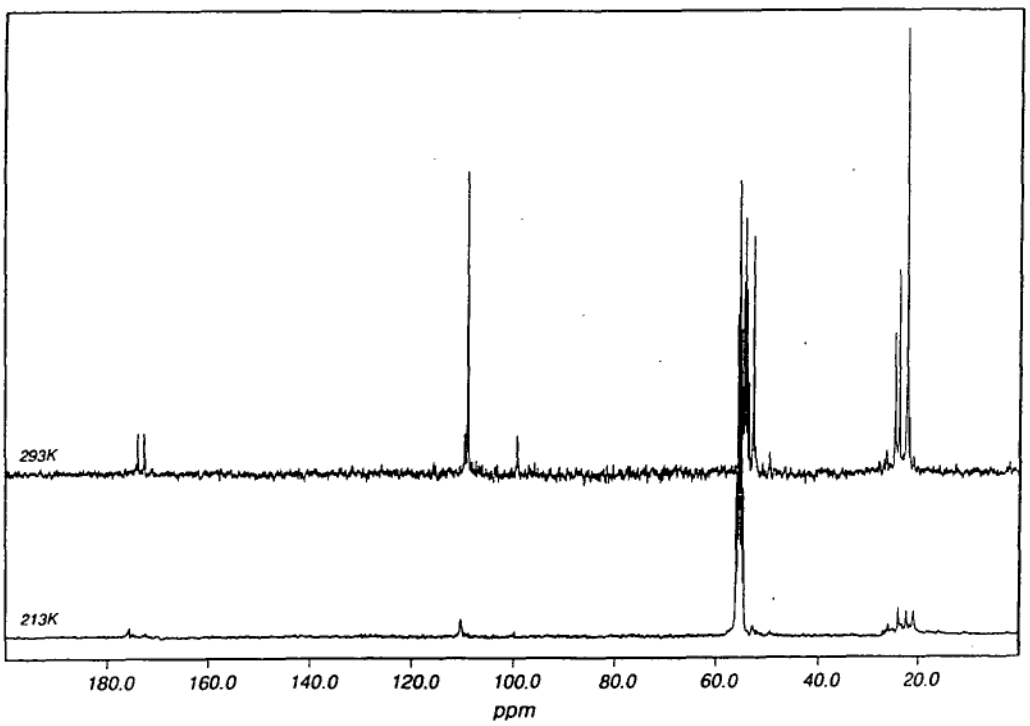

B.2.0. In-Situ FORMATION OF (R-Nacac)$_2$ZrBz$_2$ Zirconium Complexes

B.2.1. $ZrBz_4$ + 2*t*-Bu-HNacac : ^{1}H-NMR in CD_2Cl_2, 0-8ppm

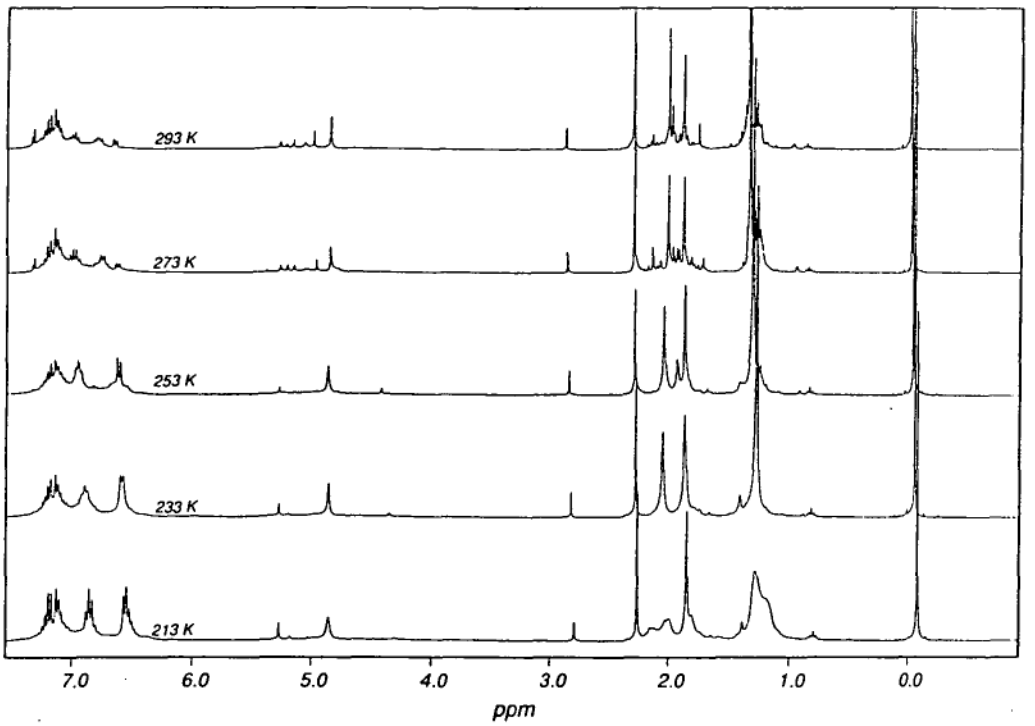

B.2.2. $ZrBz_4$ + 2cy-HNacac : ^{1}H-NMR in CD_2Cl_2, 0-12ppm

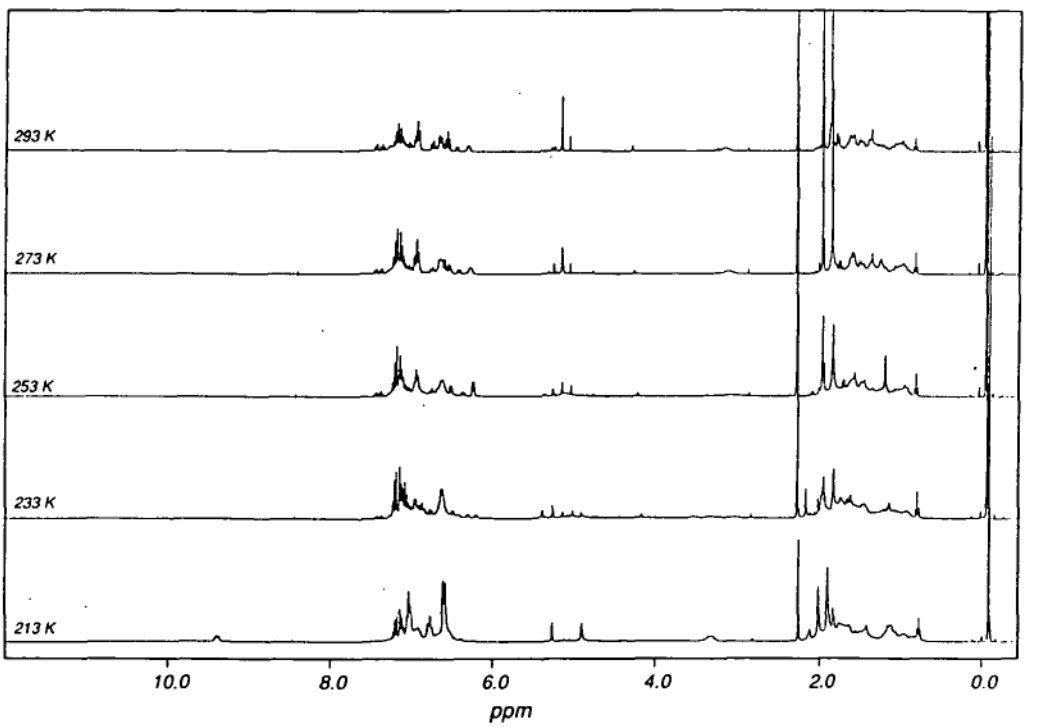

B.2.3. $ZrBz_4$ + 2*i*-Pr-HNtfac : ^{1}H-NMR in CD_2Cl_2, 0-8ppm

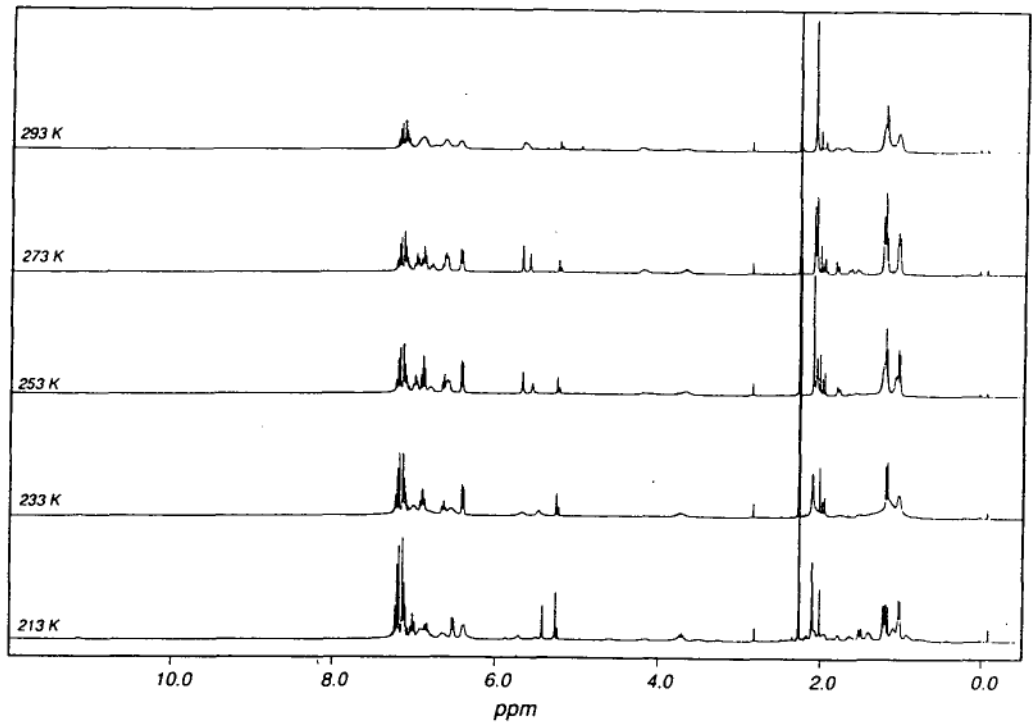

B.2.4. $ZrBz_4$ + 2Ph-HNacac : ^{1}H-NMR in CD_2Cl_2, 0-12ppm

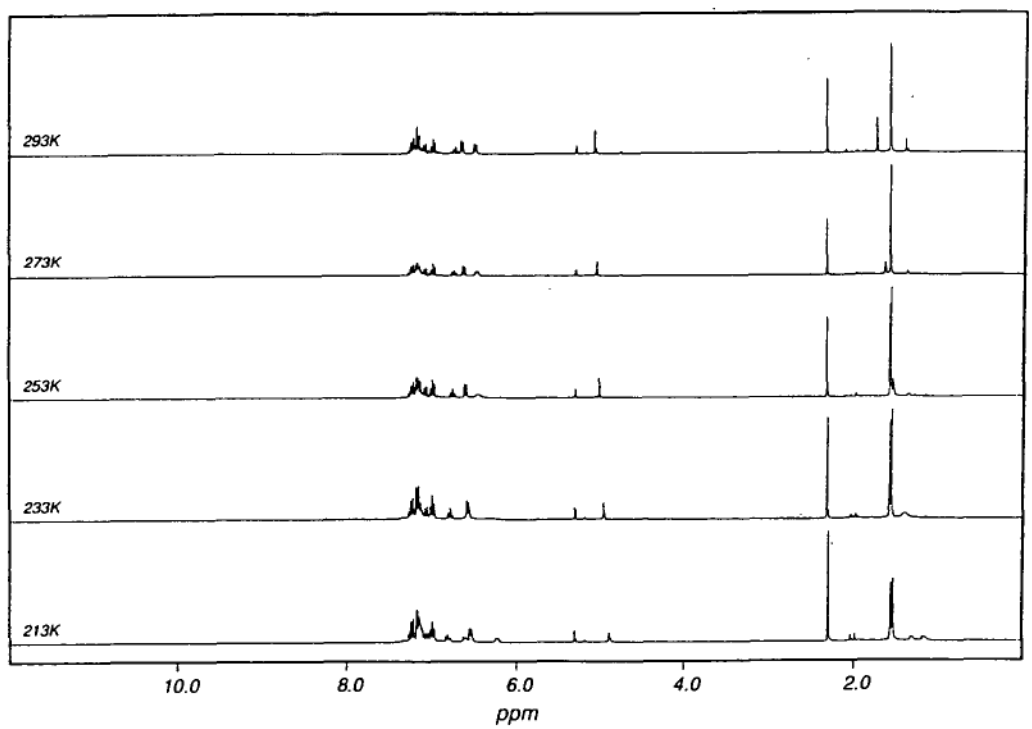

B.2.5. $ZrBz_4$ + 2HSacPhac : ^{1}H-NMR in CD_2Cl_2, 0-12ppm

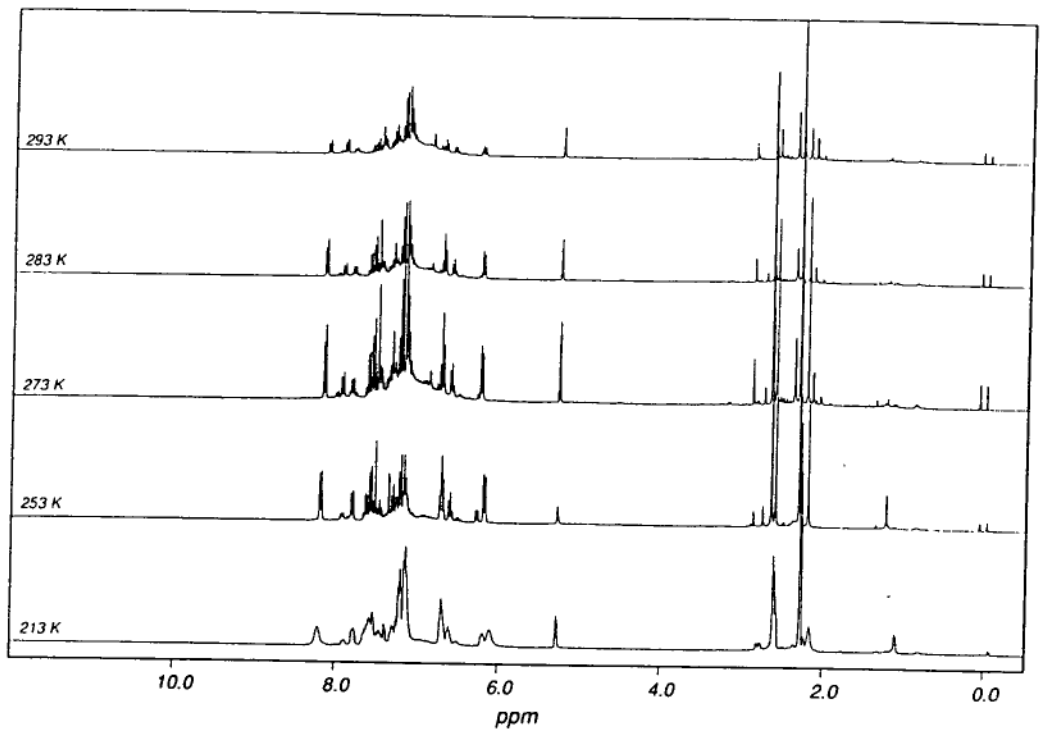

B.2.6. $ZrBz_4$ + 2*i*-Pr-HNacSac : ^{1}H-NMR in CD_2Cl_2, 0-16ppm

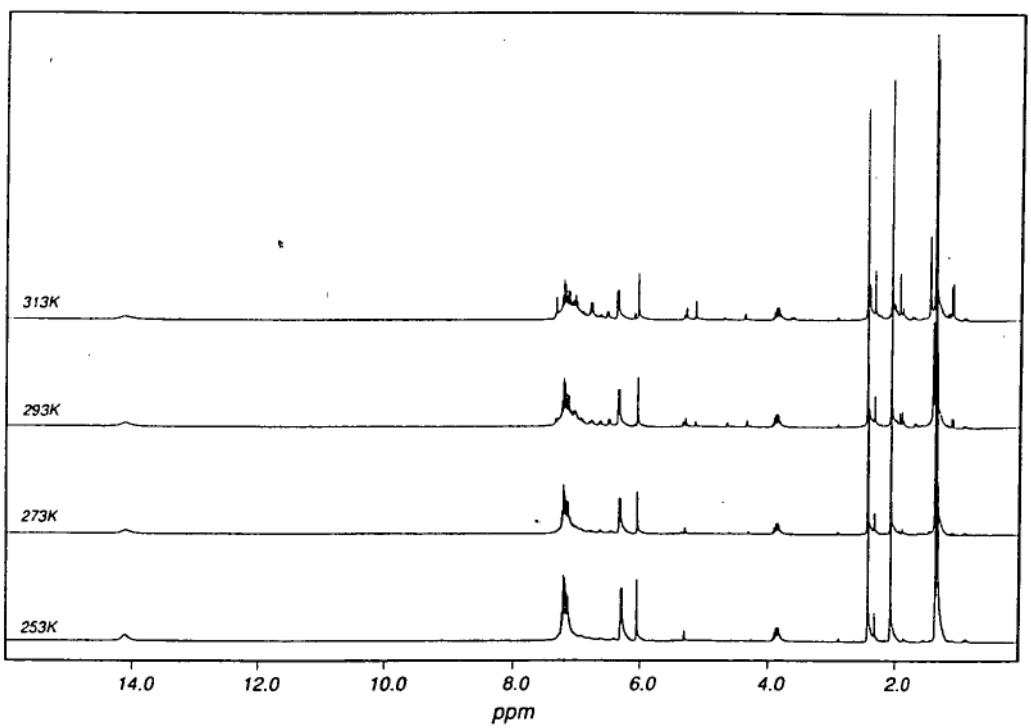

B.2.7. $ZrBz_4$ + 2*i*-Pr-NPhOH : ^{1}H-NMR in CD_2Cl_2, 0-10ppm

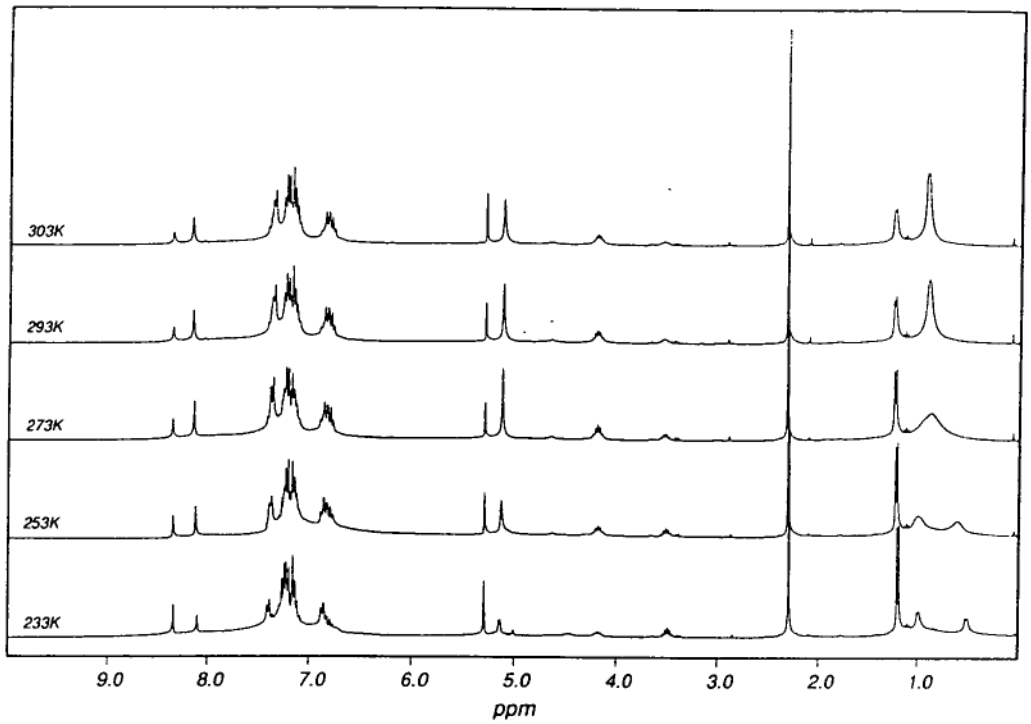

B.2.8. $ZrBz_4$ + HOPh-HNacac : ^{1}H-NMR in CD_2Cl_2, 0-8ppm

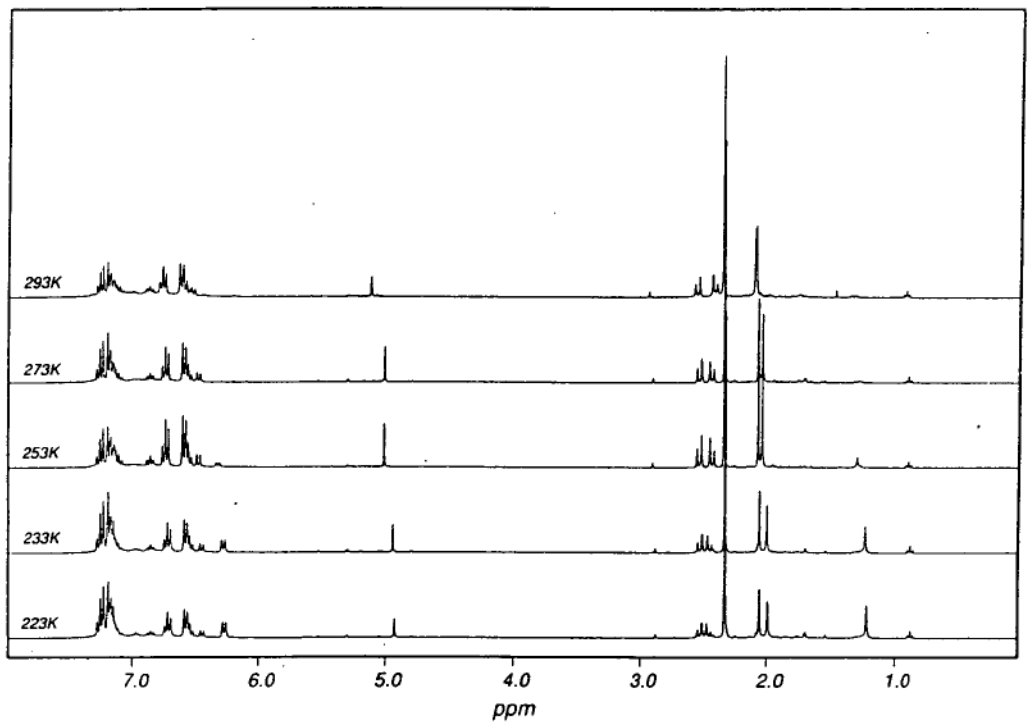

B.3.0. (R-Nacac)$_2$ZrBz$_2$ Zirconium Complexes

B.3.1. (cy-Nacac)$_2$ZrBz$_2$: ^{1}H-NMR in CD_2Cl_2, 0-8ppm

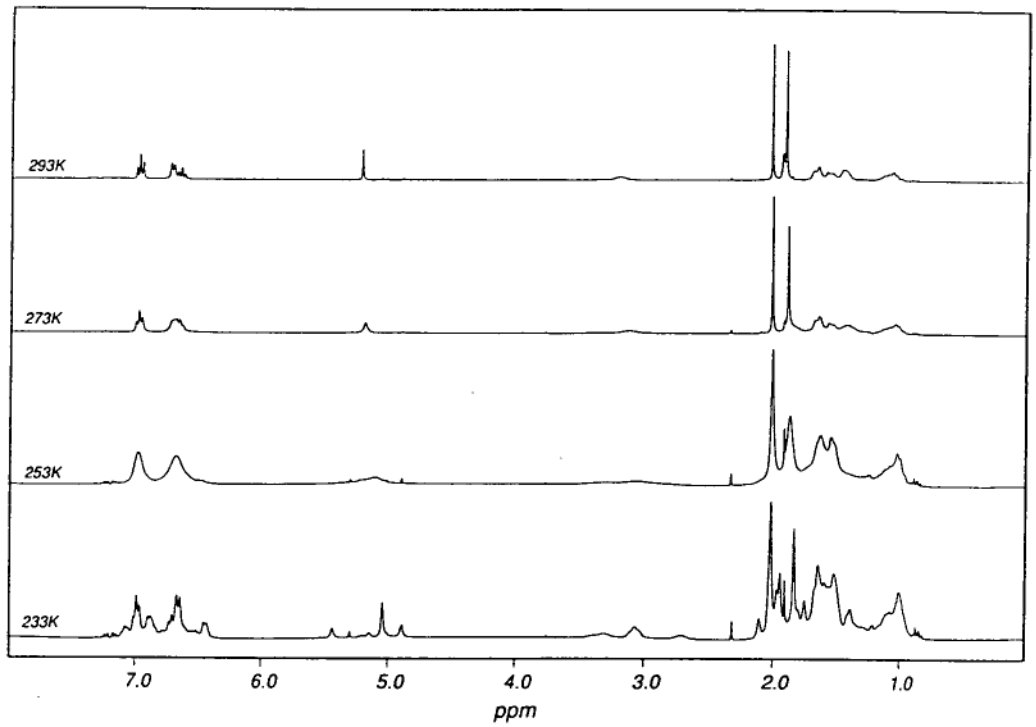

B.3.2. (cy-Nacac)$_2$ZrBz$_2$: ^{13}C{^{1}H}-NMR in CD_2Cl_2, 0-200ppm

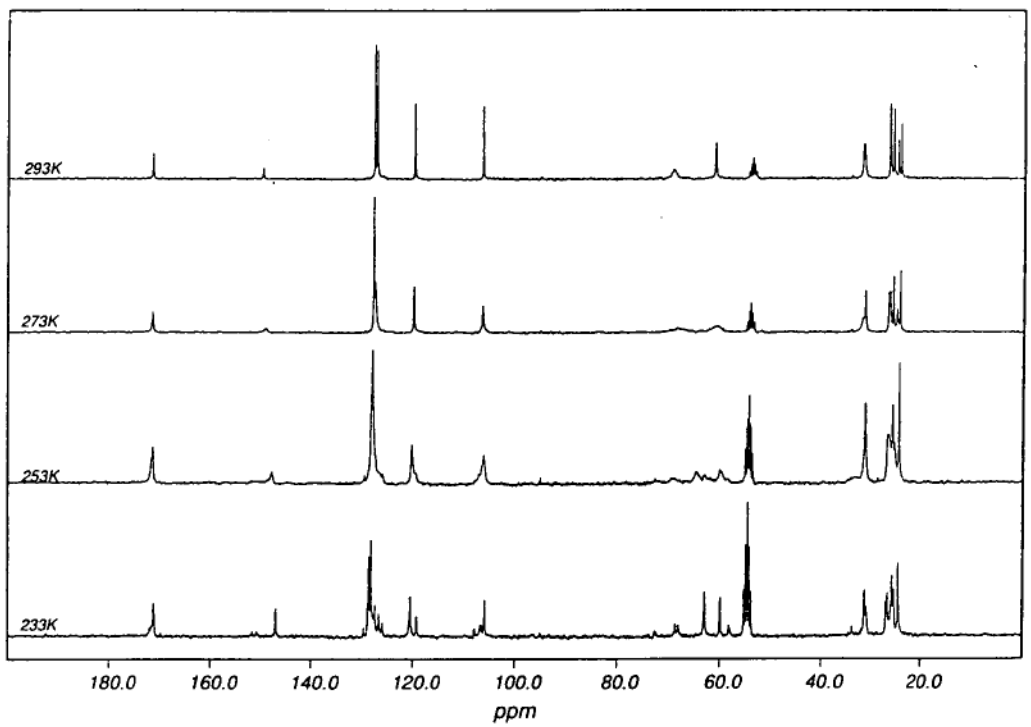

B.3.3. (i-Pr-Ntfac)$_2$ZrBz$_2$: ^{1}H-NMR in CD_2Cl_2, 0-8ppm, 273-313K

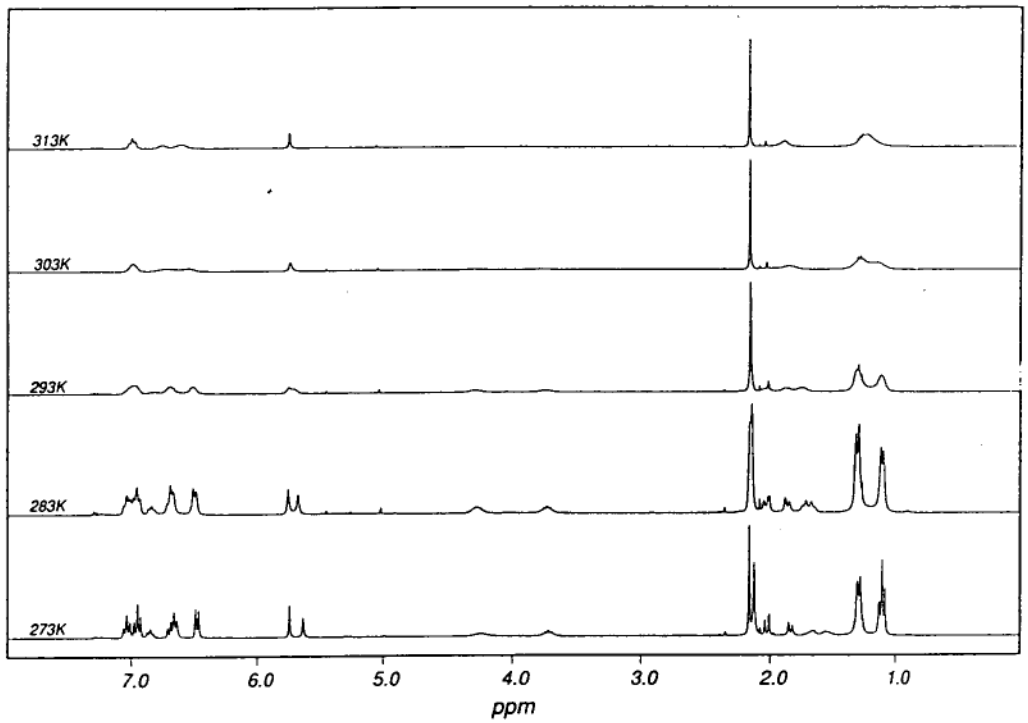

B.3.4. (i-Pr-Ntfac)$_2$ZrBz$_2$: ^{1}H-NMR in CD_2Cl_2, 0-8ppm, 233-283K

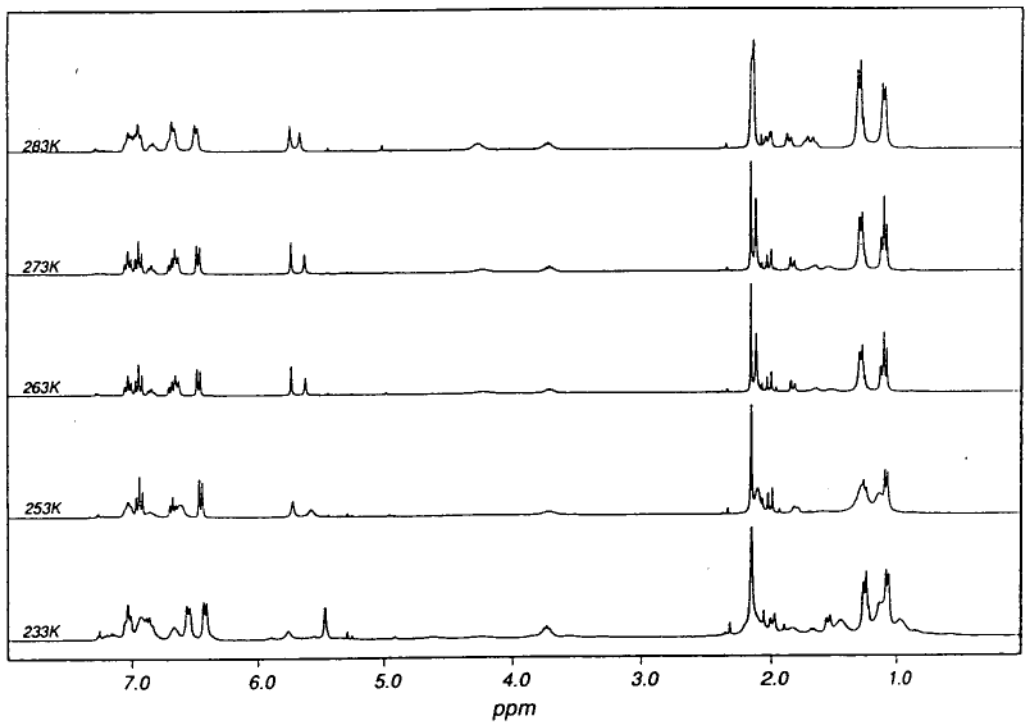

B.3.5. (*i*-Pr-Ntfac)$_2$ZrBz$_2$: $^{13}C\{^1H\}$-NMR in CD_2Cl_2, 0-200ppm, 273-313K

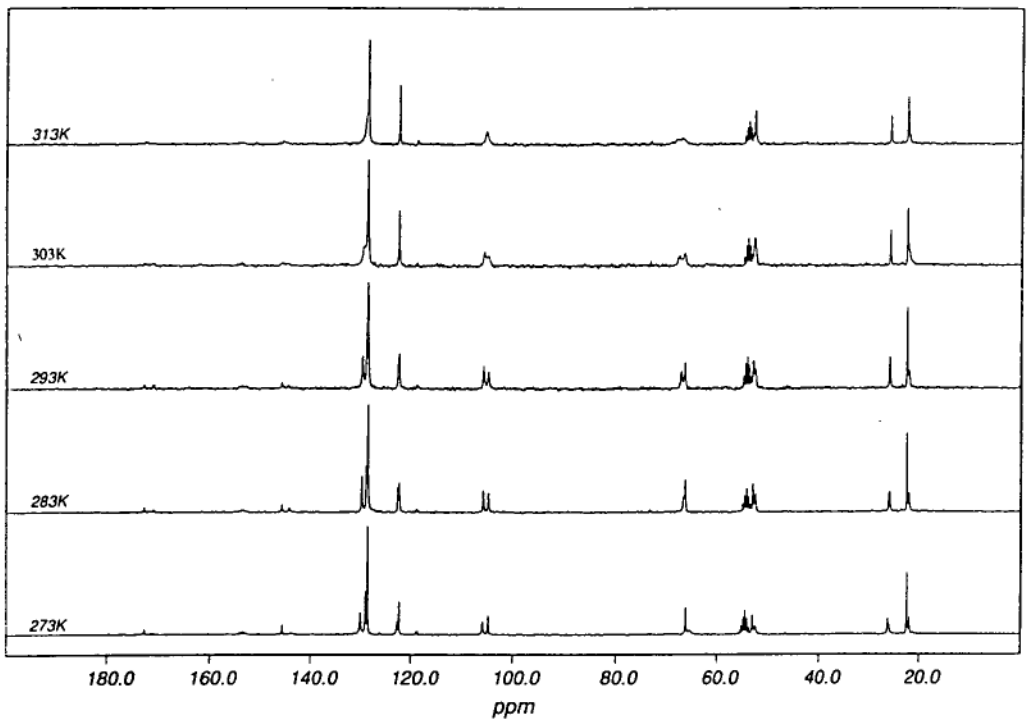

B.3.6. (*i*-Pr-Ntfac)$_2$ZrBz$_2$: $^{13}C\{^1H\}$-NMR in CD_2Cl_2, 0-200ppm, 233-283K

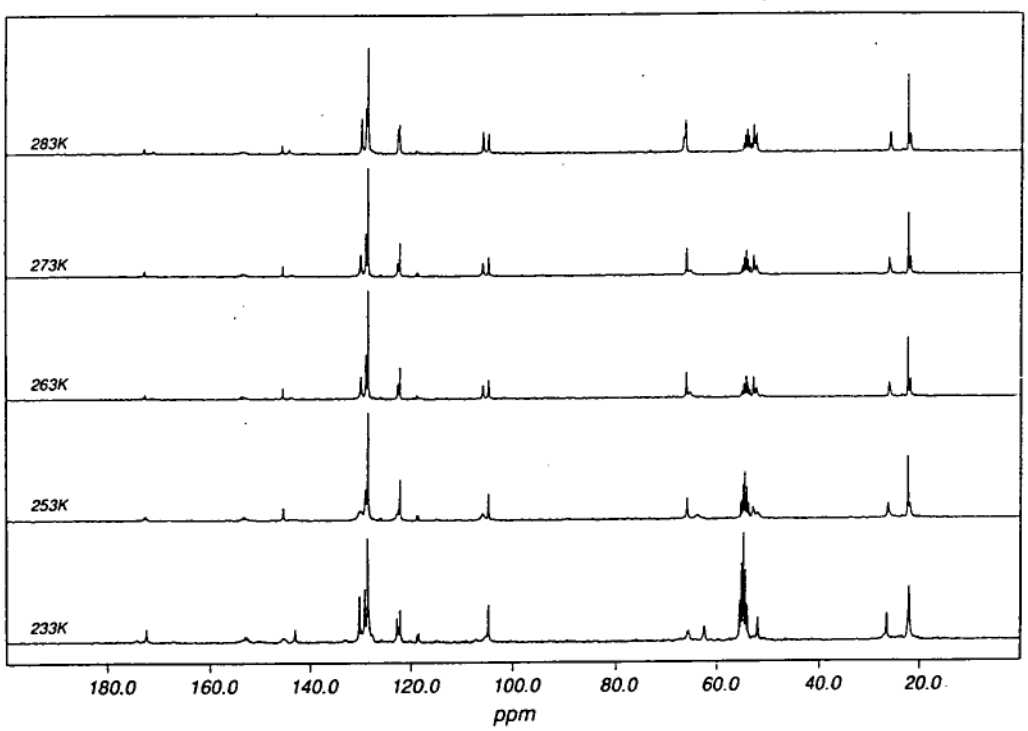

B.3.7. (i-Pr-Ntfac)$_2$ZrBz$_2$: ^{13}C-NMR in CD_2Cl_2, 0-200ppm

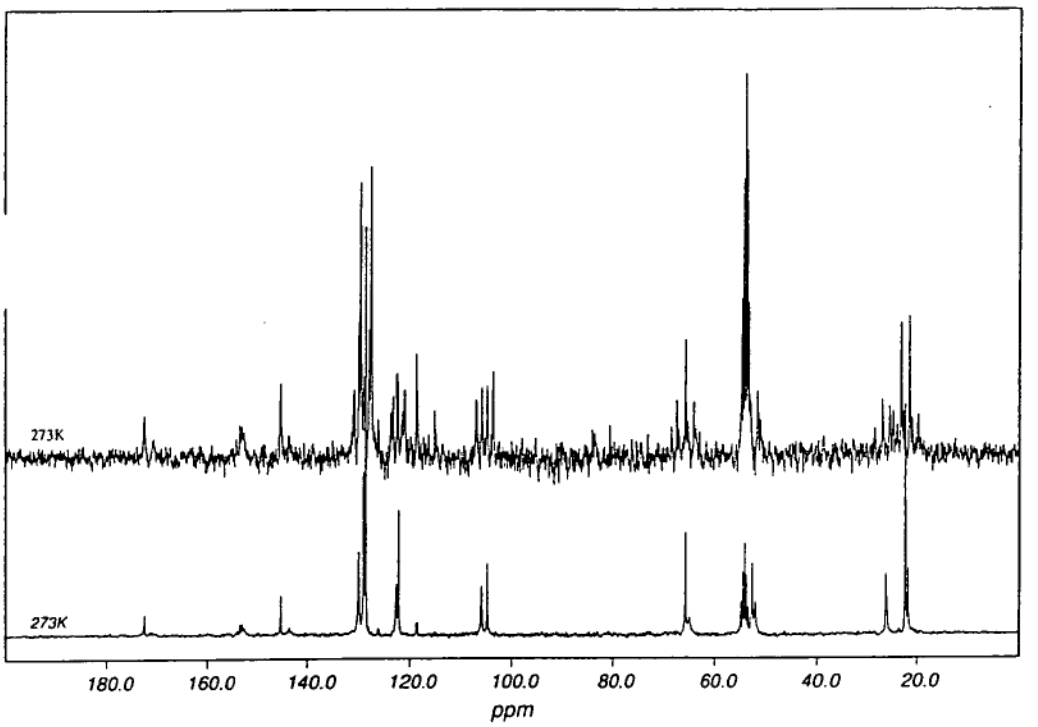

B.3.8. $(Ph\text{-}Nacac)_2ZrBz_2$: ^{13}C-NMR in CD_2Cl_2, 0-200ppm

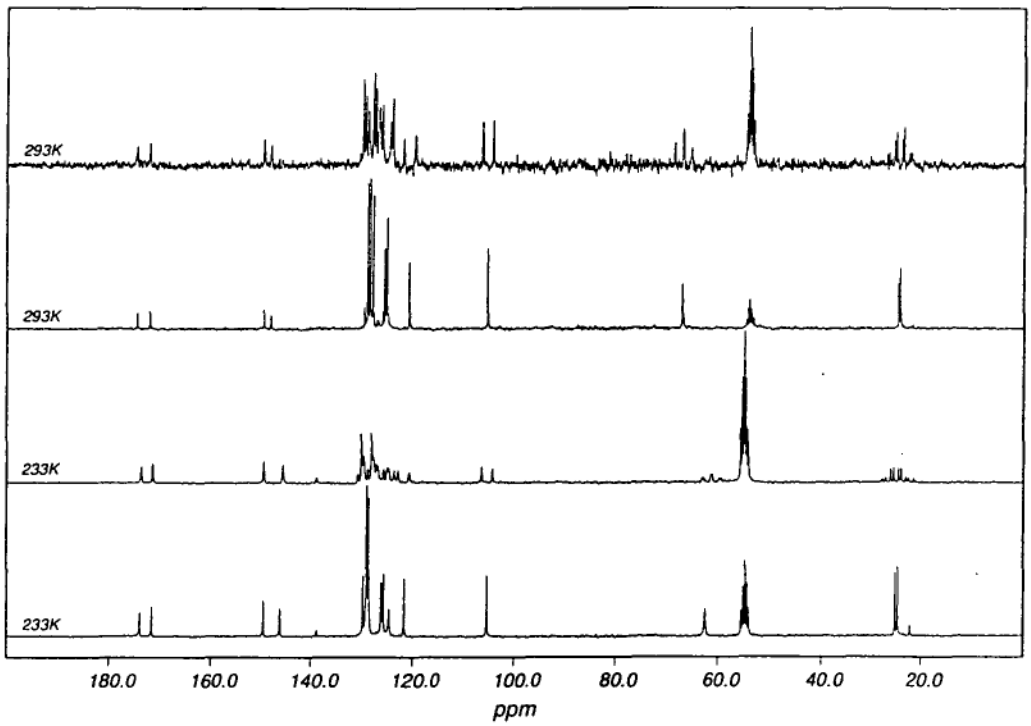

B.3.9. $(Ph\text{-}Nacac)_2ZrBz_2$: ^{13}C-NMR in CD_2Cl_2, 100-140ppm

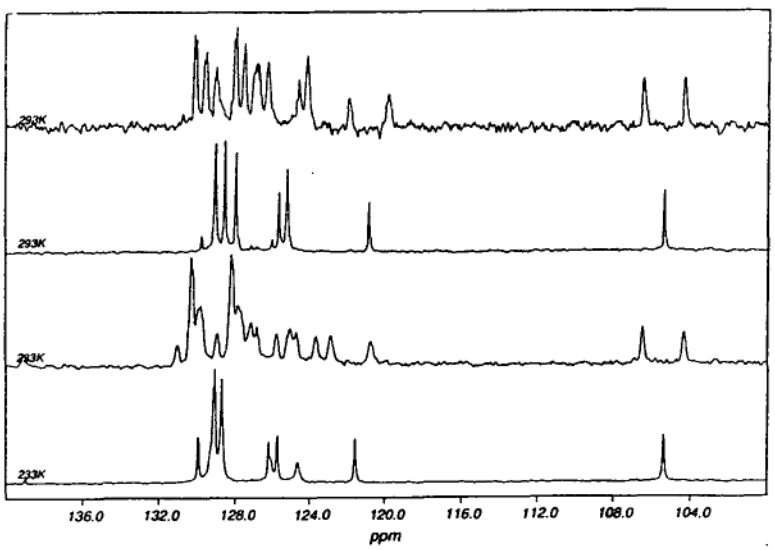

Appendix III

CONTENTS

B.4.0. EASC Interactions with Ligands or Zirconium Complexes

B.4.1. EASC : ^{1}H-NMR in C_6D_6, 0-6ppm, 298-348K

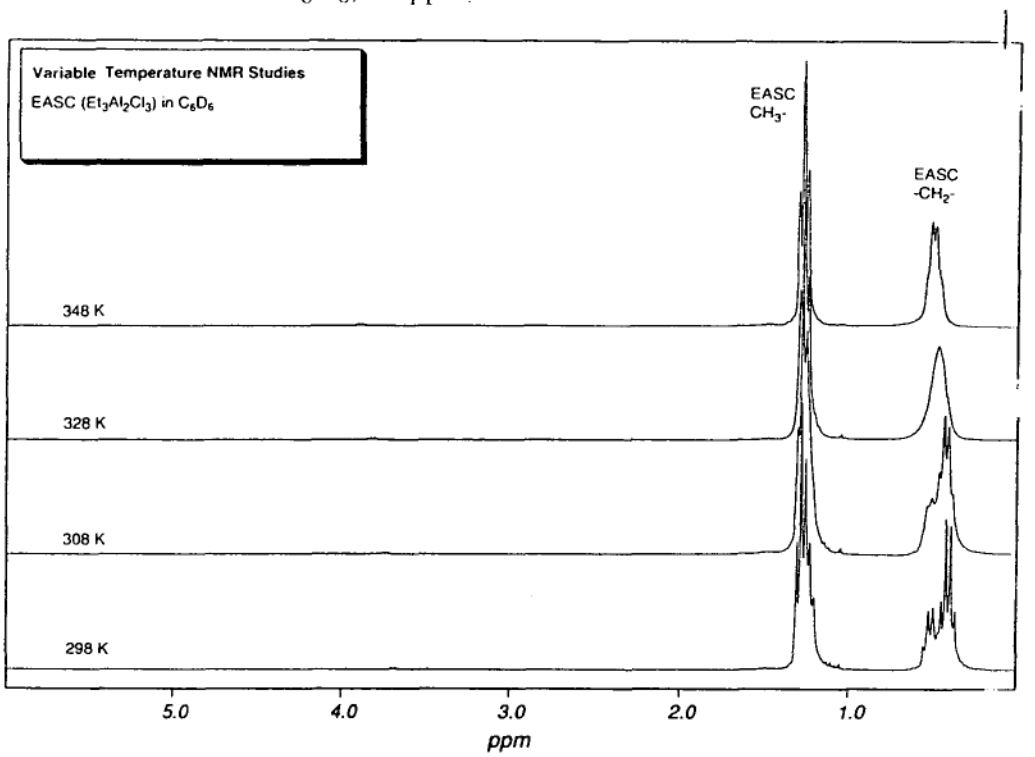

B.4.2. *i*-Pr-HNacac : ^{1}H-NMR in C_6D_6, 0-6ppm, 298-348K

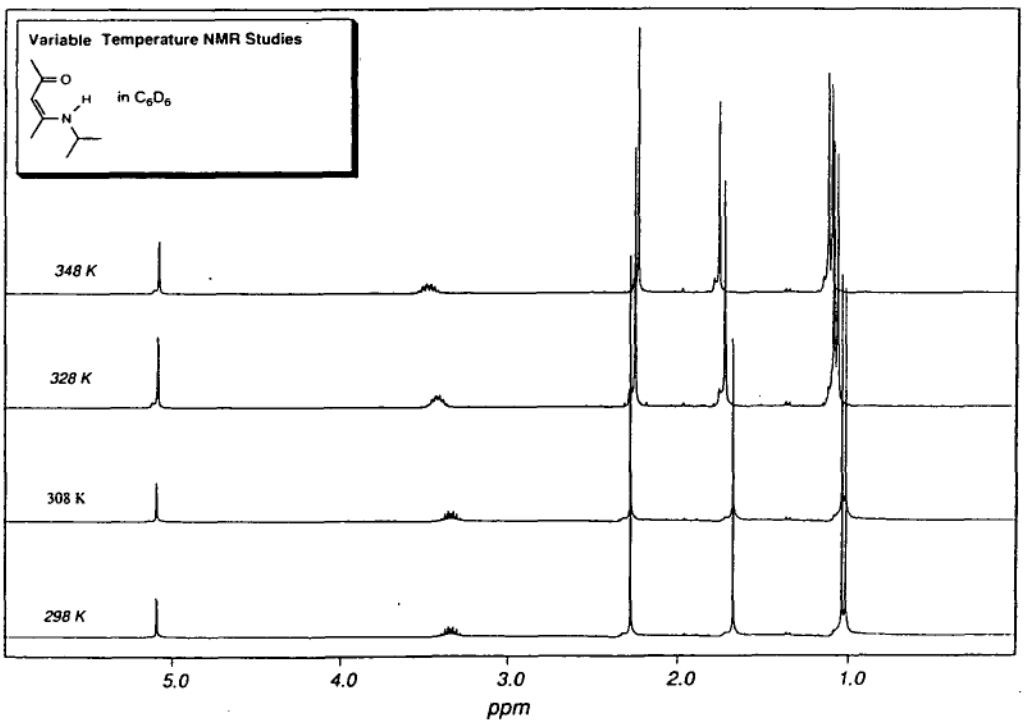

B.4.3. $ZrCl_4$:2*i*-Pr-HNacac / 2EASC : ^{1}H-NMR in C_6D_6, 0-6ppm, 298-348K

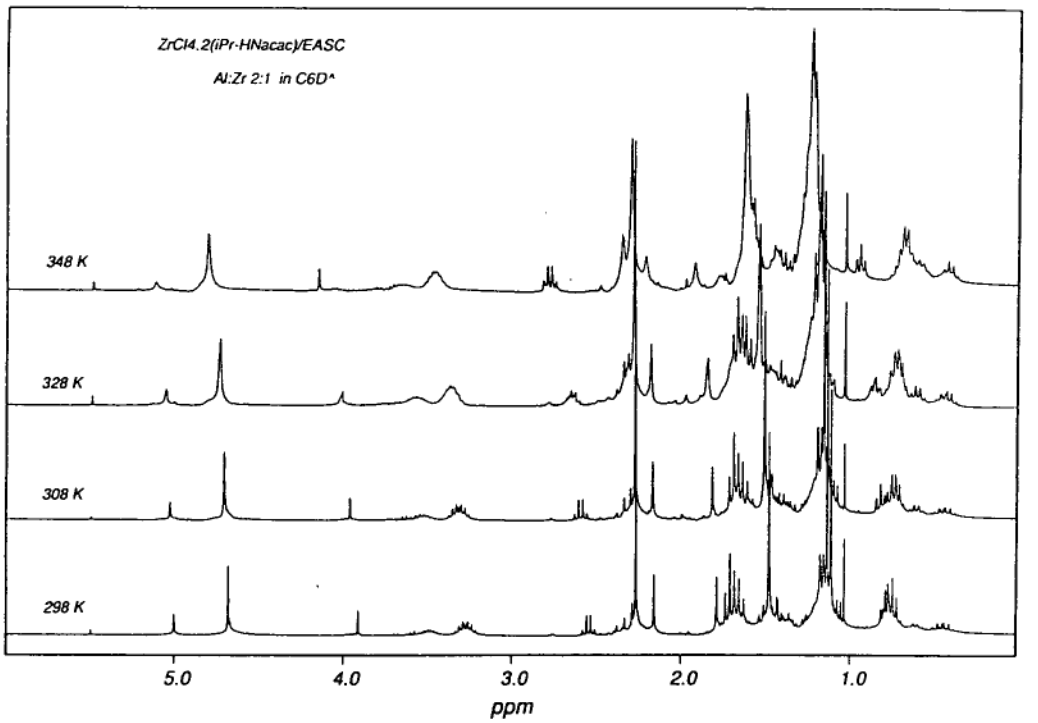

B.4.4. Ph-HNacac : ^{1}H-NMR in Toluene-d_8, 0-6ppm, 298-348K

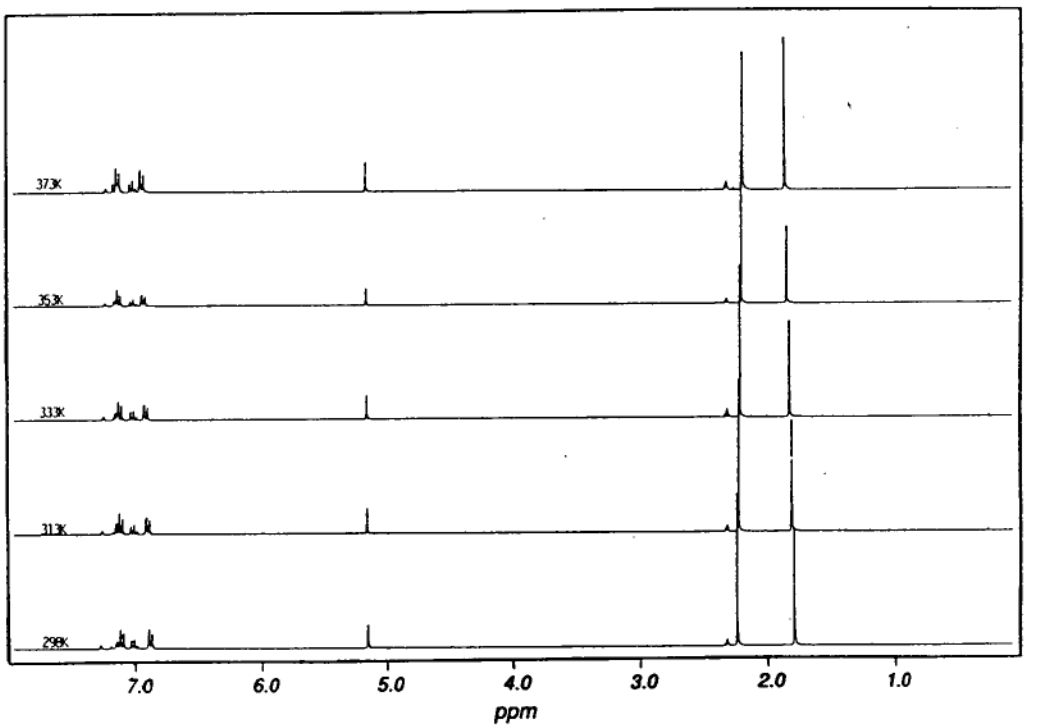

B.4.5. $ZrCl_4$.2Ph-HNacac + 5EASC: ^{1}H-NMR in Toluene-d_8, 0-8ppm, 298-373K

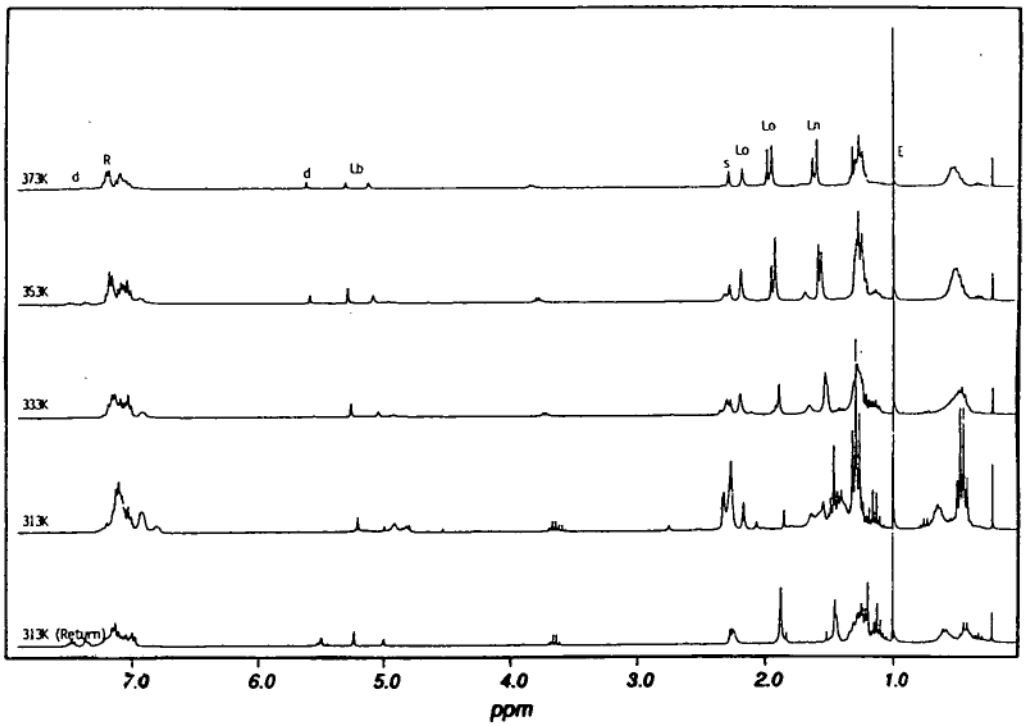

Temperature cycled from 313K to 373K before returning to 313K (bottom Spectrum);Where: d=decomposition products.

B.4.6. $ZrCl_4$.2Ph-HNacac + 5EASC + Ethylene: ^{1}H-NMR in Toluene-d_8, 0-8ppm, 313K

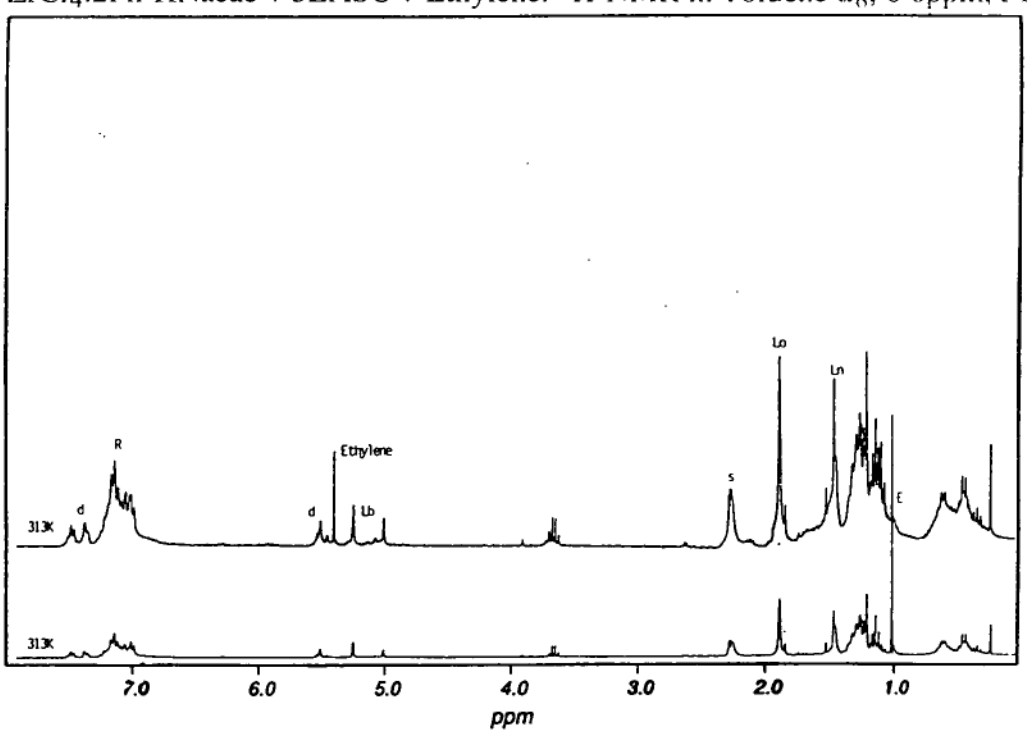

Where: d=decomposition products.

B.4.7. (Ph-Nacac)$_2$ZrCl$_2$ + 5EASC: ^{1}H-NMR in Toluene-d_8, 0-8ppm, 313-373K

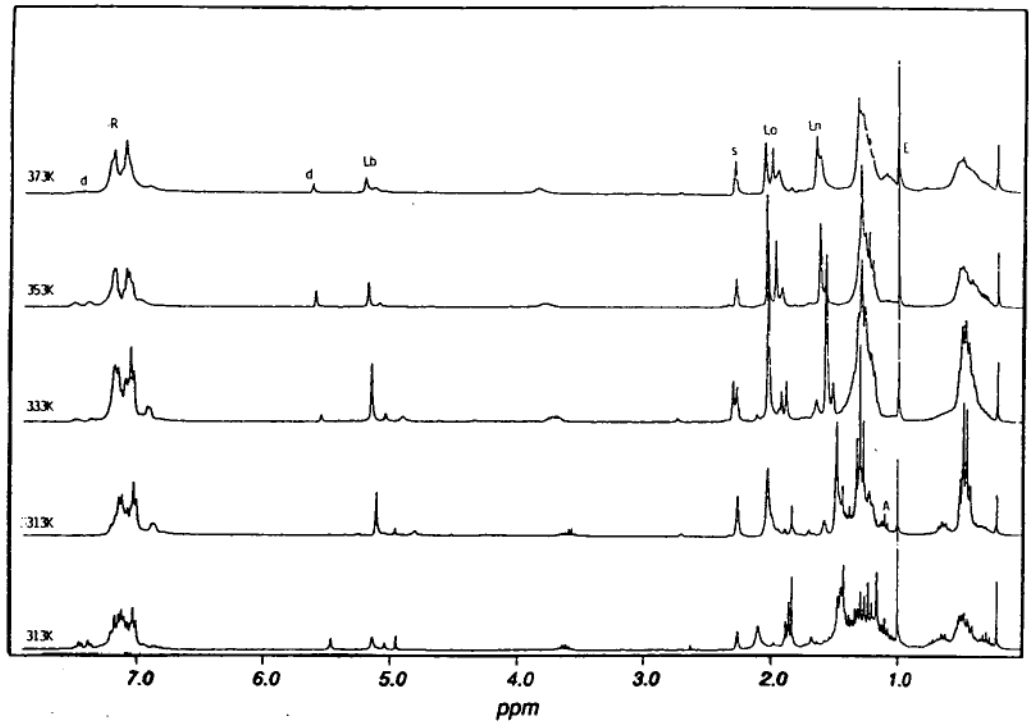

Temperature cycled from 313K to 373K before returning to 313K (bottom Spectrum);Where: d=decomposition products.

B.4.8. (Ph-Nacac)$_2$ZrCl$_2$ + 5EASC + Ethylene: ^{1}H-NMR in Toluene-d_8, 0-8ppm, 313K

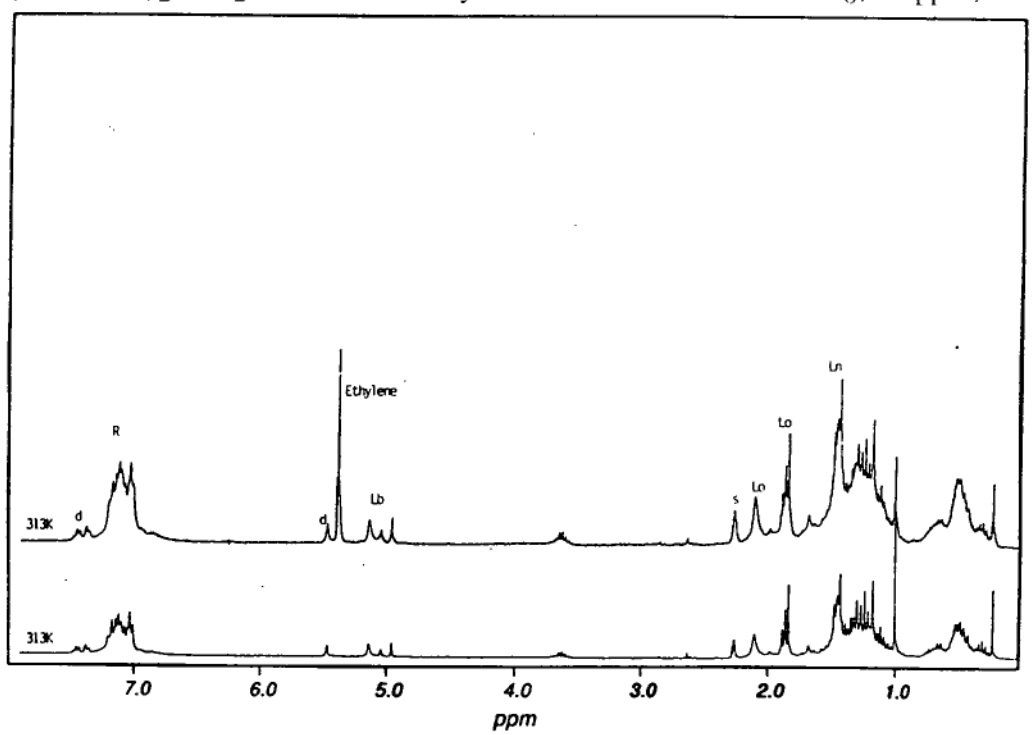

Where: d=decomposition products.

B.4.9. $ZrCl_4$:2MeOPh-HNacac+ 10EASC: ^{1}H-NMR in Toluene-d_8, 0-8ppm, 298-323K

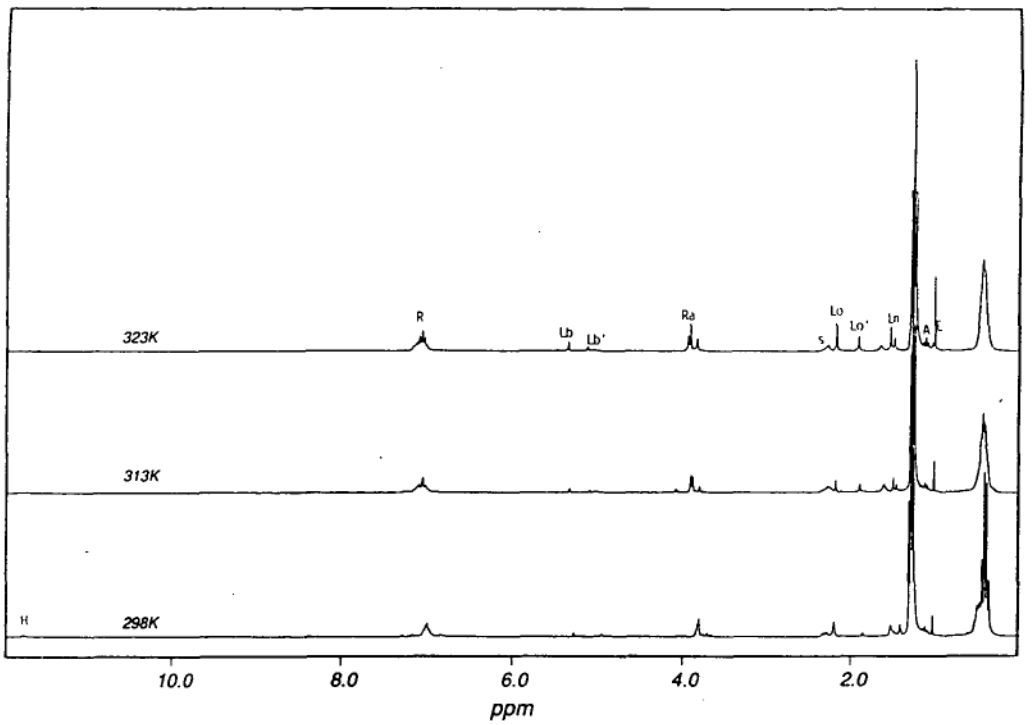

Temperature cycled from 298K to 323K; Where: Ligand backbone: Lo & Lo'=carbonyl methyls; Ln=amino carbon methyl, Lb & Lb'=methine; N-phenyl substituent: R=phenyl protons, Ra=methoxy methyl; E=ethane, A=metal alkylation.

B.4.10. $(MeOPh\text{-}Nacac)_2ZrCl_2$+ 10EASC + Ethylene: ^{1}H-NMR in Toluene-d_8, 0-8ppm, 298-323K

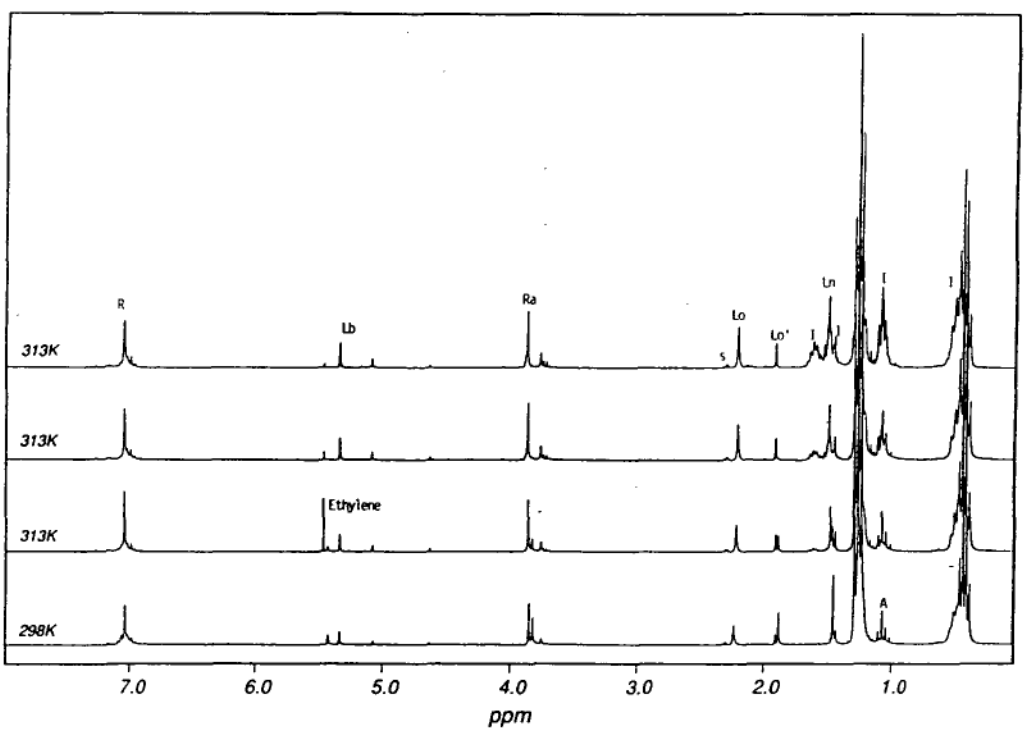

Where: A=metal alkylation, I=ethylene insertion product.

B.4.11 (MeOPh-Nacac)$_2$ZrCl$_2$+ 10EASC + Ethylene: $^{13}C\{^1H\}$-NMR in Toluene-d_8, 0-8ppm, 298-313K

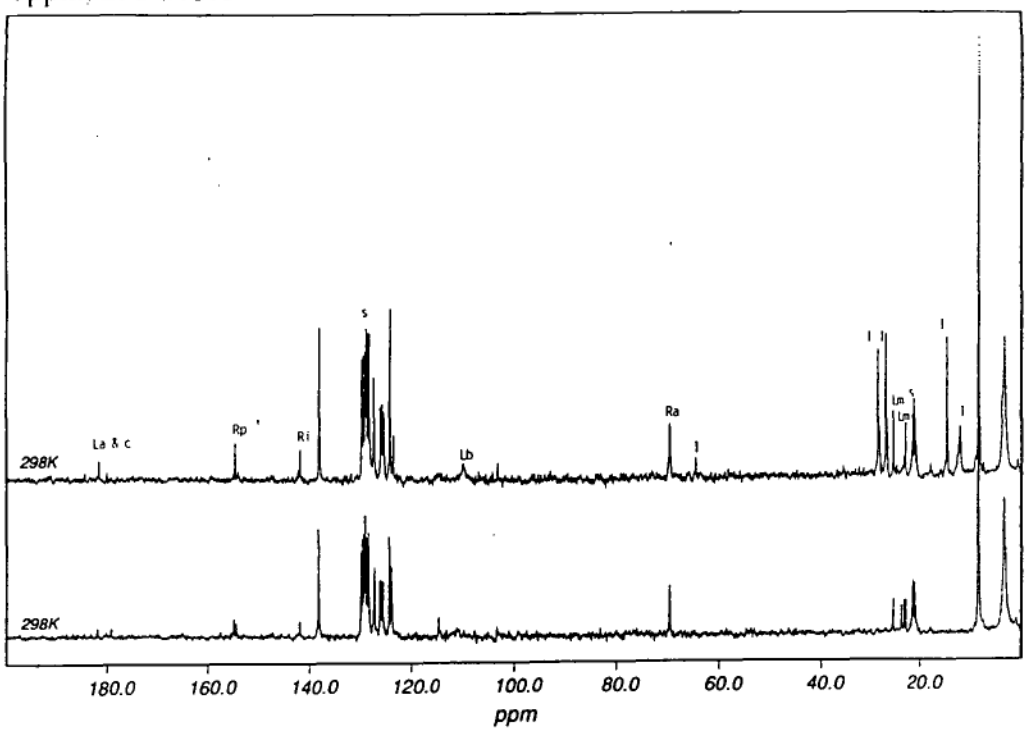

Where: Ligand backbone: La=cabonyl carbon, Lc=amino carbon, Lm=methyls; N-phenyl substituent: Rp=*para*-Ph, Ri=*ipso*-Ph; A=metal alkylation, I=ethylene insertion product; No ethylene added at 298K.

B.4.12. (MeOPh-HNacac)$_2$ZrCl$_2$ + 10EASC : $^{13}C\{^1H\}$-NMR in Toluene-d_8, 0-40ppm, 298K

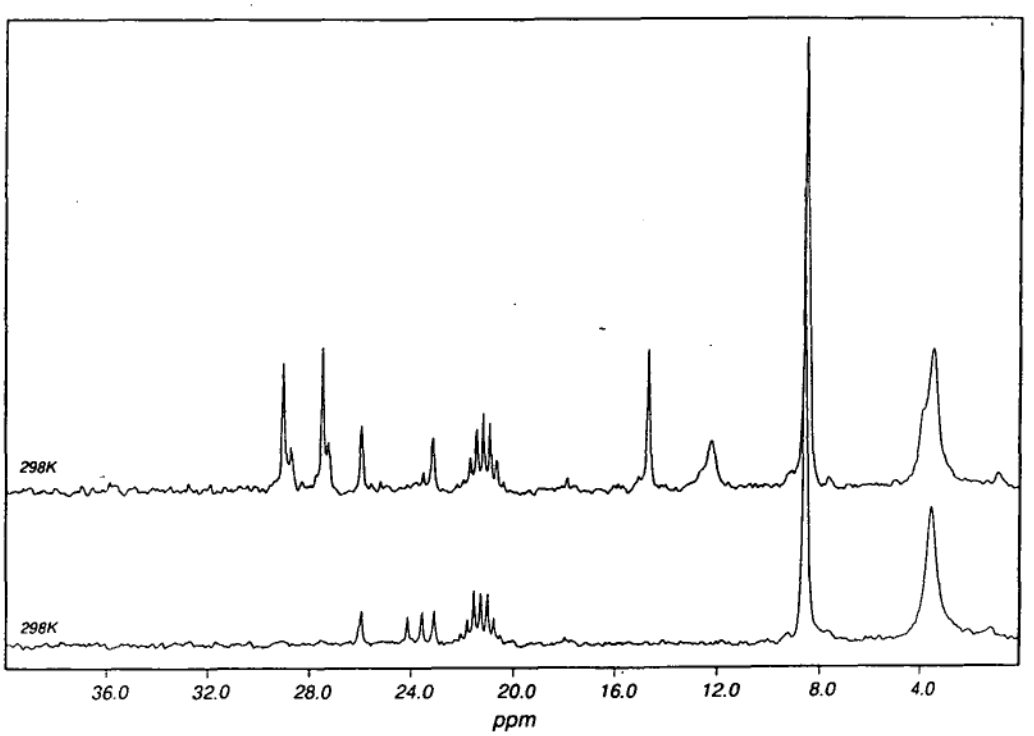

Appendix IV

CONTENTS

Crystal Structure Data

C.1.0. Crystal Structure Data for $ZrCl_4.2i$-Pr-HNacac

Molecular Formula $C_{16}H_{30}Cl_4N_2O_2Zr$
Molecular Weight 515.46
F(0)(0)=264.0
a=8.6361Å
b=9.0897Å
c=9.1174Å
V=582.5667Å^3
space group P1q z=2
2θmax=35°
I≥3.0σ(I)
ρ_c=1.4692 g/ccm
Radiation wavelength = 0.7107Å
N, No = 5755, 3815
R, R' = 0.043, 0.057

C.1.1. Structure of $ZrCl_4.2i$-Pr-HNacac

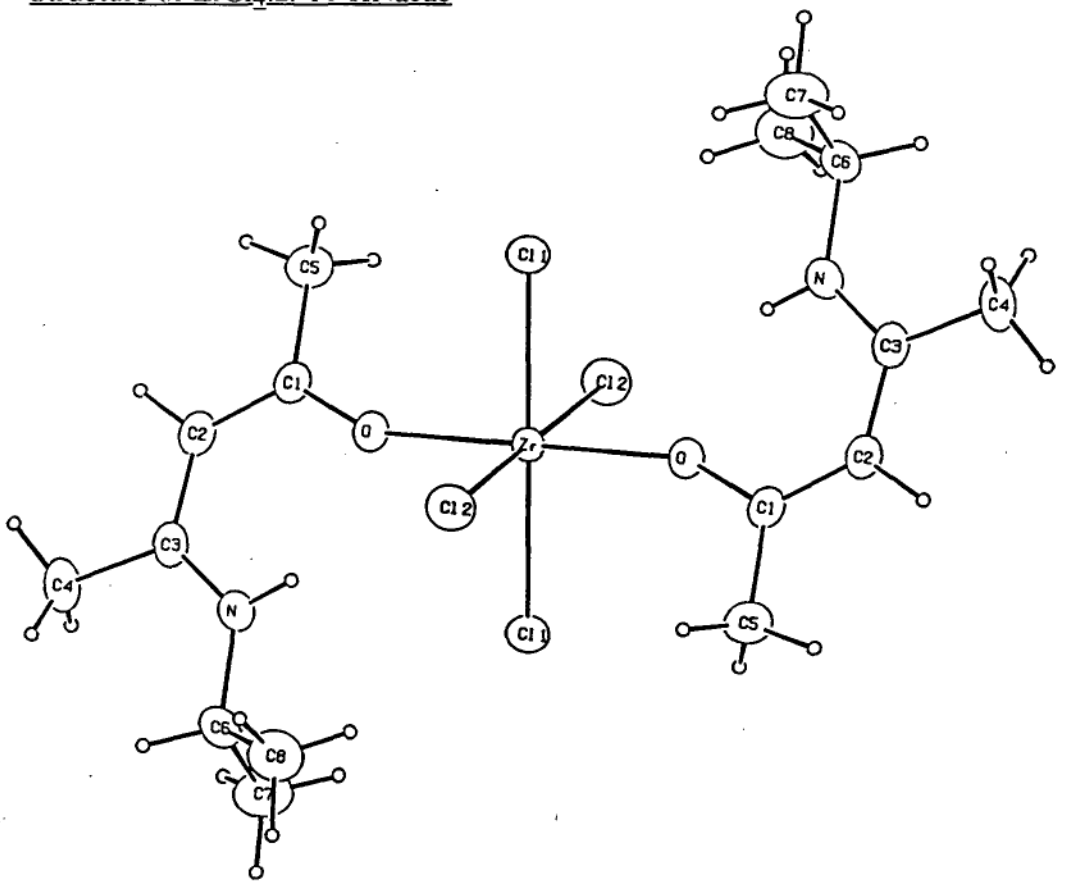

C.1.2. Bond Distances for $ZrCl_4.2i$-Pr-HNacac

Bond Lengths (Angstroms)

O-C1	1.303(2)	C6-C7	1.511(4)
N-C3	1.307(3)	C6-C8	1.517(4)
N-C6	1.470(3)	C6-H6	0.980(2)
N-H	0.81(3)	C7-H7a	0.980(3)
C1-C2	1.363(3)	C7-H7b	0.980(3)
C1-C5	1.489(3)	C7-H7c	0.980(4)
C2-C3	1.425(3)	C8-H8a	0.980(3)
C2-H2	0.980(2)	C8-H8b	0.980(3)
C3-C4	1.496(3)	C8-H8c	0.980(3)
C4-H4a	0.980(3)	Zr-Cl1	2.4676(5)
C4-H4b	0.980(3)	Zr-Cl1	2.4676(5)
C4-H4c	0.980(3)	Zr-Cl2	2.4632(6)
C5-H5a	0.980(3)	Zr-Cl2	2.4632(6)
C5-H5b	0.980(3)	Zr-O	2.052(1)
C5-H5c	0.980(3)	Zr-O	2.052(1)

C.1.3. Torsion Angles for $ZrCl_4.2i$-Pr-HNacac

Torsion Angles (Degrees)

Atom 1	Atom 2	Atom 3	Atom 4	Angle
Cl1	Zr	O	C1	-138.45 (0.40)
Cl2	Zr	O	C1	-48.33 (0.40)
Zr	O	C1	C2	172.73 (0.28)
Zr	O	C1	C5	-6.26 (0.54)
C6	N	C3	C2	-176.11 (0.25)
C6	N	C3	C4	2.33 (0.40)
H	N	C3	C2	4.40 (2.62)
H	N	C3	C4	-177.17 (2.60)
C3	N	C6	C7	89.77 (0.34)
C3	N	C6	C8	-148.06 (0.28)
H	N	C6	C7	-90.77 (2.78)
H	N	C6	C8	31.39 (2.79)
O	C1	C2	C3	-1.63 (0.42)
C5	C1	C2	C3	177.32 (0.26)
C1	C2	C3	N	2.72 (0.42)
C1	C2	C3	C4	-175.75 (0.26)

C.1.4. Bond Angles for $ZrCl_4.2i$-Pr-HNacac

Bond Angles (Degrees)

C3-N-C6	127.5(2)	N-C6-C7	109.7(2)
C3-N-H	113.(2)	N-C6-C8	108.5(2)
C6-N-H	120.(2)	N-C6-H6	111.1(2)
O-C1-C2	122.3(2)	C7-C6-C8	111.6(2)
O-C1-C5	117.1(2)	C7-C6-H6	106.9(2)
C2-C1-C5	120.6(2)	C8-C6-H6	109.0(2)
C1-C2-C3	126.5(2)	C6-C7-H7a	109.0(3)
C1-C2-H2	117.1(2)	C6-C7-H7b	110.3(3)
C3-C2-H2	116.4(2)	C6-C7-H7c	109.4(2)
N-C3-C2	123.1(2)	H7a-C7-H7b	109.3(3)
N-C3-C4	119.7(2)	H7a-C7-H7c	109.3(4)
C2-C3-C4	117.1(2)	H7b-C7-H7c	109.5(3)
C3-C4-H4a	109.7(2)	C6-C8-H8a	109.4(3)
C3-C4-H4b	109.1(2)	C6-C8-H8b	110.1(3)
C3-C4-H4c	109.6(2)	C6-C8-H8c	109.3(3)
H4a-C4-H4b	109.5(2)	H8a-C8-H8b	109.3(3)
H4a-C4-H4c	109.5(2)	H8a-C8-H8c	109.3(3)
H4b-C4-H4c	109.5(3)	H8b-C8-H8c	109.5(3)
C1-C5-H5a	110.7(2)	Cl1-Zr-Cl1	180.(0)
C1-C5-H5b	108.2(2)	Cl1- Zr-Cl2	90.19(2)
C1-C5-H5c	108.6(2)	Cl1-Zr-Cl2	89.81(2)
H5a-C5-H5b	109.9(3)	Cl1-Zr-O	88.01(4)
H5a-C5-H5c	109.9(3)	Cl1-Zr-O	91.99(4)
H5b-C5-H5c	109.5(3)	Cl1-Zr-Cl2	89.81(2)
Cl1-Zr-Cl2	90.19(2)	Cl2-Zr-O	88.05(5)
Cl1-Zr-O	91.99(4)	Cl2-Zr-O	88.05(5)
Cl1-Zr-O	88.01(4)	Cl2-Zr-O	91.95(5)
Cl2-Zr-Cl2	180.(0)	O-Zr-O	180.(0)
Cl2-Zr-O	91.95(5)		

C.2.0. Crystal Structure Data for $(Ph\text{-}Nacac)_2ZrCl_2$

Molecular Formula $C_{22}H_{24}Cl_2N_2O_2Zr$
Molecular Weight 510.6
F_{000}=2080
a=17.221(3)Å
b=16.448(12)Å
c=16.584(4)Å
V=4697(4)Å^3
space group Pbca z=8
cad4(cad1) diffractometer
$2\theta max=50°$
$I \geq 3\sigma(I)$
$\mu(MoK\alpha)$ = 7.1 cm^{-1}
A^k(min, max) = 1.20, 1.27 (gaussian)
crystal dimensions 0.28*0.65*0.36 mm
weighting scheme n=4*10^{-4}
N, No = 4141, 2619
R, R' = 0.037, 0.037

C.2.1. Structure of $(Ph\text{-}Nacac)_2ZrCl_2$

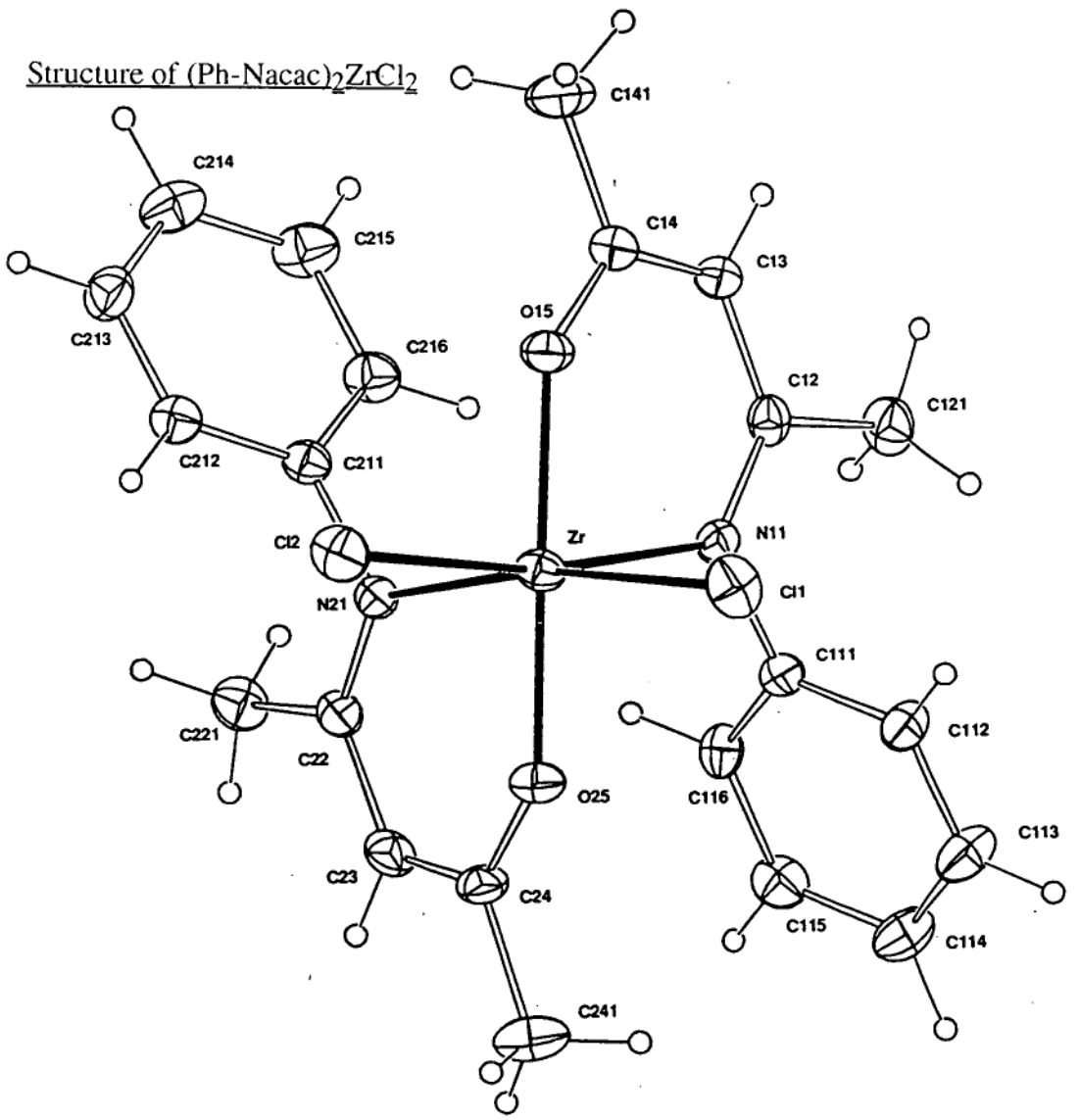

C.2.2. Unit Cell of $(Ph\text{-}Nacac)_2ZrCl_2$

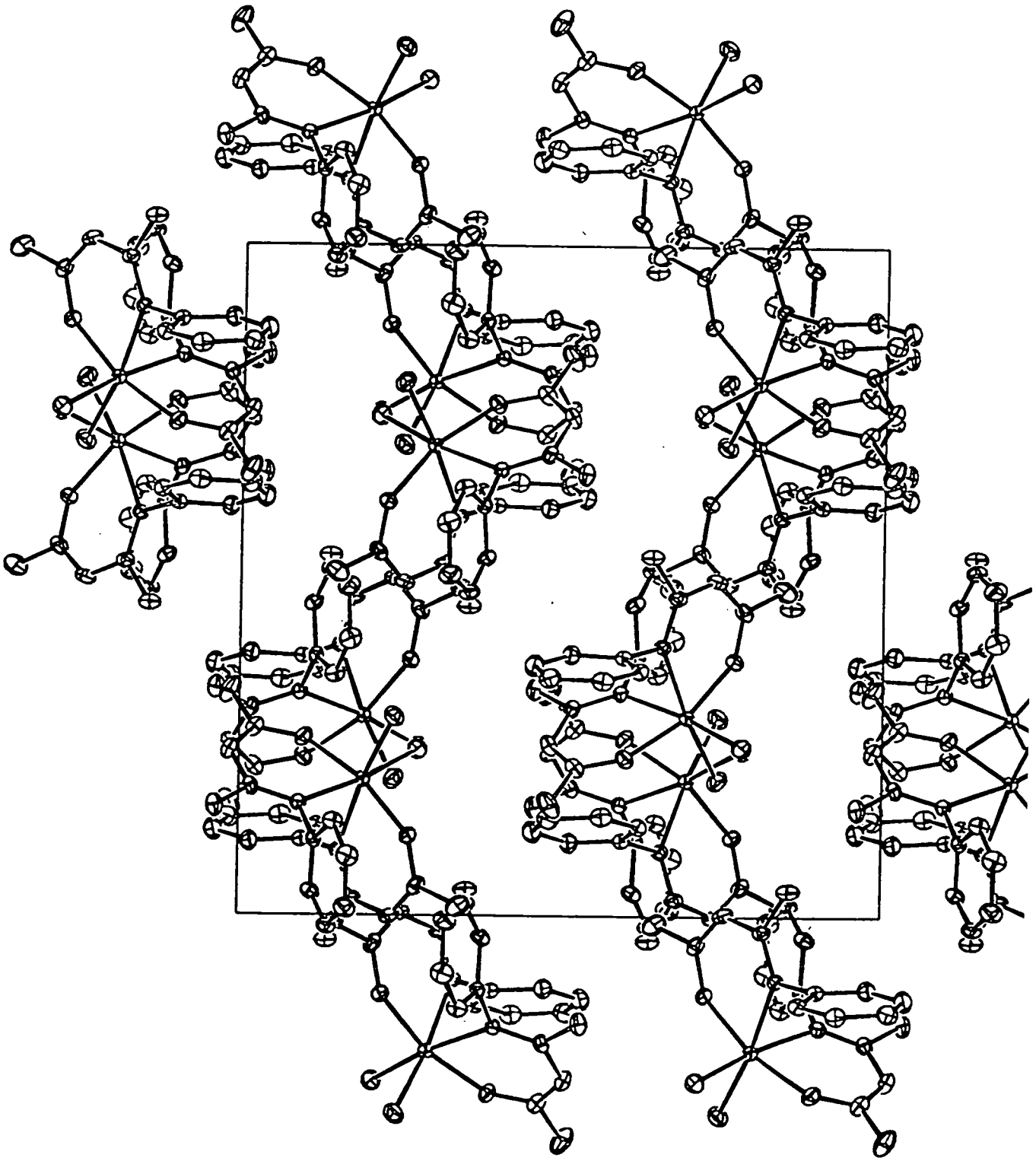

C.2.3. Bond Distances for $(Ph\text{-}Nacac)_2ZrCl_2$

Bond Distances	(Angstroms)
Zr-Cl(1)	2.432(2)
Zr-Cl(2)	2.421(2)
Zr-N(11)	2.312(3)
Zr-O(15)	2.007(3)
Zr-N(21)	2.299(3)
Zr-O(25)	2.012(3)
N(11)-C(111)	1.436(6)
N(11)-C(12)	1.321(5)
C(111)-C(112)	1.376(7)
C(111)-C(116)	1.388(6)
C(112)-C(113)	1.377(7)
C(113)-C(114)	1.379(8)
C(114)-C(115)	1.379(8)
C(115)-C(116)	1.373(7)
C(12)-C(121)	1.498(7)
C(12)-C(13)	1.430(7)
C(13)-C(14)	1.337(7)
C(14)-C(141)	1.498(8)
C(14)-O(15)	1.323(6)
N(21)-C(211)	1.445(6)
N(21)-C(22)	1.331(6)
C(211)-C(212)	1.370(7)
C(211)-C(216)	1.379(7)
C(212)-C(213)	1.385(7)
C(213)-C(214)	1.385(8)
C(214)-C(215)	1.378(8)
C(215)-C(216)	1.376(8)
C(22)-C(221)	1.500(7)
C(22)-C(23)	1.412(7)
C(23)-C(24)	1.348(7)
C(24)-C(241)	1.508(8)
C(24)-O(25)	1.320(6)

C.2.4. Bond Angles for $(Ph\text{-}Nacac)_2ZrCl_2$

Bond Angles (Degrees)

Cl(1)-Zr-Cl(2)	95.58(6)		
Cl(1)-Zr-N(11)	89.6(1)		
Cl(1)-Zr-O(15)	97.41(9)		
Cl(1)-Zr-N(21)	168.87(9)		
Cl(1)-Zr-O(25)	92.34(9)		
Cl(2)-Zr-N(11)	169.04(9)		
Cl(2)-Zr-O(15)	92.6(1)		
Cl(2)-Zr-N(21)	90.5(1)		
Cl(2)-Zr-O(25)	97.64(9)		
N(11)-Zr-O(15)	77.1(1)		
N(11)-Zr-N(21)	86.0(1)		
N(11)-Zr-O(25)	91.7(1)		
O(15)-Zr-N(21)	91.6(1)		
O(15)-Zr-O(25)	165.1(1)		
N(21)-Zr-O(25)	77.6(1)		
Zr-N(11)-C(111)	113.8(3)	Zr-N(21)-C(211)	114.6(3)
Zr-N(11)-C(12)	129.8(3)	Zr-N(21)-C(22)	129.4(3)
C(111)-N(11)-C(12)	116.3(3)	C(211)-N(21)-C(22)	116.0(4)
N(11)-C(111)-C(112)	120.2(4)	N(21)-C(211)-C(212)	119.5(4)
N(11)-C(111)-C(116)	120.3(4)	N(21)-C(211)-C(216)	119.9(4)
C(112)-C(111)-C(116)	119.5(4)	C(212)-C(211)-C(216)	120.7(4)
C(111)-C(112)-C(113)	119.9(5)	C(211)-C(212)-C(213)	119.3(4)
C(112)-C(113)-C(114)	120.5(5)	C(212)-C(213)-C(214)	120.6(5)
C(113)-C(114)-C(115)	119.6(5)	C(213)-C(214)-C(215)	119.1(5)
C(114)-C(115)-C(116)	120.0(4)	C(214)-C(215)-C(216)	120.6(5)
C(111)-C(116)-C(115)	120.4(4)	C(211)-C(216)-C(215)	119.7(5)
N(11)-C(12)-C(121)	121.3(4)	N(21)-C(22)-C(221)	120.4(4)
N(11)-C(12)-C(13)	123.1(4)	N(21)-C(22)-C(23)	123.3(4)
C(121)-C(12)-C(13)	115.7(4)	C(221)-C(22)-C(23)	116.3(4)
C(12)-C(13)-C(14)	125.2(4)	C(22)-C(23)-C(24)	125.5(4)
C(13)-C(14)-C(141)	123.0(5)	C(23)-C(24)-C(241)	122.8(5)
C(13)-C(14)-O(15)	122.4(4)	C(23)-C(24)-O(25)	122.3(4)
C(141)-C(14)-O(15)	114.6(4)	C(241)-C(24)-O(25)	114.9(4)
Zr-O(15)-C(14)	142.4(3)	Zr-O(25)-C(24)	141.6(3)